Understanding the role of microRNA expression in the response to phenobarbital toxicity in the rat

Michael Craig Osborne

Computational and Systems Medicine

Division of Surgery and Cancer

Faculty of Medicine

Imperial College London

Thesis presented for the degree of Doctor of Philosophy at Imperial College London

30th September 2015

Statement of originality

I confirm that all work presented herein is my own original work, unless otherwise stated and referenced accordingly.

Michael Osborne

30th September 2015

‘The copyright of this thesis rests with the author and is made available under a Creative Commons Attribution Non-Commercial No Derivatives licence. Researchers are free to copy, distribute or transmit the thesis on the condition that they attribute it, that they do not use it for commercial purposes and that they do not alter, transform or build upon it. For any reuse or redistribution, researchers must make clear to others the licence terms of this work’

Abstract

New chemical entities that humans and animals are likely to be exposed to are tested using various *in vitro* and *in vivo* toxicological assays to understand the potential for harm. The increasing power of *in silico* analysis in combination with *in vitro* techniques is being exploited for the ability to predict *in vivo* outcomes such as toxicity, thereby reducing the requirement for animal testing. Previous studies in our laboratory have found that dietary phenobarbital treatment of rats results in dysregulation of the hepatic miRNAome, including prominent alteration of the expression of the miR-200a/b/429 cluster and miR-182/96 cluster. In this thesis I explore the use of a cell culture system, rat hepatocyte-like B13/H cells, to interrogate the underlying mechanisms of phenobarbital-mediated toxicity. Through this model I explore the function of phenobarbital-dysregulated microRNAs to determine their roles as markers of phenobarbital treatment in the rat. We find that the B13/H cells provide a useful system for studying the phenobarbital response *in vitro*, and how these responses relate to the effects of oral exposure to phenobarbital *in vivo* in the rat. In this respect, the B13/H cells appear representative of the rat response to phenobarbital, which is different to that of the mouse. With a focus on the phenobarbital-mediated dysregulation of the miR-182/96 cluster, I have explored the consequences of phenobarbital treatment on the B13/H cell model and related this to the *in vivo* effects. The data suggest that these microRNAs appear to control phenobarbital-mediated perturbation of glycolysis, cell transformation and methylation patterns.

If you don’t go after what you want, you’ll never have it.

If you don’t ask, the answer is always no.

If you don’t step forward, you’re always in the same place.

Nora Roberts

Acknowledgements

I would like to express my upmost thanks to my supervisor, Professor Gooderham, for his supervision of my PhD, his valuable input and direction, and his unwavering support and motivation towards my academic progression, as well as his compassion throughout my turbulent time at Imperial. I would like to thank my industrial supervisors Dr Richard Currie and Dr Jayne Wright for their critical input, which has helped me to produce a well formed and completed work. I would also like to thank my previous teachers and supervisors who have helped me to develop myself to a standard capable of embarking on this PhD. I also thank the BBSRC and Syngenta for their financial support.

I am indebted to the whole of the Gooderham group for their support, advice and comradery: Dr Costas Koufaris, Dr Leanne Harling, Dr Saroor Patel, Tianlai Yang, Kuanwei Chen, and my fellow 4th floor companions. In particular I would like to mention group members: Dr Rhiannon David for her invaluable teachings and advice, Dr Qianxin Wu as my cell culture mentor, Dr Abdullah Alkandari for teaching me qPCR, as well as his many welcome and varied discussions in the evenings in the lab, Mariana Flores Torres for her support in my project and as a fellow phenobarbital researcher, Durr Shahwar Malik as my companion throughout my time at Imperial, Oliver Graham for his discussions in and out of the lab, and unofficial honorary group member, Michael Kyriakides, for his coffee break diversions.

Finally, I would like to thank my family and friends who have supported me throughout. I would like to make special mention to my mother who encouraged me to be the best that I could be, and to my father who supported me when my mother no longer could, and to Katie who has held my hand through everything. This thesis is dedicated to you.

Table of Contents

1. Introduction 19

1.1 Chemical exposure 19

1.1.1 Biotransformation 19

1.1.2 In vitro toxicology testing 22

1.2 Phenobarbital (PB) 25

1.2.1 Car/Pxr functions 26

1.2.2 Car/Pxr activation 28

1.2.3 PB-mediated indirect activation of Car 31

1.2.4 PB is non-genotoxic 34

1.2.5 PB-mediated tumourigenesis 36

1.3 microRNAs 39

1.3.1 Biogenesis 39

1.3.2 Activity/Function 41

1.4 Concluding statements 44

1.5 Hypothesis 44

1.6 Aims 44

2. Characterising rat hepatocyte-like AR42J-B13/H cells as an in vitro model for phenobarbital treatment 45

2.1 Introduction 45

2.1.1 The rat AR42J-B13/H (B13/H) cell model - origin 45

2.1.2 The rat AR42J-B13/H (B13/H) cell model - differentiation 46

2.1.3 Hypothesis..... 48

2.1.4 Aims 48

2.2 Methods 49

2.2.1 Cell culture..... 49

2.2.2 Cyp450 enzyme activity - PROD..... 49

2.2.3 BCA assay 53

2.2.4 Nuclear localisation - Subcellular fractionation 53

2.2.5 RNA extraction..... 55

2.2.6 qRT-PCR 56

2.2.7 Semi-qPCR..... 59

2.2.8 Statistics 60

2.3 Results and Discussion 61

2.3.1 Aim 1: Characterising the differentiation of AR42J-B13 (B13) to hepatocyte-like AR42J-B13/H (B13/H) cells in response to dexamethasone..... 61

2.3.2 Aim 2: Assess the B13/H cell response to PB and PB-like compounds. 66

2.3.2.1 Assess the B13/H cell response to PB 66

2.3.2.2 Cyp2b activity and Cyp mRNA expression in 2 week dexamethasone transdifferentiated B13/H cells in response to PB 73

2.3.2.3 Temporal- and dose-dependent response of Cyp2b activity in 2 week dexamethasone-differentiated B13/H cells in response to PB and PB-like compounds 77

2.3.3 Aim 3: Explore the effect of PB and PB-like compounds on miRNA expression in B13/H cells. 82

2.4 Conclusions 87

3. Cross-talk between growth factor signalling and phenobarbital signalling pathways 90

3.1 Introduction 90

3.1.1 PB antagonises Egfr in the mouse to activate Car 90

3.1.2 Effects of Egf on PB-mediated gene transcription in the rat 92

3.1.3 Hypothesis 94

3.1.4 Aims 94

3.2 Methods 95

3.2.1 Tissue Samples 95

3.2.2 Cell culture 95

3.2.3 Cell counts & alamarBlue® 95

3.2.4 Cyp450 enzyme activity - PROD 96

3.2.5 Chemical treatments – cell signalling 97

3.2.6 Immunoblots 97

3.2.7 Meso Scale Discovery (MSD) multi-spot assay system 101

3.2.8 Statistics 102

3.3 Results and Discussion 103

3.3.1 Aim 1: Optimise growth factor treatment dose and time for Erk and Akt activation in B13/H cells. 103

3.3.1.1 Optimising treatment doses 103

3.3.1.2 Optimising growth factor treatment time for Erk and Akt activity 107

3.3.1.3 Effect of phenobarbital alone on Erk or Akt pathway activity in B13/H cells 109

3.3.2 Aim 2: Assess the B13/H cell response to PB in combination with either growth factor to determine potential roles of these signalling pathways in the rat. 111

3.3.2.1 Phenobarbital potentiates Egf-mediated Erk and Akt phosphorylation in B13/H cells 111

3.3.2.2 Phenobarbital potentiates Hgf-mediated Akt phosphorylation in B13/H cells 114

3.3.2.3 The role of Akt activation in PB plus Egf/Hgf treatments 116

3.3.3 Aim 3: Assess the activation of these pathways in the rat *in vivo*. 120

3.3.3.1 Growth factor pathways are unchanged in the rat *in vivo* 120

3.4 Conclusions 125

4. Regulation of phenobarbital-induced miRNAs 129

4.1 Introduction 129

4.1.1 Regulation of miR-182/96 129

4.1.3 Aims 134

4.2 Methods 135

4.2.1 Tissue samples 135

4.2.2 Cell culture and chemical treatments 135

4.2.3 RNA extraction 136

4.2.4 qRT-PCR 136

4.2.5 DNA extraction 136

4.2.6 Bisulphite conversion 137

4.2.7 Bisulphite PCR 139

4.2.8 Pyro-sequencing 139

4.2.9 Statistics 140

4.3 Results and Discussion 141

4.3.1 Aim 1: Explore miRNA expression in PB treated WT and Car KO rats to determine underlying molecular stimulus for perturbed expression. 141

4.3.1.1 MiR-182 is time-dependently expressed in PB treated rats 141

4.3.1.2 Car as a regulator of miR-182/96 expression in PB treated Car wild type and knockout rats 143

4.3.1.3 Car as a regulator of miR-429/200b expression in PB treated Car wild type and knockout rats 145

4.3.1.4 Inhibiting Car in the B13/H model 147

4.3.2 Aim 2: Interrogate the activity of potential miRNA regulators using PB treated rat liver tissue. 150

4.3.2.1 Hnf-4α as a regulator of miR-182/96 expression in PB treated rats 150

4.3.2.2 Methylation changes as a regulator of miR-182/96 expression in PB treated rats 151

4.3.2.3 P53 as a regulator of miR-182/96 expression in PB treated rats 154

4.3.2.4 ROS as a regulator of miR-182/96 expression in PB treated rats 155

4.3.2.5 Tgf-β as a regulator of miR-182/96 expression in PB treated rats 156

4.4 Conclusion 158

5. Function of phenobarbital-induced miRNAs 162

5.1 Introduction 162

5.1.1 PB responsive miRNAs in the mouse 162

5.1.2 PB responsive miRNAs in the rat 163

5.1.3 Hypothesis 165

5.1.4 Aims 165

5.2 Methods 166

5.2.1 Tissue samples 166

5.2.2 In silico analysis 166

5.2.3 qRT-PCR 166

5.3 Results and Discussion 167

5.3.1 Aim 1: Use *in silico* analyses to identify potential targets of miR-182/96. .. 167

5.3.1.1 miR-182/96 sequence 167

5.3.1.2 Validated miR-182/96 targets 168

5.3.1.3 Predicted miR-182/96 targets 172

5.3.2 Aim 2: Confirm targets through selected targeted analysis. 178

5.3.2.1 MiR-182/96 targets chosen for validation *in vivo* 178

6. Discussion 188

6.1 General conclusions and future work..... 188

6.1.1 Thesis aim 1: Characterise the B13/H cell line and its response to PB and PB-like compounds. 188

6.1.2 Thesis aim 2: Explore the interaction with PB and growth factor signalling in vitro and *in vivo*. 190

6.1.3 Thesis aim 3: Identify potential regulators of PB-induced miRNAs *in vivo*. 192

6.1.4 Thesis aim 4: Elucidate the potential function of PB-induced miRNAs *in vivo*. 193

6.2 Consolidation – the big picture 196

6.2.1 If not Egfr, what could be the rat PB receptor? 197

6.2.2 Thesis hypothesis 199

References 201

List of figures

Figure 1.1: Liver architecture 20
Figure 1.2: Hepatic lobule structure 21
Figure 1.3: Structure of phenobarbital 25
Figure 1.4: Rat Car - linear structure 31
Figure 1.5: Indirect activation of Car in the mouse 32
Figure 1.6: PB-mediated tumourigenesis in the mouse 38
Figure 1.7: MiRNA biogenesis 41
Figure 2.1: Dexamethasone-mediated differentiation of B13 cells 47
Figure 2.2: Excitation and emission wavelengths for resorufin detection 51
Figure 2.3: PROD substrate and resorufin fluorescence 52
Figure 2.4: B13/H subcellular fractionation markers 55
Figure 2.5: TaqMan PCR 58
Figure 2.6: B13 dexamethasone treatment plan 61
Figure 2.7: Markers of the transdifferentiation phenotype of B13/H cells 63
Figure 2.8: Effect of PB treatment on Cyp2b actvity in B13/H cells 67
Figure 2.9: Car subcellular localisation 71
Figure 2.10: MiR-122 expression in PB treated B13/H cells 73
Figure 2.11: Effect of media on Cyp2b activity in B13/H cells 75
Figure 2.12: Cyp mRNA expression in PB treated B13/H cells 77
Figure 2.13: Time-response of Cyp2b activity in B13/H cells treated with PB and PB-like compounds 79
Figure 2.14: Dose-response of Cyp2b activity in B13/H cells treated with PB and PB-like compounds 81
Figure 2.15: miRNA expression in B13/H cells treated with PB and PB-like compounds 84
Figure 2.16: Comparing miRNA expression in B13/H cells between 3 and 9 days 86
Figure 3.1: Activation of Car by PB in the mouse 91
Figure 3.2: Alamar blue reduction 96
Figure 3.3: Growth factor and PB dose response 106
Figure 3.4: Twenty ng/mL Hgf time response - Erk/Akt activity 108
Figure 3.5: Sixty minute PB treatment - Erk/Akt activity 110
Figure 3.6: Thirty minutes treatment with PB followed by 60 minutes with 5ng/mL Egf - Erk/Akt activity 113
Figure 3.7: Thirty minutes treatment with PB followed by 60 minutes with 20ng/mL Hgf - Erk/Akt activity 115
Figure 3.8: Thirty minutes treatment with 20ng/mL Hgf followed by 60 minutes with PB - FoxO1 activity 117
Figure 3.9: Thirty minutes 20ng/mL Hgf followed by 48 hours PB 118
Figure 3.10: Erk and Elk activity in PB treated rat liver 121
Figure 3.11: MAPK pathway activity in PB treated rat liver 122
Figure 3.12: Akt and FoxO1 activity in PB treated rat liver 123
Figure 3.13: Car activation in the mouse and rat 126
Figure 3.14: The effect of PB on Erk and Akt activity in the rat 127
Figure 4.1: Potential miR-182/96 regulators 133
Figure 4.2: Pyro-sequencing methodology 137
Figure 4.3: Methylation assessment optimisation 138

Figure 4.4: MiR-182 expression in subchronic PB treatment study 142
Figure 4.5: Cyp mRNA expression and Cyp2b activity in wild type and Car KO rats 143
Figure 4.6: MiR-182 and miR-96 expression in wild type and Car KO rats 145
Figure 4.7: MiR-429 and miR-200b expression in wild type and Car KO rats 146
Figure 4.8: Cyp activity in B13/H cells treated with PB and androstenol 148
Figure 4.9: Analysis of miR-182/96 upstream sequence 151
Figure 4.10: Site-specific methylation levels after PB treatment in vivo 153
Figure 4.11: p21 expression in PB treated rats 154
Figure 4.12: β-Gal and Hif-1α expression in PB treated rats 156
Figure 4.13: Tgf-β expression in PB treated rats 157
Figure 4.14: β-Catenin or methylation as miR-182/96 regulators 160
Figure 5.1: MiR-182/96 sequence 167
Figure 5.2: In silico analysis of validated miRNA targets (1) 169
Figure 5.3: In silico analysis of validated miRNA targets (2) 171
Figure 5.4: In vivo FoxO1 correlation with miR-182 172
Figure 5.5: In silico analysis of predicted miRNA targets 175
Figure 5.6: In silico Gnmt correlation with miR-96 177
Figure 5.7: FoxO1 as a target for miR-182 179
Figure 5.8: In vivo FoxO1 protein expresion 180
Figure 5.9: Gnmt as a target for miR-182 181
Figure 5.10: In vivo Gnmt protein expression 182
Figure 5.11: MiRNA-mediated glycolysis 184
Figure 5.12: MiRNA-mediated methylation 186
Figure 5.13: MiR-mediated effect on EMT 187
Figure 6.1: Proposed PB signalling pathway in rat hepatocytes 198

List of tables

Table 2.1: qRT-PCR conditions 57
Table 2.2: Semi-q PCR primer details 60
Table 2.3: Semi-q PCR amplification conditions 60
Table 5.1: MiR-182/96 targets 178
Table 5.2: Proposed function of miR-182/96 184

List of abbreviations

Abbreviation	Meaning
5hmc	5-hydroxymethylcytosine
8-OHdG	8-hydroxy-2'-deoxyguanosine
AF2	trans-activation domain
Ago	argonaute
Ampk	AMP-activated protein kinase
Androstenol	5α-androstan-16-en-3α-ol
ANOVA	analysis of variance
APS	ammonium persulphate
Azaserine	O-diazoacetyl-L-serine
B13	AR42J-B13
B13/H	AR42J-B13/H
BCA	bicinchoninic acid
BP	benzophenone
BrdU	bromodeoxyuridine
BSA	bovine serum albumin
Car/Nr1i3	constitutive androstane receptor
Ccrp	cytoplasmic Car retention protein
C/EBP-β	CCAAT enhancer binding protein-β
ceRNAs	competing endogenous RNAs
CITCO	6-(4-chlorophenyl)imidazo[2,1-b][1,3]thiazole-5-carbaldehyde O-(3,4-dichlorobenzyl)oxime
c-Myc	myelocytomatosis oncogene
CpG	cytosine-guanine pair
CRR	cytoplasmic retention region
Cyp	cytochrome P-450
DDX	dead box helicase
DEN	N-diethylnitrosamine
Dex	dexamethasone
dmH_2O	demineralised H_2O
DMSO	dimethyl sulfoxide
Dnmt	DNA methyltransferase enzyme
dNTPs	deoxynucleotide triphosphates
DR	direct repeat
DTT	DL-Dithiothreitol
EDTA	edetic acid
Egf	epidermal growth factor
Egfr	Egf receptor
EMT	epithelial to mesenchymal transition
ER	everted repeat
Erk	extracellular signal regulated mitogen-activated kinase
FBS	foetal bovine serum
FoxO1	forkhead box O1
G6pase	glucose-6-phosphatase
G6pt	glycerol-6-phosphate transporter
GABA	γ-aminobutyric acid

Gadd45β	growth arrest and DNA-damage-inducible 45β
Gapdh	glyceraldehyde-3-phosphate dehydrogenase
Gnmt	glycine N-methyltransferase
GRIP	glucocorticoid receptor interacting protein
Gsk-3β	glycogen synthase kinase 3β
HEPES	4-(2-Hydroxyethyl)piperazine-1-ethanesulfonic acid
Hgf	hepatocyte growth factor
HI-DCC	heat inactivated dextran coated charcoal
Hif-1α	hypoxia-inducible factor-1α
Hnf-4α/Nr2a1	hepatocyte nuclear factor 4α
HRP	horseradish peroxidase
Hsp90	heat shock protein 90
Jnk	Jun N-terminal kinase
KCl	potassium chloride
kDa	kilodaltons
KO	knockout
MAPK	mitogen-activated protein kinase
Mek	mitogen-activated protein kinase kinase
$MgCl_2$	magnesium chloride
miR/miRNA	microRNA
miRLC	miRNA loading complex
MSD	meso scale discovery
NaCl	sodium chloride
NADPH	nicotinamide adenine dinucleotide phosphate
NES	nuclear export signal
NF	nuclear factor
NKCC1/Slc12a2	Na^+-K^+-$2Cl^-$ cotransporter
OAA	okadaic acid
Oat	organic anion transporter
Olr59	olfactory receptor 59
P16	cyclin-dependent kinase inhibitor 2A
P21	cyclin-dependent kinase inhibitor 1A
P38	p38 MAPK
PAZ	PIWI-AGO-Zwille
PB	phenobarbital
PBREM	phenobarbital-responsive enhancer module
PBRU	PB-responsive enhancer unit
PBS	phosphate buffered saline
Pc	pyruvate carboxylase
PCN	pregnenolone 16α-carbonitrile
Pepck	phosphoenolpyruvate carboxykinase
PGC	peroxisome proliferator-activated receptor γ coactivator
PHx	partial hepatectomy
PP1/2A	phosphatase 1/2A
Pp2ac	catalytic subunit of protein phosphatase 2A
Ppm	parts per million
PROD	penoxyresorufun-O-dealkylase
Pxr/Nr1i2	pregnane x receptor
qRT-PCR	quantitative real time PCR
Rack1	receptor for activated C kinase 1

Rb1	retinoblastoma 1
RISC	RNA induced silencing complex
ROS	reactive oxygen species
RT	reverse transcription
Rxr	retinoid x receptor
SD	standard deviation
SDS	sodium dodecyl sulphate
SEM	standard error of the mean
semi-q	semi-quantitative
SGK1	serum- and glucocorticoid-regulated kinase 1
Slc	solute carrier family
Smad4	mothers against decapentaplegic homolog 4
Src	steroid receptor co-activator
SV	splice variant
TBE	tris-borate-EDTA
TCA	tricarboxylic acid
TCPOBOP	1,4-Bis[2-(3,5-dichloropyridyloxy)]benzene
TEMED	tetramethylethylenediamine
Tgf	transforming growth factor
Tomm40l (yeast)-like	translocase of outer mitochondrial membrane 40 homolog
Ugt	UDP-glucuronosyl transferases
Vdr/Nr1i1	1,25-$(OH)_2$-vitamin D3 receptor
Vegf	vascular endothelium growth factor
WT	wild type
XRS	xenochemical response signal
Zeb	zinc-finger E-box binding homeobox

1. Introduction

1.1 Chemical exposure

Exposure to lipophilic chemical entities from foreign (xenobiotic) or endogenous (endobiotic) sources requires biotransformation and excretion to prevent harmful accumulation (Ennulat et al., 2010). Biotransformation refers to biologically-mediated chemical changes, for example by xenobiotic metabolising enzymes, which aim to reduce a chemical's lipophilicity and aid elimination (Botts et al., 2010). Most tissues in the body are capable of xenobiotic biotransformation, however the liver has the largest capacity to produce xenobiotic metabolising enzymes and is the major defence of the body to chemical exposure (Ennulat et al., 2010; Hardisty & Brix, 2005).

1.1.1 Biotransformation

The liver is a multifunctional organ involved in xenobiotic metabolism (Sturgill & Lambert, 1997), energy regulation (Bollen, Keppens, & Stalmans, 1998), bile production, fat absorption and cholesterol homeostasis (T. Li & Chiang, 2014). The liver is a heterogeneous mix of cells, dominated by parenchymal hepatocyte cells, which are the main cell type involved in expressing proteins for biotransformation (Decaens, Durand, Grosse, & Cassio, 2008) and make up to 60-70% of the cell population. The most abundant non-paranchymal cell populations consist of cholangiocytes, sinusoidal cells, Kupffer cells and hepatic stellate cells. There are variable reports on their density within the liver, but each have been reported to be 1-20% of the total cell population (Damm et al., 2013; Malarkey, Johnson, Ryan, Boorman, & Maronpot, 2005). The cholangiocytes are epithelial cells, which line the liver bile ducts and are important in the transport of bile from hepatocytes into the

bile canaliculi to the bile duct (N. Kanno, LeSage, Glaser, Alvaro, & Alpini, 2000) (Figure 1.1). Kupffer cells are resident macrophages and are involved in mediating the liver immune response (Damm et al., 2013). Sinusoidal endothelial cells form capillaries that facilitate the transport of molecules between hepatocytes and the blood (Figure 1.1), which is enabled by the sinusoidal cell's porous structure, known as fenestrations (Damm et al., 2013). Finally, hepatic stellate cells, which are located in the space of Disse (between the basolateral membrane of hepatocytes and anti-luminal surface of sinusoidal cells (Figure 1.1)), are involved in liver regeneration, retinol storage and immune regulation (Y.-S. Lee & Jeong, 2012).

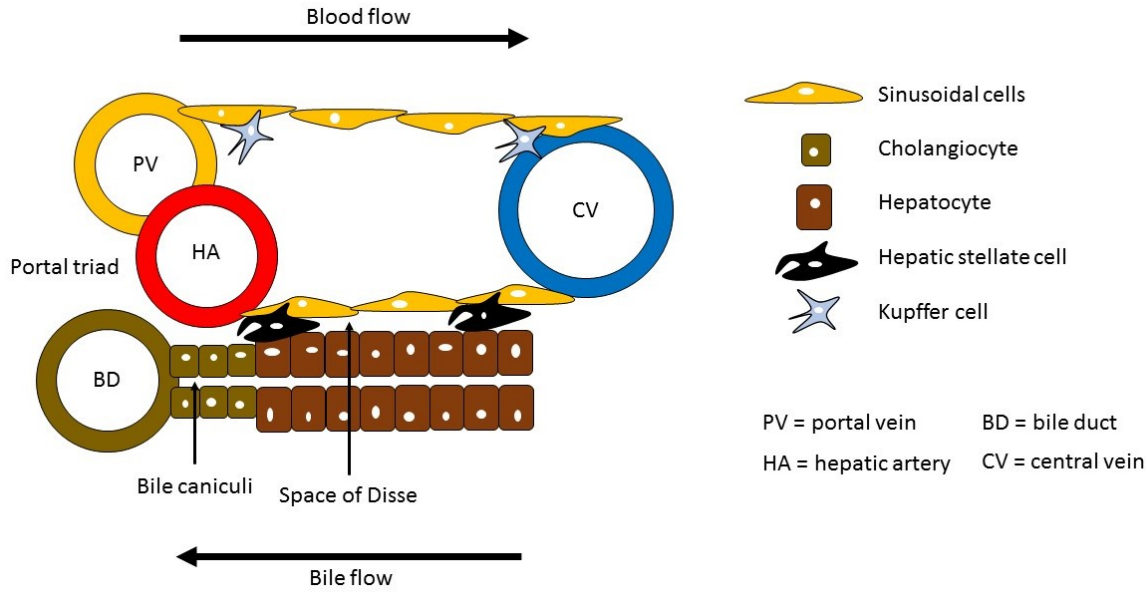


Figure 1.1: Liver architecture

Figure 1.1 depicts the human liver architecture, demonstrating the cellular arrangement and blood and bile flow. Adapted from Kang *et al.,* (Kang, Mars, & Michalopoulos, 2012).

The architecture of the human liver is arranged as many hexagonal-like hepatic lobules, where blood flows into the liver lobule from the portal triad (Figure 1.1 and Figure 1.2). Blood flows into the liver from the intestine, stomach, spleen and

pancreas *via* the portal vein, and from the heart *via* the hepatic artery. Blood flow leaves the liver through the central vein where it travels back to the heart (Malarkey et al., 2005) (Figure 1.1 and Figure 1.2). Bile flows in the opposite direction towards the portal triad; produced by the hepatocytes and leaves *via* the bile duct to the gall bladder (Malarkey et al., 2005) (Figure 1.1 and Figure 1.2). The hepatic lobule is split into 3 zones, (1) the outer periphery, or periportal zone, containing the portal triads, (2) the pericentral zone and (3) the inner transitional, or centilobular, zone (Figure 1.2). The periportal zone is associated with highest oxygen context, transitioning to the centrilobular zone, which is linked to the highest levels of metabolised xenobiotics and lowest oxygen levels (Kang et al., 2012; Malarkey et al., 2005).

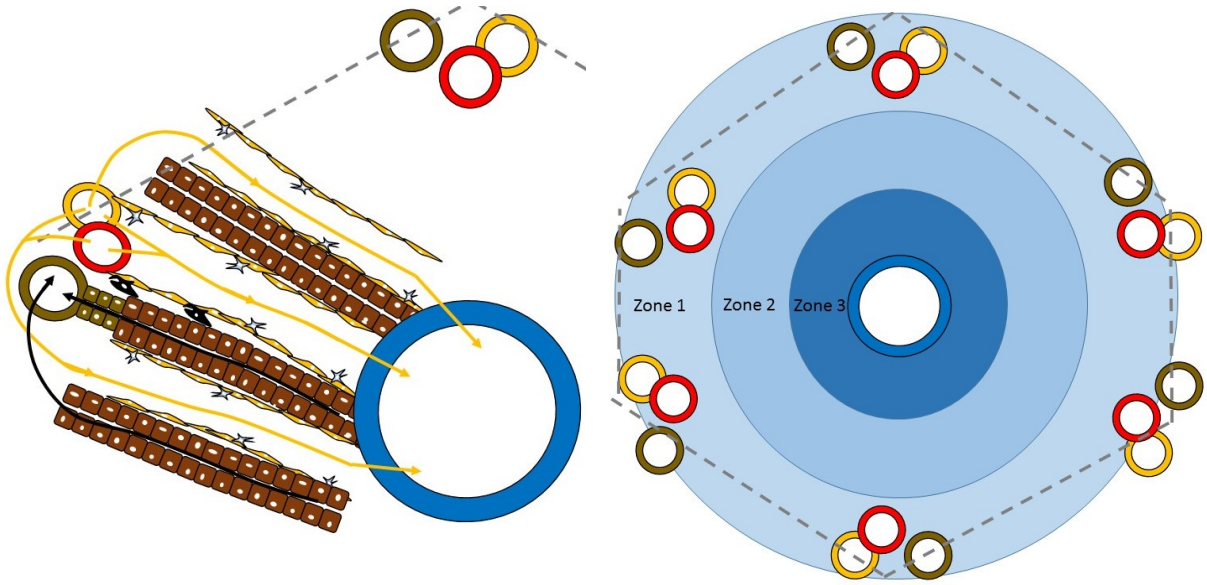


Figure 1.2: Hepatic lobule structure

Figure 1.2 demonstrates the layout of the human hepatic lobule structure as hexagonal units that repeat throughout the liver. In the left panel, blood flow and bile flow are represented using yellow and black arrows respectively. Adapted from Kang *et al.,* (Kang et al., 2012).

Xenobiotic biotransformation can be split into 3 distinct phases. Phase 1 metabolism refers to the creation of a functional group on a lipophilic xenobiotic (such as an

hydroxyl group by oxidation from cytochrome P450 monooxygenases (Cyps)), which allows the subsequent conjugation of a polar moiety (phase 2) (such as glucuronide formation by UDP-glucuronosyl transferases (Ugt)). Addition of the polar group increases the hydrophilicity of the xenobiotic for transport and excretion (phase 3) (by transporter proteins such as, organic anion transporter (Oat)) (B. D. Wallace & Redinbo, 2013).

1.1.2 In vitro toxicology testing

In order to interrogate the underlying molecular mechanism(s) of a chemical's potential for harm, one needs to investigate and characterise an appropriate *in vitro* model. Hepatic models will be discussed herein due to the hepatic effects of phenobarbital.

Cultured primary hepatocytes are the current gold standard for hepato-toxicology testing. However primary hepatocytes are unstable and rapidly lose their hepatic phenotype (within 48-72 hours of culturing) and data is not easily reproducible due to donor variation and health. Liver slices can be used but they are also subject to similar problems associated with primary cells (Soldatow, LeCluyse, Griffith, & Rusyn, 2013). Maintenance of the primary hepatocyte cell phenotype are reported to be improved through co-culture with additional cell types (Khetani, Szulgit, Del Rio, Barlow, & Bhatia, 2004) or by 3D spheroid culture (Chang & Hughes-Fulford, 2014) when compared to monolayer cultures. However, it remains difficult to maintain appropriate oxygen and nutrient flow in 3D cultures, which are key effectors of spheroid formation and hepatocyte differentiation (Nugraha et al., 2011; Soldatow et

al., 2013). One way to circumvent these hurdles is through the use of microfluidics based approaches. In systems such as this, hepatocytes can be cultured either as mono- or co-cultures, or even as spheroids, and cell medium with or without xenobiotics can be perfused over the cells producing a dynamic and zonal environment (Soldatow et al., 2013). Results demonstrate that the functional life span of primary hepatocytes can be improved with these methods (Legendre et al., 2013). It is thought that these above 3D methods improve upon primary cell mono-cultures due to the formation of cell polarity and inter cell contacts and communication, which is believed to be key in the pleiotropic functionality of hepatocytes (Decaens et al., 2008; Treyer & Musch, 2013).

Other more readily available cell systems have been extensively used to understand hepatic responses to chemical exposure such as immortalised human cells: HuH7 (Nakabayashi, Taketa, Miyano, Yamane, & Sato, 1982), HepG2 (Knowles, Howe, & Aden, 1980) and HepaRG (Gripon et al., 2002) cells. HuH7 cells are derived from a well differentiated hepatocellular carcinoma, which are Cyp450 inducible as demonstrated by increased enzyme activity of CYP2B6 and CYP3A4 when treated with PB or rifampicin respectively (Choi et al., 2014). HepG2 cells are human hepatoblastoma derived cells that are also Cyp450 inducible, and to a greater degree than Huh7 cells (Choi et al., 2014). HepG2 cells are useful in studying phase 1 (oxidative) detoxication of a parent compound but have lower metabolic capacity for the metabolites (phase II metabolism) (Gerets et al., 2012) and have been shown to exhibit altered phenotypic changes with increased passage (Soldatow et al., 2013). Equivalent hepatoma derived cells from the rat have also been used to understand xenobiotic metabolism, such as the Reuber H35 rat hepatoma derived:

Fao, 2sFou and C2Rev7 cells (Pitot, Peraino, Morse, & Potter, 1964; Reuber, 1961). These cell lines exhibit aldrin epoxidase activity in response to PB treatment (Wiebel, Kiefer, & Murdia, 1984), which is suggestive of Cyp2b activation (Khan et al., 1998). Increased Cyp2c6 mRNA has been reported in Fao cells after PB treatment (Shaw, Adesnik, Weiss, & Corcos, 1993) and Fao cells treated with benzo[b]fluoranthene also demonstrate increased Cyp1a activity (Alessandro Chiarolini, Maria Teresa, 1997). More recently the HepaRG cell line, a bipotent human hepatocellular carcinoma cell line, has been shown to display enhanced Cyp450 inducibility compared to HepG2 cells (Gerets et al., 2012). Upon reaching confluency, HepaRG cells differentiate into hepatocyte-like and biliary-like cells and express liver function genes such as phase I and II drug metabolising enzymes and the nuclear receptors, Car and Pxr. Treating HepaRG cells with 2% DMSO and hydrocortisone has been reported to further improve their liver-like functions (Gripon et al., 2002).

Hepatocytes or hepatocyte-like cells can be derived from stem cell populations, either from embryonic stem cells or from differentiated somatic cells as induced stem cells (Hu & Li, 2015). Induced pluripotent stem cells derived from differentiated cells allows expansion of patient specific cells for experimental manipulation (Lu et al., 2015). Yet thus far, stem-cell derived hepatocyte models do not exhibit the full complement of normal hepatocyte activity and in particular the full range and inducibility of Cyp enzyme functionality and are also subject to dedifferentiation problems as well as typically requiring complex culture media (Soldatow et al., 2013). However, unlike other stem-cell derived hepatocytes, the differentiated rat B13/H hepatocyte-like cells do express a range of inducible and constitutively expressed Cyp enzymes and have been demonstrated to act as a functional and

useful hepatic model (Philip M E Probert et al., 2014), and will be used herein as an *in vitro* model to assess responses to phenobarbital exposure.

1.2 Phenobarbital (PB)

Phenobarbital (PB) is a commonly prescribed antiepileptic drug that has been in use since its inception over 100 years ago (Brodie & Kwan, 2012). PB has a low cost-efficacy ratio and is recommended by the World Health Organisation as a first-line treatment in countries with low resources (Ilangaratne, Mannakkara, Bell, & Sander, 2012), demonstrating similar efficacy and tolerability as with other antiepileptic drugs such as phenytoin and carbamazepine (Brodie & Kwan, 2012). However, increased teratogenic effects have been reported in 1 year old infants whose mothers were treated with PB (≥150mg/day compared to <150mg/day). Teratogenic effects were also noted with other antiepileptic drugs and all treatments demonstrated increased probability of congenital abnormalities if there was a parental history of such malformations (Tomson et al., 2011).

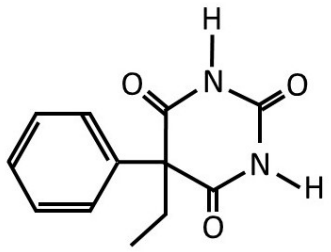


Figure 1.3: Structure of phenobarbital

Figure 1.3 shows the chemical structure of phenobarbital (PB).

PB is a lipophilic barbiturate (Figure 1.3), which exerts its antiepileptic effects through binding γ-aminobutyric acid (GABA) ion channels in the neocortex. Through PB binding to $GABA_A$ receptors, PB potentiates the neuro-suppressive effects of GABA by keeping the Cl^- channel open and hyperpolarising the postsynaptic neuron (Löscher & Rogawski, 2012). PB is also known to cause a myriad of phenotypic effects beyond its original therapeutic outcomes. These are

typically mediated by PB's interaction with the nuclear receptors, the constitutive androstane receptor (Car/Nr1i3) and the pregnane x receptor (Pxr/Nr1i2).

Nuclear receptors are ligand-activated transcription factors whose activation are controlled by lipophilic compounds, such as hormones and xenobiotics and are involved in a variety of biological processes. They consist of a variable N-terminal trans-activation domain with a DNA binding domain and a hinge region linked to the C-terminal ligand binding and trans-activation domain (AF2) (Aranda, Aranda, Pascual, & Pascual, 2001; Y. Kanno & Inouye, 2008). Car and Pxr belong to the Nr1i family of nuclear receptors, which, including the 1,25-$(OH)_2$-vitamin D3 receptor (Vdr/Nr1i1), are all functionally involved in regulating the expression of xenobiotic metabolising enzymes (Reschly & Krasowski, 2006). Car and Pxr control the expression of shared and unique genes involved in xenobiotic metabolism, as well as genes involved in apoptosis, inflammation and cell cycle control (Tojima et al., 2012; Ueda et al., 2002).

1.2.1 Car/Pxr functions

Exogenous activators & functions The synthetic steroid, pregnenolone 16α-carbonitrile (PCN) is an efficacious activator of mouse and rat Pxr (Kliewer et al., 1998) while the antibiotic rifampicin is an human Pxr activator (Y. Chen, Ferguson, Negishi, & Goldstein, 2004; Kliewer & Willson, 2002). PB is typically regarded as the prototypical indirect activator of Car, although Car is also activated by 1,4-Bis[2-(3,5-dichloropyridyloxy)]benzene (TCPOBOP) in the mouse (Omiecinski, Coslo, Chen, Laurenzana, & Peffer, 2011; Tzameli, Pissios, Schuetz, & Moore, 2000), and 6-(4-

chlorophenyl)imidazo[2,1-*b*][1,3]thiazole-5-carbaldehyde *O*-(3,4-dichlorobenzyl)oxime (CITCO) in humans (Maglich et al., 2003). Pxr possesses a large C-terminal ligand binding domain, which results in promiscuous activation by a variety of ligands. Whereas Car has a smaller repertoire of direct ligands due to a smaller ligand binding site, but can also be indirectly activated. Therefore Car/Pxr can be activated by, and induce the metabolism of, a wide range of chemicals (Honkakoski, Zelko, Sueyoshi, & Negishi, 1998; Omiecinski et al., 2011; Sueyoshi, Kawamoto, Zelko, Honkakoski, & Negishi, 1999; Suino et al., 2004). CAR/PXR induction of CYP2B6/3A4 (Lehmann et al., 1998; Sueyoshi et al., 1999) have been reported as involved in the metabolism of >50% of clinical drugs, highlighting the important role these nuclear receptors play in xenobiotic metabolism (Rendic, 2015).

Endogenous activators & functions The bile acid, lithocholic acid, is a Pxr agonist and increases expression of the bile acid metabolising enzyme, Cyp3a11, and inhibits the cholesterol metabolising (and bile acid synthesising) enzyme, Cyp7a1 (Staudinger et al., 2001). Increased bilirubin levels can also activate Car and Pxr resulting in the expression of genes involved in bilirubin metabolism (such as the carrier protein Slc12a6, which mediates bilirubin uptake, and Ugt1a1, which glucuronidates bilirubin) (Huang et al., 2003).

Other functions Acute activation of Car and Pxr is reported to induce transient increases in cell cycle genes, such as *cyclin A2*, *cyclin-dependent kinase 1* and *cyclin B2* (Luisier et al., 2014). Car and Pxr activation is also associated with decreased glucose levels due to reduced activity of gluconeogenic genes, such as

forkhead box O1 (*FoxO1*) (Kodama, Koike, Negishi, & Yamamoto, 2004). Car and Pxr have been shown to reduce adiposity through induction of *insulin induced gene 1*, which is involved in inhibiting the nuclear localisation of the lipogenic transcription factor, sterol regulatory element binding protein 1 (Roth et al., 2008). It has also been reported that Pxr and the immune and inflammatory mediator, nuclear factor-κB, regulate each other through a negative feedback loop (Zhou et al., 2006). Hence, as well as xenobiotic metabolism, Car and Pxr are also associated with bile acid and bilirubin metabolism, energy metabolism, regulation of adiposity and negative regulation of the immune response.

1.2.2 Car/Pxr activation

Coactivator binding Activated Car and Pxr form heterodimeric complexes with the retinoid x receptor α (Rxr) (Suino et al., 2004). Agonist activation and binding of Car/Pxr to Rxr *via* their ligand binding domain (Suino et al., 2004) is thought to stabilise subsequent binding of coactivators, such as steroid receptor co-activator-(Src-)3 (T. Chen et al., 2012). Coactivators bind to α-helix (H)12 (AF2) within the ligand binding domain of nuclear receptors (Dussault et al., 2002; Suino et al., 2004).

In the absence of a ligand, corepressors bind H3 of the nuclear receptor's ligand binding domain, *via* the repressor's receptor interaction domain. Repressors are displaced upon ligand binding due to a conformational change of AF2, which also aids coactivator binding (Dussault et al., 2002). Uniquely among nuclear receptors, Car demonstrates constitutive activity due to a short AF2 helix, which is stabilised by surrounding helixes, allowing coactivator binding in the absence of a bound ligand

(Dussault et al., 2002; Suino et al., 2004). Coactivator binding is thought to facilitate DNA binding (Dussault et al., 2002).

Car/Pxr DNA binding Car/Rxr bind response elements containing direct repeat- (DR)3, DR-4 and everted repeat- (ER)6 motifs, while Pxr/Rxr also bind DR-5, ER-8 and inverted repeat- (IR)6 motifs (Dawson & Xia, 2012). The repeat sequences typically consist of the consensus sequence, AG(G/T)TCA, followed by:

- a chronological repeat of this first consensus sequence (direct repeat),
- the reverse complement of the first consensus sequence (inverted repeat) or,
- the first sequence is the reverse complement of the consensus sequence, which is followed by the consensus sequence (everted repeat).

The 2 sequences are separated by 'n' nucleotides as indicated in each case. For example, DR-3 represents 2 direct repeating sequences separated by 3 nucleotides (Beaudet, Desrochers, Lachaud, & Anderson, 2005; Horie-Inoue, Bono, Okazaki, & Inoue, 2004; Y.-M. Wang, Ong, Chai, & Chen, 2012).

Cyp2b expression is often used as a marker of Car activation by PB (Honkakoski et al., 1998; Sueyoshi et al., 1999), and Cyp3a for Pxr (Kliewer et al., 1998; Lehmann et al., 1998); although both receptors have been reported to regulate both genes (B Goodwin, Moore, Stoltz, McKee, & Kliewer, 2001; Bryan Goodwin, Hodgson, D'Costa, Robertson, & Liddle, 2002). The mouse PB-inducible gene, *Cyp2b10,* has been shown to be regulated by an upstream enhancer sequence; the phenobarbital-responsive enhancer module (PBREM) (Honkakoski et al., 1998) (also known as the

PB-responsive enhancer unit; PBRU (Czekaj, 2000)). The PBREM contains a nuclear factor (NF)1 binding site, surrounded by DR-4 nuclear receptor binding sites: NR1 and NR2 and a 5' NR3 motif; of which, NR1 is conserved between the mouse, rat and human and thought to be the key component for PB-responsiveness (J. Kim, Min, & Kemper, 2001; Sueyoshi et al., 1999). Car/Rxr are thought to bind to the NR1 site within the PBREM to increase target gene expression (Honkakoski et al., 1998), as well as nuclear factor 1 protein binding, which potentiates Car/Rxr binding to NR2 (J. Kim et al., 2001).

Car cellular localisation Due to Car's constitutive activity, Car-mediated gene expression is controlled *via* its sequestration to the cytoplasm. Nuclear import of rat Car is dependent on a conserved C-terminal leucine rich peptide, the xenochemical response signal (XRS) (Zelko, Sueyoshi, Kawamoto, Moore, & Negishi, 2001), as well as nuclear localisation signals (NLS) 1 and 2, in the hinge region and ligand binding domain, respectively (Figure 1.4). While a cytoplasmic retention region (CRR) containing a nuclear export signal (NES) (NES2) within the ligand binding domain, and a second NES surrounding the XRS, are implicated in Car cytoplasmic localisation (Figure 1.4). Whereas for Pxr nuclear translocation it is reported that AF2, NLS and XRS are implicated (Y. Kanno et al., 2007; Y. Kanno, Suzuki, Nakahama, & Inouye, 2005).

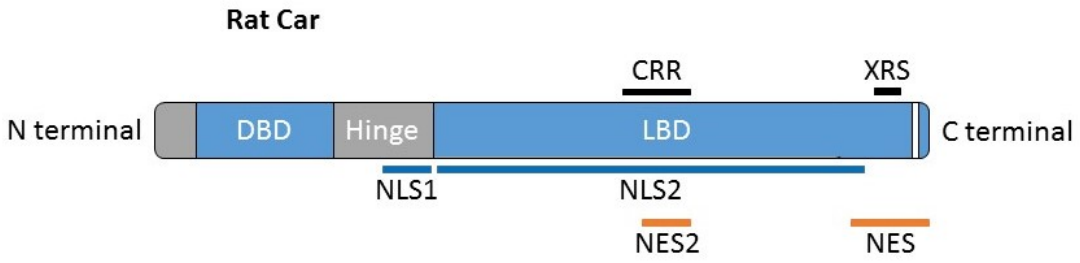


Figure 1.4: Rat Car - linear structure

Figure 1.4 shows the linear structure of rat Car, with domains reported to be important in cellular localisation labelled. The activation helix, H12/AF2, is shown as a white bar. Adapted from Suino *et al.,* (Suino et al., 2004) Kanno *et al.,* (Y. Kanno et al., 2007). Abbreviations: DBD, DNA binding domain; LBD, ligand binding domain; CRR, cytoplasmic retention region; XRS, xenochemical response signal; NLS, nuclear localisation signal; NES, nuclear export signal.

1.2.3 PB-mediated indirect activation of Car

Mutoh *et al.,*(Mutoh et al., 2013) demonstrated in the mouse that PB indirectly activates Car by binding and inhibiting the epidermal growth factor receptor (Egfr), decreasing phosphorylation of the receptor Tyrosine^{845} and Tyrosine^{1173} residues, and therefore decreasing phosphorylation of receptor for activated C kinase 1 (Rack1), on Tyrosine^{52}. De-phosphorylated Rack1 forms a complex with Car and the catalytic subunit of protein phosphatase 2A (Pp2ac) to stimulate de-phosphorylation of Car-Threonine^{38} (Figure 1.5). Hosseinpour *et al.,*(Hosseinpour, Moore, Negishi, & Sueyoshi, 2006) also identified Serine^{202} as a key residue in the de-phosphorylation and subsequent nuclear translocation of mouse Car.

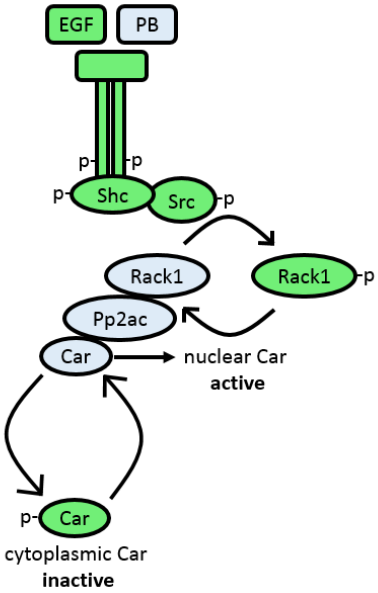


Figure 1.5: Indirect activation of Car in the mouse

Figure 1.5 depicts the proposed indirect activation of Car by PB in the mouse *via* antagonism of the Egfr. Adapted from (Mutoh et al., 2013)

Under normal conditions Car is retained in the cytosol by cytoplasmic Car retention protein (Ccrp), which also aids recruitment of heat shock protein 90 (Hsp90) (Kobayashi, Sueyoshi, Inoue, Moore, & Negishi, 2003). Treatment-induced de-phosphorylation and nuclear translocation of Car is dependent on an intact microtubular network (Y. Kanno, Miyama, Ando, & Inouye, 2009) as well as cytosolic proteins such as Hsp90 (Yoshinari, Kobayashi, Moore, Kawamoto, & Negishi, 2003) and Rack1 (Mutoh et al., 2013), which aid in Pp2ac recruitment and de-phosphorylation of Car. Oligomerisation of the membrane bound subunit of protein phosphatase 1 (Ppp1r16a) and its association with Car have also been implicated in the nuclear receptor's translocation into the nucleus (Sueyoshi, Moore, Sugatani, & Matsumura, 2008). Translocation into the nucleus is reported to be *via* a Ran-GTPase and importin 13-dependent process potentially through interactions with Car's NLS2 domain (Y. Kanno, Miyazaki, & Inouye, 2010).

Other kinases such as cAMP-dependent protein kinase, mitogen-activated protein kinase kinase (Mek)1/2, protein kinase c and extracellular regulated mitogen-activated kinase (Erk) have been reported as negative regulators of PB-mediated gene transcription (F Joannard, Galisteo, Corcos, Guillouzo, & Lagadic-Gossmann, 2000; Kawamura, Yoshida, Kimura, Oda, & Kakinuma, 1999; Koike, Moore, &

Negishi, 2007; Osabe & Negishi, 2011), while Ca^{2+}/calmodulin-dependent protein kinase II has been reported as an enhancer of PB-mediated gene expression (Pustylnyak et al., 2005). Furthermore, Rencurel *et al.,*(Rencurel et al., 2005) showed that in the HepG2 cell derivative, WGA cells, dominant negative AMP-activated protein kinase (AMPK) mutant cells exhibited reduced PB-mediated Cyp induction, and that PB (2.5mM) activated AMPK through reduced ATP levels in human WGA cells and rat primary hepatocytes. PB mediated increase in AMPK activity was also demonstrated *in vivo* for the mouse and rat (Shindo, Numazawa, & Yoshida, 2007). It has been proposed that PB-mediated AMPK activation is through the upstream kinase, LKB1 (Blättler, Rencurel, Kaufmann, & Meyer, 2007), which is proposed as a putative target of miR-122, a microRNA (miRNA) shown to be reduced by PB (100mg/kg) *in vivo* (Shizu, Shindo, Yoshida, & Numazawa, 2012), as a result of Car-mediated inhibition of hepatocyte nuclear factor 4α (Hnf-4α/Nr2a1) (Kazantseva, Yarushkin, Mostovich, Pustylnyak, & Pustylnyak, 2015). Dominant negative AMPK was also shown to reduce activity from the Car binding site, NR1 (Rencurel et al., 2005). Furthermore, Pascussi *et al.,* (Pascussi, Gerbal-Chaloin, Fabre, Maurel, & Vilarem, 2000) demonstrated that dexamethasone-mediated (100nM) nuclear translocation of Car did not induce CYP2B6, suggesting other nuclear activities are required for full activation. Taken together these data suggest that, once Car is in the nucleus, AMPK may mediate NR1 site binding of Car for full activation, which is further indicated by the fact that AMPK activation alone is not sufficient for PB induced gene expression (Shindo et al., 2007). However, AMPK-mediated inhibition of Car target genes has also been demonstrated by others (H. Yang et al., 2014), which complicates the interpretation of such data.

1.2.4 PB is non-genotoxic

The hallmarks of a non-genotoxic carcinogen include the ability to cause cancer without directly damaging DNA (Hernández, van Steeg, Luijten, & van Benthem, 2009), and has been reported to be through diverse mechanisms such as endocrine modification, tumour promotion, inflammation, and epigenetic carcinogenesis (Hernández et al., 2009; Williams & Whysner, 1996). Epigenetics is defined as the adaptation of chromosomal arrangement to initiate or potentiate activity state, such as by DNA methylation (Bird, 2007). The DNA methyl modification, 5-methylcytosine, is found on the cytosine of cytosine–guanine pairs. Typically, gene promoters that are extensively methylated are associated with transcriptional silencing. This is thought to be due to recruitment of proteins, which bind the methylated sites and, in conjunction with other proteins, compact the chromatin and inhibit transcription. Whereas the de-methylated intermediate, 5-hydroxymethylcytosine, is associated with enhancer regions and transcription start sites of actively transcribed genes (Thomson, Moggs, Wolf, & Meehan, 2013). MicroRNAs add to the complexity of epigenetic regulation through post-transcriptional and post-translational regulation of gene expression, and will be discussed later (Malumbres, 2012).

Testing compounds for carcinogenic potential requires 2 approaches. The first is an assessment of the chemical as a genotoxin, a DNA reactive chemical, for example benzo[a]pyrene (Ling et al., 2004), in assays such as the Ames test (Ames, McCann, & Yamasaki, 1975). The second is an assessment of the chemical as a non-genotoxic carcinogen. As mentioned above, non-genotoxic carcinogens are typically thought to cause cancer without damaging DNA. Due to these indirect methods of

carcinogenesis, genotoxicity assays do not positively identify such compounds. Therefore, the gold standard test for non-genotoxic chemicals requires treatment with the chemical of animals in a lifetime bioassay (Boobis et al., 2009). PB does not directly damage DNA, but when given to rodents after a DNA damaging event in a lifetime bioassay, does promote the progression of hepatic tumours and as such is a non-genotoxic carcinogen.

PB is widely used as a model non-genotoxic carcinogen in rodents, whereby PB acts as a tumour promoter in the rat (Butler, 1978; Hagiwara et al., 1999), and induces hepatocellular carcinomas in mice predisposed to tumours, such as C3H and B6C3F, while C57BL appear resistant (Becker, 1982). Due to the different sensitivities of rats and mice, tumour promotion studies are often conducted with PB following a DNA damaging compound, such as *N*-diethylnitrosamine (DEN), which when given to mice at 6 weeks of age will increase tumour burden with PB compared to DEN alone (Braeuning, 2013). However, PB is not reported to cause cancer in humans (Elcombe et al., 2014) and is currently classified as a class 2B carcinogen; possibly carcinogenic to humans (Braeuning, 2014).

Using genetic mouse models, research groups have tried to determine the relevance of PB as a human carcinogen. Wildtype and humanised Car/Pxr C57BL/6J mice treated with PB (80mg/kg/day) by intraperitoneal injection for 4 days showed that the PB treated humanised mice did not present with hyperplasia as seen in the wildtype mice (Ross et al., 2010). However, Luisier *et al.,* (Luisier et al., 2014) demonstrated in the same model that PB treatment (0.05% w/v in drinking water) does induce

hyperplasia in humanised mice. This dose is roughly equivalent to 87mg/kg/day (0.05% w/v corresponds to 500mg/L, and the daily dose was subsequently calculated using a dose conversion factor for a subacute study with male mice; 0.174, as determined by the European Food Safety Authority (Antunović et al., 2011)) therefore suggesting that the disparity could be an issue of dose method. Furthermore, the authors show that the transcriptomic profile is similar between wildtype and humanised mice (Luisier et al., 2014). It has also been demonstrated that using the same strains, humanised Car/Pxr mice do develop tumours when treated with DEN (single intraperitoneal injection at 90mg/kg body weight) for 1 week followed by dietary PB (0.05% w/v) for 40 weeks, albeit at a lower tumour burden than in wildtype mice with the same treatment (Braeuning et al., 2014). These data suggest that rodent and human Car are capable of inducing tumours, but that receptor activity also needs to be considered in the context of other factors beyond the receptor. This is corroborated by Yamada *et al.,* (Yamada et al., 2014) who demonstrate that chimeric CD1 mice with human hepatocytes do not show PB-mediated hyperplasia (up to 1500 parts per million (ppm) for 7 days).

1.2.5 PB-mediated tumourigenesis

Acute PB exposure Treatment with PB is associated with a myriad of molecular and physiological changes in the liver. PB is a prototypical Cyp2b inducer *via* indirect activation of Car (Honkakoski et al., 1998; Sueyoshi et al., 1999) and Pxr (B Goodwin et al., 2001). PB induces adaptive hepatic responses, consolidated as hepatomegaly – liver enlargement (P. Carthew, Edwards, & Nolan, 1998; Waterman et al., 2010). In the rat, PB induces compensatory transient hyperplasia during the first 3 days of treatment (Waterman et al., 2010), which is associated with increased

Car activation and enhanced by concomitant Pxr activation (Shizu et al., 2013), followed by reversible hepatocyte hypertrophy (Isenberg et al., 2001). Within the first 7 days of PB treatment there is an increase in growth factor expression in mice (Orton, Doughty, Kalinowski, Lord, & Wadsworth, 1996) and rats (Lindroos, Tsai, Zarnegar, & Michalopoulos, 1992), which are thought to be involved in mediating PB-induced transient hyperplasia. Activation of Car is also associated with cell cycle progression (Osabe et al., 2008), and expression of cell cycle genes (Luisier et al., 2014; Waterman et al., 2010). The induction of the transcription factor myelocytomatosis oncogene (c-Myc) in mice (Blanco-Bose et al., 2008) and transient hypermethylation in the promoter region of the tumour suppressor gene *cyclin-dependent kinase inhibitor 2A* (*p16*) in the rat (Kostka, Urbanek, & Ludwicki, 2007) and decreased miR-199a-3p (Koufaris, 2011) have also been suggested as contributing to this proliferative response. Typically more than 7 days treatment with PB has been shown to reduce responsiveness to growth factors in both the mouse (Fletcher, Orton, Chipman, & Strain, 1997) and rat (Tsai & Michalopoulos, 1991; Tsai, Zarnegar, & Michalopoulos, 1991) potentially due to the phenotypic switch from hyperplasia to mitoinhibition (Fletcher et al., 1997).

Chronic PB exposure It has been demonstrated in mice that chronic activation of Car is necessary for PB-induced tumours (Figure 1.6), potentially through upregulation of Mdm2 and inhibition of p53-mediated apoptosis (Huang et al., 2005; Yukio Yamamoto, Moore, Goldsworthy, Negishi, & Maronpot, 2004) and growth arrest and DNA-damage-inducible 45β- (Gadd45β) induced inhibition of apoptosis (Y Yamamoto & Negishi, 2008). Furthermore, several other signalling components have been identified as pertinent to the tumour promoting effects of PB. It has been

demonstrated in DEN/PB studies that PB promotes the growth of β-catenin activated tumours (Aydinlik, Nguyen, Moennikes, Buchmann, & Schwarz, 2001) (Figure 1.6) and that deletion of β-catenin results in loss of PB-induced tumours in the mouse (Rignall, Braeuning, Buchmann, & Schwarz, 2011). PB is known to interfere with gap-junction signalling, which is thought to promote neoplastic cell growth due to the impaired signalling. In fact, loss of connexin 32 suppresses PB-mediated tumour promotion, suggesting PB requires functional gap-junction signalling to induce tumours (Moennikes et al., 2000) (Figure 1.6). A comprehensive analysis of the liver methylome of PB-treated mice has shown that the level and type of methylation induced by long-term PB treatment are associated with sensitivity to PB-induced tumours in the mouse, as well as altered gene expression (Phillips, Burgoon, & Goodman, 2009; Phillips, Yamamoto, Negishi, Maronpot, & Goodman, 2007; Thomson et al., 2012; Thomson, Hunter, et al., 2013) (Figure 1.6).

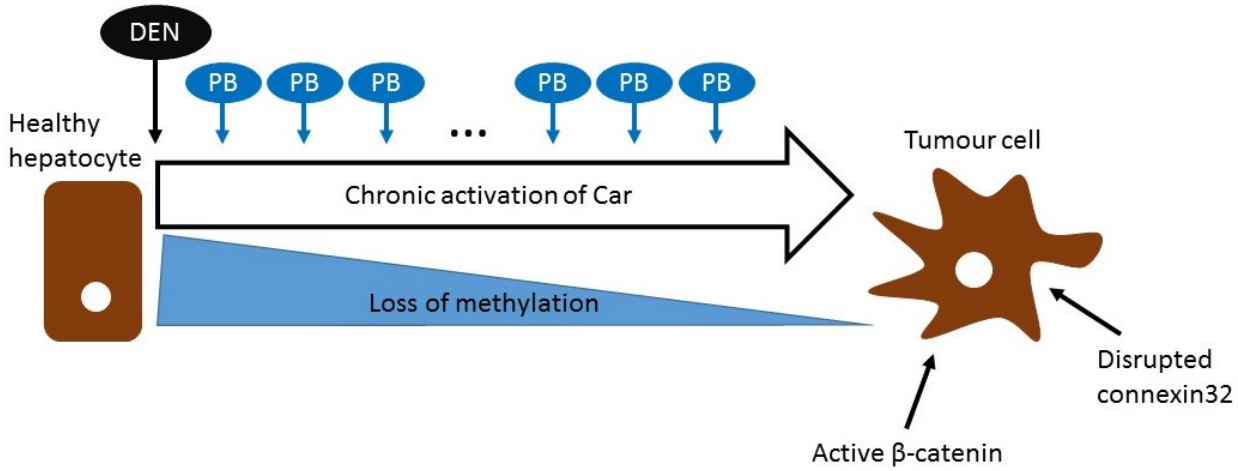


Figure 1.6: PB-mediated tumourigenesis in the mouse

Figure 1.6 Depicts key molecular markers and components of PB-induced tumourigenesis in the mouse, as described in text.

Recent work has demonstrated that chronic exposure to PB also induces time- and dose-dependent changes in rat (Koufaris, Wright, Currie, & Gooderham, 2012; Koufaris, Wright, Osborne, Currie, & Gooderham, 2013) and mice miRNAomes (Lempiäinen et al., 2013).

1.3 microRNAs

The first miRNA to be discovered was lin-4 in *Caenorhabditis elegans* (R. C. Lee, Feinbaum, & Ambros, 1993), and was initially dismissed as a component of *C.elegan*s genetics that was unrelated to other organisms. However, since then it has been established that miRNAs play an important role in gene regulation; being predicted to target >50% of human genes, as well as having been identified as biomarkers of different cancers, and a multitude of other diseases and even as therapeutic treatments (reviewed in Doxakis, (Doxakis, 2013) and Zhang *et al.,* (B. Zhang, Pan, Cobb, & Anderson, 2007)).

1.3.1 Biogenesis

MiRNAs are found in the introns and exons of genes, where they are processed in tandem with the mRNA (Rodriguez, Griffiths-Jones, Ashurst, & Bradley, 2004), or miRNAs are found in intergenic regions being controlled by their own promoter (Saini, Griffiths-Jones, & Enright, 2007). MiRNAs can be transcribed as single units (monocytronic) or in clusters (polycistronic) (reviewed in (Doxakis, 2013).

Mammalian miRNAs are transcribed by DNA polymerase II into primary-miRNA (pri-miRNA) transcripts, which are 3' poly-adenylated and 5' 7-methyl guanosine capped, forming hairpin secondary structures (Y. Lee et al., 2004) (Figure 1.7). Flanking pri-miRNA nucleotides are cleaved to form the hairpin precursor-miRNA (pre-miRNA) containing a 2 nucleotide 3' overhang, by the RNase III endonuclease Drosha, with the RNA binding protein Pasha (also known as DGCR8) (Han et al., 2004; Y. Lee et al., 2003) (Figure 1.7), and RNA helicases, dead box helicase- (DDX-)5 and DDX17 and tumour suppressor, breast cancer 1, early onset (Kawai & Amano, 2012). Pre-miRNAs can also be produced from the introns of mRNAs (Y.-K. Kim & Kim, 2007). After pre-miRNA processing, the nucleo-cytoplasmic receptor, Exportin-5, transports the pre-miRNA into the cytoplasm (Figure 1.7) through an interaction with the pre-miRNA's 3' overhang, in a Ran-GTP dependent process (Yi, Qin, Macara, & Cullen, 2003). Once in the cytoplasm, the pre-miRNA is bound by the miRNA loading complex (miRLC) comprising Argonaute2 (Ago2) (also known as eIF2C2), and other proteins, including the RNase III endonuclease, Dicer, and trans-activating response RNA-binding protein (Maniataki & Mourelatos, 2005) (Figure 1.7). Dicer recognises the 3' overhang of the pre-miRNA *via* Dicer's PAZ (PIWI-AGO-Zwille) domain and cleaves ~22 base pairs (bp) from this site (Vermeulen et al., 2005). The miRNA is unwound and the guide strand is selected by Ago2, and the passenger strand is discarded. Generally, in the duplex the strand with lowest thermodynamic stability at its 5' terminus is selected as the guide strand, which results in either retention of the 5' end of the miRNA (miR-5p) or the 3' end (miR-3p) (Schwarz et al., 2003) (Figure 1.7). It is thought that once the mature miRNA (guide strand) is selected, the accessory proteins dissociate leaving the miRNA and Ago2 as the functional RNA induced silencing complex (RISC) (Maniataki & Mourelatos, 2005). Ago2 secures the

miRNA seed sequence (discussed below) *via* an interaction with the miRNA 5' terminus and the protein's Mid domain, thereby exposing the seed region of the mature miRNA to enable target interactions (Lambert, Gu, & Zahler, 2011).

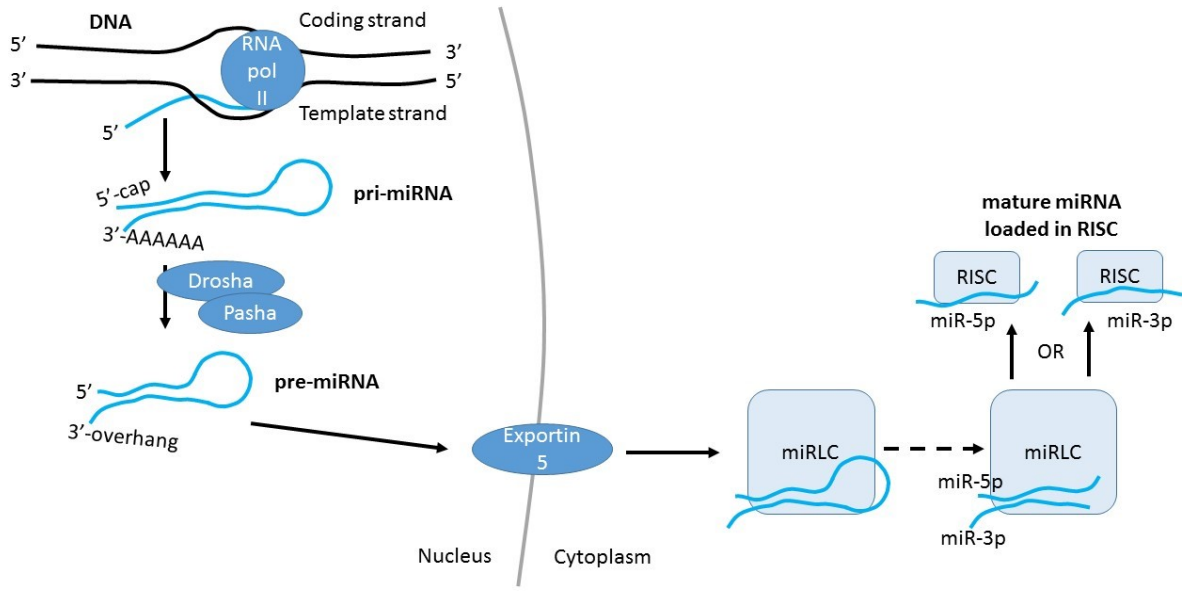


Figure 1.7: MiRNA biogenesis

Figure 1.7: depicts the pathway for miRNA biogenesis and formation of RISC as described in text.

1.3.2 Activity/Function

The mature miRNA transcript is approximately 22 nucleotides long and has a functional region known as the seed sequence in the 5' terminal end of the miRNA, which exhibits homology to the mRNA target. The seed sequence can be between residues 2-7 (known as a 6mer site match to the mRNA) or 2-8 (known as a 7mer or 7mer-m8 site match to the mRNA). Sequence complementarity as an extension of the seed sequence is also thought to influence miRNA-mRNA target interactions if the miRNA possesses a matching adenosine in the position of the first nucleotide, (therefore between nucleotides 1-7 of the miRNA; known as a 7mer-A1 site match of

the mRNA), or if the miRNA contains both matching residues in positions 1 and 8 (known as an 8mer site match of the mRNA) (B. Lewis, Burge, & Bartel, 2005).

MiRNAs silence gene expression based on the level of complementation between the miRNA seed sequence and its mRNA target, resulting in either mRNA target degradation or translation inhibition. It is still not fully understood what the mechanisms are that control these two outcomes, but it appears to be highly context specific and dependent on the diversity and proximity of miRNA binding sites (Doench & Sharp, 2004; Grimson et al., 2007). MiRNAs have been shown to target the mRNA within the 3'-untranslated region (UTR), as well as with the 5'-UTR (I. Lee et al., 2009), and introns (Tan et al., 2007).

Typically, it is thought that complete sequence complementarity mediates Ago-induced cleavage of the mRNA, while mismatches induces translation suppression (discussed in (R. W. Carthew & Sontheimer, 2009)). MiRNA target degradation or translation suppression is dependent on the recruitment of deadenylase and decapping complexes to the RISC *via* Ago interaction with the GW182 (TNRC6A-C) protein, and that the final outcome may also be dependent on which proteins are recruited (Behm-Ansmant, Rehwinkel, & Izaurralde, 2006).

MiRNA down-stream regulation is becoming increasingly complex; with the ability of miRNAs to regulate gene expression of the parent cell, but also the secretion of miRNAs to act in inter-cellular communication as evidenced by the presence of miRNAs in many biological fluids (Boon & Vickers, 2013), the ability of miRNAs to

act as toll-like receptor ligands or “hormone miRNAs” (Fabbri, 2012), and even potentially cross-kingdom associations (L. Zhang et al., 2012). The roles of miRNAs are further complicated by the observation that RNAs can act as competing factors, pseudo-targets, to mediate miRNA function and availability, known as competing endogenous RNAs (ceRNAs) (Salmena, Poliseno, Tay, Kats, & Pandolfi, 2011). It has been suggested that microRNAs provide robustness to biological systems – the ability to maintain appropriate function when under intrinsic or extrinsic stresses (Ebert & Sharp, 2012).

1.4 Concluding statements

This thesis is concerned with understanding the toxicity of PB *in vivo* and developing *in vitro* models to assess the mechanisms of toxicity. Furthermore, as the rat model is reported to be resistant to PB-induced tumourigenesis, when PB is treated in the absence of a DNA damaging compound, this thesis attempts to establish to what extent PB-inducible miRNAs *in vivo* impart robustness and maintenance of homeostasis, with a focus on miR-182/96.

1.5 Hypothesis

I hypothesise that the rat hepatocyte-like, B13/H, cell system can provide robust mechanistic insights into the PB phenotype. Additionally, that the regulation and function of PB-induced miRNAs can be explored using *in vivo* samples, and provide context-specific relationships relevant to chronic PB exposure.

1.6 Aims

1. Characterise the B13/H cell line and its response to PB and PB-like compounds.
2. Explore the interaction with PB and growth factor signalling *in vitro* and *in vivo*.
3. Identify potential regulators of PB-induced miRNAs *in vivo*.
4. Elucidate the potential function of PB-induced miRNAs *in vivo*.

2. Characterising rat hepatocyte-like AR42J-B13/H cells as an in vitro model for phenobarbital treatment

2.1 Introduction

In this chapter I will evaluate the hepatocyte-like AR42J-B13/H (B13/H) cell as a model to characterise the *in vitro* effect of phenobarbital (PB) treatment.

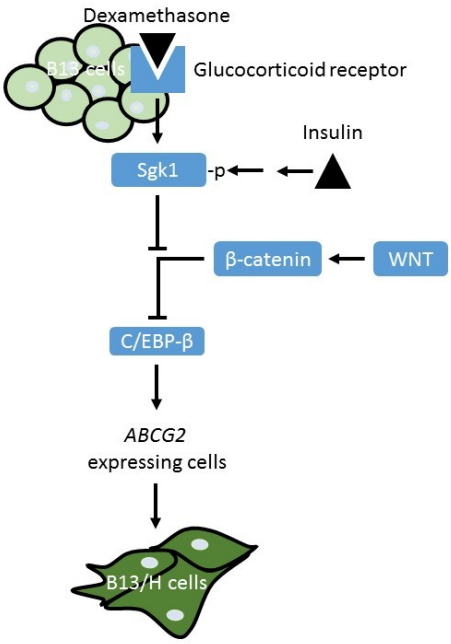
2.1.1 The rat AR42J-B13/H (B13/H) cell model - origin

Wistar/Lewis rats were treated with azaserine (*O*-diazoacetyl-L-serine) to generate pancreatic tumour cells, which were subsequently harvested to form the acinar derived pancreatic adenocarcinoma AR42J cell line (Longnecker, Lilja, French, Kuhlmann, & Noll, 1979). Azaserine is a pancreatic carcinogen with potent DNA adduct forming abilities. AR42J cells possess exocrine and neuroendocrine properties and treatment with activin A plus betacellulin will convert approximately 10% of cells from amylase production to insulin production (Hirosato Mashima et al., 1996). This was also noted when AR42J cells were treated with activin A plus Hgf, and it is from this sub-population of cells that the AR42J-B13 (B13) cell line originated (H Mashima, Shibata, Mine, & Kojima, 1996). The switch to insulin producing β-cells is thought to be due to activation of neurogenin 3 and downstream transcription factors Nkx6.1 or MafA (Akinci, Banga, Greder, Dutton, & Slack, 2012; Ogihara et al., 2008).

2.1.2 The rat AR42J-B13/H (B13/H) cell model - differentiation

It has been demonstrated *in vivo* that the pancreas can develop hepatic-like foci, for example as noted in Fisher rats following 60-72 weeks ciprofibrate treatment (Reddy et al., 1984), as well as after glucocorticoid treatment of Sprague-Dawley rats for 25 days (K. Wallace, Marek, Currie, & Wright, 2009). This differentiation was also shown in B13 cells. Shen *et al.,* (Shen, Slack, & Tosh, 2000) were able to demonstrate that B13 exocrine-like cells transdifferentiated into hepatocyte-like cells, AR42J-B13/H (B13/H), upon stimulation with 10nM dexamethasone for 2 weeks. The differentiated B13/H cells are no longer proliferative and display phenotypic and molecular markers of hepatocytes (Philip M. E. Probert et al., 2015).

The current dogma is that the differentiation of B13/H cells is through dexamethasone-mediated activation of the glucocorticoid receptor and increased expression of the serine/threonine protein kinase serum- and glucocorticoid-regulated kinase 1 (Sgk1), which when activated, phosphorylates and reduces the total levels of cellular β-catenin. Reduced levels of β-catenin transiently suppresses downstream components of WNT signalling, which results in activation of the transcription factor CCAAT enhancer binding protein-β (C/EBP-β) (Shen et al., 2000; K. Wallace, Long, Fairhall, Charlton, & Wright, 2011; K. Wallace, Marek, Hoppler, & Wright, 2010), followed by activation of Hnf-4α and phenotypic change of the cell towards an hepatic fate (Z. D. Burke, Shen, Ralphs, & Tosh, 2006). Furthermore, endogenous expression of insulin in B13 cells through activation of the Pi3k/Akt pathway augments the transdifferentiation of B13 to B13/H cells (Wu et al., 2010). This is likely the stimulus for activation of Sgk1 described by Wallace *et al.,* due to



the sensitivity of Sgk1 phosphorylation to the Pi3k inhibitor, LY294002 (K. Wallace et al., 2011) (Figure 2.1) .

Figure 2.1: Dexamethasone-mediated differentiation of B13 cells

Figure 2.1 shows the proposed molecular pathway controlling dexamethasone-mediated differentiation of B13 cells to hepatocyte-like B13/H cells (Shen et al., 2000; K. Wallace et al., 2011; K. Wallace, Marek, et al., 2010; Wu et al., 2010).

Furthermore, the Shen group later demonstrated that during transdifferentiation an intermediate cell type is generated, which express the stem/progenitor cell marker ABCG2 (Wu et al., 2010). Treatment with oncostatin M has been shown to improve the differentiated phenotype (Shen et al., 2000).

Expression of hepatocyte markers has been extensively studied in B13/H cells, whereby B13 cell markers amylase, synaptophysin, and neurofilament were suppressed, albumin is secreted and Cyp2e1, 3a1, 2b1, 7a1 and UGT (Z. D. Burke et al., 2006) and the hepatocyte marker transferrin, as well as ductal cell markers cytokeratin 7 and 19 are expressed (Al-Adsani et al., 2010). Further studies have demonstrated functional increases in phase I and II xenobiotic metabolism enzymes and drug transporter genes highlighting this model as a useful system to study chemical exposure (Marek, Cameron, Elrick, Hawksworth, & Wright, 2003; Philip M E Probert et al., 2014; Philip M. E. Probert et al., 2015).

2.1.3 Hypothesis

That the AR42J-B13/H cell line can be used as an *in vitro* tool to further understand and mechanistically test cellular responses to phenobarbital treatment.

2.1.4 Aims

1. Characterising the differentiation of AR42J-B13 (B13) to hepatocyte-like AR42J-B13/H (B13/H) cells in response to dexamethasone.
2. Assess the B13/H cell response to PB and PB-like compounds.
3. Explore the effect of PB and PB-like compounds on miRNA expression in B13/H cells.

2.2 Methods

2.2.1 Cell culture

Unless stated otherwise, all cell culture consumables were bought from Life Technologies, Gibco & Invitrogen (Paisley, UK). All cell culture consumables and chemicals were sterile filtered or autoclaved before use. Rat pancreatic progenitor AR42J-B13 cells (B13) were a gift from Professor Matthew Wright (Newcastle University). Rat pancreatic progenitor B13 cells were cultured in standard conditions with GIBCO low glucose (1g/L) Dulbecco's Modified Eagle Medium and 10% foetal bovine serum (FBS), with L-glutamine (233.6µg/mL) and antibiotics, penicillin (80Units/mL) and streptomycin (80µg/mL). Rat pancreatic B13 cells were treated with dexamethasone (10nM) (Sigma-Aldrich, Dorset, UK) for 13 days, with media changes every 3-4 days to stimulate differentiation into hepatocyte-like (B13/H) cells (Shen et al., 2000). Dexamethasone was removed from the culture media for 24 hours after 13 days continuous differentiation to control for potential confounding effects on Cyp2b (Audet-Walsh & Anderson, 2009). Undifferentiated B13 cells were maintained by trypsinization and subculture. Trypsin (0.25%) was used to detach cells, and an equal volume of serum-containing media to inactivate the trypsin. Seeding densities and treatments are detailed in the following sections. Cell culture plastics were purchased from Corning (NY, USA).

2.2.2 Cyp450 enzyme activity - PROD

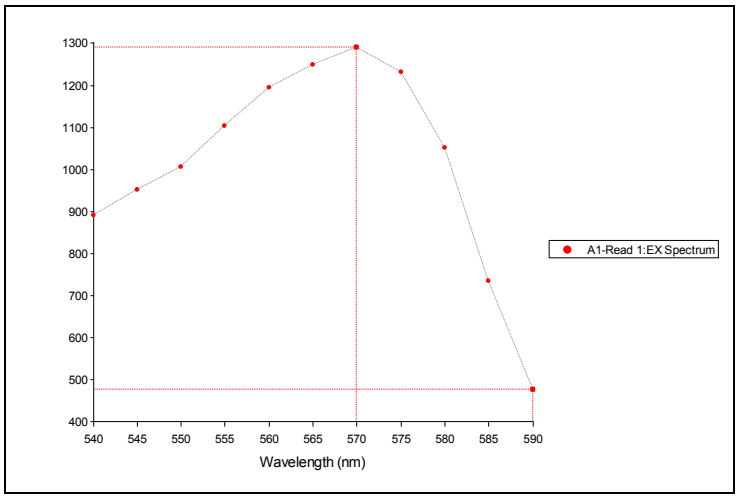
All compounds used for PROD were purchased from Sigma-Aldrich (Dorset, UK), unless stated otherwise. To assess drug metabolising competency of the cell culture model, activity was assessed by the pentoxyresorufin-*O*-dealkylase (PROD) assay,

which is catalysed mainly by Cyp2b1/2, but also 2c11, Cyp26 and Cyp3a2 (M. Burke, Thompson, Weaver, Wolf, & Mayer, 1994; Langouët et al., 1997). B13 cells were seeded at $2x10^4$ cells per well in 24-well plates and differentiated to B13/H cells as described above. B13/H cells were treated with phenobarbital-sodium (PB) (BDH Chemicals Ltd, UK) (solvated in media), benzophenone (BP) (Alfa Aesar, Lancashire, UK) (solvated in dimethyl sulfoxide [DMSO]), clotrimazole (solvated in ethanol), or 1,4-Bis[2-(3,5-dichloropyridyloxy)]benzene (TCPOBOP) (solvated in DMSO) for 1, 2, 3, 7 and 9 days. After treatments, cells were washed in serum-free media as assay activity is maintained at higher levels with cells in serum-free media (Hammond & Fry, 1992). Rat liver aroclor induced S9 (40µg) was used as a positive control for PROD. The PROD assay controls were run in a buffer containing Tris HCl (100mM), nicotinamide adenine dinucleotide phosphate (NADPH) (500µM), glucose-6-phosphate (10mM), magnesium chloride ($MgCl_2$) (2mM) and glucose-6-phosphate-dehydrogenase (3 units) (based on (D. M. Burke & Mayer, 1974), whereas samples were run in serum-free media.

A Synergy H1 Hybrid plate reader and Gen5 Data Analysis Software (BioTek, Swindon, UK) were used to collect data with optimized excitation (λ565nm) and emission (λ590nm) wavelengths (Figure 2.2) to measure the production of resorufin from the pentoxyresorufin substrate (Figure 2.3 A). The assay was started by adding pentoxyresorufin (resorufin pentyl ether, final concentration of 6µM). It should be noted that Cyp450 activity might be underestimated in this assay due to potential incomplete pentoxyresorufin uptake into the cells, as well as phase 2 conjugation of resorufin resulting in a reduced fluorescence signal, such as through the activity of

glucuronidation and sulphation enzymes, which are reported to be highly expressed in the B13/H cells (Philip M. E. Probert et al., 2015).

Excitation wave length



Emission wave length

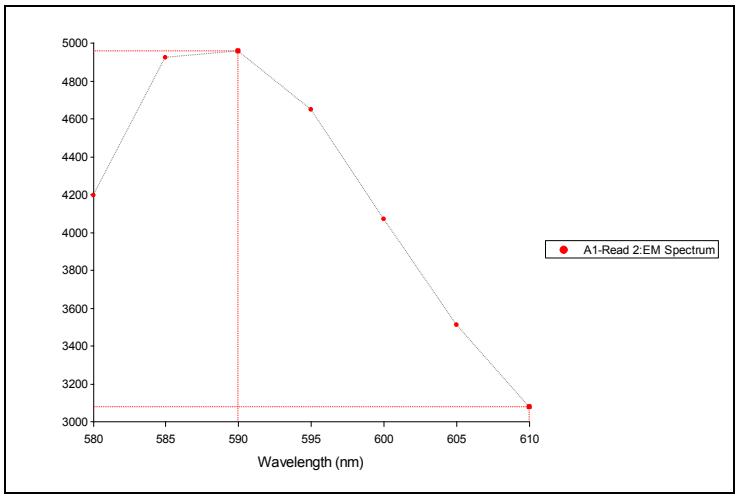


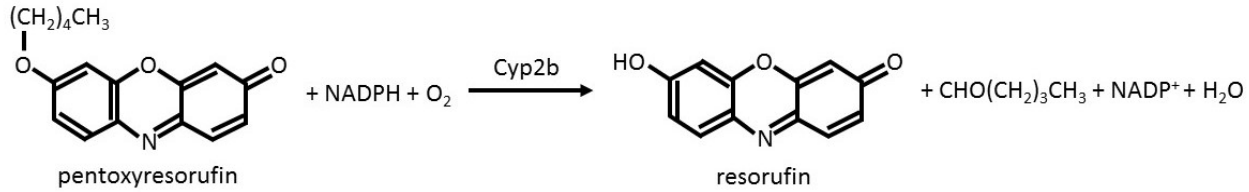
Figure 2.2: Excitation and emission wavelengths for resorufin detection

Figure 2.2 shows optimised excitation and emission wavelengths of resorufin with relative fluorescence units (RFU) on the y-axis indicative of signal strength.

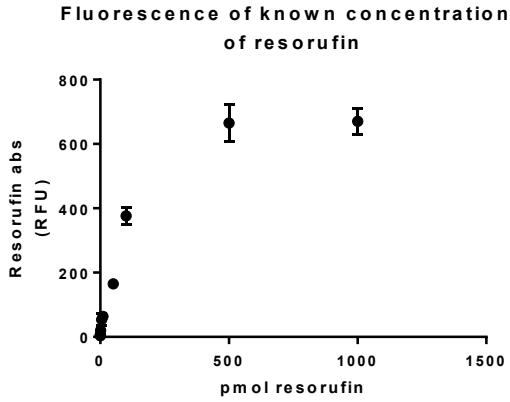
Fluorescence readings were taken every 10 minutes for 2 hours and the rate of resorufin was calculated by normalising to a blank of pentoxyresorufin only.

Fluorescence was converted to pmol of resorufin using a set of known standards (Figure 2.3 B and C), then the linear rate of reaction was calculated per minute per mg of total protein. Total cellular protein was determined using the BCA assay described later. The two highest concentrations of the resorufin standard (Figure 2.3 B) were not included in calculating the change in fluorescence with resorufin concentration due to the plateau in signal strength.

A



B



C

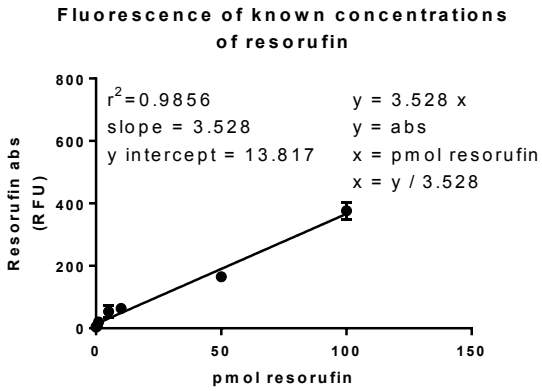


Figure 2.3: PROD substrate and resorufin fluorescence

Figure 2.3 shows the structure of pentoxyresorufin and its O-dealkylated product, resorufin, and aldehyde (**A**) (adapted from Sigma-Aldrich) with resorufin fluorescence (**B**, **C**). Data are representative of 3 dilutions, shown as mean + SEM. The y-axis plots the relative fluorescence units.

2.2.3 BCA assay

The bicinchoninic acid (BCA) assay protein quantification kit was from Pierce, ThermoScientific (IL, USA). A reaction mix of buffers B and A were made at 1:50, and 200µL was mixed with 10µL sample. The sample-buffer mixture was incubated at 37^{o}C for 30 minutes. Cupric ions (Cu^{2+}) in the buffer are reduced by and bind to protein molecules of $\geq$3 peptides in length, and the subsequent cuprous ions (Cu^{1+}) chelate with BCA to produce a colour change that can be quantified by absorbance at 560nm (Goldring, 2012). Absorbance of each sample was compared to the absorbance of a set of standard BSA concentrations (25, 125, 250, 500, 750, 1000, 1500, 2000µg/mL), using the equation:

y = "gradient" x where y = absorbance and x = protein concentration (µg/mL)

2.2.4 Nuclear localisation - Subcellular fractionation

Phenobarbital induces nuclear translocation of Car protein, and to assess this in the cell culture model used here, nuclear and cytoplasmic fractions were harvested and protein changes interrogated by immunoblot. B13 cells were seeded at 1x10^{6} cells per T175 flask and differentiated to B13/H as described above. B13/H cells were treated with phenobarbital-sodium (PB) (dissolved in media), for 72 hours. After treatments, cells were detached using trypsin (0.25%), centrifuged at 250g for 8 minutes and washed with ice cold phosphate buffered saline (PBS) (Fisher Scientific, PA, USA). The cell pellet was re-suspended in 500µL of buffer A containing 4-(2-Hydroxyethyl)piperazine-1-ethanesulfonic acid (HEPES) (10mM) pH 7.9, $MgCl_2$ (1.5mM), potassium chloride (KCl) (10mM), DL-Dithiothreitol (DTT) (500µM) (Sigma-Aldrich, Dorset, UK) and Halt Protease Inhibitor (diluted in buffer mixture to 1:100)

(ThermoScientific, IL, USA), for 60-70 minutes on ice. All buffers were made up to the required volume using demineralised (dm)H_2O.

Typically a Dounce homogenizer is used to disrupt the cell membrane while leaving the nucleus intact. The B13/H cells however appear susceptible to the hypotonic conditions of the low KCl concentration used here and ruptured without the need of a Dounce homogenizer. The success of fractionation can be crudely tested at this stage by haemocytometer and trypan blue (Sigma-Aldrich, Dorset, UK), where successfully lysed cells fail to exclude the impermeable dye. Leaving the cells for 60-70 minutes on ice as described above produced >90% lysis by trypan blue exclusion.

Samples were centrifuged for 5 minutes at 250g and 4^oC to pellet the intact nuclear material and the supernatant was collected as the cytoplasmic fraction. The nuclear pellet was re-suspended in 500µL of buffer B containing sucrose (250mM) (BDH Chemicals Ltd, UK) $MgCl_2$ (10mM) and Halt Protease Inhibitor (diluted in buffer mixture to 1:100). The nuclear fraction was then layered over a sucrose gradient of 1mL buffer C containing sucrose (862.5mM), $MgCl_2$ (500µM) and 1x Halt Protease Inhibitor (diluted in buffer mixture to 1:100). In order to remove lighter, non-nuclear, contaminants samples were centrifuged for 10 minutes at 3500g and 4^oC. The pellet was retained and re-suspended in buffer C (100µL) as the nuclear fraction. Samples were discarded if they showed signs of being insoluble as this is indicative of lysed nuclei and subsequent nuclear contamination in cytoplasmic fractions. Samples were stored at -20^oC, or lysed directly using equal volumes of RIPA buffer (Sigma-Aldrich, Dorset, UK). Contamination was checked using protein markers when samples were

run on immunoblots; Lamin B1 as the nuclear marker, and β-actin as the cytoplasmic marker (Figure 2.4).

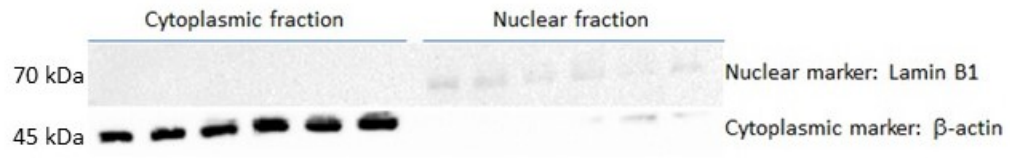


Figure 2.4: B13/H subcellular fractionation markers

Figure 2.4 shows the cytosolic and nuclear separation of B13/H cells and the respective compartment-specific markers. Abbreviations kDa, kilodaltons.

This fractionation protocol was based on the Lamond Lab Protocol (2007):

http://greproteomics.lifesci.dundee.ac.uk/webpage%20front%20page/dreamweaver%20webpage/CellFractionation.pdf

2.2.5 RNA extraction

To avoid contamination and RNA degradation all surfaces and tips were cleaned with 70% ethanol and RNase*ZAP* (Sigma-Aldrich, Dorset, UK) prior to any handling of RNA/cDNA. RNA extractions were performed using MirVana PARIS RNA extraction kits (Life Technologies, Paisley, UK) following manufactures protocol. Tissue culture wells were washed with ice cold PBS followed by addition of ice cold kit disruption buffer for 10 minutes. Samples were then transferred to DNase/RNase free 2mL centrifuge tubes. An equal volume of kit 2x Denaturing Solution was added to the homogenate at room temperature and samples were incubated for 5 minutes on ice. Samples were mixed with an equal volume of Acid-Phenol:Chloroform (to

denature proteins) and then separated by high speed centrifugation for 10 minutes (20,000g) to isolate the protein into the lower phase. Acidic conditions reduces gDNA contamination in the upper aqueous phase, which contains the RNA (Chomczynski & Sacchi, 2006). A volume of 1.25x 100% ethanol was added to the aqueous phase aliquot and passed through a silica filter, which binds the RNA. A series of wash steps with kit washes were used to remove salt contamination and purified total RNA was eluted from the filter into clean collection tubes by adding 95^{o}C DNase/RNase free water. RNA was quantified using the IMPLEN – nanophotometer (Implen, Gmbh, Munich, Germany). RNA was stored at -20^{o}C until required. RNA quality was determined using absorbance at A260 (nucleic acids)/A280 (proteins) and A260/A230 (phenol and salts), with ratios of $\geq$1.8 indicative of good quality.

2.2.6 qRT-PCR

To assess mRNA and miRNA expression in cell samples, quantitative real time PCR (qRT-PCR) was used. Endogenous controls were used to control for loading differences – β-actin, 18S rRNA or glyceraldehyde-3-phosphate dehydrogenase (Gapdh) for mRNA and sno or U6 RNA for miRNA. mRNA reverse transcription (RT) was performed using RNA template (500ng-1µg) with random hexamers (300ng) (Life Technologies, Paisley, UK) made up to a final volume in DNase/RNase free water (15µL). To denature RNA secondary structures prior to RT, the samples were heated for 5 minutes at 65^{o}C. RT was performed using Superscript II (Life Technologies, Paisley, UK) using a final volume of 23.5µL per sample including deoxynucleotide triphosphates (dNTPs) (425µM) (Sigma-Aldrich, Dorset, England), first strand buffer (diluted in reaction mixture to 1:5), DL-dithiothreitol (DTT) (8.5mM),

and superscript II enzyme (100 units). To check for contamination in the RT mixture a no template control was included and a no enzyme control to check for genomic DNA (gDNA) contamination in the RNA. The samples were run on a PTC-200 Peltier Thermal Cycler using conditions described in Table 2.1.

MiRNA RT was performed using TaqMan MicroRNA Reverse Transcription Kit (Life Technologies, Paisley, UK) with a final volume of 7.5µL per sample containing: RNA (5ng), dNTP (1mM), reverse transcriptase (25 units), RT buffer (diluted in reaction mixture 1:10), RNase inhibitor (1.9 units) and RT primers (diluted in reaction mixture 1:5), and run on a thermal cycler using conditions described in Table 2.1. Negative controls were not necessary for the miRNA RT as the primers used for this reaction are specific to the miRNA and do not amplify gDNA (C. Chen et al., 2005). Reverse transcription product was stored at -20^{o}C until needed.

Table 2.1: qRT-PCR conditions

RT/PCR	Step 1	Step 2	Step 3	Step 4	Step 5
RT (miRNA)	16^{o}C 30min	42^{o}C 30min	85^{o}C 5min	4^{o}C ∞	
RT (mRNA)	25^{o}C 10min	37^{o}C 120min	85^{o}C 5min	4^{o}C ∞	
qPCR	95^{o}C 10min	95^{o}C 15sec	60^{o}C 60sec	Repeat step 2-3 x39	4^{o}C ∞

PCR amplification of the mRNA and miRNA RT product was performed using TaqMan Fast Universal PCR Master Mix, No AmpErase UNG (Life Technologies, Paisley, UK). PCR master mix was made to a final volume of 10µL with master mix

(diluted in reaction mixture to 1:2), primers (diluted in reaction mixture to 1:20), and mRNA cDNA (0.8µL) or miRNA cDNA (0.67µL). Samples were run as technical triplicates for each primer. PCR analysis was performed using the 96-well fast block setting on the 7500 Fast Real-Time PCR System (Applied Biosciences, Life Technologies, Paisley, UK) (Table 2.1) and quantified by the comparative Ct method ($2^{-\Delta Ct}$) relative to an internal control (Schmittgen & Livak, 2008). Changes in housekeeping genes were assessed using the inverse log2 of the Ct values (2^{-Ct}) (Schmittgen & Livak, 2008).

TaqMan PCR signals are detected through conventional primer based amplification of target cDNA with addition of a target-specific 5'-FAM-labelled probe, which will only fluoresce after polymerase-mediated cleavage of the probe and subsequent release of the 3' quencher from the probe (Figure 2.5). A tailed 5' binding forward primer is used to adjust melting temperature. MiRNAs are specifically reverse transcribed by a 3' binding stem-loop primer, which provides specificity and stability for amplifying short sequences (Figure 2.5). TaqMan PCR amplification is similar between mRNAs and miRNAs (C. Chen et al., 2005).

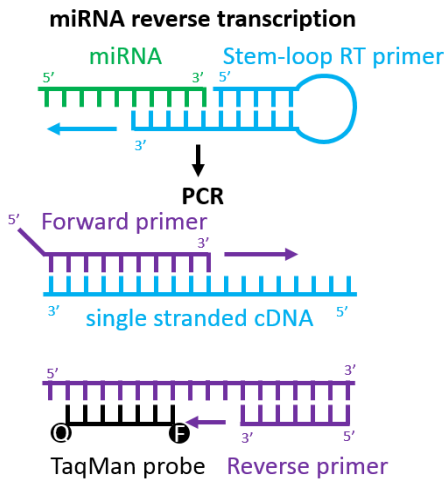


Figure 2.5: TaqMan PCR

Figure 2.5 details the TaqMan miRNA RT and universal PCR process; 5'-FAM-label (F) and 3' quencher (Q) of the TaqMan probe are shown. Adapted from Chen *et al.,* (C. Chen et al., 2005).

2.2.7 Semi-qPCR

Semi-quantitative (semi-q) PCR was also used to assess cell type markers after differentiation of rat pancreatic B13 cells to the hepatocyte-like B13/H cell. RT reactions were performed as described above for mRNA in the qRT-PCR section (chapter 2.2.6).

PCR amplification was performed using the Tfi polymerase kit to a final volume of 20µL per sample, containing cDNA (2µL), Tfi polymerase (2.5 units), 1x reaction buffer (diluted in reaction mixture to 1:5), $MgCl_2$ (3mM), dNTPs (200µM), and forward and reverse primers (200nM each) (Life Technologies, Paisley, UK). Negative controls were included as described for mRNA qRT-PCR. Primer details & optimised PCR conditions can be found in Table 2.2 and Table 2.3 respectively. PCR products were resolved using 2% agarose gel (Sigma-Aldrich, Dorset, UK) of Tris-borate-EDTA (TBE) solution containing ethidium bromide (5µL) (ICN Biomedicals Inc, OH, USA). Products were separated by applying a charge of 150V for 45 minutes to the loaded gel; using a 100bp ladder as reference (New England Biolabs, MA, USA). The negative charge of the phosphate backbone in DNA causes the product to migrate towards the anode, allowing separation by size. The DNA intercalates with the ethidium bromide, which fluoresces under UV light enabling sample detection (LePecq & Paoletti, 1967). Analysis was performed using the Image Lab on the Gel Doc XR+ System and the KODAK image station 4000MM (Carestream molecular imaging, CT, US).

Table 2.2: Semi-q PCR primer details

mRNA semi-qPCR primers (Life Technologies)		
Primer	Sequence (5'-3')	Amplicon size (bp)
Gapdh Fwd	GGACCAGGTTGTCTCCTGTG	322
Gapdh Rev	GGCCCCTCCTGTTGTTATGG	
Albumin Fwd	GCTGAGGCCAAGGATGTCTT	470
Albumin Rev	CACTTGGTGACCTTCTCGCT	
Amylase 2a3 Fwd	TGGTTCTCCCAAGGAAGCAG	834
Amylase 2a3 Rev	CTCTTACAACTTTGAGTCGGCAT	
Nr1i3 Fwd	AAAGCTGATGGGCCTGCTA	369
Nr1i3 Rev	GAGGCTCCTGTCTTTCCCA	

Table 2.3: Semi-q PCR amplification conditions

PCR	Step 1	Step 2	Step 3	Step 4	Step 5	Step 6	Step 7
Gapdh	94°C 2min	94°C 30sec	59°C 30sec	72°C 30sec	Repeat 2-4 x29	72°C 10min	4°C ∞
Albumin	94°C 2min	94°C 30sec	60°C 30sec	72°C 30sec	Repeat 2-4 x29	72°C 10min	4°C ∞
Amylase	94°C 2min	94°C 30sec	59°C 30sec	72°C 60sec	Repeat 2-4 x29	72°C 10min	4°C ∞
Nr1i3	94°C 2min	94°C 30sec	58°C 30sec	72°C 30sec	Repeat 2-4 x29	72°C 10min	4°C ∞

2.2.8 Statistics

All data are shown as mean ± standard error of the mean (SEM) with sample size shown in figure legends. Student's t tests were used to compare treatment with control, or one way analysis of variance (ANOVA) with Dunnett's comparison for comparing multiple groups to a control. Graphs and analysis were produced/performed using Graph Pad 6 (La jolla, California). Statistical significance was defined as $p<0.05$ (*), $p<0.01$ (**), $p<0.001$ (***), $p<0.001$ (****).

2.3 Results and Discussion

2.3.1 Aim 1: Characterising the differentiation of AR42J-B13 (B13) to hepatocyte-like AR42J-B13/H (B13/H) cells in response to dexamethasone.

Upon treatment with 10nM dexamethasone for 2 weeks, B13 cells transdifferentiate into hepatocyte-like B13/H cells (Shen et al., 2000) and these cells can be maintained in culture for up to 30 days (Marek et al., 2003). To determine the most appropriate time-course of dexamethasone-induced differentiation, B13 cells were treated for 2, 3 or 4 weeks with 10nM dexamethasone as detailed in Figure 2.6. Ninety-six hours after the removal of the dexamethasone, the cells were assessed for expression of the hepatic phenotype. For comparison, untreated B13 cells were examined in parallel.

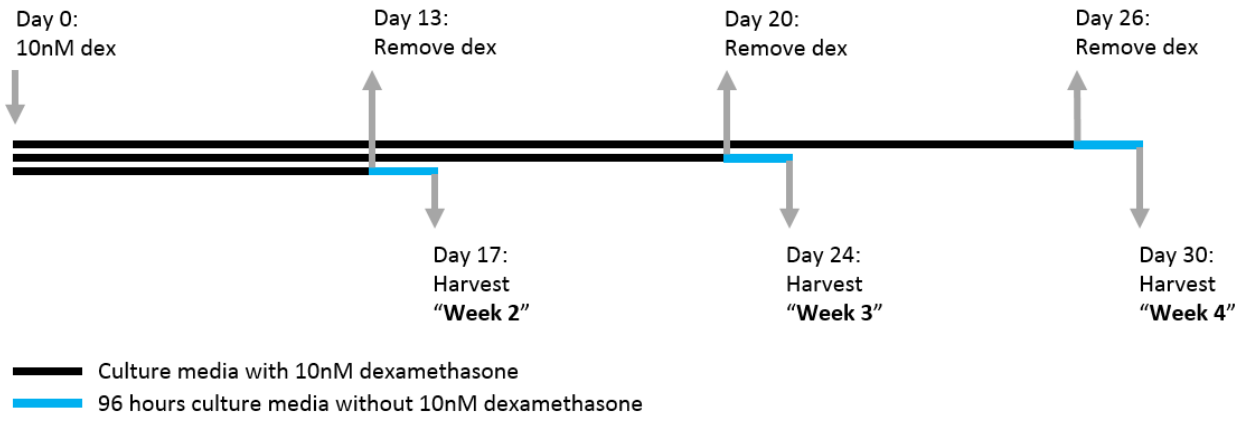


Figure 2.6: B13 dexamethasone treatment plan

Figure 2.6 represents the treatment scheme of 10nM dexamethasone- (dex) mediated differentiation of B13 cells to hepatocyte-like B13/H cells.

Cyp2b activity Cyp2b activity (PROD) was used as a marker of the hepatocyte phenotype and functionality (Philip M E Probert et al., 2014). Figure 2.7 A shows that 2 and 3 weeks dexamethasone treated B13 cells were able to metabolise

pentoxyresorufin at a rate significantly higher than that of untreated B13 cells, indicative of an increased hepatocyte-like phenotype. Although PROD activity was reduced at the 4 week time point, it was still higher than the undifferentiated B13 cells.

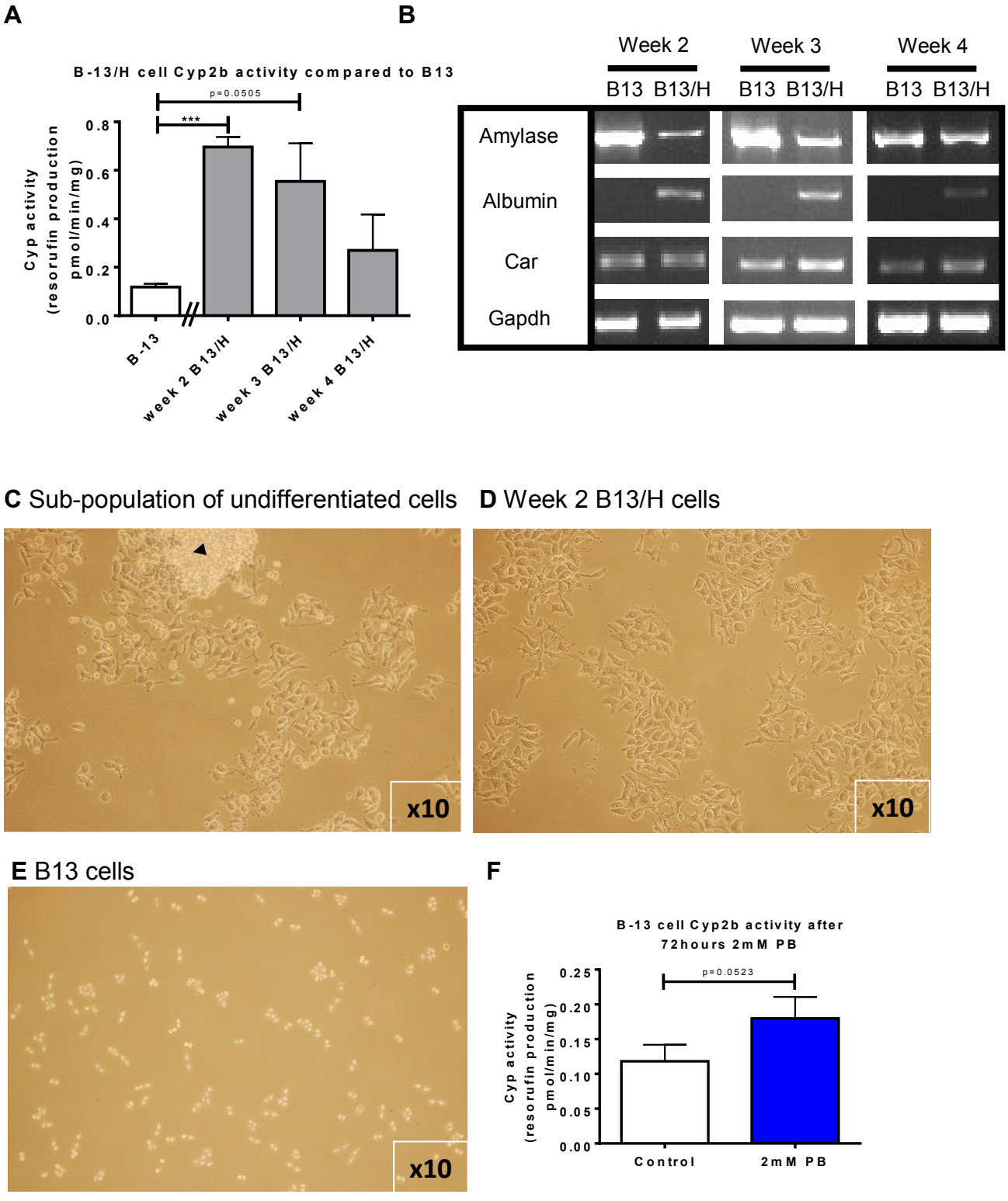


Figure 2.7: Markers of the transdifferentiation phenotype of B13/H cells

Figure 2.7. **A** Cyp2b activity in B13/H cells by PROD compared to B13 cells. Y-axis is mean ± SEM of Cyp activity determined by the rate of resorufin production of 3 independent cultures. Student's t test compared B13/H to B13 cells. ***p<0.001. **B** Representative semi-q PCR of B13 and B13/H cells differentiated for different times

as indicated. This experiment was repeated with similar results for 3 independent cultures. Brightfield images are shown of: B13/H cells with undifferentiated B13 cells (**C**), 2 weeks differentiated B13/H cells (**D**) and undifferentiated B13 cells (**E**). Images are typical of cell morphology and were taken at x10 magnification. **F** Cyp2b activity in B13 cells treated with 2mM PB for 72 hours. Values were mean ± SEM for 3 independent cultures.

Expression of B13/H marker genes Semi-q PCR analysis confirmed the expression of the liver marker, albumin, at all 3 time points in the B13/H cells, whereas there was no detectable albumin expression in the B13 cells (Figure 2.7 B). As expected, amylase expression was still present within the dexamethasone treated cells, probably as there are always sub-populations of undifferentiated cells (Al-Adsani et al., 2010), which can clearly be identified as clusters of circular cells using brightfield microscopy (Figure 2.7 C, arrow head).

I confirmed the expression of Car mRNA in the B13/H cells (Figure 2.7 B). Surprisingly I also detected Car mRNA in the B13 cells, in contrast to Probert *et al.,* (Philip M E Probert et al., 2014) who were unable to detect Car mRNA in B13 cells. Assessing primer sets between both studies *via* Primer-BLAST (Ye et al., 2012) showed that the primers used by Probert *et al.,* (Philip M E Probert et al., 2014) (Fwd 5'-CTCTCCTGACAGGCCTGGGGT-3': Rev 5'-CGAAGCTCAGCTAGCAGGCCC-3') detected the *Car* splice variant (SV) 1 at 156 base pairs and SVs 2 and 3 at 174 base pairs, while the primers used herein (Fwd 5'-AAAGCTGATGGGCCTGCTA-3': Rev 5'-GAGGCTCCTGTCTTTCCCA-3') additionally detected *Car* SV4, at 369 base pairs. My primer pair also detected the predicted gene, *translocase of outer mitochondrial membrane 40 homolog (yeast)-like (Tomm40l), SV X1*, which overlaps the *Car* gene. This suggests that either, Car SVs are expressed in B13 and B13/H

cells, or that the predicted gene, *Tomm40l*, is actually expressed in this cell model. To assess the functionality of Car expression in the non-differentiated B13 cells, I examined the induction of Cyp2b activity in B13 cells, which is a Car-mediated event (Sueyoshi et al., 1999; Wei, Zhang, Egan-Hafley, Liang, & Moore, 2000). Treating B13 cells with a single dose of 2mM PB for 72 hours produced a 50% increase in Cyp2b activity ($p=0.0523$) (Figure 2.7 F), consistent with a functional Car response.

Cell morphology After treatment with dexamethasone there was a clear morphological change in the cell phenotype. B13/H cells exhibited the hepatocyte-like flattened and elongated shape with finger-like projections (Figure 2.7 D), whereas B13 cells were smaller circular cells that proliferated in clusters (Figure 2.7 E). These morphological traits were used as a checkpoint to determine successful differentiation.

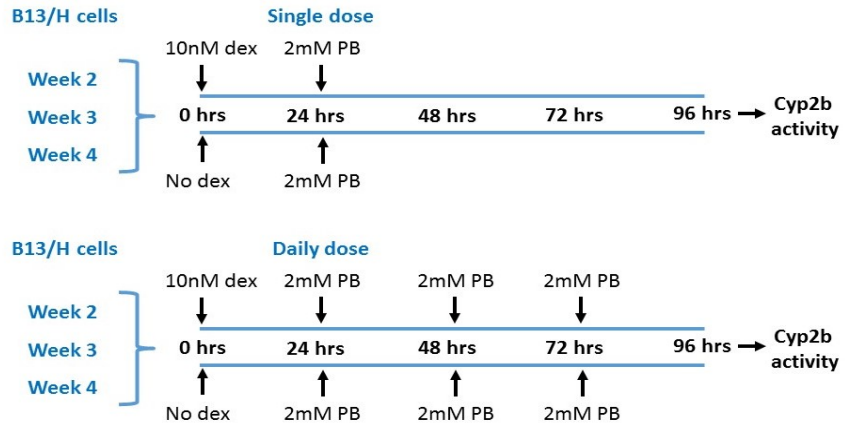
Summary – These results indicate that a 2 week dexamethasone treatment successfully transdifferentiated B13 cells to an hepatocyte-like phenotype, with a gain of albumin expression, increased Cyp2b expression and reduced (but not lost) amylase expression. Additionally, the morphology of the B13/H cells differed from the undifferentiated B13 cells. Furthermore, the transdifferentiated phenotype could be maintained for at least 4 weeks.

2.3.2 Aim 2: Assess the B13/H cell response to PB and PB-like compounds.

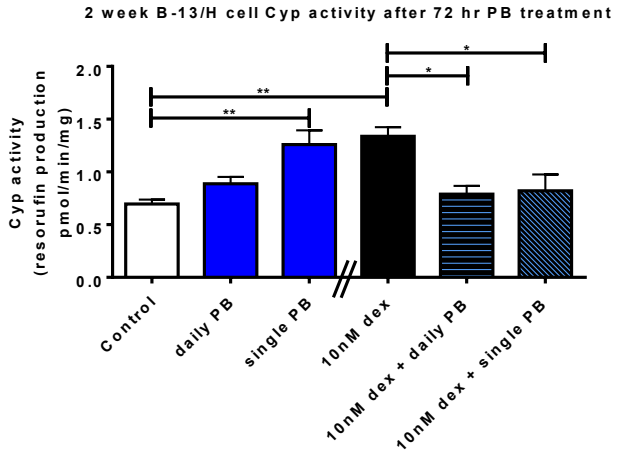
2.3.2.1 Assess the B13/H cell response to PB

Cyp2b activity Using markers from the literature (Philip M E Probert et al., 2014; Shen et al., 2000) I have shown that I am able to produce B13/H cells, which appear to behave as hepatocyte-like cells. I then went on to assess the response of B13/H cells to PB to determine appropriate dosing regimens, as well as confirm their hepatocyte-like functionality. B13/H cells were differentiated as described previously (Figure 2.6) for 2, 3 or 4 weeks, with subsequent PB treatment for 72 hours. Dexamethasone has been shown to augment PB-mediated affects in human primary hepatocytes (Pascussi, Gerbal-Chaloin, et al., 2000). However it has also been reported that dexamethasone decreases Cyp2b mRNA, but not protein, in Fao cells (de Waziers et al., 1992) and suppresses Cyp2b6 expression in HepG2 cells (Sueyoshi et al., 1999). To explore the effect of dexamethasone on PB's induction of Cyp2b, B13/H cells were either treated with PB in media lacking, or supplemented with, dexamethasone (10nM). The former treatment group had 24 hours in dexamethasone-free media prior to PB treatment, as detailed in Figure 2.8 A. PB treatments were either: single doses of PB (2mM) for 72 hours (single dose), or 3 doses of PB (2mM), one every 24 hours (daily dose), with respective vehicle controls.

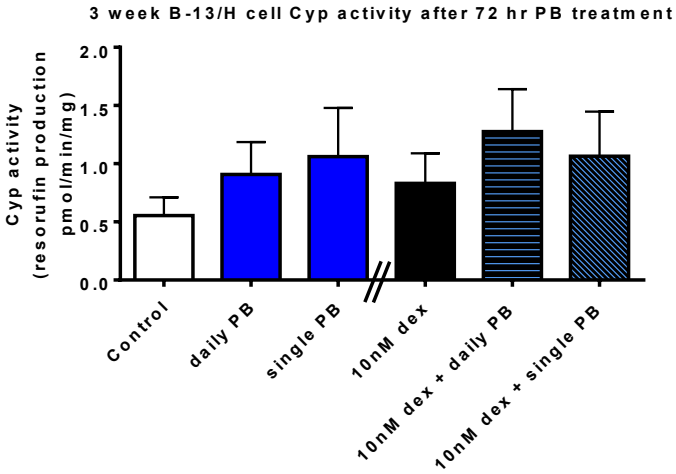
A



B



C



D

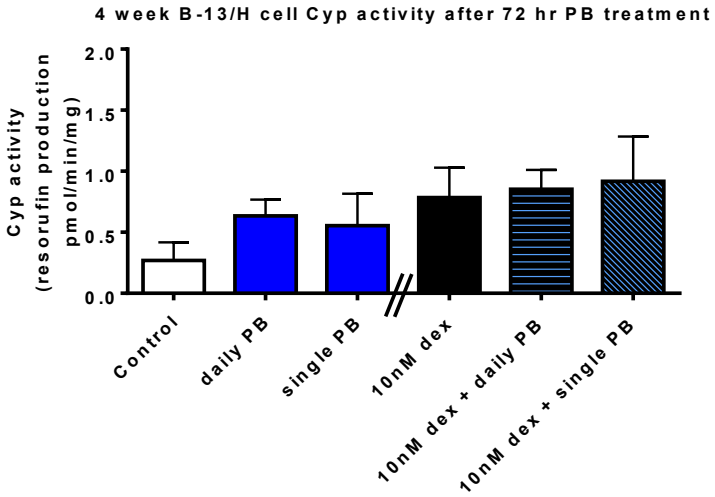


Figure 2.8: Effect of PB treatment on Cyp2b actvity in B13/H cells

Figure 2.8 (**A**) depicts the treatment plan for measuring Cyp2b with various PB and dexamethasone treatments. Cyp2b activity in B13/H cells by PROD after 2mM PB and/or 10nM dexamethasone treatment at 2 (**B**), 3 (**C**) and 4 (**D**) weeks dexamethasone-induced differentiation. Results were representative of 3 independent cultures, and Y-axis is mean ± SEM of Cyp activity determined by PROD. Student's t test compared control with 10nM dex (dexamethasone), and one way ANOVA with Dunnett's comparison compared control to PB, and dex to dex + PB. *p<0.05, **p<0.01.

Cyp2b activity (PB without dexamethasone) This data demonstrates that at 2 weeks differentiation, B13/H cells had significantly increased Cyp2b activity with a single dose of 2mM PB compared to control (B13/H cells with no PB treatment), and that daily doses of PB did not significantly increase Cyp2b activity, in fact it attenuated the response (Figure 2.8 B).

Cyp2b activity (PB with dexamethasone) Two week differentiated B13/H cells treated with 10nM dexamethasone also showed increased Cyp2b activity compared to B13/H cells treated with the dexamethasone vehicle (Figure 2.8 B). At the dose of dexamethasone used, this could be through canonical activation of the glucocorticoid receptor, which has been shown to activate both Pxr and Car in primary human hepatocytes (Pascussi et al., 2001). Furthermore, co-treatments with dexamethasone (10nM) and PB (2mM) showed an inhibition in Cyp2b activity, at both daily and single PB doses at 2 weeks transdifferentiation (Figure 2.8 B).

Summary – This demonstrates that in B13/H cells co-treatments with dexamethasone and PB attenuated Cyp2b activity. Interestingly, B13/H cells transdifferentiated for 3 and 4 weeks showed reduced capacity for both PB- and dexamethasone-mediated induction of Cyp2b activity (Figure 2.8 C and D). This suggests that for maximal Cyp2b induction by PB, optimal differentiation of B13 to B13/H cells in our hands is after 2 weeks treatment with dexamethasone. This is consistent with the decline in basal Cyp2b activity from 2 weeks onwards as shown in Figure 2.7 A.

Subcellular localisation of Car Under basal conditions in primary cells, Car is sequestered in the cytosol. However in immortalised cells, Car appears to have escaped its regulatory control and is found primarily in the nucleus (reported in HepG2 cells) (Kawamoto et al., 1999). In this respect, B13/H cells appear to display this key characteristic of primary hepatocytes, I therefore attempted to confirm the subcellular localisation of Car.

B13/H cells were differentiated for 2, 3 and 4 weeks and treated with PB, or vehicle control, for 72 hours in media devoid of dexamethasone (as shown in Figure 2.8 A - single PB dose without dexamethasone). I have shown that PB treatment for 72 hours significantly induced Cyp2b activity at 2 weeks transdifferentiation of B13/H cells (Figure 2.8 B). Treated B13/H cells were harvested and nuclear and cytoplasmic fractions obtained for Car protein detection *via* immunoblot. To assess subcellular fractions and contamination, a cytoplasmic marker, β-actin, and a nuclear marker, Lamin B1, were used. In all cases there was minimal nuclear contamination in the cytoplasmic fractions, whereas there was evidence of cytoplasmic contamination in the nuclear fraction (Figure 2.9). Treatment with PB (2mM) suggests there was an increase in Car protein within the nuclear fraction compared to the nuclear fraction of control cells (Figure 2.9 A). However, it is difficult to unequivocally confirm this response due to the increase in the nuclear marker Lamin B1 with PB treatment. Koike *et al.,* (Koike, Moore, & Negishi, 2005) previously assessed Lamin B1 as a marker for PB-mediated nuclear localisation for Car, which appeared to show a subtle (not quantified) increase with PB compared to control, suggesting a different nuclear marker may have been more appropriate. Interestingly at all 3 time points tested, Car was found to be in the nucleus of control samples and

not detected in the cytoplasm, indicating that B13/H cells are more similar to immortalised cells with regards to Car localisation.

Summary – From these data I have shown that optimised transdifferentiation of B13 cells was with 2 weeks of 10nM dexamethasone (from now on reference to B13/H cells indicates 2 weeks differentiation) and optimal Cyp2b activity was obtained by treating with single doses of PB. We have also established that while B13/H cells are responsive to PB, the location of Car in B13/H cells is primarily nuclear and therefore likely to be more similar to that of immortalised cells than compared with primary hepatocyte cells.

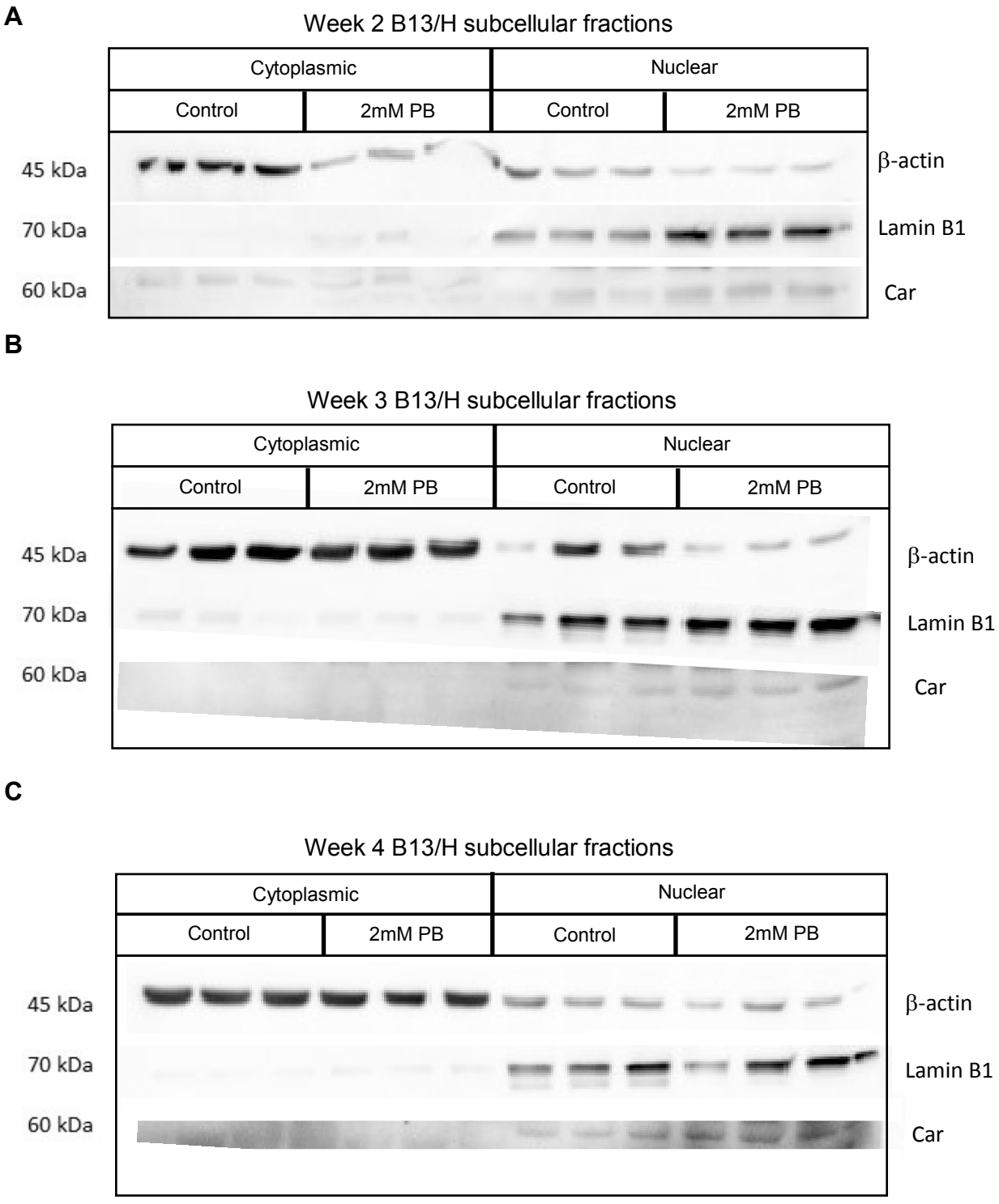


Figure 2.9: Car subcellular localisation
Figure 2.9 depicts immunoblots of Car and loading controls, β-actin and Lamin B1, in 2 (**A**), 3 (**B**) and 4 (**C**) weeks dexamethasone-differentiated B13/H cells with 72 hours 2mM PB treatment. Each lane was derived from an independent culture.

Due to the constitutive activity of Car, if this nuclear receptor is present in the nucleus, why do we appear to demonstrate a PB response? It is possible that, due to the overlapping nature of Car and Pxr downstream targets, the response shown is due to Pxr activation? However, it has been reported that nuclear location of Car is not sufficient for gene expression alone, and may require further molecular changes (Pascussi, Gerbal-Chaloin, et al., 2000). In this respect, I argued in chapter 1 that Ampk activation may be part responsible for this (chapter 1.2.3). Activation of Ampk has been suggested to be due to decreased expression of miR-122 (Shizu et al., 2012) as a result of Car-mediated Hnf-4α suppression (Kazantseva et al., 2015). Both Car (Miao, Fang, Bae, & Kemper, 2006) and Pxr (Bhalla, Ozalp, Fang, Xiang, & Kemper, 2004) have been reported to inhibit Hnf-4α-mediated gene expression. Therefore it is possible that basal Car activity or activation of Pxr, as a result of PB treatment, inhibits Hnf-4α, which results in decreased miR-122 and subsequent Ampk activation and nuclear activation of Car. In fact, Figure 2.10 shows that PB treatment (4mM) in 2 weeks dexamethasone-transdifferentiated B13/H cells significantly reduced miR-122 expression after 24 hours. It would be interesting to determine if PB-mediated inhibition of miR-122 may be involved in the activation of Car in B13/H cells. To explore this further would require additional treatment times to be examined in order to correlate miR-122 expression with Cyp mRNA expression and activity. To confirm the role of miR-122 and Car activation it would be interesting to over-express the miRNA and assess if the B13/H cells remain responsive to PB.

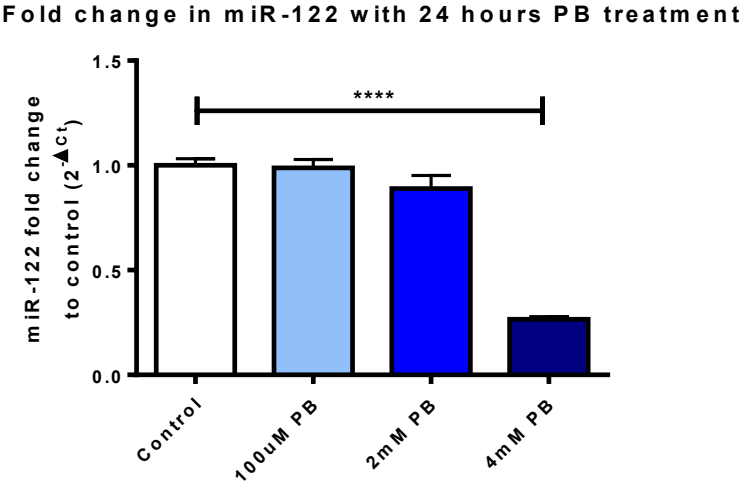


Figure 2.10: MiR-122 expression in PB treated B13/H cells

Figure 2.10 depicts the expression of miR-122 in B13/H cells following 24 hours PB treatment. Results were representative of 3 independent cultures, and Y-axis is mean ± SEM of miR-122 expression using $2^{-\Delta Ct}$ to present fold change of target to time matched control. One way ANOVA with Dunnett's comparison was used to compare PB (100µM, 2mM or 4mM) to control. ****p<0.0001

Summary – This data shows that PB reduced miR-122 levels in B13/H cells, as seen in male C3H mice and human HepG2 cells (Shizu et al., 2012).

2.3.2.2 Cyp2b activity and Cyp mRNA expression in 2 week dexamethasone transdifferentiated B13/H cells in response to PB

Cyp2b activity Primary hepatocytes often require culturing in complex conditions in order to maintain their hepatic functions (K. Wallace, Fairhall, Charlton, & Wright, 2010). Yusof *et al.,* (Yusof & Edwards, 1990) demonstrated that by culturing primary rat hepatocytes in Williams' medium E containing: Egf (10ng/mL), dexamethasone (30nM), insulin (300nM) and FBS (3% v/v) (referred to herein as hepatocyte media) at sub-confluency improved the transient hyperplasic response associated with PB

treatment *in vivo*. From this I hypothesised that culture of B13/H cells in an hepatocyte defined medium might improve the *in vitro* PB response. I first sought to test if differentiated B13/H cells cultured with this hepatocyte media would exhibit an improved response to PB-mediated induction of Cyp2b activity, when compared to standard culturing conditions. By comparing the effect of different cell media on Cyp2b activity I demonstrated that an hepatocyte defined medium produced a higher basal Cyp2b activity compared to standard B13 culture media and a serum stripped media (Figure 2.11 A). However, the standard B13 culture media appeared to be optimal for PB-mediated induction of Cyp2b (Figure 2.11 B, C and D). I included a serum stripped media as growth factors have been shown to inhibit PB signalling (Mutoh et al., 2013; Osabe & Negishi, 2011), and I wanted to explore the possibility that in a medium lacking hormones and certain growth factors, PB induction of Cyp2b would be improved. This did not appear to be the case.

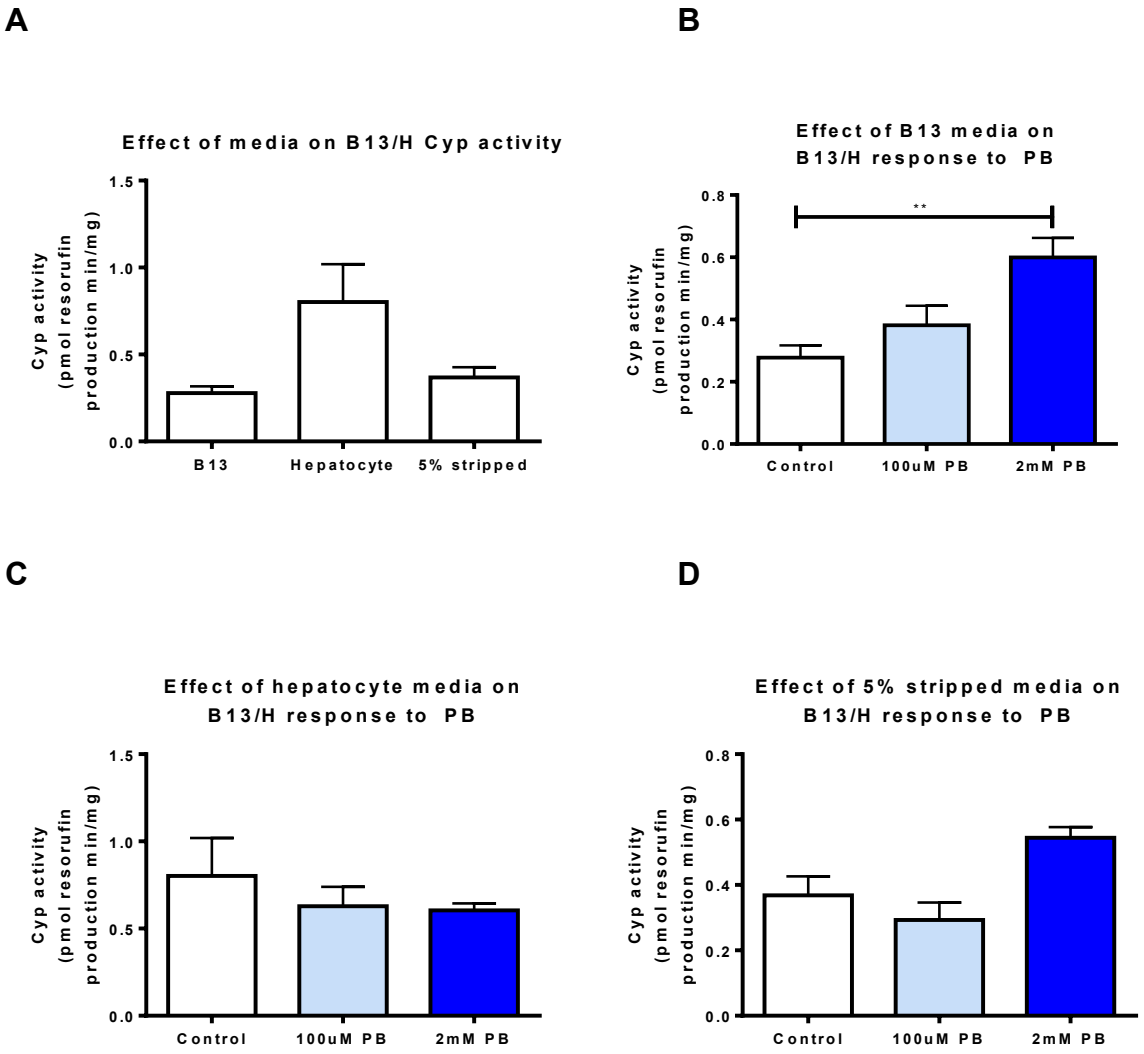


Figure 2.11: Effect of media on Cyp2b activity in B13/H cells

Figure 2.11 shows Cyp2b activity (PROD) in B13/H cells in different media types (**A**), and after PB treatment for 72 hours (**B**/**C**/**D**). Results were mean ± SEM for 4 independent cultures. Y-axis is of Cyp activity determined by the rate of resorufin production. Control treatment was compared to PB (100μM and 2mM) by one way ANOVA with Dunnett's comparison. **p<0.01.

Summary – The data confirmed that B13/H cells are capable of responding to PB treatment in a simple culture media without the requirement of many added supplements, and that the defined hepatocyte media tested here is unlikely to improve the B13/H cell response to PB. Therefore, culturing B13/H cells in B13

media (lacking dexamethasone) is optimal for eliciting a PB response, as measured by PROD.

Expression of Cyp2b mRNA I confirm that Cyp2b1 mRNA was increased with PB (2mM) after 6 hours treatment (Figure 2.12 A), although expression was diminished after 24 hours (Figure 2.12 B) and undetectable after 72 hours (data not shown). Furthermore, I confirm that B13/H cells expressed the male specific Cyp2c11 (Philip M E Probert et al., 2014), which did not appear to be induced by PB (Figure 2.12 C and D).

In agreement with my data, Probert *et al.,* (Philip M E Probert et al., 2014) report that B13/H cells treated with PB exhibit similar responses as determined by qPCR and PROD, and demonstrate the reproducibility of this cell line.

Summary – These data show that B13/H cells are capable of responding to PB and producing typical markers of PB exposure, in a manner comparable to independent laboratory groups.

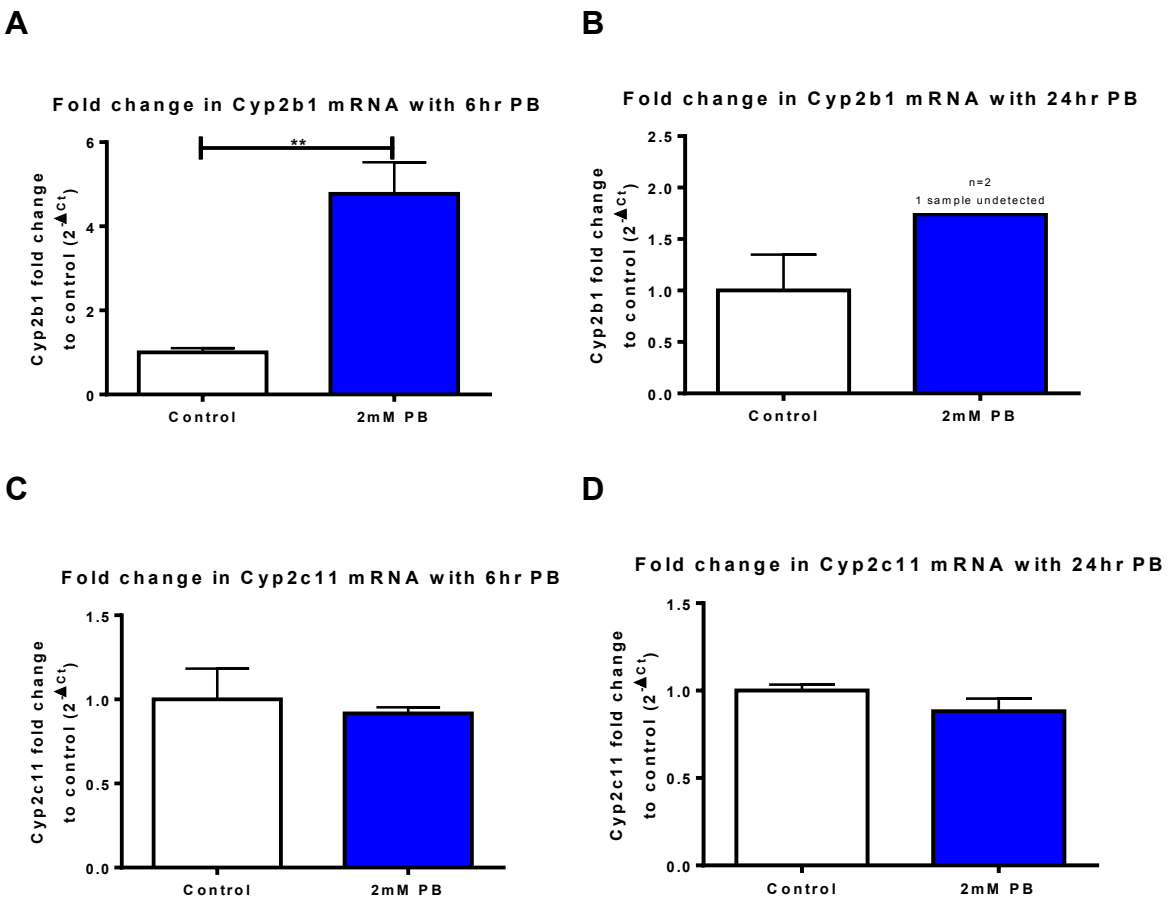


Figure 2.12: Cyp mRNA expression in PB treated B13/H cells

Figure 2.12 depicts mRNA expression by qRT-PCR of Cyp2b1 and Cyp2c11 after 6 hours (**A**/**C**) or 24 hours (**B**/**D**) 2mM PB. Results were representative of 3 independent cultures, and Y-axis is mean ± SEM using $2^{-\Delta Ct}$ to present fold change of target to control. Student's t test compared control to PB. **p<0.01.

2.3.2.3 Temporal- and dose-dependent response of Cyp2b activity in 2 week dexamethasone-differentiated B13/H cells in response to PB and PB-like compounds

Data presented in Figure 2.13 and Figure 2.14 were obtained in collaboration with Myriam Haltalli (Department of Surgery and Cancer, Imperial).

I have established that treatment with PB (2mM) for 72 hours in 2 weeks dexamethasone-differentiated (10nM) B13/H cells provoked a reliable and reproducible induction of Cyp2b activity (by PROD). It has been suggested that B13/H cells are capable of being cultured for extended timeframes and so offer an advantage over the short-term chemical exposures required when working with primary hepatocytes. Here, by assessing Cyp2b activity at different times we hoped to identify an appropriate regime for *in vitro* PB exposure beyond 72 hours, and explore the effect of extended chemical treatments in these cells. Furthermore, we interrogated the response to PB and PB-like compounds to assess if the cells elicited reproducible responses to chemicals with similar phenotypic effects. The following data is from B13/H cells exposed to PB and PB-like compounds for the times indicated in Figure 2.13, with the media and compound refreshed every 72 hours. My previous data demonstrated that PB induces Cyp2b activity under this condition (Figure 2.8 B).

Rat Car activators Two millimolar PB significantly induced Cyp2b activity at 3 and 9 days (Figure 2.13 A), and we confirmed that doses of 2mM PB and above were able to significantly induce Cyp2b activity at 72 hours (Figure 2.14 A). The PB-like compound benzophenone (BP) was also tested. BP is used in agricultural chemical synthesis as well as a fragrance enhancer and flavour. BP was identified as a Cyp2b inducer, demonstrating similar adaptive responses in the liver as PB treated rats (Boobis et al., 2009; Chhabra, 2000), as well as similar molecular changes (Koufaris et al., 2012). We tested a dose response to BP at 72 hours where PB induced Cyp2b activity (PROD) (Figure 2.13 A and Figure 2.14 A) and found that doses of 750µM or 1mM induced Cyp2b activity compared to control ($p<0.05$ by Student's t test) (Figure

2.14 B). Clotrimazole has been identified as a direct activator of rat Car (Omiecinski et al., 2011). We showed that 10μM clotrimazole increased Cyp2b activity (PROD) at 1, 3 and 9 days treatment compared to control (Figure 2.13 B). To support this finding we also examined the effect of clotrimazole dose on PROD after 72 hours treatment and found induction only occurred at 10μM (Figure 2.14 C).

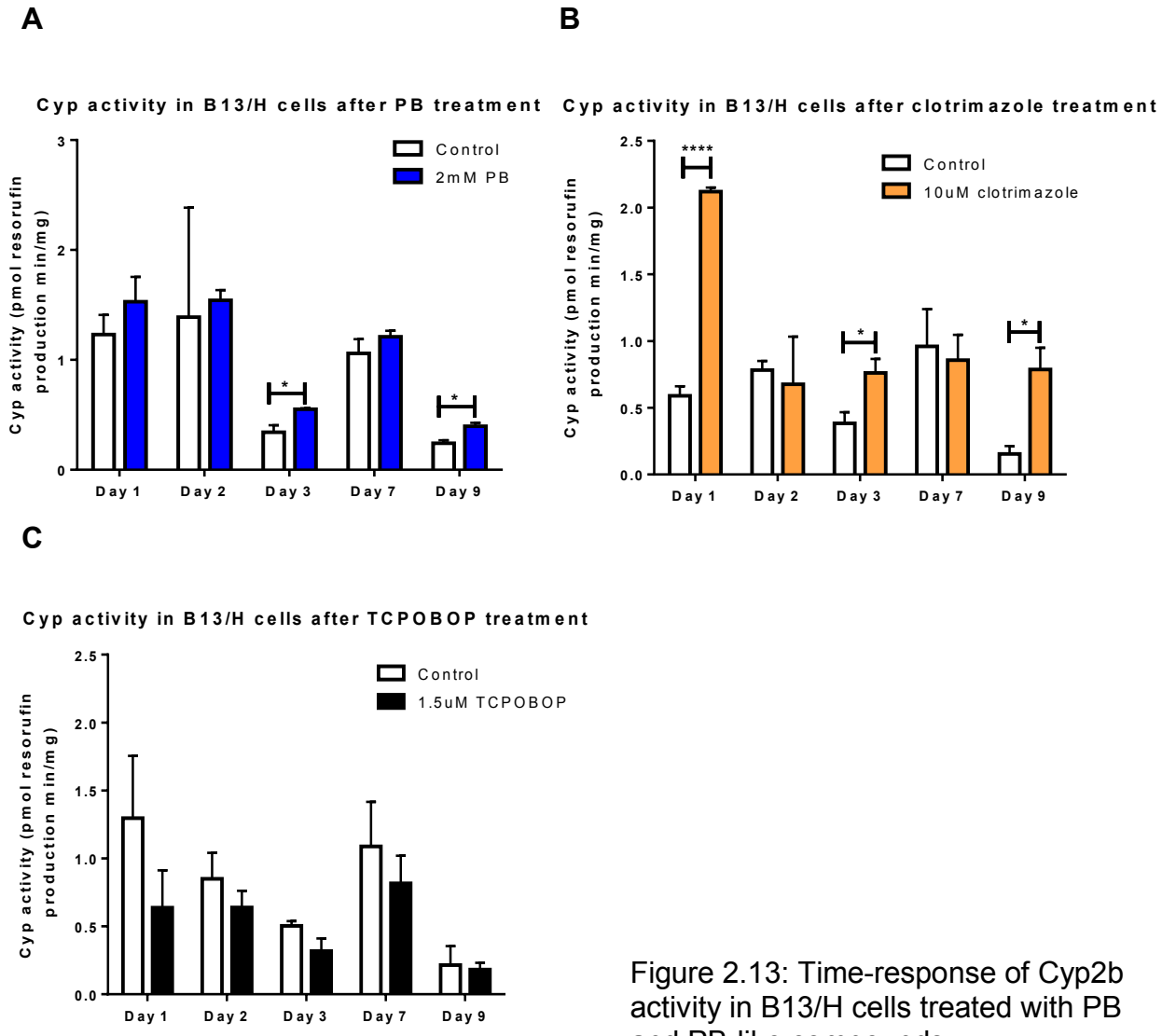


Figure 2.13: Time-response of Cyp2b activity in B13/H cells treated with PB and PB-like compounds

Figure 2.13 illustrates Cyp2b activity in B13/H cells by PROD after 2mM PB (**A**), 10μM clotrimazole (**B**), or 1.5μM TCPOBOP (**C**) treatments for the times indicated. Treatment and media were refreshed every 72 hours. Results were representative of 3 independent cultures, and Y-axis is mean + SEM of Cyp activity determined by the rate of resorufin production. Student's t test compared control to time matched treatment. *p<0.05, ****p<0.0001.

Mouse Car activator Car is known to respond to chemicals in a species-specific manner. For example, the rat Car activator clotrimazole is a human Car inverse agonist (Moore et al., 2000; Omiecinski et al., 2011), and the Car activator TCPOBOP has been reported to be mouse-specific (Omiecinski et al., 2011; Tzameli et al., 2000). To confirm that in the B13/H cells Car responded in a rat-specific manner, we treated B13/H cells with 1.5μM TCPOBOP (Philip M E Probert et al., 2014). We found that there was no significant change in PROD compared to control at any time point tested (Figure 2.13 C). Although the response to TCPOBOP was variable, the data indicates that TCPOBOP was not a Car activator in the rat B13/H model.

Summary – These data suggest that optimal treatment of B13/H cells, based on Cyp2b activity, requires single doses of PB or PB-like compounds for 72 hours, and that increases in Cyp2b activity can be maintained for up to 9 days exposure to compounds. Furthermore, B13/H cells responded to activation of Car in a rat-specific manner.

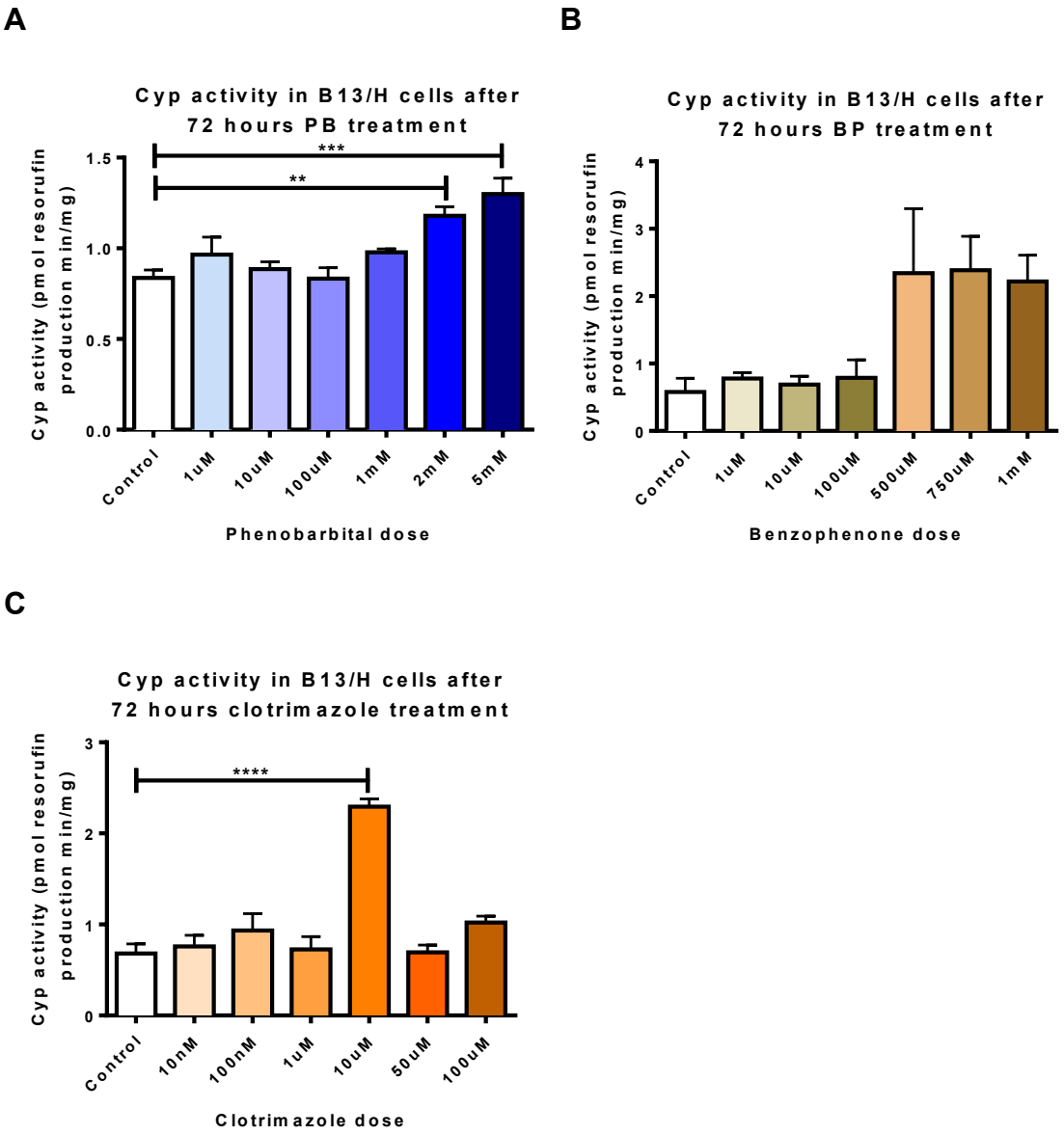


Figure 2.14: Dose-response of Cyp2b activity in B13/H cells treated with PB and PB-like compounds

Figure 2.14 describes the effect of chemical dose-response on Cyp2b activity in B13/H cells by PROD after PB (**A**), BP (**B**) or clotrimazole (**C**) exposure for 72 hours. Results were representative of 3 independent cultures, and Y-axis is mean ± SEM of Cyp activity determined by the rate of resorufin production. One way ANOVA with Dunnett's comparison was used to compare treatment to control. **p<0.01, ***p<0.001, ****p<0.0001.

2.3.3 Aim 3: Explore the effect of PB and PB-like compounds on miRNA expression in B13/H cells.

Data presented in Figure 2.15 were obtained in collaboration with Myriam Haltalli.

Data from Koufaris *et al.,* (Koufaris et al., 2012, 2013) reported that miRNA expression profiles can be used to predict mechanisms of action of different chemicals. The authors showed that PB induced miR-182/96 and miR-200a/b/429 in a time- and dose-dependent manner, and the PB-like compound BP also increased expression of these miRNAs. The regulation and function of these miRNAs will be discussed further in chapter 4 and 5. Importantly, the *in vivo* time-dependent induction of these miRNAs by PB is such that at 1, 3 and 7 days 1000ppm PB treatment, the miRNAs were not significantly changed from control. However from 14 days onwards the miRNAs were significantly increased by 1000ppm PB (demonstrated with miR-200a, miR-200b and miR-96) (Koufaris et al., 2013). We therefore wanted to further test the B13/H cell model with extended treatments. By treating with PB and BP, as well as the Car activator clotrimazole, we explored the reproducibility of the B13/H cells in responding to chemicals with similar mechanisms of action by analysing if the *in vivo* identified miRNAs were sensitive to these treatments.

MiRNA expression after PB and PB-like treatments Treatment with PB (100μM and 2mM) did not significantly alter the expression of miR-182 or miR-96 at 3 days treatment compared to control (Figure 2.15 A and B), despite induction of Cyp2b

under these conditions (2mM PB) (Figure 2.13 A). However at 9 days, where we showed Cyp2b induction (Figure 2.13 A), PB (2mM) significantly induced both miRNAs compared to control (Figure 2.15 A and B). This suggests that PB was able to time-dependently induce miR-182 and miR-96 in the B13/H cells in a similar fashion as shown *in vivo*. Furthermore, we show that miR-96 was induced by BP (500µM) in the same manner (Figure 2.15 C). Our data demonstrates that two compounds, PB and BP, which display similar hepatic responses *in vivo*, both induced the expression of associated miRNA markers *in vitro*. Interestingly, the induction of miR-96 expression by clotrimazole (10µM) at 3 days treatment (Figure 2.15 D) was consistent with clotrimazole's rapid induction of Cyp2b (Figure 2.13 B). Finally, we confirmed that the mouse-specific Car agonist TCPOBOP (1.5µM) did not induce either miR-182 or miR-96 under the conditions used here (Figure 2.15 E and F).

We also determined the expression of miR-200b in B13/H cells but in these samples the Ct values were such that the target was considered not to be expressed (Ct >35) (data not shown).

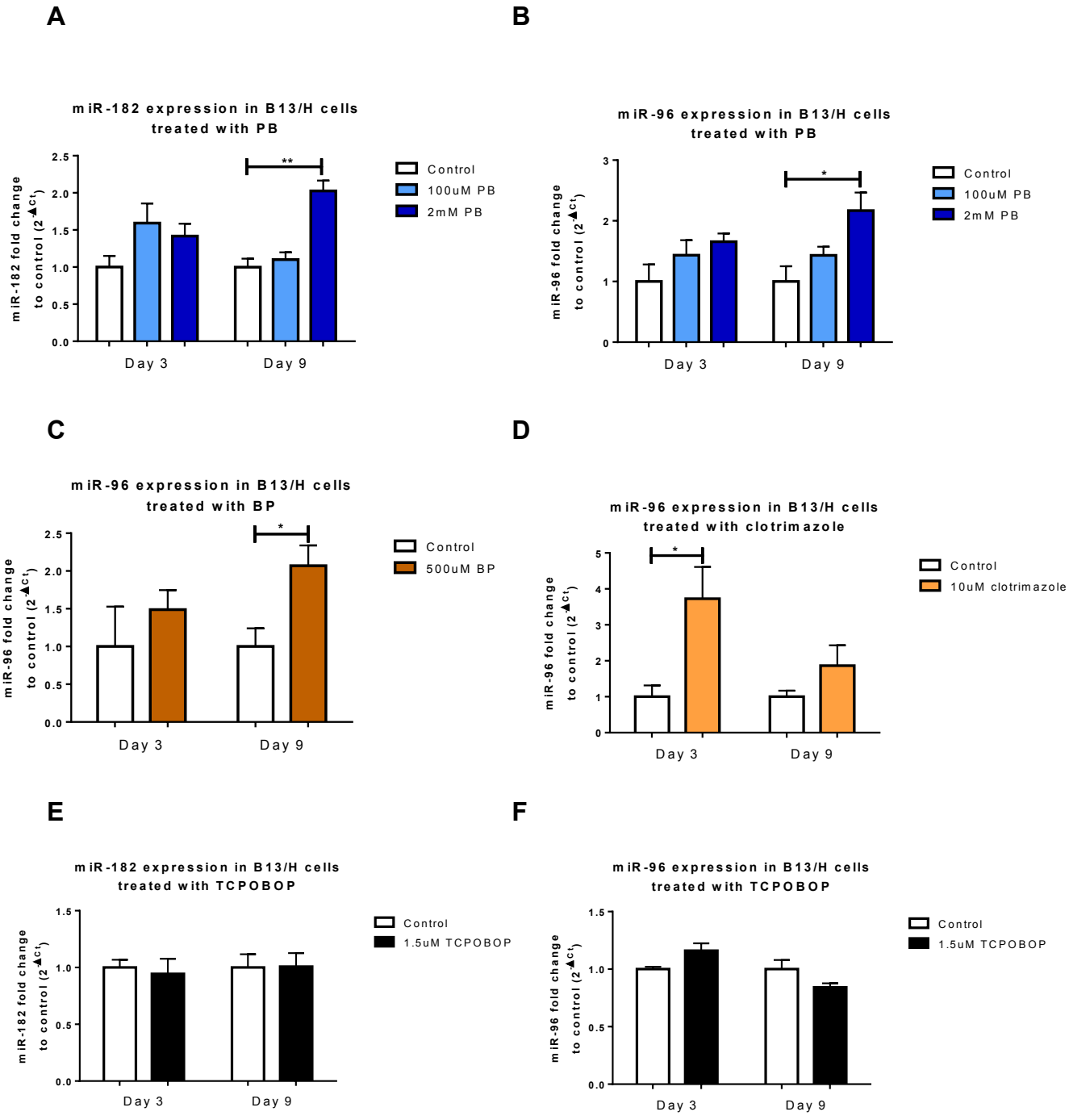


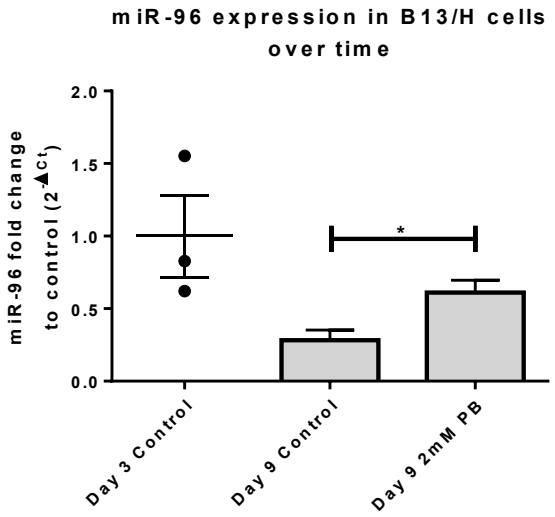
Figure 2.15: miRNA expression in B13/H cells treated with PB and PB-like compounds

Figure 2.15 shows miRNA expression by qRT-PCR of miR-182 (**A**) and miR-96 (**B**) after treatment with PB, miR-96 in response to BP (**C**) or clotrimazole (**D**) and miR-182 (**E**) and miR-96 (**F**) after TCPOBOP treatment. Results were representative of 3 independent cultures, and values were mean ± SEM using $2^{-\Delta Ct}$ to present fold change of target to time matched control. One way ANOVA with Dunnett's comparison was used to compare PB (100μM or 2mM) to control, and Student's t test compared control to PB. *p<0.05. **p<0.01.

MiRNA expression in B13 and B13/H cells Transdifferentiation of B13 to B13/H cells results in an increase in expression of miR-182 (data not shown) and PB has also been used to maintain primary hepatocytes in a differentiated state (Miyazaki et al., 1998). It is therefore possible that removal of dexamethasone and PB might result in dedifferentiation of B13/H cells and the levels of the miRNAs might be expected to reduce in the control cells over time. To explore this, I have assessed the change in miR-182 cluster partner, miR-96, over the treatment course. Figure 2.16 compares the expression of miR-96 between control samples at day 3 and control samples at day 9. The data shows that miR-96 expression, although variable, at 3 days did not significantly decrease over time in the control treatment groups (Figure 2.16 A and B). This suggests that PB was not required to maintain the hepatocyte-like phenotype in B13/H cells. Furthermore, Figure 2.15 D indicates that 3 days treatment with clotrimazole (10μM) was sufficient to induce miR-96, suggesting that the B13/H cells are responsive to PB and PB-like compounds.

Summary – Collectively these data suggest that B13/H cells produced a miRNA response similar to that seen *in vivo* in rats with PB and PB-like compounds.

A



B

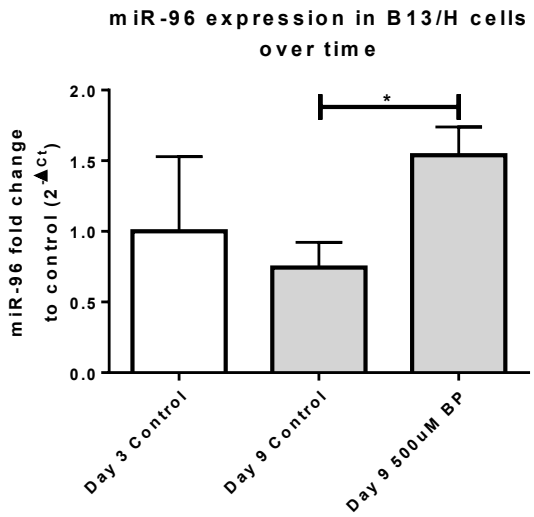


Figure 2.16: Comparing miRNA expression in B13/H cells between 3 and 9 days

Figure 2.16 shows mRNA expression by qRT-PCR of miR-96 expression in control and PB (**A**) or BP (**B**) treated B13/H cells respectively. Results were representative of 3 independent cultures, and values were mean $\pm$ SEM using $2^{-\Delta Ct}$ to present fold change of target to day 3 control. Student's t test compared day 3 to day 9 control or day 9 control to day 9 PB. *$p<0.05$.

2.4 Conclusions

B13/H cells provide Toxicologists with a reproducible, cost-effective and simple model for interrogating hepatocyte-like responses *in vitro* (Philip M. E. Probert et al., 2015). Here we demonstrated that 2 weeks dexamethasone-induced (10nM) transdifferentiated B13/H cells can respond to PB and PB-like compounds with increased Cyp2b activity as well as associated changes in miRNAs in a manner similar to the rat *in vivo* (Koufaris et al., 2012, 2013; Waterman et al., 2010).

Probert *et al.,* (Philip M E Probert et al., 2014) could not detect Cyp2b1 protein but did detect 2b1 mRNA and activity by PROD assay after PB treatment, in agreement with the data presented here. This could suggest that perhaps the induction of PROD activity is independent of Cyp2b1 protein and could involve Cyp2c11 and/or Cyp3a2 (Langouët et al., 1997). Our data suggested that although Cyp2c11 was expressed in B13/H cells, it was not induced after 6 or 24 hours PB treatment (2mM) (Figure 2.12 C and D), which is in agreement with the rat *in vivo* (Kot & Daniel, 2007). PB has been shown to induce Cyp3a2 in Sprague-Dawley and Wistar rats (Kishida et al., 2008), and CYP3A has been shown to be induced by PXR in human primary hepatocytes (Pascussi, Drocourt, Fabre, Maurel, & Vilarem, 2000); this could suggest that the Cyp450 activity measured by the PROD assay here may be through PB-mediated activation of Pxr. This could also have implications on Car expression in B13 cells discussed earlier (Figure 2.7 B and F). However, the increase in Cyp2b1 mRNA with PB treatment (Figure 2.12 A) is indicative of Car activation, which is corroborated by Marek *et al.,* (Marek et al., 2003) who show that testosterone is

metabolised in B13/H cells and that in the presence of PB generates a testosterone metabolite indicative of Cyp2b1/2 activation.

Interestingly, Probert *et al.,* (Philip M E Probert et al., 2014) show that TCPOBOP at the same dose used in our work did induce Cyp2b1 and Cyp3a1 mRNA in B13/H cells, although the reason for this was not discussed. To fully explore the possibility that B13/H cells respond to TCPOBOP a dose response should be performed. Tzameli *et al.,* (Tzameli et al., 2000) show that peak activation of a Car expression vector in HepG2 cells was at approximately 300nM TCPOBOP with an half maximal effective concentration (EC_{50}) of 20nM. TCPOBOP is a mouse Car activator, and a human Pxr activator (Moore et al., 2000), it is therefore possible that at the high concentrations used here in my study that TCPOBOP may induce Cyp450 mRNA. Nonetheless, our data demonstrates that under the conditions used herein Car activation in the B13/H cells was rat specific. However, subcellular fractionation of PB treated B13/H cells and immunoblot analysis showed that Car protein was undetectable in the cytoplasm of control or PB treated B13/H cells. This suggests that despite the B13/H cell's metabolic capacity and PB responsiveness, subcellular localisation of Car in B13/H cells was more similar to immortalised cells than to primary cells.

Chapter 2 Conclusions – Overall our data suggest that the B13/H cells are a useful model for exploring the molecular effects induced by PB and PB-like compounds, and that B13/H cells produce similar responses to PB and PB-like compounds as has been reported *in vivo* (Koufaris et al., 2012, 2013). However, future research into

characterising this model should focus on the extent of PB-mediated induction of Car and Pxr and the potential effects of TCPOBOP in this cell line. In this respect, the next chapter will focus on the interaction of PB with growth factors to begin to interrogate the role of growth factor responses in PB signalling.

3. Cross-talk between growth factor signalling and phenobarbital signalling pathways

3.1 Introduction

Chapter 2 focussed on characterising the B13/H cells and their response to PB. In this chapter I interrogate the effect of PB on epidermal growth factor (Egf) and hepatocyte growth factor (Hgf) signalling pathways to explore potential regulatory interactions with PB signalling.

3.1.1 PB antagonises Egfr in the mouse to activate Car

As discussed in chapter 1.2.3, PB indirectly activates Car through a signalling pathway, which dephosphorylates Car. This causes Car to dissociate from cytoplasmic chaperones and subsequently to translocate into the nucleus (Kawamoto et al., 1999; Kobayashi et al., 2003; Yoshinari et al., 2003). In the mouse, PB is thought to initiate these events through antagonising the Egf receptor pathway (Egfr) (Mutoh et al., 2013).

Phosphorylated & cytoplasmic Car Under growth factor stimulation the adapter protein, Shc, is phosphorylated by an activated receptor, and bound by another adapter protein, Grb2, *via* its phospho-tyrosine (Src homology 2 domain: SH2) binding domain. The guanine nucleotide exchange factor, Sos, is then recruited, which facilitates activation of ras through the transfer of GTP to ras (Ravichandran, 2001). Raf can then bind to ras *via* its ras-binding domain, resulting in a number of

de-phosphorylation and phosphorylation steps to activate raf. Raf then binds, phosphorylates and activates Mek1/2, which binds, phosphorylates and activates extracellular signal regulated mitogen-activated kinase (Erk)1/2 (Matallanas et al., 2011). Osabe and Negishi (Osabe & Negishi, 2011) reported that 2mM PB was able to inhibit Erk signalling in mouse primary hepatocytes, which is believed to be associated with decreased phosphorylation of Car (Figure 3.1). Furthermore, both Egf (10µg/mL) and Hgf (10µg/mL) were able to inhibit 1.5mM PB induced expression of Cyp2b10 mRNA in mouse primary hepatocytes, which the authors attributed to Erk activation (Koike et al., 2007). Activated Erk was suggested as the intrinsic cell signal for Car phosphorylation, which maintains Car in the cytoplasm; thereby inhibiting Car-mediated gene transcription (Koike et al., 2007; Osabe & Negishi, 2011).

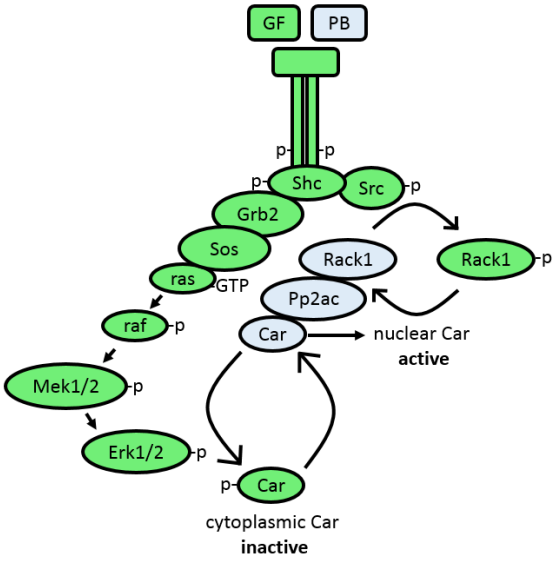


Figure 3.1: Activation of Car by PB in the mouse

Figure 3.1 PB is reported to antagonise growth factor signalling in the mouse to induce Car translocation to the nucleus. Growth factor-mediated cytoplasmic sequestration of Car is shown in green, while the antagonistic PB-induced response is shown in blue. Adapted from (Matallanas et al., 2011; Mutoh et al., 2013).

Dephosphorylated & nuclear Car Shc can also interact with Src *via* their proline rich domains (Src homology 3 domain: SH3) (Ravichandran, 2001). Active Src has been reported to phosphorylate receptor for activated C kinase (Rack)1 and abolish Rack1 association with protein phosphatase 2a (Pp2ac) (Mutoh et al., 2013). Mutoh *et al.,* (Mutoh et al., 2013) reported that PB-mediated antagonism of the Egfr enabled de-phosphorylation of Car by co-recruitment of de-phosphorylated Rack1 to Pp2ac (Figure 3.1), which is known to be the signal for Car nuclear translocation (Mutoh et al., 2013). Rack1 is a scaffold protein involved in stabilising, anchoring and shuttling proteins within the cell (Adams, Ron, & Kiely, 2011).

Therefore, it is thought that in the mouse PB indirectly activates Car through antagonism of the Egfr and through inhibition of the downstream kinase, Erk.

3.1.2 Effects of Egf on PB-mediated gene transcription in the rat

Cyp2b1/2 mRNA were significantly induced by 2mM PB in Male Wistar rat primary hepatocytes. This induction was shown to be inhibited by simultaneous treatment with Egf (20ng/mL), which was also able to suppress PB-mediated induction of *Ugt2*. Treatment with Hgf (20ng/mL) was unable to inhibit the expression of either *Cyp2b1/2* or *Ugt2* by PB (Kawamura et al., 1999). The ability of Egf (10ng/mL) to inhibit PB-mediated (1.5mM) expression of Cyp2b mRNA and activity were also demonstrated by Aubrecht *et al.,* (Aubrecht et al., 1995) in male Wistar rats. Furthermore, indirectly inhibiting Erk1/2 through inhibition of its upstream kinase, Mek1/2, augmented PB-mediated induction of *Cyp2b1/2* and *Cyp3a1/2* (F Joannard et al., 2000; Florence Joannard et al., 2006). These data here suggest that Erk

inhibits expression of PB-regulated genes in the mouse and rat. Interestingly, Joannard *et al.,* (Florence Joannard et al., 2006) reported that 15 minute treatment with 5mM PB increased Erk activity in male Sprague-Dawley rat primary hepatocytes. However, it is not clear to what extent PB interacts with the Egfr pathway in rat B13/H cells, compared to primary rat hepatocytes.

To begin to explore the association with PB and the Egfr pathway in the rat I have utilised the B13/H cells described in chapter 2 in combination treatments with PB plus Egf or Hgf. Hgf was included to determine if the PB interaction was specific to the Egfr pathway, as indicated above. In order to begin interrogating these pathways, 2 common downstream kinases (Berasain et al., 2009) were chosen to assess changes in activity with the combination treatments: (1) Erk was selected as it was reported that PB modulated Erk activity in mouse primary hepatocytes (Osabe & Negishi, 2011), and rat primary hepatocytes (Florence Joannard et al., 2006); (2) Akt was chosen as it has previously been reported that the Akt activator, Pi3k, had minimal effect on PB-mediated *Cyp* expression (F Joannard et al., 2000).

3.1.3 Hypothesis

If B13/H cells resemble primary rat hepatocytes, then PB will augment Egf-induced Erk activity but not Akt activity. Furthermore, neither Hgf-induced Erk, nor Akt activity will be affected by PB treatment.

3.1.4 Aims

4. Optimise growth factor treatment dose and time for Erk and Akt activation in B13/H cells.
5. Assess the B13/H cell response to PB in combination with either growth factor to determine potential roles of these signalling pathways in the rat.
6. Assess the activation of these pathways in the rat *in vivo*.

3.2 Methods

3.2.1 Tissue Samples

Ethics approval and *in vivo* experimentation were conducted by Syngenta. This study has been previously described (Waterman et al., 2010). Briefly, male Fischer rats were fed a diet containing 1000ppm PB or control diet *ad libitum* for 90 days with liver collections at 1, 3, 7, 14 and 90 days. These samples were snap frozen and stored at -80^{o}C, until thawed for protein extraction. All studies were performed on left lobe liver samples.

3.2.2 Cell culture

As detailed in chapter 2.2.1.

Culture conditions were as previously described with 13 days differentiation with 10nM dexamethasone. Cell media was then replaced with dexamethasone-free, 5% heat inactivated dextran coated charcoal (HI-DCC) stripped FBS supplemented media for 24 hours before PB treatment for 72 hours to assess changes in Cyp2b activity by PROD, or for 72 hours prior to growth factor treatments.

3.2.3 Cell counts & alamarBlue®

Cell counts were performed using the Moxi Z (ORFLO, Ketchum, ID). Cells were passed through a passage with a voltage applied, as the cells move through, the Moxi measures the number of cells and their volume relative to the impedance of the voltage (http://orflo.com/howitworks.html).

AlamarBlue® can be used to measure cell viability. Viable cells incorporate the assay's non-fluorescent compound, resazurin, which is reduced in the cytosol to the fluorescent product, resorufin. The production of resorufin is dependent on cytosolic reducing enzymes and is proportional to the number of cells, and so this assay is often used to determine viability/proliferation, and has been shown to be comparable with, and a quicker assay than, [^{3}H]thymidine incorporation (Ahmed, Gogal, & Walsh, 1994). Data obtained in collaboration with Mariana Flores-Torres (Figure 3.2) demonstrates the change in alamarBlue® reduction is proportional to B13/H cell density.

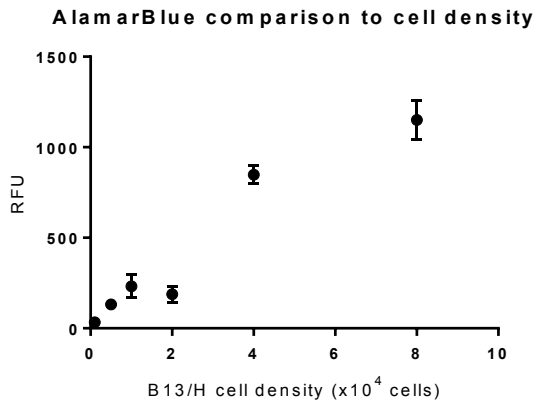


Figure 3.2: Alamar blue reduction

Figure 3.2 shows the relative fluorescence units (RFU) from alamarBlue® reduction at different cell densities, from 3 independent cultures.

3.2.4 Cyp450 enzyme activity - PROD

Pentoxyresorufin-*O*-dealkylase (PROD) assay was used to determine Cyp2b activity, as described in chapter 2.2.2.

3.2.5 Chemical treatments – cell signalling

To explore the roles of growth factors and phenobarbital signalling, B13/H cells were treated with rat epidermal growth factor (Egf) (Sigma-Aldrich, Dorset, UK) (solvated in 0.1% bovine serum albumin [BSA]) or human hepatocyte growth factor (Hgf) (PeproTech EC Ltd, London, UK) (solvated in 0.1% BSA), with specific inhibitors to the Egf receptor, Erlotinib (Cayman Chemical, MI, USA) (made to concentration in DMSO), or to the Hgf receptor, SU11274 (VWR International Ltd, Leicestershire, UK) (solvated in DMSO), in combination with phenobarbital (made up in 5% stripped media). Treatment combinations are described in figure legends. B13 cells were seeded at $4x10^4$ cells per well in 24-well plates and differentiated as described previously. At 13 days differentiation the cell culture media was substituted for media containing 5% HI-DCC-stripped FBS for 72 hours prior to any treatments with growth factors to reduce background signalling (http://www.lifetechnologies.com/uk/en/home/life-science/cell-culture/mammalian-cell-culture/fbs/specialty-serum/charcoal-stripped-fbs.html; date accessed 14/06/2015). Protein was harvested from samples and subsequently analysed by immunoblotting as described below.

3.2.6 Immunoblots

Unless stated otherwise chemicals were obtained from Sigma-Aldrich (Dorset, UK).

Cell lysis Cell samples were lysed directly from the culture plate on ice after washing with ice cold PBS. Lysis was performed with RIPA buffer containing Halt

Protease Inhibitor and phosphatase inhibitor cocktail 2 and 3 (at final dilutions of 1:100) for at least 10 minutes. In order to assess phospho-proteins by immunoblot it was important to use phosphatase inhibitor cocktails 2 and 3, to inhibit tyrosine and serine/threonine phosphatases respectively. The cell lysate was centrifuged at 10,000g to collect the soluble protein supernatant.

Tissue lysis Frozen rat liver tissue samples of 50-100mg were homogenised in lysis buffer prepared in dmH_2O with constituents: Igepal (0.1%), sodium chloride (NaCl) (150mM), tris (1mM) (Fisher Scientific, PA, USA), edetic acid (EDTA) (1mM) and Halt Protease Inhibitor and phosphatase inhibitor cocktail 2 and 3 (at final concentrations of 1:100), using a T25 basic IKA Labortechnik tissue homogeniser. Samples were incubated on ice for 10 minutes then centrifuged at 10,000g to pellet insoluble material. Supernatant was collected for protein quantification.

Protein concentration was quantified using the BCA assay, as described in chapter 2.2.3.

SDS-PAGE gel preparation An acrylamide resolving gel (10% acrylamide/bis-acrylamide) under reduced (i.e. β-mercaptoethanol in the loading buffer) and denaturing conditions (i.e. SDS, and sample heating) was prepared with constituents: Tris (500mM), sodium dodecyl sulphate (SDS) (3.4mM), ammonium persulphate (APS) (2.7mM) and tetramethylethylenediamine (TEMED) (10.3mM). A bis-acrylamide (5%) stacking gel was set on top of the resolving gel, containing Tris

(284mM), SDS (7.9mM), APS (8.7mM) and TEMED (6.6mM), and a 15 well 1.5mm well-forming comb was set in place.

Sample preparation Protein samples were lysed and then quantified by the BCA assay as mentioned above. Samples were diluted to 1µg/µL. Twenty micrograms of protein per sample were loaded with 5µL SDS loading buffer, containing SDS (350mM), Tris-HCl (200mM), glycerol (2.7M), bromophenol blue (1.6mM) and supplemented with β-mercaptoethanol (1:20). Samples and biotinylated protein ladder (Cell Signalling, MA, USA) were heated to 95^{o}C for 5 or 2 minutes, respectively, and then centrifuged at 4,000g for 5 minutes. Samples, biotinylated protein ladder and Novex Sharp pre-stained protein standard (Life Technologies, Paisley, UK) were then loaded into the prepared gel.

Gel electrophoresis Upon addition of a current, proteins migrate down an agarose gel relative to their mass and charge. Samples were run at 60V through the 5% gel until they were stacked along the junction with the 10% gel. Samples were then run at 100V to separate proteins in order of size. Electrophoresis was performed using Biorad tanks, containing a running buffer of tris (2.5mM), glycine (25mM), and SDS (3.5mM).

Protein transfer Protein was transferred onto a protran nitrocellulose membrane (0.45µm pore) (Bio-Rad, Hertfordshire, UK) pre-soaked in a Tris-glycine-methanol transfer buffer (25mM-186mM-20%v/v). The protein was transferred from gel to

membrane through semi-dry or wet transfer. For semi-dry transfer a BioRad Trans-Blot SD semi-dry electrophoretic transfer cell was used running at 20V for 40 minutes. For wet transfers Biorad tanks were used with samples transferred at 150V for 1 hour 20 minutes. Successful transfer was checked using the protein dye Ponceau S solution.

Immunoblotting Membranes were blocked for one hour in a blocking buffer containing skimmed milk (5%) made up in PBS-Tween20 (0.1% Tween20). Blocking limits nonspecific binding of subsequent antibodies. Between blocking and antibody incubations, membranes were washed 3x 5 minutes with PBS-Tween20 to remove contaminants. Target proteins were visualised using antibodies diluted in a blocking buffer. Protein-fixed nitrocellulose membranes were incubated with primary antibodies overnight at 4^{o}C or at room temperature for 2 hours, and incubations with secondary antibodies were at room temperature for 2 hours. In cases where phospho-antibody and total antibody were used, the blot was stripped using reblot solution (Millipore, MA, USA) for 20 minutes, after first visualising the phospho-target protein. Secondary antibodies were linked to horseradish peroxidase (HRP), which oxidises luminol in a chemiluminescence reaction and this was detected on a Gel Doc XR+ System (Kodac). Luminata Forte (Millipore, MA, USA) was used as the substrate for the chemiluminescence.

Primary antibodies mouse α-Gapdh (1:1,000 dilution, Abcam ab8245), rabbit α-β-tubulin (1:500, Abcam ab6046), rabbit α-Akt (1:200, Santa Cruz sc-8312), rabbit α-pAkt (Ser 473) (1:350, Santa Cruz sc-7985-R), rabbit α-Erk (1:200, Santa Cruz sc-

94), mouse α-pErk (human tyr 204) (1:200, Santa Cruz sc-7383), rabbit α-Elk1 (1:200, Santa Cruz sc-355), mouse α-pElk1 (Ser 383) (1:200, Santa Cruz sc-8406), rabbit anti-FoxO1A (1:1000, Abcam ab133893) and rabbit anti-pFoxO1A (Ser 256) (1:500, Abcam ab131339).

Secondary antibodies α-biotin-HRP (1:1,000, Cell signalling #7075P5), goat α-mouse-HRP (1:10,000, Abcam ab6789), goat α-rabbit-HRP (1:5,000, Abcam ab97051).

3.2.7 Meso Scale Discovery (MSD) multi-spot assay system

The MAP Kinase Phosphoprotein Assay Whole Cell Lysate Kit (MSD, MD, USA) was used to quantify the levels of phospho-p38 at Thr180/Tyr182, phospho-Erk1/2 at Thr202/Tyr204 and Thr185/Tyr187 and phospho-Jnk at Thr183/Tyr185 in the rat liver samples following the manufacturer's protocol. Briefly, the assay plate was blocked with a kit derived blocking solution to prevent non-specific binding of proteins, and then washed to remove excess solution. Samples were loaded at 20µg of tissue lysate per well. Each well was pre-coated with three different antibodies, one antibody for phospho-p38, one for phospho-Erk1/2 and one for phospho-Jnk, with each antibody located in its own spot within the well. The analytes of interest bind to the capture antibodies by incubating the plate and samples at room temperature for 3 hours on a plate shaker (500 rpm). The plate was washed again to remove unbound sample and the detection antibodies were added. The detection antibodies were diluted to a final concentration of 1:50 and bind to the sequestered analyte, recognising total p38, total Erk1/2 or phospho-Jnk. The detection antibodies were

conjugated with an electrochemiluminescent tag that emits light when a voltage is applied during measuring of the assay plate on a SECTOR Imager 2400A, allowing the relative levels of each analyte to be quantified.

3.2.8 Statistics

In vitro as described in chapter 2.2.8.

In vivo statistics were also performed using Graph Pad 6 as above, except showing standard deviation (SD) and comparing treatment groups with control using Mann-Whitney.

3.3 Results and Discussion

3.3.1 Aim 1: Optimise growth factor treatment dose and time for Erk and Akt activation in B13/H cells.

3.3.1.1 Optimising treatment doses

B13/H cells were differentiated for 2 weeks with 10nM dexamethasone as detailed in chapter 2. Upon differentiation, dexamethasone was removed and cells were cultured in 5% HI-DCC stripped FBS supplemented media for 72 hours prior to growth factor treatments. HI-DCC stripped FBS was used in order to reduce the background signal of growth factor signalling pathways. As a quick and effective method to test Hgf and Egf dose responses in the B13/H cells, the alamarBlue® assay was used.

Growth factors B13/H cells were treated with a dose range of Hgf (1-50ng/mL) (Figure 3.3 A) or Egf (0.1-10ng/mL) (Figure 3.3 B) for 24 hours. The dose range for Hgf was selected based on Kawamura *et al.,* (Kawamura et al., 1999) who reported that Hgf (20ng/mL) did not inhibit *Cyp2b* expression induced by PB (2mM). The dose range for Egf was based on the report by Aubrecht *et al.,* (Aubrecht et al., 1995) who demonstrated that Egf (10ng/mL) could inhibit the induction of *Cyp2b* by PB (1.5mM).

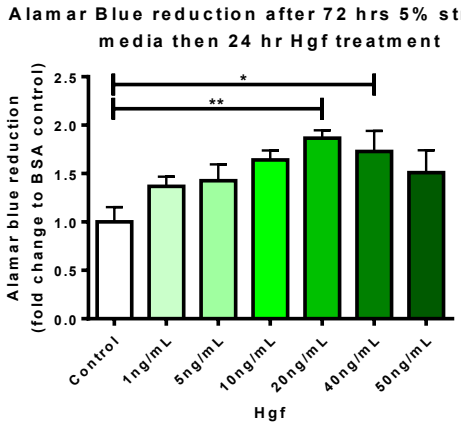
Hgf produced a significant dose-dependent increase in resorufin production up to 20ng/mL (Figure 3.3 A). Egf also significantly increased resorufin production in a dose-dependent manner up to 10ng/mL (Figure 3.3 B). This response was lost after

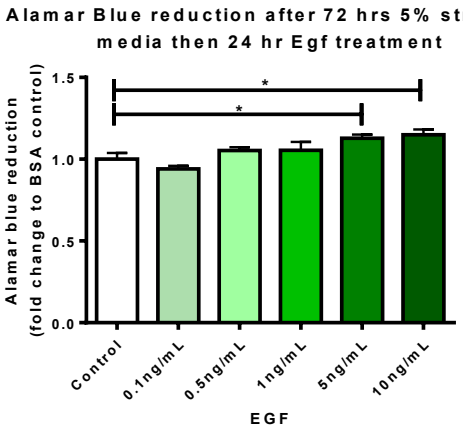
48 hours for Hgf and Egf (data not shown). It has been previously reported that B13/H cells do not proliferate in the presence of Egf (100ng/mL) (Philip M E Probert et al., 2014) for 4 days, as measured by bromodeoxyuridine (BrdU) incorporation during S phase of the cell cycle. The disparity between the data presented here and that of Probert *et al.,* (Philip M E Probert et al., 2014) could be due to the different treatment times used, as the data shown here indicated a minimal and transient effect of mitogens only at 24 hours treatment. However, as B13/H cells cultured in normal media are quiescent, and the Hgf- and Egf-mediated increase in resorufin production shown here are transient, it would suggest that Hgf and Egf may be inducing signalling activities that resulted in resorufin production, but not stimulating proliferation within the cells. This was confirmed using a cell count assessment (data not shown).

Summary – Twenty ng/mL Hgf and 5ng/mL Egf were selected as optimal treatment doses for B13/H cells.

3. Cross-talk between growth factor signalling and phenobarbital signalling pathways

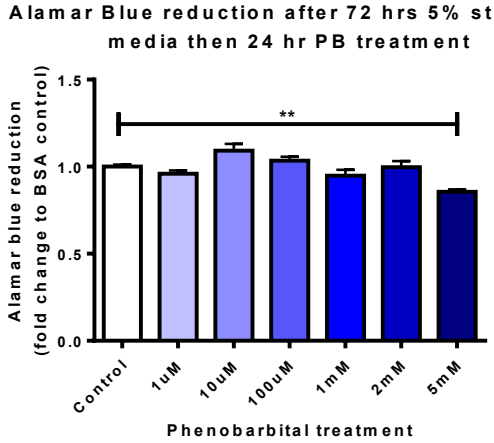
A



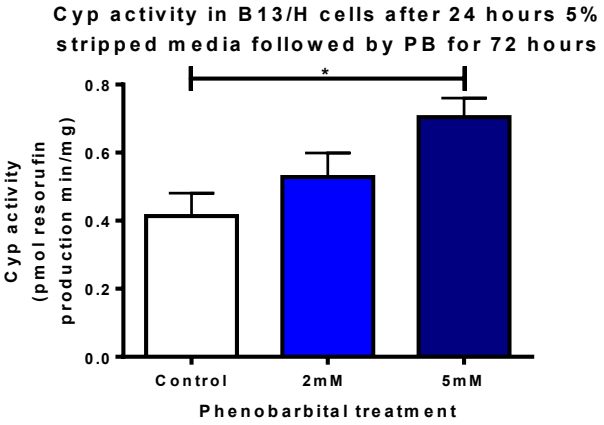


B

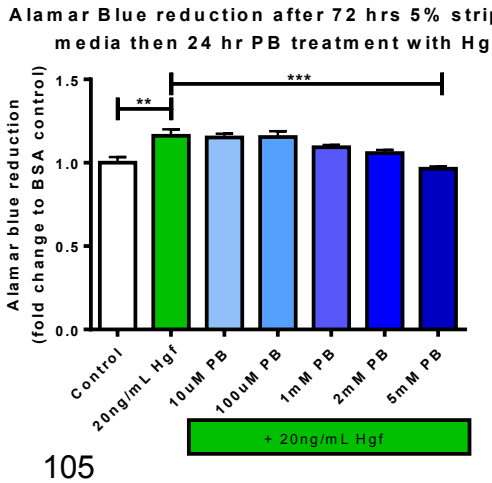
C



D



E



F

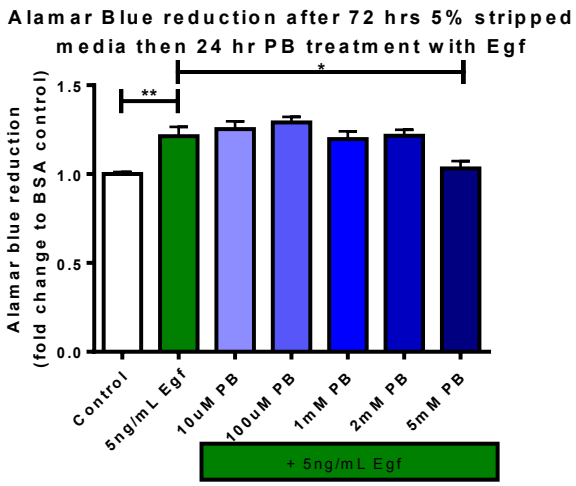


Figure 3.3: Growth factor and PB dose response

Figure 3.3 shows alamarBlue® reduction of B13/H cells treated with a dose range of Hgf (n=3) (**A**), Egf (n=4) (**B**), or PB (n=4) (**C**) for 24 hours, or in combination (**E**/**F**) (n=3/4). Cyp2b activity in B13/H cells after 72 hours PB treatment in 5% stripped media (5% HI-DCC stripped FBS supplemented media) was shown (n=4) (**D**). Data were mean ± SEM, with y-axis as fold change to vehicle control. Significance was tested by one way ANOVA with Dunnett's comparison to respective control, or Student's t test comparing control with growth factor alone.

PB The effect of PB on alamarBlue® reduction was then assessed. PB alone (10μM-5mM) for 24 hours was shown not to be mitogenic, and at the highest concentration (5mM) showed a decrease in resorufin production (Figure 3.3 C). Furthermore, 5mM PB was able to significantly induce Cyp2b activity as determined by PROD, after 72 hours treatment in 5% HI-DCC stripped FBS supplemented media (Figure 3.3 D).

PB plus growth factors Previous work has suggested that PB ≤1.5mM in combination with Egf was mitogenic, yet higher doses suppressed proliferation in primary rat hepatocytes (Jirtle & Meyer, 1991). Treating B13/H cells with Hgf (20ng/mL) or Egf (5ng/mL) in the presence of PB (10μM-5mM) for 24 hours, we failed to reproduce the biphasic effect of PB as reported by others (Figure 3.3 E and F). However, 5mM PB was suppressive in these co-treatments, reducing resorufin production to a level comparable to control cells.

Summary – Five mM PB was selected as the optimal treatment dose for combination treatments with growth factors.

3.3.1.2 Optimising growth factor treatment time for Erk and Akt activity

To confirm a functional growth factor signalling response and optimal treatment duration, B13/H cells were treated with 20ng/mL Hgf for 30, 60, 90 and 120 minutes and Erk and Akt activity were assessed by immunoblots (Figure 3.4). Treatment for up to 90 minutes with Hgf significantly increased Erk (Figure 3.4 A) and Akt (Figure 3.4 B) activation (as measured by a ratio of phospho-protein to total protein) compared to time-matched control. The immunoblots shown (Figure 3.4 C and D) demonstrated clear changes in phospho-protein compared to control.

Summary – Hgf treatment induced significant activation in Erk and Akt up to 90 minutes, therefore 60 minutes and 90 minutes growth factor treatments were selected as optimal for treatment combinations.

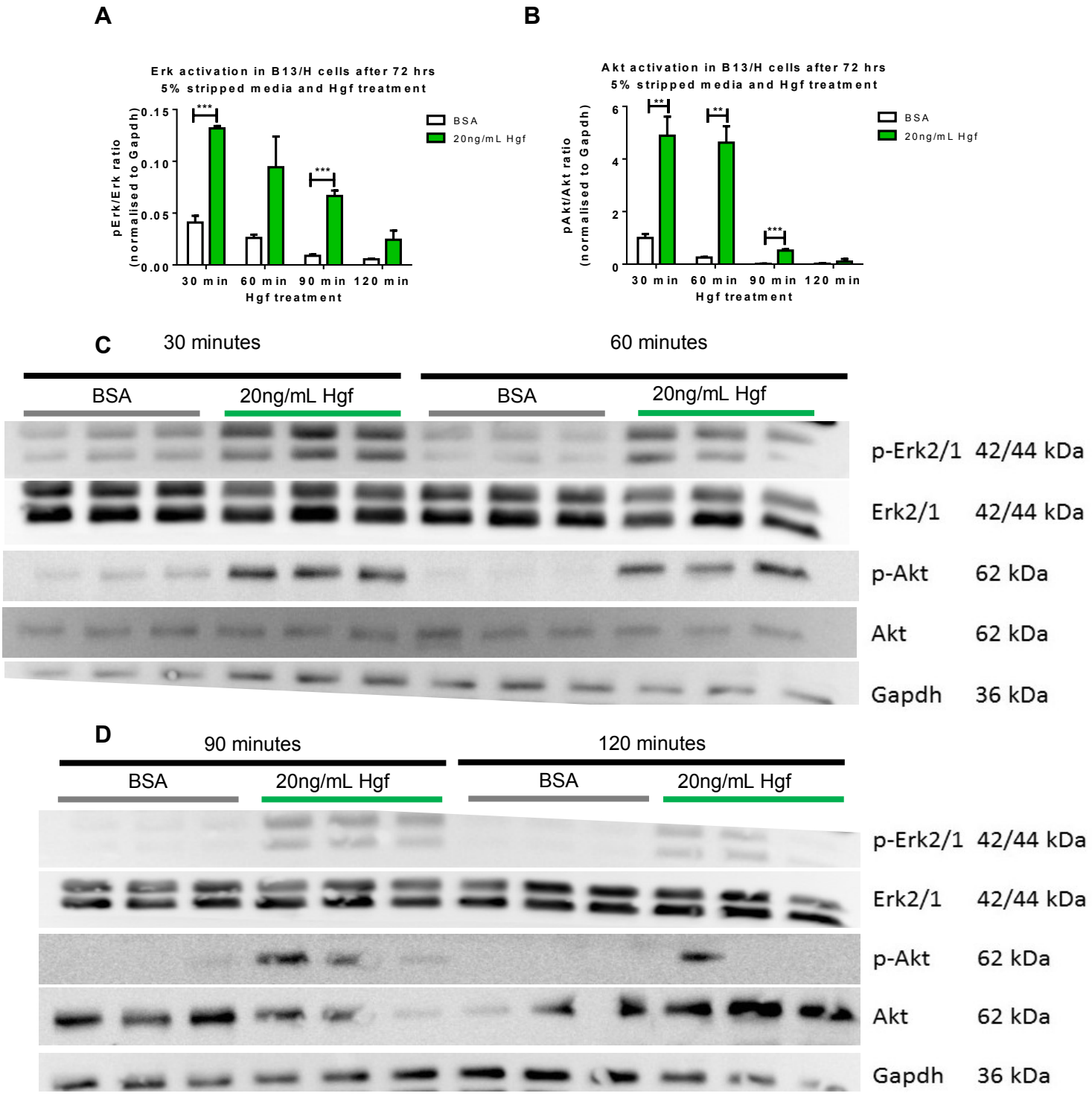


Figure 3.4: Twenty ng/mL Hgf time response - Erk/Akt activity

Figure 3.4 details Hgf activation on Erk (**A**) and Akt (**B**) signalling pathways after 30-120 minutes treatment, with immunoblots shown for 30-60 mintes (**C**) and 90-120 minutes (**D**). Data were representative of 3 independent cultures, showing mean ± SEM and with y-axis as Erk and Akt activity measured as a ratio of phospho-protein to total protein normalised to Gapdh. Significance was tested by Student's t test comparing time matched vehicle with Hgf.

3.3.1.3 Effect of phenobarbital alone on Erk or Akt pathway activity in B13/H cells

PB (2mM) treatment for 1 hour has been shown to reduce Erk activity in male C3H mouse primary hepatocytes (Osabe & Negishi, 2011). This was not reproduced by us in rat B13/H cells when treated with PB alone (Figure 3.5 A). This is in concordance with the alamarBlue® data showing that PB alone was not mitogenic (Figure 3.3 C). However, the inhibition of Erk (and Akt) activity with erlotinib (Figure 3.5 A (and B)) was found to not be significant and the data reported here was interpreted with caution. Therefore, through stimulating pathway activation with growth factors I aim to increase Erk and Akt pathway signalling to interrogate the effect of PB on these pathways.

A lower dose of PB (1μM) was chosen after preliminary alamarBlue® data suggested resorufin production at this dose (data not shown). In this experiment and subsequent experiments using Egf, the Egfr inhibitor, erlotinib was included as a negative control. Erlotinib inhibits the Egfr by competing with ATP for its receptor binding site (Schettino, Bareschino, Ricci, & Ciardiello, 2008); the dose chosen demonstrated effective inhibition of EGF-induced (10ng/mL) EGFR phosphorylation with 10μM erlotinib (Buck et al., 2006). The Erk phospho-residue measured here, is the same as that assessed by Osabe and Negishi (tyrosine-204) in the mouse (Osabe & Negishi, 2011), although the antibody used by Osabe and Negishi also recognised threonine-202. These 2 residues are both phosphorylated by mitogen-activated protein kinase kinase (Mek) and both require phosphorylation for full activation of Erk (Butch & Guan, 1996).

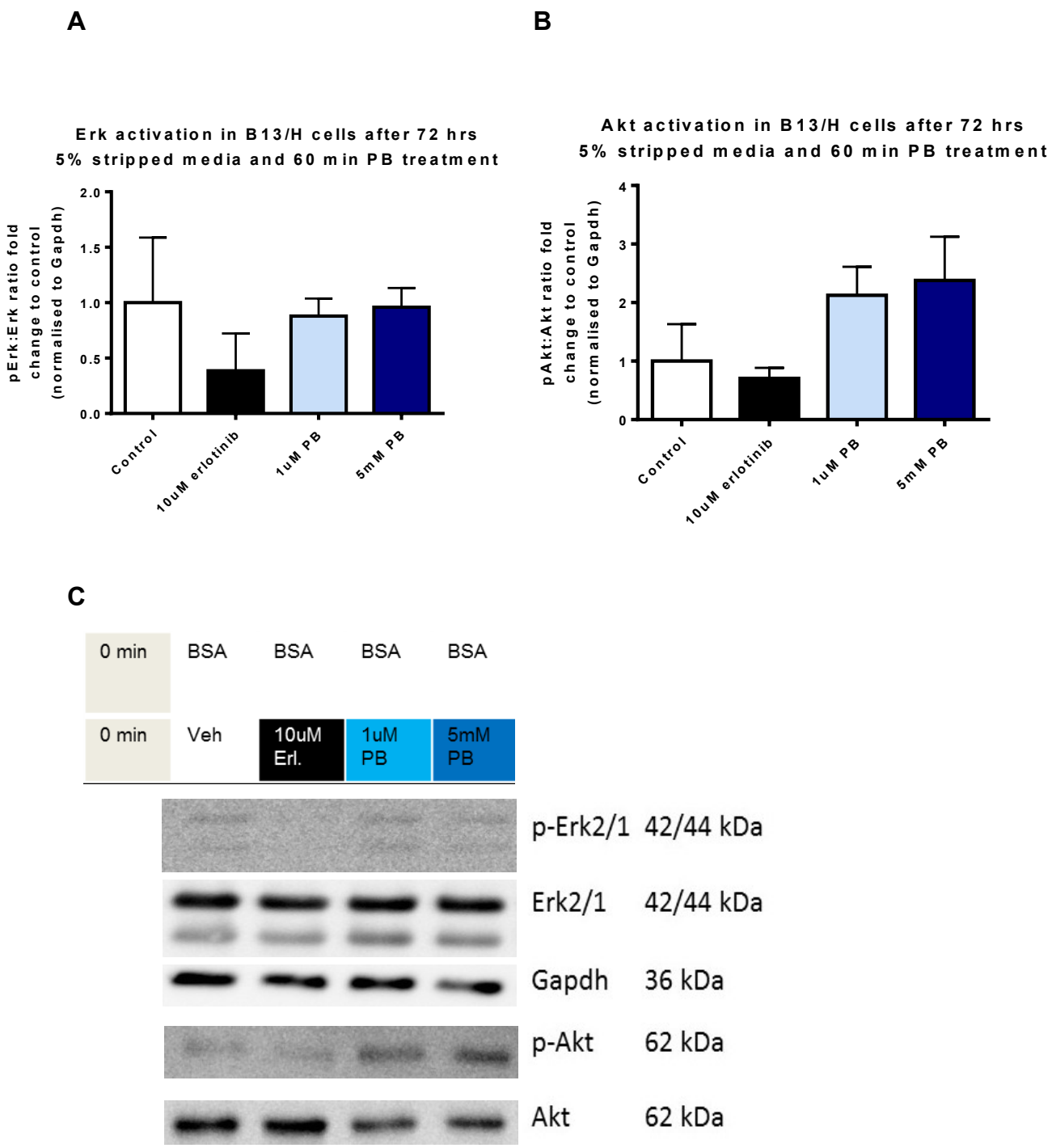


Figure 3.5: Sixty minute PB treatment - Erk/Akt activity

Figure 3.5 details the effect of 60 minutes PB on Erk (**A**) and Akt (**B**) activity. Representative blots shown (**C**). Data were representative of 3 independent cultures, showing mean ± SEM and with y-axis as fold change to vehicle control. Erk and Akt activity were measured as a ratio of phospho-protein to total protein normalised to Gapdh from 3 separate immunoblots. Significance was tested by one way ANOVA with Dunnett's comparison to control.

3.3.2 Aim 2: Assess the B13/H cell response to PB in combination with either growth factor to determine potential roles of these signalling pathways in the rat.

3.3.2.1 Phenobarbital potentiates Egf-mediated Erk and Akt phosphorylation in B13/H cells

As described previously, Mutoh *et al.,* (Mutoh et al., 2013) reported that the Egfr acted as the PB receptor, in which PB antagonised Egfr phosphorylation to allow the nuclear translocation of Car and gene transcription. The authors demonstrated that in mouse primary hepatocytes, Egfr phosphorylation induced by 30 minutes pre-treatment with Egf (100µg/mL) could be antagonised by the addition of PB (2.5mM), and that pre-treating with PB for 30 minutes could retard the effects of Egf. However, using optimized treatment conditions, treating B13/H cells with PB (5mM) for 30 minutes followed by Egf (5ng/mL) for 60 minutes resulted in a significant increase in both Erk and Akt phosphorylation compared to Egf alone (Figure 3.6 A and B respectively). PB with growth factor vehicle did not significantly alter pathway activation (Figure 3.6 A and B).

If the treatment of the B13/H cells with PB responded similarly to the mouse it would be expected that PB would suppress Erk phosphorylation while have no effect on Akt, yet surprisingly, PB increased Egf-mediated phosphorylation of both Erk and Akt. This is in agreement with the data from Joannard *et al.,* (Florence Joannard et al., 2006) who reported that PB increased Erk activity in primary rat hepatocytes. This suggests that in B13/H cells, unlike in the mouse, Erk is activated by PB. The

function of increased Erk may be as a negative regulator of PB-mediated activation of Car genes. This was indicated by Mek inhibition, which has been shown to potentiate PB induction of Cyp2b1/2 and Cyp3a1/2 mRNA expression in male Sprague-Dawley rat primary hepatocytes (F Joannard et al., 2000; Florence Joannard et al., 2006). Assessing Cyp gene expression in B13/H cells under these treatment conditions would confirm the negative feedback of Erk activity.

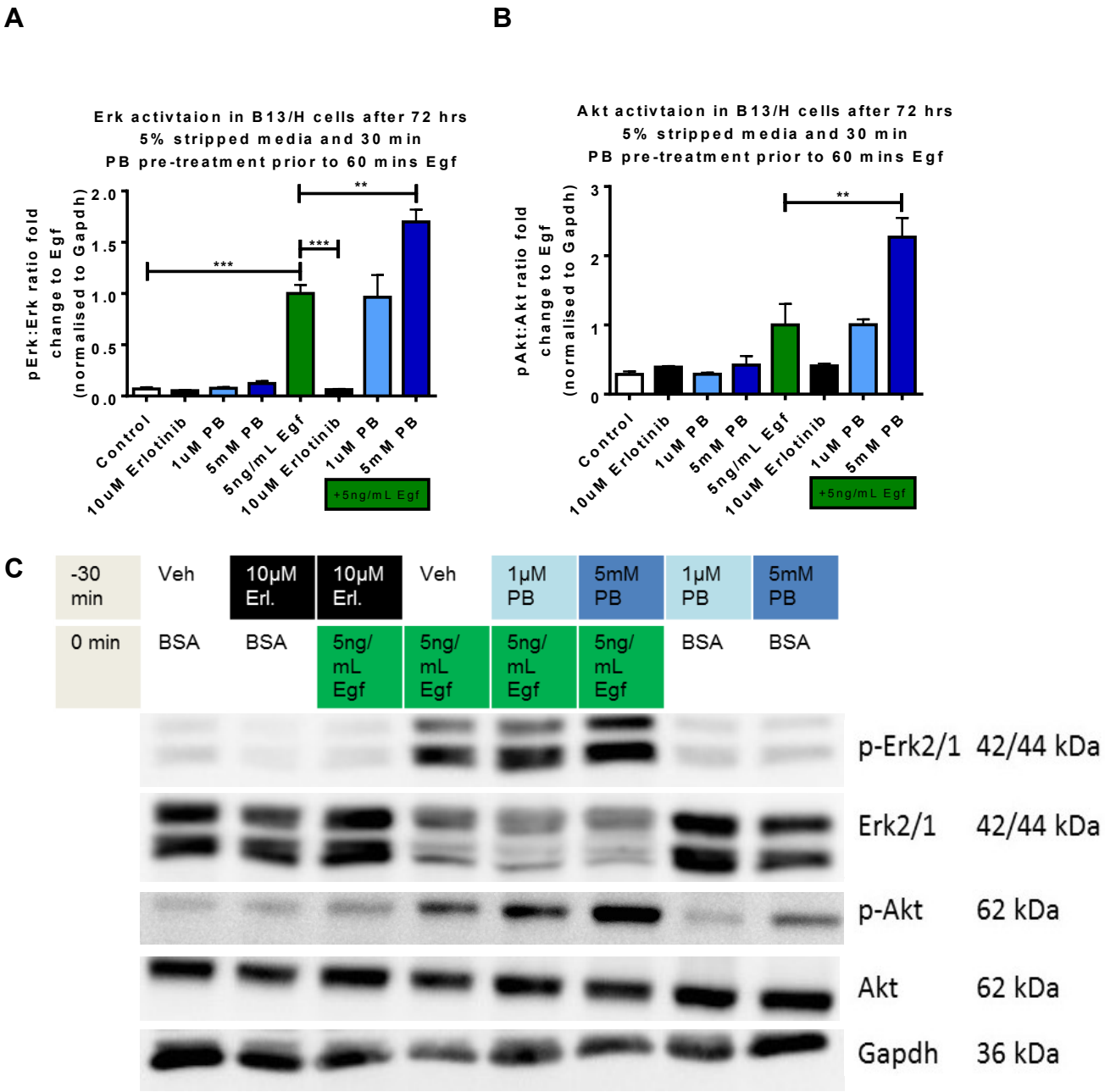


Figure 3.6: Thirty minutes treatment with PB followed by 60 minutes with 5ng/mL Egf - Erk/Akt activity

Figure 3.6 shows the effect of pre-treating PB or inhibitor for 30 minutes followed by BSA vehicle or Egf (5ng/mL) for 60 minutes on Erk (**A**) and Akt (**B**) activity. Representative blots shown (**C**). Data were representative of 3 independent cultures, showing mean ± SEM and with y-axis as fold change to Egf alone. Erk and Akt activity were measured as a ratio of phospho-protein to total protein normalised to Gapdh from 3 separate immunoblots. Significance was tested by one way ANOVA with Dunnett's comparison to control or Egf alone, and Student's t test to compare control with Egf alone.

Summary – PB has the ability to potentiate Erk and Akt phosphorylation in the presence of Egf in rat B13/H cells. These data suggest Egf-Erk could be involved in PB-mediated gene expression, and that gene expression in B13/H cells in response to PB is likely to be similar to that of rat primary hepatocytes. The function of Akt is discussed below.

3.3.2.2 Phenobarbital potentiates Hgf-mediated Akt phosphorylation in B13/H cells

Regulation of PB-induced genes in the rat has been reported to be controlled by Egf but not Hgf (Kawamura et al., 1999). Therefore rat B13/H cells were treated with Hgf (20ng/mL) for 60 minutes, after pre-treatment with PB (5mM) for 30 minutes. This potentiated Hgf-induced Akt activity, but was not as obvious for Erk activation (Figure 3.7 A and B). Interestingly, PB treatment (5mM) in the absence of Hgf (90 minutes total treatment time) resulted in increased Akt activity (although not significant) (Figure 3.7 B and C). This suggests that PB may influence Akt activation independently of growth factor treatments. A trend for increased Akt activation was also noted in Figure 3.5 B and Figure 3.6 B without growth factors, albeit at lower levels than seen in Figure 3.7 B. The Hgf receptor inhibitor, SU11274 (100nM), was included as a negative control (Berthou et al., 2004). Unfortunately, at 100nM SU11274 there was no effect on pathway activity (data not shown). These data suggest this inhibitor may not be effective in these cells, or require a higher dose.

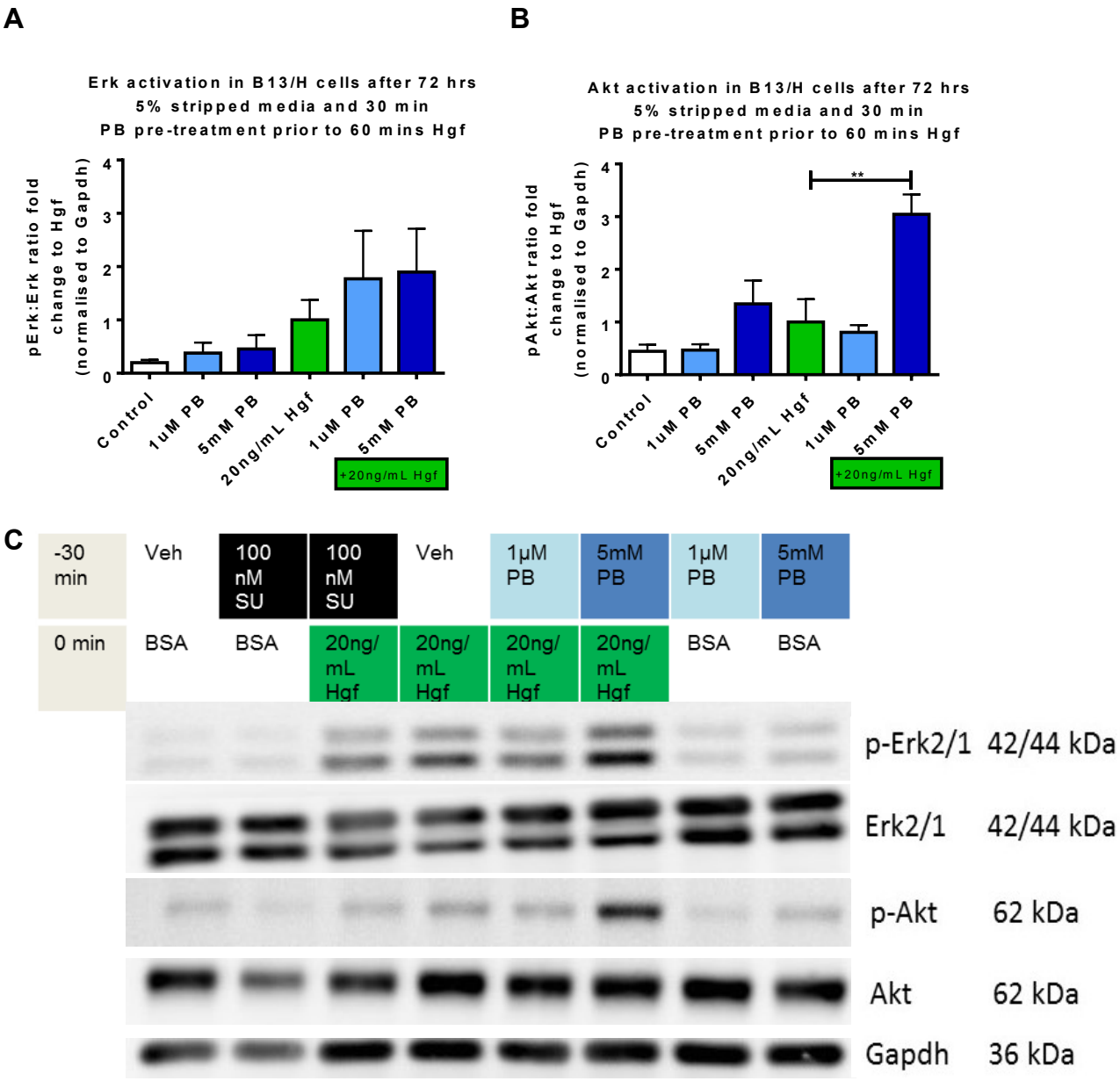


Figure 3.7: Thirty minutes treatment with PB followed by 60 minutes with 20ng/mL Hgf - Erk/Akt activity

Figure 3.7 shows the effect of pre-treating PB or inhibitor for 30 minutes followed by BSA vehicle or Hgf (20ng/mL) for 60 minutes on Erk (**A**) and Akt (**B**) activity. Representative blots shown (**C**). Data were representative of 3 independent cultures, showing mean ± SEM and with y-axis as fold change to Hgf alone. Erk and Akt activity were measured as a ratio of phospho-protein to total protein normalised to Gapdh from 3 separate immunoblots. Significance was tested by one way ANOVA with Dunnett's comparison to control or Hgf alone, and Student's t test to compare control with Hgf alone.

Summary – PB increased Hgf-mediated phosphorylation of Akt, and not Erk, suggesting Hgf-Erk signalling is not involved in regulating the PB response, and that PB-mediated potentiation of Erk activation is specific to Egf signalling. Furthermore, Akt activity was increased by PB (5mM) in the absence of growth factors, suggesting growth factor-independent activation. The function of Akt signalling is discussed below.

3.3.2.3 The role of Akt activation in PB plus Egf/Hgf treatments

Due to increased Akt phosphorylation demonstrated in Hgf/PB treatments some of these samples were examined for changes in the downstream Akt target, FoxO1. FoxO1 is a transcription factor that controls expression of gluconeogenic, anti-proliferative and pro-apoptotic genes (Puigserver et al., 2003; X. Zhang, Tang, Hadden, & Rishi, 2011). Pre-treating with PB (5mM) for 30 minutes significantly increased Hgf-mediated (20ng/mL) Akt activation (Figure 3.7 B), as did the reverse experiment; pre-treating with Hgf (20ng/mL) for 30 minutes followed by PB (5mM) for 60 minutes (Figure 3.8 A). In the same samples that showed increased Akt phosphorylation with Hgf plus PB compared to Hgf alone (Figure 3.8 A), FoxO1 activity appeared to be increased with Hgf (20ng/mL) treatment, as well as in pre-treated PB (5mM) samples, compared to control (Figure 3.8 B). However, the lack of a significant increase in FoxO1 activity in both treatment groups could reflect the time-dependent process of phosphorylation after Hgf/PB treatment and would require optimising as performed for Erk and Akt (Figure 3.4) to confirm pathway changes.

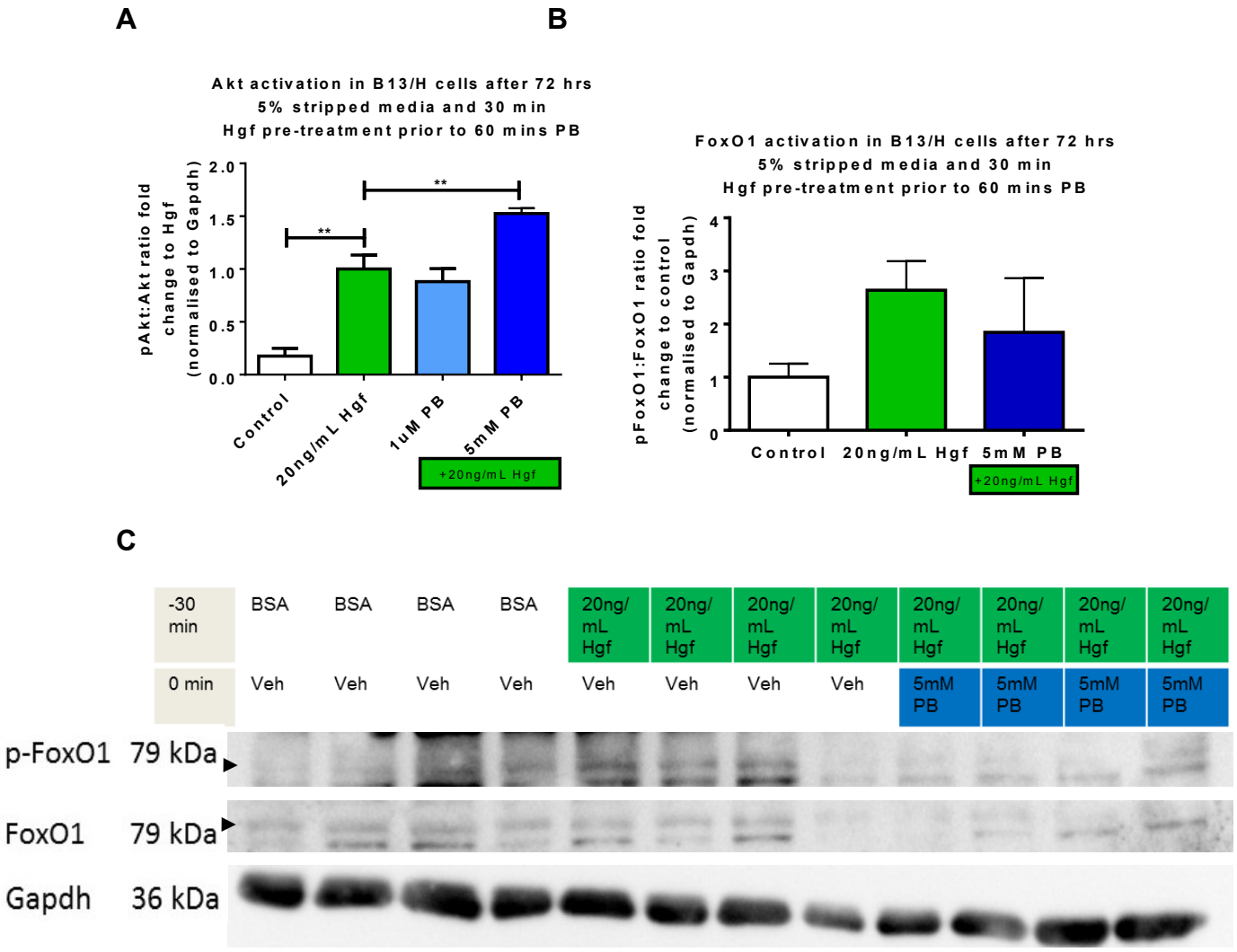


Figure 3.8: Thirty minutes treatment with 20ng/mL Hgf followed by 60 minutes with PB - FoxO1 activity

Figure 3.8 shows the effect of pre-treating with 20ng/mL Hgf for 30 minutes followed by PB for 60 minutes on Akt activity (**A**) and FoxO1 activity (**B**). FoxO1 immunoblots shown (**C**). Data were representative of 4 independent cultures, showing mean ± SEM and with y-axis as fold change to control. FoxO1 activity was measured as a ratio of phospho-protein to total protein normalised to Gapdh from 1 immunoblot. Significance was tested by one way ANOVA with Dunnett's comparison to Hgf alone. FoxO1/p-FoxO1 were the top bands of the pairs (as indicated by the arrow head).

B13/H cells were also treated with Hgf (20ng/mL) for 30 minutes followed by PB (5mM) for 48 hours to assess if under conditions where short term PB increased Akt phosphorylation, whether this influenced Akt-mediated cell survival or hypertrophy (Matsui, Nagoshi, & Rosenzweig, 2003). The data in Figure 3.9 demonstrates that

PB (5mM) in the presence of Hgf (20ng/mL) induced subtle changes in cell count (Figure 3.9 A) and cellular hypertrophy (Figure 3.9 B) (as determined by the ratio of cell count to total protein (Das et al., 2014)); the magnitude of these responses suggest the effects of Akt on cellular hypertrophy and cell count were not dramatic.

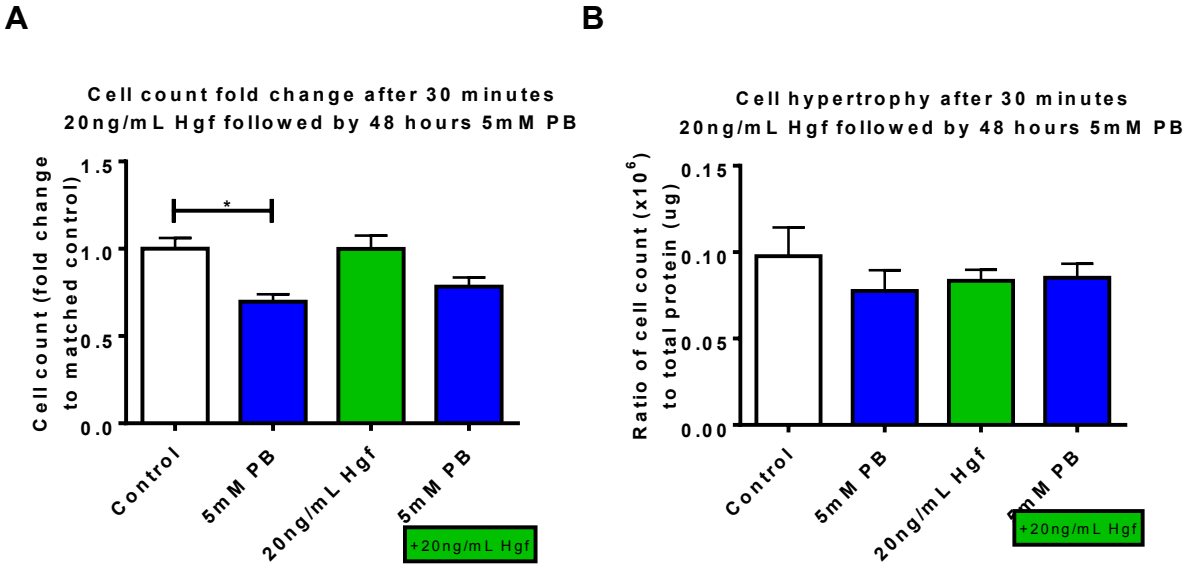


Figure 3.9: Thirty minutes 20ng/mL Hgf followed by 48 hours PB

Figure 3.9 shows B13/H cells treated with 20ng/mL Hgf for 30 minutes followed by PB for 48 hours. Cell counts between control and Hgf samples treated with PB (5mM) are shown (**A**) and the effect of cellular hypertrophy (**B**). Hypertrophy was measured as the ratio of cell count to total protein. Results were mean ± SEM. Significance was determined by Student's t test to compare control to PB, and Hgf to Hgf + PB. *p<0.05.

Summary – Although PB appeared to increase Hgf-mediated Akt phosphorylation the functional output of this is uncertain at the moment, as cell counts, hypertrophy and activity of a downstream Akt target, FoxO1, are unchanged with PB plus Hgf compared to Hgf alone.

To understand the changes seen with Erk and Akt phosphorylation further, rat liver tissues were also assessed for changes in pathway activation following PB treatment.

3.3.3 Aim 3: Assess the activation of these pathways in the rat *in vivo*.

3.3.3.1 Growth factor pathways are unchanged in the rat in vivo

Joannard *et al.,* (Florence Joannard et al., 2006) showed that 15 minutes 5mM PB treatment increased activation of Erk, Jnk and p38 in male Sprague-Dawley rat primary hepatocytes. Erk was reported to act as a negative regulator of *Cyp2b* induction, while p38 was a positive regulator. Furthermore, 3 days PB treatment in the rat *in vivo* has been shown to induce a transient state of hyperplasia (Waterman et al., 2010) and this has previously been associated with increased plasma Hgf (Lindroos et al., 1992). Akt activation is known to effect cell proliferation (Manning & Cantley, 2007) and as B13/H cells demonstrated changes in Akt phosphorylation with PB plus growth factors (described above), I interrogated these pathways *in vivo*.

The first 14 days of PB exposure were analysed (days 1, 3, 7 and 14) from an acute *in vivo* PB treatment study (previously described by Waterman *et al.,* (Waterman et al., 2010)) as this covers the phase of PB-induced adaptive hepatomegaly concluding with mitoinhibition. Ninety days treatment were also included to determine if prolonged PB exposure effected these pathways.

Erk pathway activity Comparing 1000ppm PB to control, Erk activity (Figure 3.10 A) and its downstream target, Elk (Figure 3.10 B), were not significantly changed with PB treatment. Although showing non-significant decreased activity at 7 (Figure 3.10 A) and 1 days (Figure 3.10 B) with PB treatment (1000ppm), respectively, the lack of

consistent changes over time suggest long-term Erk activity was not affected by PB treatment *in vivo*.

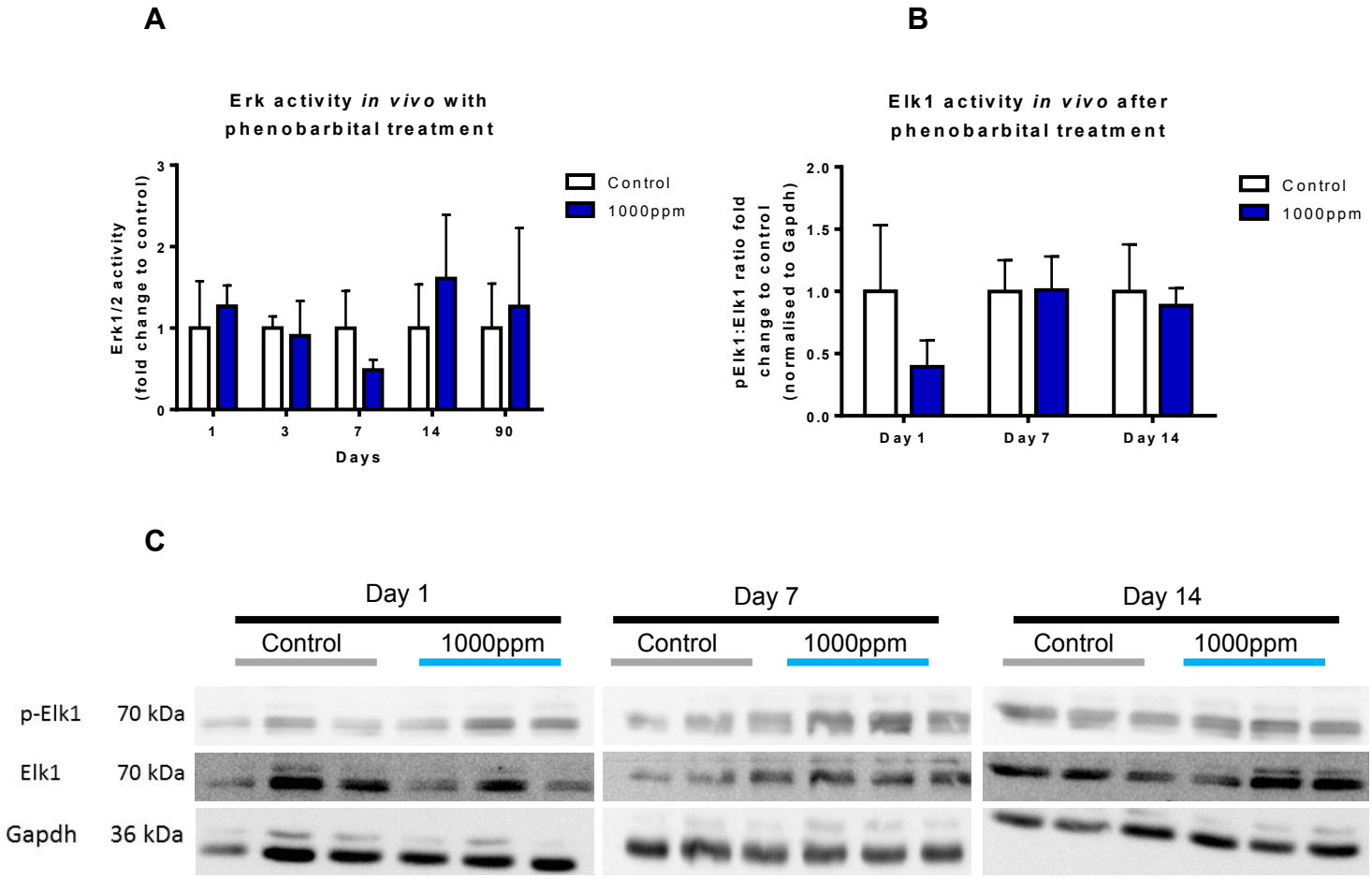


Figure 3.10: Erk and Elk activity in PB treated rat liver

Figure 3.10 shows Erk activity in the livers of 1, 3, 7, 14 and 90 days 1000ppm PB treated rats using the MSD platform (**A**). Pathway activity was measured as change in phospho-protein normalised to total protein loaded. Elk activity was also assessed in the livers of 1, 7 and 14 days 1000ppm PB treated rats (**B**) *via* immunoblots (**C**). Elk activity was measured as a ratio of phospho-protein to total protein normalised to Gapdh from 1 immunoblot. Data were representative of 3 samples, showing mean ± SD and with y-axis as fold change to time matched vehicle control. Significance was tested by Mann-Whitney between time matched control and treatment.

Jnk and p38 activity Erk is part of a signalling hub known as the mitogen-activated protein kinase (MAPK) pathway. The MAPK pathway consists of 2 other signalling kinases, p38 MAPK (p38) and Jun N-terminal kinase (Jnk). These 2 other kinases

are also activated through growth factor pathways (as well as through environmental stress and inflammatory signals) and are involved in the regulation of cell survival (Wagner & Nebreda, 2009) and have been implicated in the PB signalling response (Florence Joannard et al., 2006). Figure 3.11 shows that at the time points tested and dose of PB used (1000ppm), there were no significant changes in MAPK activity compared to control.

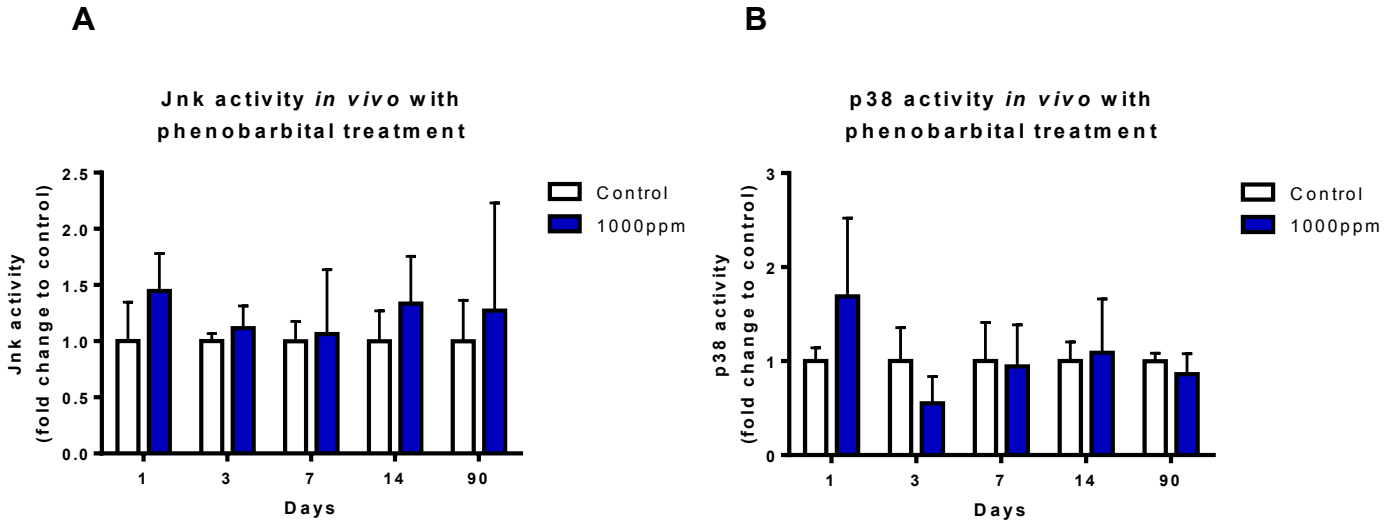


Figure 3.11: MAPK pathway activity in PB treated rat liver

Figure 3.11 shows MAPK pathway activity in the livers of 1, 3, 7, 14 and 90 days 1000ppm PB treated rats using the MSD platform. Jnk (**A**) and p38 (**B**) pathways were analysed. Data were representative of 3 independent samples, showing mean ± SD and with y-axis as fold change to time matched control. Pathway activity was measured as change in phospho-protein normalised to total protein loaded. Significance was tested by Mann-Whitney between time matched control and treatment.

Akt pathway activity The activity of Akt and its downstream target, FoxO1, were also assessed, due to increased Akt activation with PB treatment *in vitro*. I found that both Akt and FoxO1 showed a non-significant increased activity at 3 days PB (1000ppm) compared to control, while there were no changes between treatment and control at 14 days with either Akt or FoxO1 (Figure 3.12). The suggestive

increase in pathway activity could reflect PB-induced hyperplasia at this time (Waterman et al., 2010).

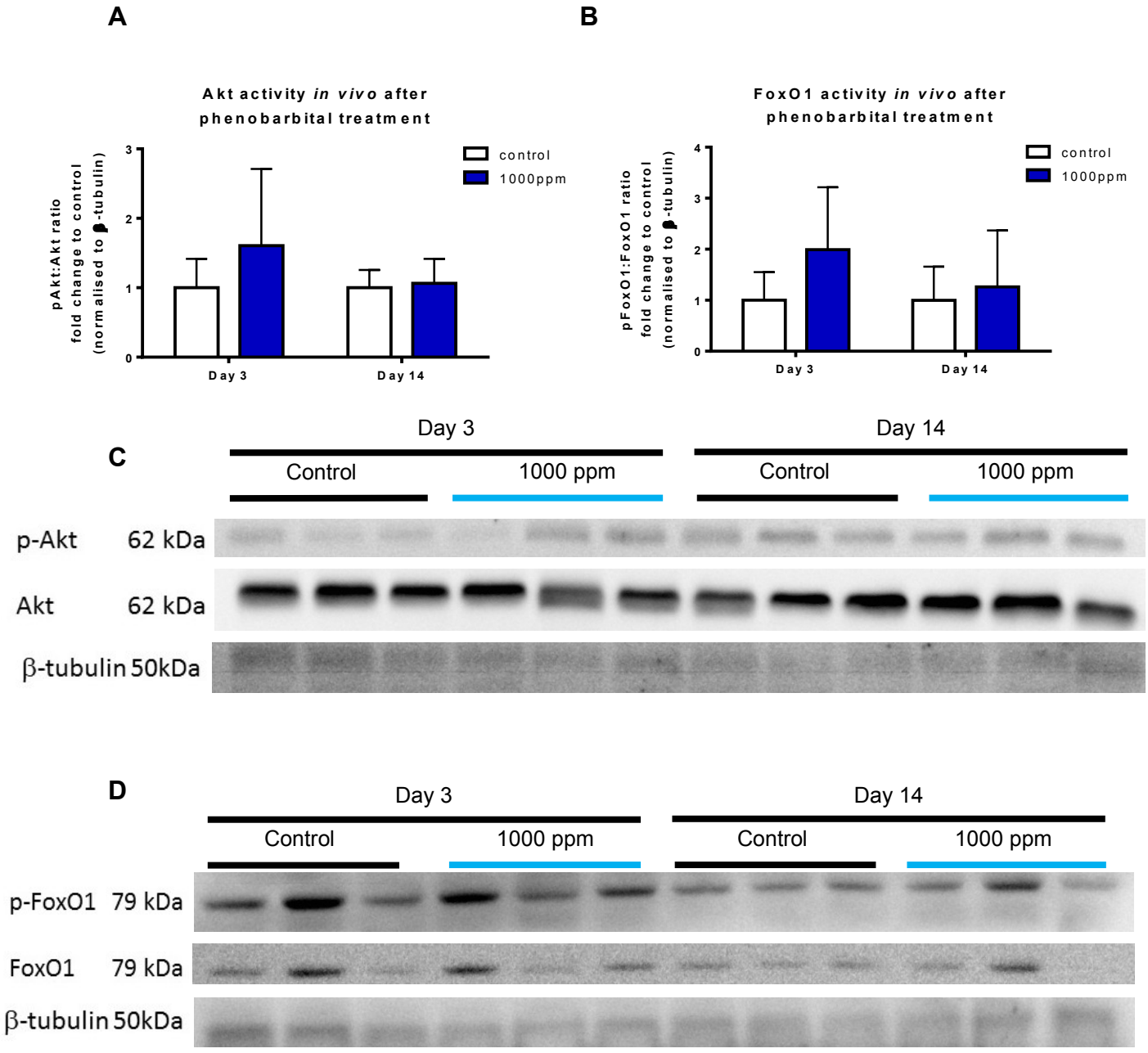


Figure 3.12: Akt and FoxO1 activity in PB treated rat liver

Figure 3.12 shows Akt (**A**) and FoxO1 (**B**) activity in the livers of 3 and 14 days 1000ppm PB treated rats. Akt and FoxO1 immunoblots shown (**C**/**D**). Data were representative of 3 samples, showing mean ± SD and with y-axis as fold change to time matched vehicle control. Akt and FoxO1 activity were measured as a ratio of phospho-protein to total protein normalised to β-tubulin from 1 immunoblot. Significance was tested by Mann-Whitney between time matched control and treatment.

Discussion – These data suggest that changes in MAPK pathway activity with PB treatment reported in the literature are likely to be early transient effects, as they are not maintained beyond 24 hours PB *in vivo*. It is known that responses to MAPK activation are dependent on duration and strength of kinase signalling. For example, as demonstrated with Jnk, whereby transient activation stimulates cell survival but prolonged activation induces apoptosis (Wagner & Nebreda, 2009). Furthermore, due to the trend for increased Akt activity *in vivo*, these data suggest that the increase in Akt activity with PB *in vitro* may reflect cell signalling changes indicative of PB-mediated transient hyperplasia.

3.4 Conclusions

In mouse primary hepatocytes, PB-mediated activation of Car has been reported to be *via* inhibition of the Egfr, allowing subsequent translocation of Car to the nucleus (Mutoh et al., 2013). Inactivation of the Egfr downstream target, Erk, has also been implicated in the nuclear translocation of Car (Koike et al., 2007; Osabe & Negishi, 2011). In the rat, Egf has been shown to suppress PB-mediated induction of Car-regulated genes, while Hgf has no effect (Kawamura et al., 1999).

PB + Egf: Erk Through treatments with Egf plus PB it was shown that compared to Egf alone, PB plus Egf potentiated Erk activity (Figure 3.6). It is unlikely that the dose of Egf used here was a saturating dose as Mutoh *et al.,* (Mutoh et al., 2013) used a much higher dose of Egf (100µg/mL and 5ng/mL respectively). This suggests that PB does not inhibit Erk activation as seen in the mouse. Further, Egf is reported to inhibit PB-mediated gene expression in the rat (Kawamura et al., 1999). Therefore, Erk activation could be part of a negative feedback loop specific to the rat, which this data suggests may be reproducible between rat primary hepatocytes (Florence Joannard et al., 2006) and the B13/H cell model. This indicates that in the rat, Car is likely activated through a disparate mechanism to the mouse (Figure 3.13).

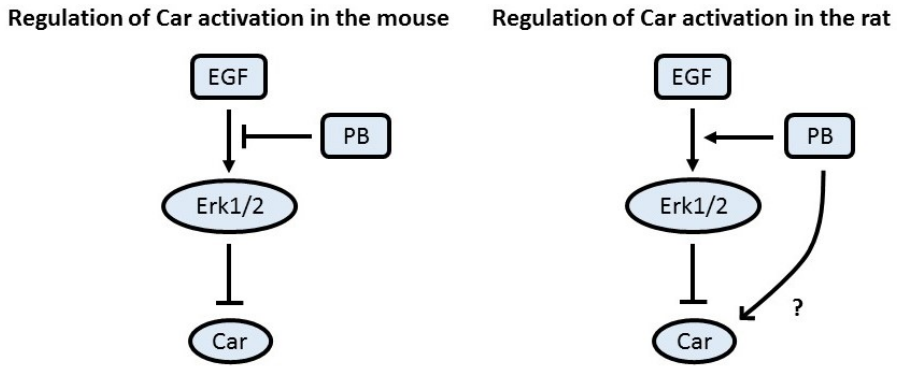


Figure 3.13: Car activation in the mouse and rat

Figure 3.13 shows the proposed model of PB-mediated Car activation comparing the mouse and rat.

PB + Egf/Hgf: Akt (FoxO1) Interestingly, PB potentiated Akt activity in combination with either Egf or Hgf compared to growth factor alone (Figure 3.6 and Figure 3.7). This could be expected given that activation of Car inhibits FoxO1 mediated gene transcription (Kodama et al., 2004), and Akt activation results in FoxO1 inactivation *via* phosphorylation and exclusion from the nucleus (X. Zhang et al., 2011). FoxO1 activity, as measured by changes in phosphorylated protein, was potentially elevated *in vivo* but not significantly (Figure 3.12 B), as was Akt activity (Figure 3.12 A). I was not able to demonstrate this for FoxO1 *in vitro* (Figure 3.8 B). To determine if PB-mediated activation of Akt does increase FoxO1 phosphorylation in this context, it would be necessary to complete a time-course of FoxO1 activity to ascertain the optimal time required to assess changes in FoxO1 phosphorylation.

PB + Egf/Hgf: Akt (hyperplasia) Akt activity is also associated with proliferation (Manning & Cantley, 2007), and the trend for increased activity seen *in vivo* (Figure 3.12 A) is suggestive of PB-induced hyperplasia. I showed increased Akt activity *in*

vitro in the presence of either Egf or Hgf, and even trends for increased Akt activity without growth factor treatment (Figure 3.5 B, Figure 3.6 B and Figure 3.7 B). This suggests that *in vitro*, PB may influence the Akt pathway independently of growth factor treatment, which could contribute to the molecular mechanisms underlying PB-induced hyperplasia (Figure 3.14).

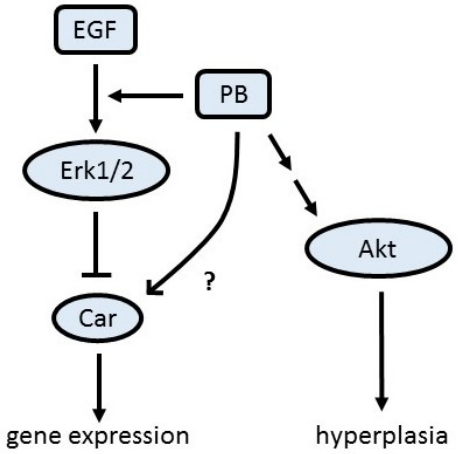


Figure 3.14: The effect of PB on Erk and Akt activity in the rat

Figure 3.14 shows the proposed model of PB-mediated growth factor-dependent effect on Erk activity, and growth factor-independent effect on Akt activity.

Akt activation is also known to induce cell survival and hypertrophy (Matsui et al., 2003), both of which showed minimal changes with PB plus Hgf compared to growth factor alone suggesting they are not greatly influenced by Akt activation in this context.

Chapter 3 Conclusions – Erk is reported to be a negative regulator of PB-induced genes in the mouse and rat, and that Erk is inhibited by PB treatment in the mouse. However, Erk is activated by PB in the rat suggesting a negative feedback loop to

modulate the PB response. This appears to be common between rat primary hepatocytes and the B13/H cell system. Furthermore, PB-mediated increased Erk activity was specific to Egf signalling and not seen with Hgf. The function of increased Akt activity in this context requires further research, but as indicated from *in vivo* data, could be contributing to PB-induced transient hyperplasia.

I conclude that although Car is found in the nucleus of untreated B13/H cells, Car is still PB-inducible and this work demonstrates that the B13/H cells are similar to rat primary hepatocytes in response to PB and its effect on growth factor signalling, which is different to that of the mouse.

4. Regulation of phenobarbital-induced miRNAs

4.1 Introduction

In this chapter I explore the molecular mechanisms of PB-mediated miRNA induction, with a focus on the miRNA cluster, miR-182/96.

4.1.1 Regulation of miR-182/96

Koufaris *et al.,* (Koufaris et al., 2012, 2013) have reported that 2 clusters of miRNAs, miR-182/96 and miR-200a/b/429, are time- and dose-dependently induced by PB treatment in the rat. This has subsequently also been demonstrated *in vitro* (chapter 2), yet the mechanisms underlying this PB-mediated response are unknown. With a focus on pathways that are related to the PB phenotype, I discuss potential regulators of the miR-182/96 cluster below, in alphabetical order. I also consider the role of Car in regulation of both clusters of miRNAs to explore function.

Car – Car is activated by PB (Honkakoski et al., 1998; Sueyoshi et al., 1999), but has not been reported as being a direct regulator of miR-182/96 or miR-200a/b/429. However, it has been suggested that these miRNAs are involved in maintaining homeostasis during PB exposure, and as Car is required for PB-induced tumours, it might be expected that these miRNAs are regulated independently of Car. It has been reported that PB can regulate genes independently of Car (Ueda et al., 2002), therefore understanding the role of Car activation on these miRNAs would prove important in exploring their homeostatic function and in identifying their upstream regulator.

Hnf-4α –PB treatment induces nuclear translocation of Hnf-4α (Bell & Michalopoulos, 2006), yet nuclear Car inhibits Hnf-4α-mediated gene transcription by competing for DR1 binding sites in gene promoter regions as well as for nuclear co-factors, glucocorticoid receptor interacting protein- (GRIP-)1 and peroxisome proliferator-activated receptor γ coactivator- (PGC-)1α (Miao et al., 2006). Furthermore, an acute PB treatment (500ppm) study in male Fisher (F344) rats predicted that Hnf-4α is induced after 2 weeks PB treatment; using the pathway prediction program, Ingenuity® Pathway Analysis (Kakehashi et al., 2013), which is in agreement with the time-dependent induction of the miRNAs. Additionally, Koufaris *et al.,* (Koufaris, 2011) identified Hnf-4α binding sites up-stream of both miR-200b and miR-96, suggesting potential regulation.

Methylation – PB has been shown to induce global hypermethylation after 14 days PB treatment (1000ppm) in male Fisher rats (Koufaris et al., 2013). There is also substantial evidence of altered methylation in PB treated mice; around the promoter proximal region of strongly induced genes there is an initial gain in the methyl-intermediate, 5-hydroxymethylcytosine (5hmc), indicating demethylation, and eventual loss of this marker and 5-methylcytosine (5mc) (Thomson, Moggs, et al., 2013; Thomson et al., 2012; Thomson, Hunter, et al., 2013). MiR-182 was found to have decreased expression in human renal cell carcinoma tissue compared to non-tumour renal tissue, and this was associated with high methylation levels up-stream of the miRNA (Xin Xu et al., 2014). Furthermore, treatment with a methyltransferase inhibitor 5-azacytidine, reduced methylation levels and increased expression of miR-

182 in renal cell carcinoma cell lines, suggesting a role of epigenetic regulation in miR-182 expression (Xin Xu et al., 2014).

P53 – The effect of PB on p53 inducibility has been explored in Female Sprague-Dawley rats treated with an initiating dose of DEN (single intraperitoneal injection at 0.3mmol/kg body weight) followed by a subsequent regime of PB (500ppm) for up to 14 months, or DEN administration (weekly intraperitoneal injection at 0.3mmol/kg body weight) for up to 3 months (Finnberg, Stenius, & Högberg, 2000). Twenty-four hours prior to sacrifice, the animals were again treated with DEN to assess the p53 induction response. The authors showed that in enzyme altered foci (characterised by glutathione-*S*-transferase pi positive staining) PB treated rats had increased p53 levels compared to DEN treated rats.

Primary hepatocytes from B6C3F1 mice treated with PB (2mM) for 23 hours have been shown to exhibit delayed p53 induction in response to the DNA damaging compound, bleomycin (16μg/mL), compared to non-PB treated cells (Gonzales et al., 1998).

Comparing *in vivo* rat with *in vitro* mouse responses is difficult, but this could suggest that PB may effect p53 induction discordantly between rats and mice; whereby rats remain sensitive to p53 induction, while mice develop retarded p53 induction in response to PB. MiR-182 has been shown to be dependent on p53 expression in human uveal melanoma cell lines, M23 and SP6.5 (Yan et al., 2012), and PB-

induced miR-182 expression is specific to the rat (Koufaris et al., 2012, 2013; Lempiäinen et al., 2013) thereby implicating p53 as a potential regulator of miR-182 in the rat.

ROS – Oxidative stress has been suggested as a mediator of PB-induced non-genotoxic carcinogenesis in rats due to increased expression of genes implicated in increased oxidative stress, such as Cyp450s and glutathione-S-transferases (GSTs) (Dail, Shack, Chambers, & Burgess, 2008; Elrick et al., 2005; Klepeisz et al., 2013), and an increase in the oxidative marker 8-hydroxy-2'-deoxyguanosine (8-OHdG) (Imaoka et al., 2004). However, a recent study in male C57BL/6J mice reported minimal effects of PB (0.05% w/v) on heme oxygenase 1 induction, a gene involved in oxidative stress pathway (Henderson, Cameron, Chatham, & Stanley, 2015), despite this dose of PB previously being reported as inducing tumours in this strain of mice, albeit with an initiating dose of the genotoxin DEN (Braeuning et al., 2014). MiR-182 and miR-200a have been reported to be induced in the human uterine leiomyoma cell line, DD-HLM, when treated with hydrogen peroxide (100μM) for a total of 48 hours after an initial treatment regime of once an hour for 5 hours (Xiaofei Xu et al., 2014). Although rat Fao cells treated with hydrogen peroxide (500μM) for 24 hours show no significant change in miR-200b compared to control (Koufaris et al., 2012). Taken together this suggests that increased ROS may be a contributing factor to miRNA induction.

Tgf-β – In rats, putative preneoplastic cells are reported to express reduced levels of the epithelial cell growth inhibitor, transforming growth factor- (Tgf-)β1, in response

to 2 months DEN (50ppm) and 3 months PB (0.1% w/v) than do surrounding normal periportal hepatocytes, which show a marked increase in Tgf-β1 levels (Jirtle & Meyer, 1991). Male Fisher rats treated with DEN (50ppm) for 1 month, then 4 months PB (0.1% w/v) also show reduced Tgf-β receptor levels in tumours compared to surrounding cells (Mansbach et al., 1996). This suggests that normal hepatocytes have increased activity of Tgf-β in response to PB, which maintains mitoinhibition compared with preneoplastic cells. Tgf-β (0.5 ng/ml) has also been shown to induce miR-182 after 12 hours treatment in human gall bladder cancer cells, GBC-SD (Qiu et al., 2014), suggesting a link between miRNA expression and Tgf-β.

These above components of the PB phenotype will be assessed as regulators of the miR-182/96 cluster (Figure 4.1) to determine the molecular mechanism underlying miRNA perturbation, in order to further understand the function of these miRNAs.

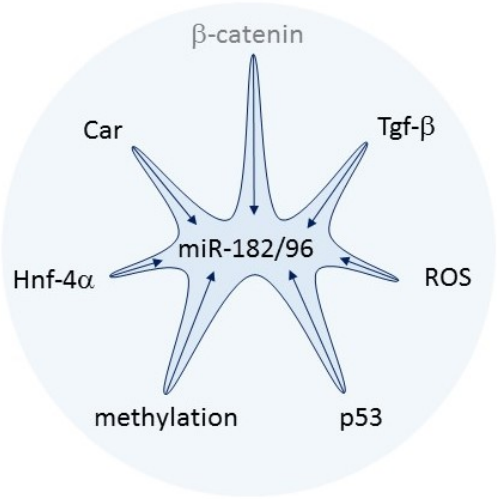


Figure 4.1: Potential miR-182/96 regulators

Figure 4.1 is an arbitrary depiction of potential positive regulators of miR-182/96 involved in the PB response, identified from the literature and discussed in text. B-Catenin is discussed later.

4.1.2 Hypothesis

The PB-induced miRNAs, miR-182/96, are regulated independently of Car *in vivo*.

4.1.3 Aims

1. Explore miRNA expression in PB treated wild type (WT) and Car knockout (KO) rats to determine underlying molecular stimulus for perturbed expression.
2. Interrogate the expression of potential miRNA regulators in PB treated rat liver tissue.

4.2 Methods

4.2.1 Tissue samples

Ethics approval and *in vivo* experimentation were performed by CXR Biosciences and Syngenta.

Car KO study Liver tissue samples from male Sprague-Dawley WT Car and KO rats were provided by CXR Biosciences (Chamberlain, Haines, & Elcombe, 2014). Rats were treated with either a control or PB (500ppm) diet for 7 days, with subsequent liver collections used herein for RNA analysis.

Methylation analysis Liver tissue samples from male Fisher rats were provided by Syngenta. Rats were treated with control or PB (1000ppm) diet for 7, 14 and 28 days, with subsequent liver collections, used herein for methylation analysis *via* pyrosequencing.

Transcriptomic analysis Liver samples used are described in chapter 3.2.1. Twenty-eight day PB (50ppm and 1000ppm) treated rat samples detailed in "Methylation analysis" (4.2.1) were also used for gene expression analysis.

4.2.2 Cell culture and chemical treatments

Cell culture was performed as detailed in chapter 2.2.1.

To explore the functional response of the B13/H cells to phenobarbital, B13/H cells were treated in combination with phenobarbital and with the Car inhibitor 5α-androst-16-en-3α-ol (androstenol) (solvated in 95% ethanol) (Sigma-Aldrich, Dorset, UK) or okadaic acid sodium salt (OAA) (solvated in DMSO) (Millipore, MA, USA). B13 cells were seeded at $2x10^5$ cells per well in 6-well plates and differentiated as in chapter 2.2.1. Samples were harvested for RNA and subsequent qRT-PCR.

4.2.3 RNA extraction

MirVana PARIS RNA extraction kits were used as detailed in chapter 2.2.5, with modification to sample lysis for tissue samples as described below. Samples were stored at -80^{o}C, and moved onto dry ice for RNA extraction. Homogenisation was performed as quickly as possible to avoid RNA degradation. Approximately 50-100mg of tissue was disrupted in ice cold MirVana kit cell disruption buffer (625µL) using a tissue homogeniser. Samples were processed one at a time, incubating on ice with denaturing solution, which contains RNase inactivating guanidinium thiocyanate and ensures integrity of the sample.

4.2.4 qRT-PCR

As detailed in chapter 2.2.6.

4.2.5 DNA extraction

The Qiagen QIAamp DNA mini kit 50 (Qiagen, Manchester, UK) was used to extract DNA from <25mg flash frozen rat liver tissue samples. Extractions were performed

following manufacturers protocols. Briefly, samples were homogenised in PBS (80µL) using a T25 basic labortechnik homogeniser. Homogenate was lysed in kit ATL buffer containing proteinase K by occasional vortexing and incubated for 3 hours at 56ºC. Lysis was completed with the addition of kit Buffer AL and incubation for 10 minutes at 70ºC. As with RNA extractions, 100% ethanol was added to the samples to aid binding to the silica mini columns, which were subjected to a series of kit buffer washes to remove salts and proteins. Samples were eluted in kit Buffer AE. DNA quality was determined as with RNA (chapter 2.2.5).

4.2.6 Bisulphite conversion

DNA methylation can be quantified by the conversion of unmethylated cytosines to uracil, which are amplified as a thymine after PCR. Methylated cytosines (within a cytosine-guanine pair [CpG]) are protected and remain unchanged following bisulphite conversion (Figure 4.2) (Frommer et al., 1992). The changes in these nucleotides can be compared across samples after PCR amplification by pyro-sequencing.

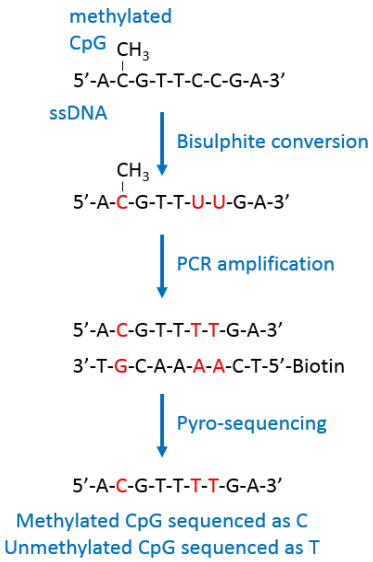


Figure 4.2: Pyro-sequencing methodology

Figure 4.2 depicts the steps involved in determining site-specific methylation status using pyro-sequencing. Adapted from Frommer *et al.,* (Frommer et al., 1992)

The EZ DNA methylation kit (Zymo research, CA, USA) was used for bisulphite conversion. DNA (500ng) in nuclease free water (50µL) containing M-Dilution buffer

(diluted to 1:10) was heated for 15 minutes at 37^{o}C followed by the addition of 2x volume of Ct conversion reagent and incubated for 16 hours at 50^{o}C in the dark. The conversion reagent chemically deaminates unmethylated cytosines to uracil (Frommer et al., 1992). Samples were chilled on ice for 10 minutes and bound to a spin column with kit M-Binding buffer. Column-bound samples were washed with a series of kit buffers to remove precipitates and finally eluted with kit M-Elution buffer. Quality control standards were also included during the bisulphite conversion for pyro-sequencing to act as references to 100% methylated rat gDNA and 0% methylated rat gDNA (Millipore, MA, USA) as well as standard rat gDNA (Affymetrix, CA, USA) (Figure 4.3).

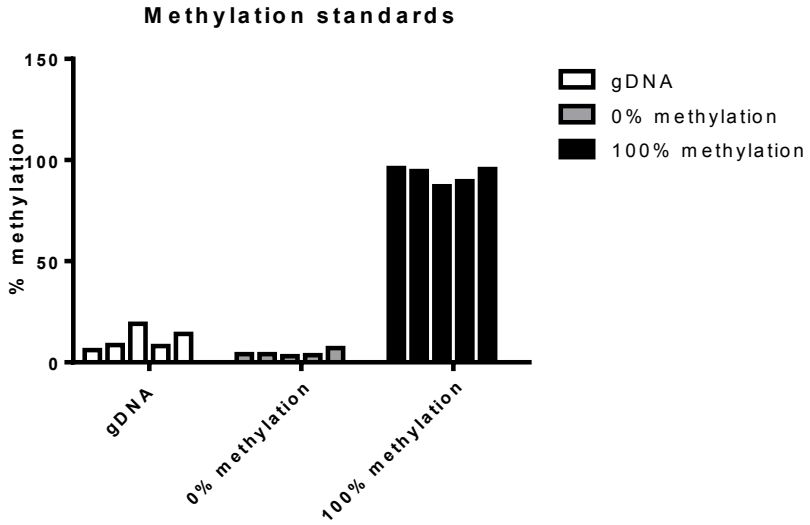


Figure 4.3: Methylation assessment optimisation

Figure 4.3 shows the mean percentage level of methylation at the 5 CpG sites measured in the three assay standards used across 2 technical replicates.

4.2.7 Bisulphite PCR

FastStart TaqDNA Polymerase, dNTPack (Roche, Hertfordshire, UK) was used for PCR amplification. PCR master mix was made per sample, which consisted of PCR buffer (diluted 1:10), dNTPs (50μM), forward primer (400nM), biotinylated reverse primer (400nM) (to allow capture of single stranded PCR product to streptavidin-coated Sepharose beads (Figure 4.2) (Royo, Hidalgo, & Ruiz, 2007)), Taq DNA polymerase (1 unit) and bisulphite DNA (10ng) made up with nuclease free water (final volume of 25μL). PCR amplification was run on a PTC-200 Peltier Thermal Cycler: 95^{o}C for 6 minutes, then 40 cycles of 95^{o}C, 59^{o}C and 72^{o}C for 30 seconds each, followed by 72^{o}C for 5 minutes and finally 4^{o}C. PCR primers used were: forward 5'-GGGTTTTTTAGTTTGGTGGGAATAT-3', reverse 5'-CTCTTCTTTCTTCCCCAACATC-3' (5' biotinylated). PCR products were run on 2% agarose gel as described in chapter 2.2.7. Temperature gradient PCR (53-60^{o}C) showed that optimal conditions were 59^{o}C for primer annealing (data not shown). Template controls were included to check for DNA contamination in the PCR mix prior to pyro-sequencing.

4.2.8 Pyro-sequencing

A Pyromark Q24 (Qiagen, Manchester, UK) was used for the pyro-sequencing. Component binding mixture was made for each PCR product, consisting of binding buffer (diluted to 1:2), sepharose beads (diluted to 1:80) and PCR product (diluted to 1:8) made to a final volume in nuclease free water (up to 80μL). The component buffer with samples were subjected to a series of washes with ethanol, denaturing buffer and wash buffer by the Pyromark vacuum pump before being transferred to a

sequencing plate containing aliquots of the sequencing primer (300nM) in annealing buffer (25µL). The sequencing plate was then heated for 2 minutes at 80^{o}C, followed by 5 minutes at room temperature to allow denaturation of sample and annealing of primers. The sequencing plate was then run on the Pyromark.

The captured template sequence was read by elongation from the sequencing primer with sequential incorporation of single nucleotides. Incorporation of a nucleotide into the sequence releases a phosphate group, which is converted to ATP by ATP-sulphurylase and reacts with luciferase to produce a light signal read by the Pyromark. The sequencing primer used was 5'- ATTTGGTTTTGAATTGTGT-3'. Negative controls were included to check for primer dimers, which cause misreading by the pyro-sequencer.

4.2.9 Statistics

In vitro analysis was performed as described in chapter 1.2.8. *In vivo* data is shown as mean ± standard deviation (SD) with sample size shown in figure legends. Kruskal-Wallis and Dunn's multiple comparison were used to compare treatment with control, as well as Spearman's correlation. Graphs and analysis were produced/performed using Graph Pad 6 (La jolla, California). Statistical significance was defined as $p<0.05$ (*), $p<0.01$ (**), $p<0.001$ (***), $p<0.001$ (****).

4.3 Results and Discussion

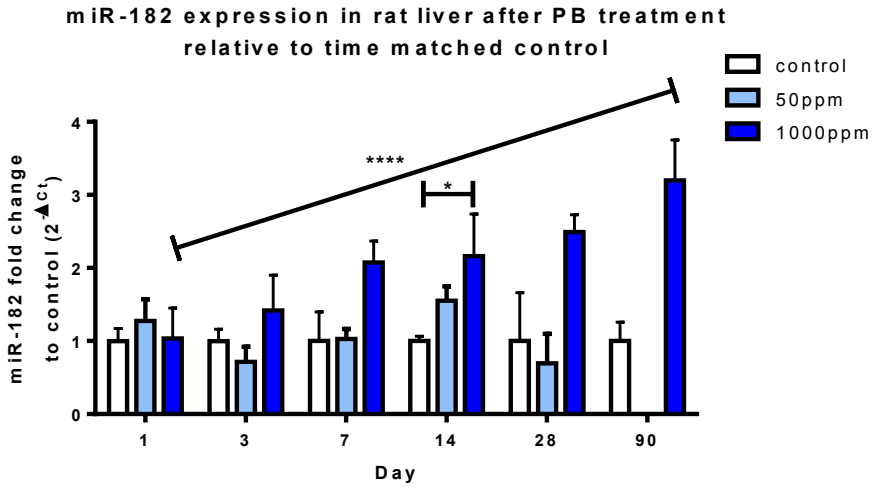
4.3.1 Aim 1: Explore miRNA expression in PB treated WT and Car KO rats to determine underlying molecular stimulus for perturbed expression.

4.3.1.1 MiR-182 is time-dependently expressed in PB treated rats

Phenobarbital treatment in the rat has been shown to significantly induce two clusters of miRNAs, the miR-200a/b/429 cluster and miR-182/96 (Koufaris et al., 2012, 2013) (Figure 4.4). This work has taken a focus on miR-182/96 to explore their regulation and function as a result of PB treatment, as little is known about their role in the context of PB exposure in the rat. MiR-183 is the third member of the miR-182/96 cluster but is not discussed herein as miR-183 expression levels were too low to be reliably quantified (Koufaris, 2011), although correlation analysis of microarray data obtained from Koufaris, (Koufaris, 2011) demonstrated miR-182 and miR-96 exhibit significant positive expression, suggesting expression of the miRNA cluster (Figure 4.4 B).

I discuss both clusters in the context of Car activation. Mounting evidence suggests that miR-200a/b/429 are involved in maintaining liver homeostasis through inhibiting epithelial to mesenchymal transition (EMT); a feature of cancer progression. In PB treated rats these miRNAs are reported to inhibit the expression of *zinc-finger E-box binding homeobox (Zeb)1/2* (Koufaris et al., 2012, 2013), which are 2 transcription factors involved in the progression of EMT *via* increasing expression of mesenchymal markers and decreasing expression of epithelial markers, such as E-cadherin (Aigner et al., 2007).

A



B

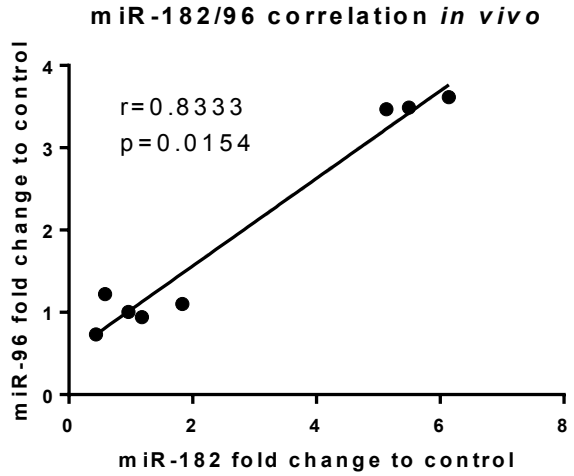


Figure 4.4: MiR-182 expression in subchronic PB treatment study

Figure 4.4 (**A**) details miR-182 expression by qPCR after PB treatment for up to 90 days. Data were mean ± SD of 3 samples, comparing treatment to control with Kruskal-Wallis and Dunn's multiple comparison. Change over time was measured by a one way ANOVA linear trend analysis of 1000ppm PB. Data were published in (Koufaris et al., 2013) (**B**) Spearman correlation of miR-182/96 fold change in 90 days 1000ppm PB and control treated rats. Adapted from miRNA microarray data (Koufaris, 2011).

Summary – MiR-182 expression was time-dependently increased with PB treatment (1000ppm) in the rat.

4.3.1.2 Car as a regulator of miR-182/96 expression in PB treated Car wild type and knockout rats

Car wild type and knockout rat samples were obtained from CXR biosciences. Car wild type samples showed increased Cyp2b1/2 mRNA expression and activity with PB (500ppm) treatment compared to control, which was abolished in the PB treatment group of Car knockout samples, indicating effective loss of Car (Chamberlain et al., 2014) (Figure 4.5 A and B).

A **B**

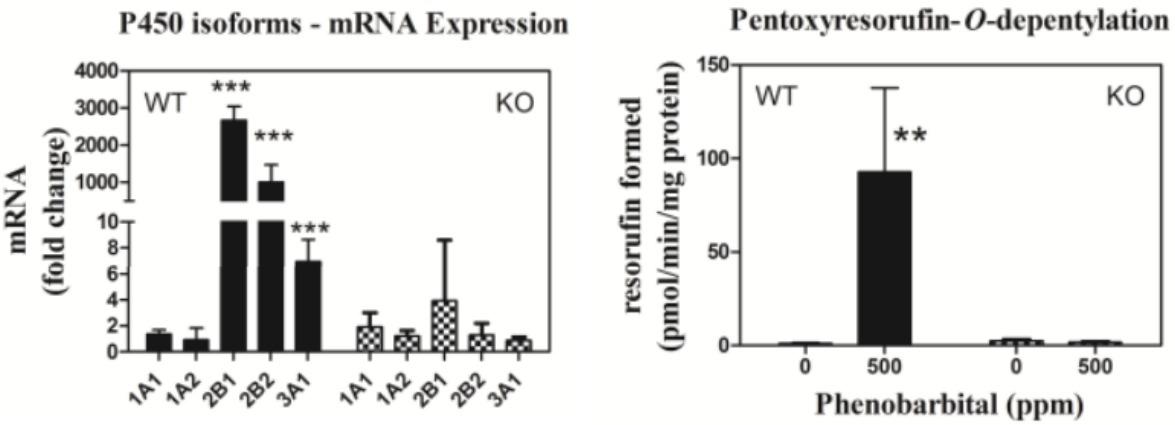


Figure 4.5: Cyp mRNA expression and Cyp2b activity in wild type and Car KO rats

Figure 4.5 details the mRNA expression of PB responsive *Cyp450* genes after 7 days treatment in Car wild type (WT) and knockout (KO) rats (**A**), and Cyp2b activity, measured by PROD (**B**). Data were representative of 5 animals, with significance determined by Student's t test. Data presented were from Chamberlain *et al.,* (Chamberlain et al., 2014).

MiR-182 and miR-96 are both time- and dose-dependently induced by PB in the rat (Koufaris et al., 2012, 2013) and are believed to play a role in the transition from hyperplasia to mitoinhibition (Koufaris et al., 2013). Interrogating the expression of these miRNAs in Car wild type and knockout samples will aid our understanding of their underlying molecular regulation. Figure 4.6 shows the expression of miR-182

was not significantly changed from control in Car wild type (A) or Car knockout (B) rats. Interestingly miR-96 expression was similar between PB (500ppm) and control in the wild type animals (C), whereas miR-96 was significantly increased with PB (500ppm) compared to control in the Car knock out individuals (D), suggesting miR-96 was not regulated by Car. This implies that there could be a disparity in the regulation of the expression of miR-182 and miR-96, whereby miR-96 expression was not Car-mediated, but miR-182 may be. However, it is important to note that this study uses a lower dose of PB compared to previous work that demonstrates significant increases in these miRNAs (1000ppm PB) (Koufaris, 2011).

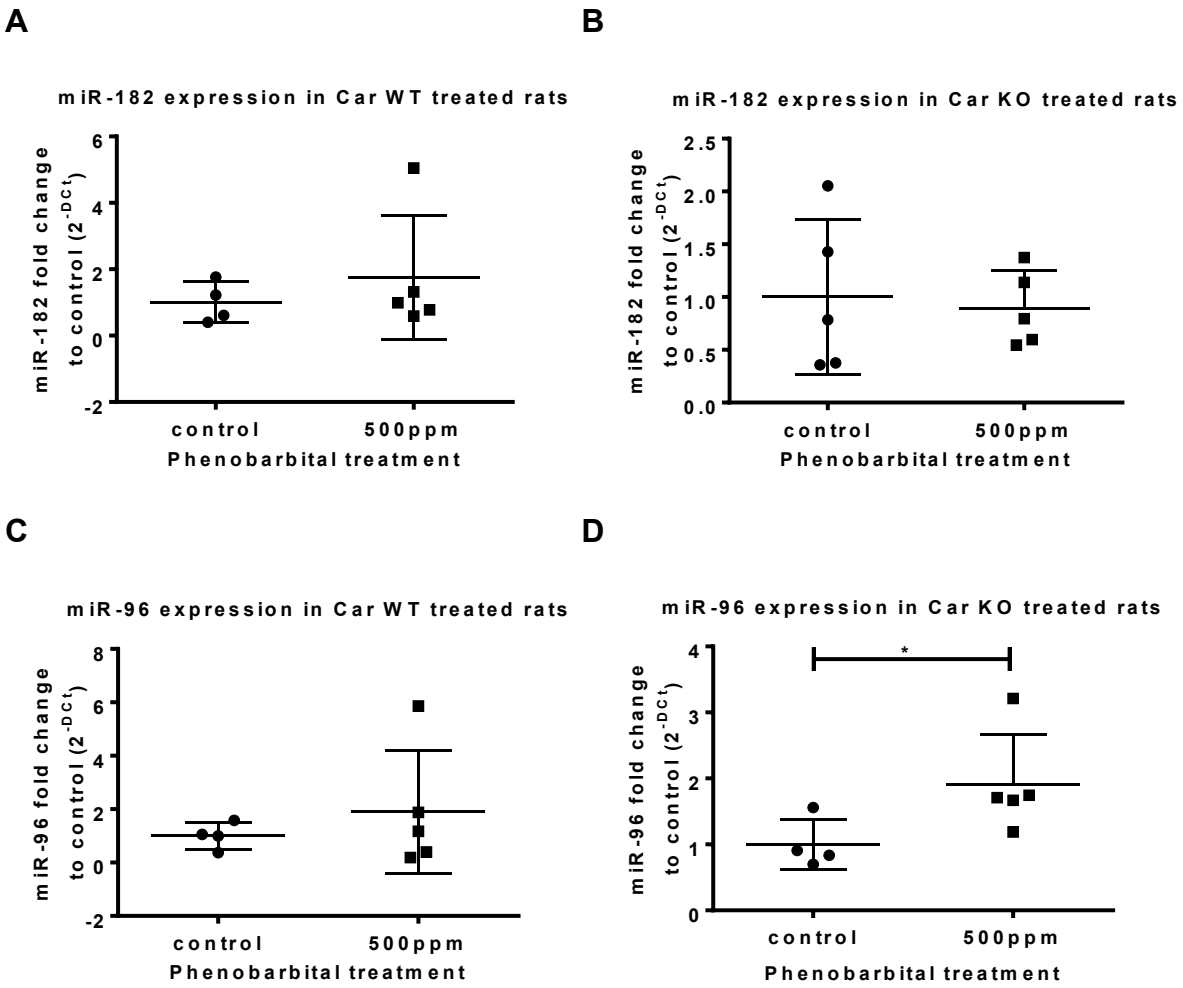


Figure 4.6: MiR-182 and miR-96 expression in wild type and Car KO rats

Figure 4.6 miR-182 (**A**/**B**) and miR-96 (**C**/**D**) expression was measured from the livers of wild type and Car knockout rats treated with 500ppm PB or control diet for 7 days. Data were mean ± SD of 4-5 samples. Mann-Whitney was used to assess statistical significance of treatment to control in genotype matched samples. *p<0.05.

4.3.1.3 Car as a regulator of miR-429/200b expression in PB treated Car wild type and knockout rats

MiR-429 and miR-200b demonstrated similar expression changes as seen with miR-182 and miR-96 when treated with 1000ppm PB in the rat (Koufaris et al., 2012, 2013). Figure 4.7 shows that miR-429 was unchanged from control in wild type (A) and in the Car knockout model (B), as was miR-200b (C/D). Due to the lack of change in expression between control and PB treated samples it was not possible to

draw any conclusions from this dataset. The lack of a response was most likely due to the lower dose used in this study (500ppm PB) compared to previous data (1000ppm) (Koufaris, 2011).

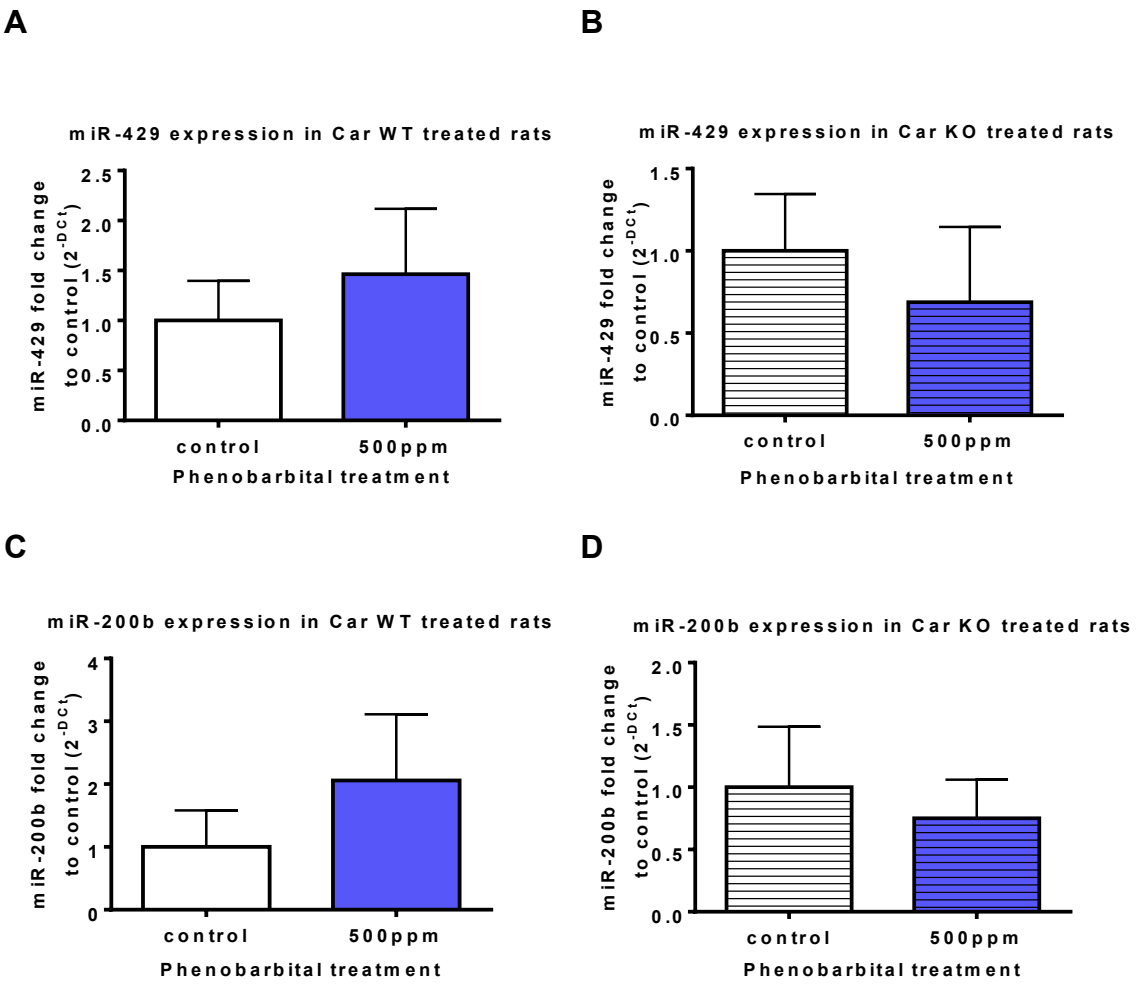


Figure 4.7: MiR-429 and miR-200b expression in wild type and Car KO rats

Figure 4.7 miR-429 (**A**/**B**) and miR-200b (**C**/**D**) expression was measured from the livers of wild type and Car knockout rats treated with 500ppm PB or control diet for 7 days. Data were mean ± SD of 4-5 samples. Mann-Whitney was used to assess statistical significance of treatment to control in genotype matched samples.

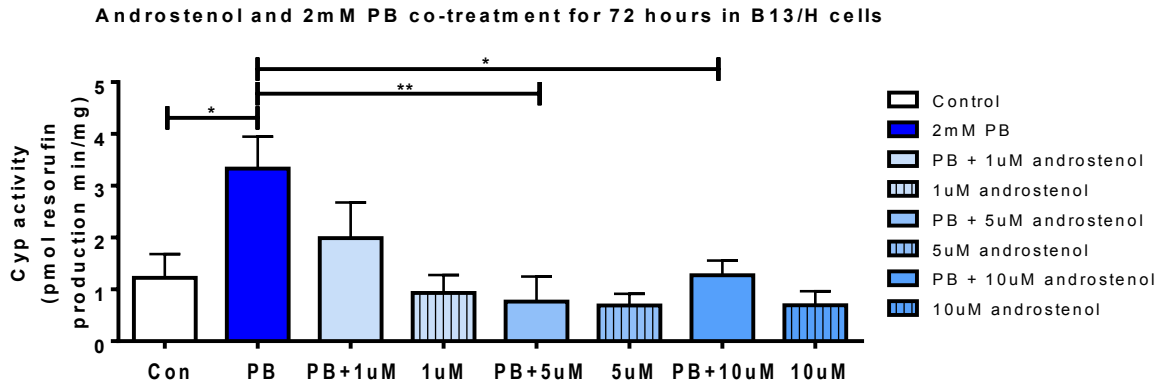
Summary – The above data suggests that miR-96 expression was not controlled by PB-mediated activation of Car, suggesting that miR-96 was induced by PB through other mechanisms. Neither miR-182, nor miR-200b/429 were affected by PB treatment in either genotype within this timeframe (7 days), suggesting the low dose

used was not sufficient to stimulate their increased expression and the duration of the treatment may not have been appropriate. I next sought to confirm if miR-96 (and miR-182) also demonstrated Car independent expression *in vitro*.

4.3.1.4 Inhibiting Car in the B13/H model

Co-treating B13/H cells with 2mM PB and 5μM or 10μM androstenol (5α-androstan-16-en-3α-ol) (Forman et al., 1998) for 72 hours significantly inhibited PB activation of Car, as determined by Cyp2b activity (Figure 4.8 A). Androstenol is a Car inverse agonist, an inhibitor of Car's constitutive activity, through binding Car and stimulating release of co-activator proteins (Forman et al., 1998) *via* repositioning of Car's co-activation domain, AF2 (Suino et al., 2004), and aiding co-repressor, Smrt, recruitment (Dussault et al., 2002). To confirm androstenol-mediated suppression of Car, I repeated the experimental conditions and assessed Cyp2b1 mRNA expression (Figure 4.8 B). PB-induced (2mM) Cyp2b1 mRNA expression was not significantly inhibited by androstenol (5μM), suggesting that androstenol was unable to completely inhibit PB activation of Car. This has been noted before in HepG2 cells, whereby 3α-androstenol did not alter nuclear localisation of GFP-Car in HepG2 cells (Kawamoto et al., 1999), although human Car is not thought to be repressed by androstanes (H. Wang & Negishi, 2003). It has been suggested that PB and PB-like inducers are able to eliminate androstane-mediated inverse agonism of Car (Waxman, 1999), which would appear to be supported by the data shown here.

A



B

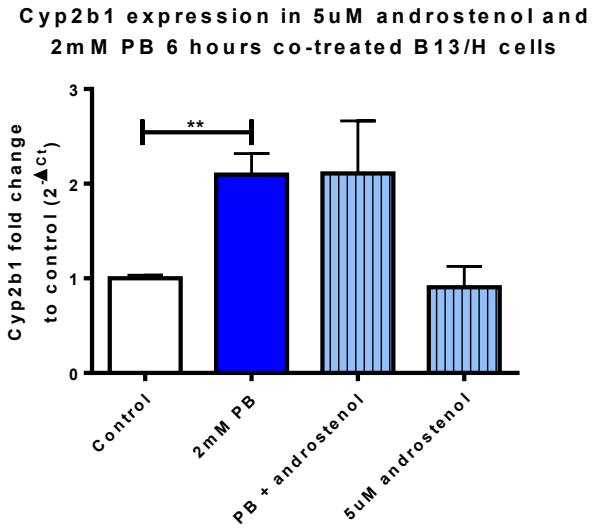


Figure 4.8: Cyp activity in B13/H cells treated with PB and androstenol

Figure 4.8 B13/H cells were treated with 2mM PB for 72 hours in the presence of the Car inverse agonist, androstenol (**A**). In a separate experiment Cyp2b1 mRNA expression was analysed in cells co-treated with 2mM PB and 5µM androstenol for 6 hours (**B**). Data were mean ± SEM of 4 independent cultures. One way ANOVA with Dunnett's multiple comparisons was used to compare PB + androstenol samples to PB alone (A), or Student's t test to compare control with PB (A/B), or PB + androstenol to PB alone (B).

As androstenol did not successfully inhibit PB-mediated activation of Car, I therefore attempted to inhibit Car in the B13/H cells using okadaic acid (OAA). OAA is a protein phosphatase (PP) 1 and 2A inhibitor, which inhibits PB-mediated de-

phosphorylation, and subsequent activation, of Car (Kawamoto et al., 1999; Sidhu & Omiecinski, 1997). Sidhu and Omiecinski (Sidhu & Omiecinski, 1997) showed that pre-treating primary rat hepatocytes with >10nM OAA for 60 minutes could ablate PB-mediated (100μM) induction of Cyp2b1/2 mRNA. Therefore B13/H cells were pre-treated with OAA (20nM and 200nM) for 60 minutes prior to PB (2mM) for 6 hours. Unexpectedly, in this experiment Cyp2b1/2 mRNA were not detected by qPCR (data not shown), suggesting that the inhibitor vehicle, DMSO, may be contributing to this result; the mechanisms behind this are unknown.

4.3.2 Aim 2: Interrogate the activity of potential miRNA regulators using PB treated rat liver tissue.

4.3.2.1 Hnf-4α as a regulator of miR-182/96 expression in PB treated rats

MiR-96 and miR-200b have been shown to possess Hnf-4α binding sites in their promoter region (Koufaris, 2011). Under normal conditions, PB induces the nuclear translocation of Car where it binds nuclear cofactors to aid binding to gene regulatory elements and induce transcription (Honkakoski et al., 1998; Kodama et al., 2004; Q. Zhang, Bae, Kemper, & Kemper, 2006). PB treatment also induces nuclear translocation of Hnf-4α (Bell & Michalopoulos, 2006), but Hnf-4α is inhibited by Car through competition for binding gene regulatory elements and nuclear cofactors (Kachaylo, Pustylnyak, Lyakhovich, & Gulyaeva, 2011; Miao et al., 2006; Yarushkin, Kachaylo, & Pustylnyak, 2013). This has been corroborated by the finding that in primary hepatocytes from Car and Pxr knockout mice, Hnf-4α is activated by PB (Tamasi, Juvan, Beer, Rozman, & Meyer, 2009). Therefore, it is possible that the induction of miR-96 in Car KO rats (Figure 4.6 D) is controlled by Hnf-4α. This may also be true for miR-182 and the lack of concordance could be an issue of dose. This could also explain the delay in miRNA induction with PB treatment in the rat, whereby miRNAs are progressively significantly increased compared to control from 14 days onwards ((Koufaris et al., 2013) Figure 4.4), mirroring the predicted increase in Hnf-4α activation at this time (Kakehashi et al., 2013). The Hnf-4α gene target, *Cyp7a1* (Miao et al., 2006) was assessed by interrogating the previously published microarray data from Waterman *et al.,* (Waterman et al., 2010) to explore if Hnf-4α was activated in a time-dependent manner. Cyp7a1 was not significantly induced over time with PB treatment (data not shown).

Summary – This suggests that Hnf-4α is unlikely to control PB-induced expression of miR-182/96.

4.3.2.2 Methylation changes as a regulator of miR-182/96 expression in PB treated rats

Methylation data were obtained in collaboration with Nahal Masrour (Department of Surgery and Cancer, Imperial College London).

Analysis of the upstream region of miR-182/96 using USCS genome browser (Kent et al., 2002) (July 14 (RGSC 6.0/rn6) Assembly of *Rattus norvegicus*) identified a 3,194 bp CpG island (highlighted in green in Figure 4.9) at 57,467,436-57,470,629 bps on chromosome 4, which is approximately 3,500 bps upstream of the first miRNA of the cluster (Figure 4.9).

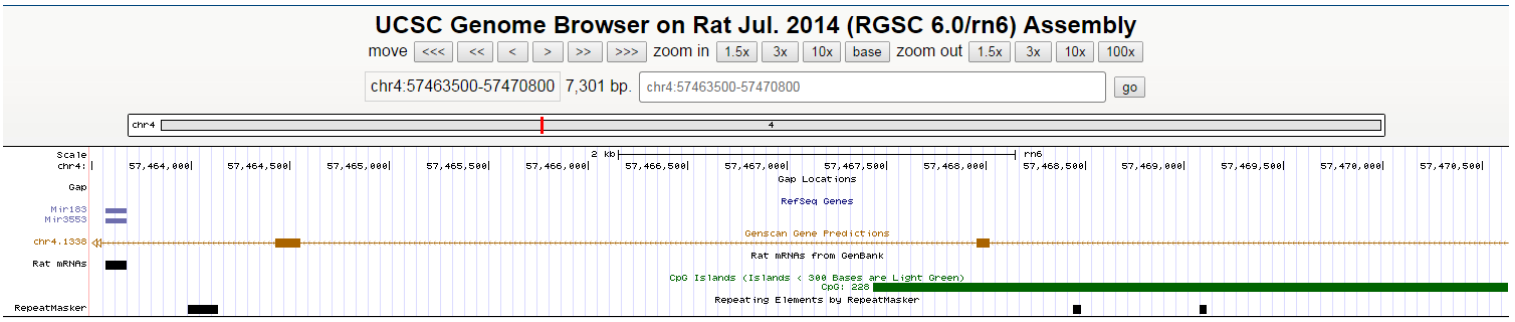


Figure 4.9: Analysis of miR-182/96 upstream sequence

Figure 4.9 shows the minus strand of *Rattus norvegicus* chromosome 4 orientated 3' to 5', upstream of the miR-182/96 (purple bar) cluster. The CpG island is shown (highlighted in green).

CpG islands are defined as >500bp in length, with G-C content ≥55% and a ratio of observed CpG / expected CpG ≥0.65 (Takai & Jones, 2002). The CpG island selected herein had a G-C content of 64% and a ratio of 0.7. Within this CpG island I identified a PB regulatory sequence known as a Barbie-box, which we designed PCR primers to amplify in order to sequence the 5 CpG sites around the Barbie-box. Barbie-boxes consist of a 10 bp PB consensus sequences (CCAAAGCNGG) that are bound by a barbiturate responsive protein(s) and found in the 5'-regulatory sequence of PB responsive genes, Cyp2b and α_1-acid glycoprotein (Fournier et al., 1994). Transfection of a promoter construct containing either functional, point mutated or deleted Barbie-box into primary rat hepatocytes showed that response to PB (2mM) was reduced in the latter two constructs (Fournier et al., 1994). Conversely, others have found that mutation of this sequence does not affect PB-mediated gene expression (Park, Li, & Kemper, 1996). However, the authors do note that mutation of the sequence in a luciferase construct containing the Cyp2b upstream regulatory sequence results in a slight increase in activity, suggesting a potential role as a negative regulator of gene expression.

RNA-sequencing identified miR-182 as significantly increased with PB treatment (1000ppm) compared to control at 28 days treatment in this sample set (Flores-Torres – thesis in 2015). Therefore methylation levels were assessed at 28 days, but also 14 days due to previous data indicating global hypermethylation with PB treatment (1000ppm) at this time (Koufaris et al., 2013). Seven days were also chosen. Cyp2b1/2 mRNA were shown to be significantly induced by PB (100ppm) compared to control at the start and cessation of the study (days 1, 3 and 28)

(Flores-Torres – thesis in 2015). Figure 4.10 shows that at the 3 time points tested there was no change in percentage methylation of the targeted CpG sites with PB treatment (1000ppm) compared to control.

Summary – These data suggest that methylation of the Barbie-box sequence within the CpG island upstream of miR-182/96 is unlikely to be involved in regulating the PB-mediated expression of these miRNAs.

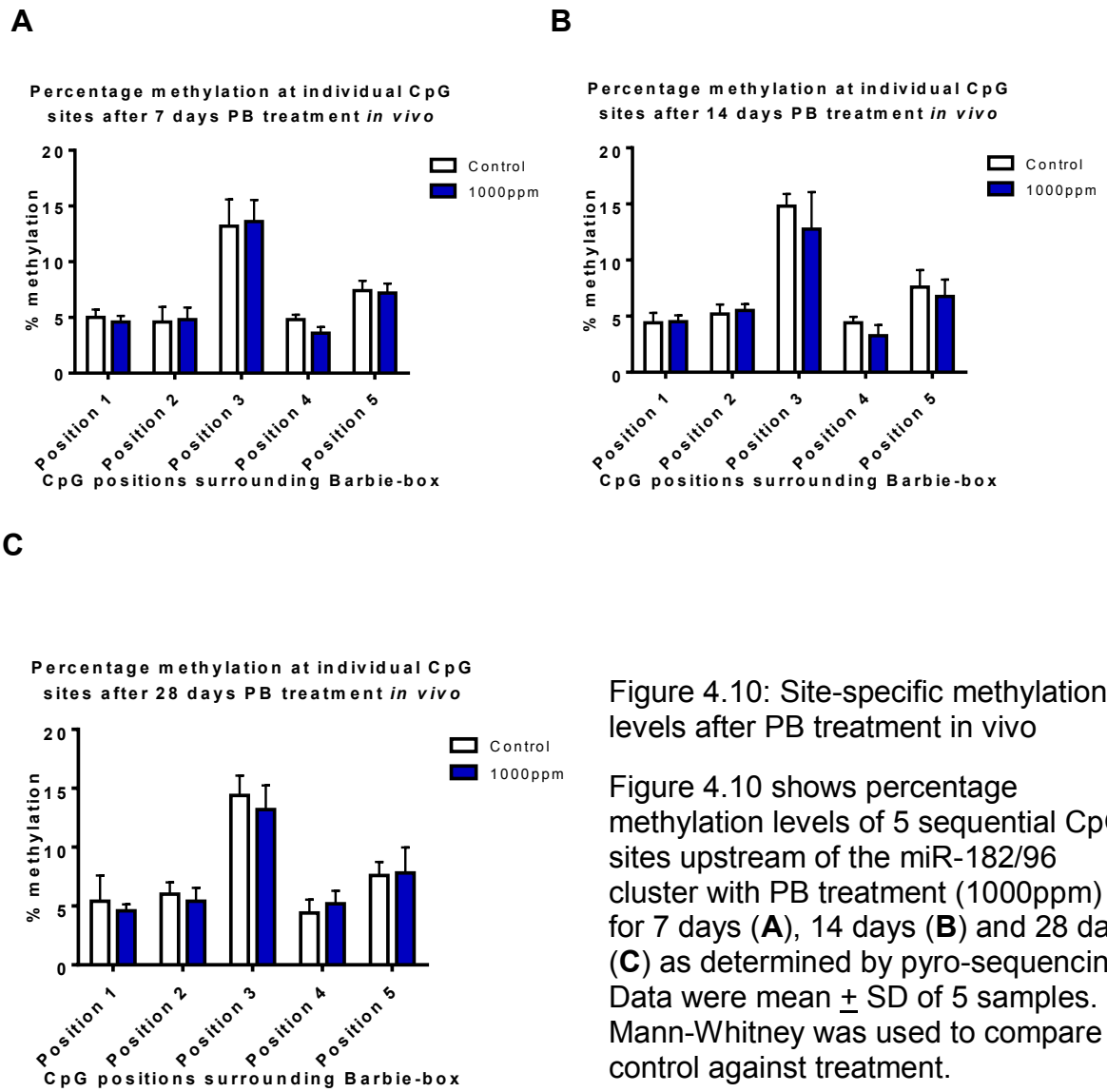


Figure 4.10: Site-specific methylation levels after PB treatment in vivo

Figure 4.10 shows percentage methylation levels of 5 sequential CpG sites upstream of the miR-182/96 cluster with PB treatment (1000ppm) for 7 days (**A**), 14 days (**B**) and 28 days (**C**) as determined by pyro-sequencing. Data were mean ± SD of 5 samples. Mann-Whitney was used to compare control against treatment.

4.3.2.3 P53 as a regulator of miR-182/96 expression in PB treated rats

To interrogate p53 as a regulator of miR-182/96, the downstream transcriptional target of p53, *cyclin-dependent kinase inhibitor 1A* (*p21*), was assessed. P21 inhibits cell cycle progression through inhibition of cyclin-dependent kinases (Harper, Adami, Wei, Keyomarsi, & Elledge, 1993). Expression of p21 was significantly decreased in the livers of PB treated (1000ppm) rats at 3 days treatment compared to control, and although decreased at 14 days, showed no significant change to control with PB treatment (1000ppm) (Figure 4.11 A and B). Three and 14 days were chosen as they reflect the time-dependent increase in miR-182 expression with PB treatment (1000ppm) (Figure 4.4).

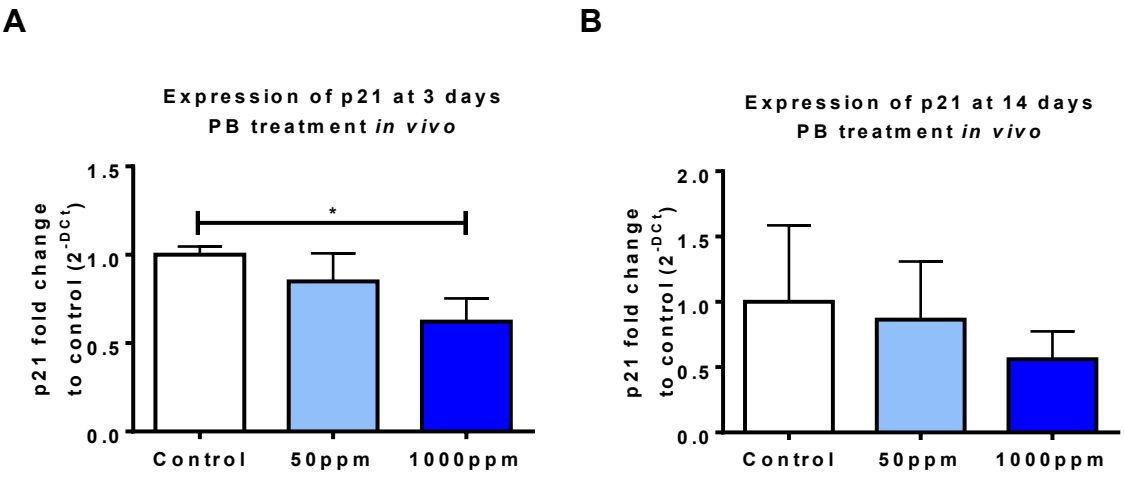


Figure 4.11: p21 expression in PB treated rats

Figure 4.11 depitcs p21 expression by qPCR after PB treatment (50ppm or 1000ppm) for 3 (**A**) or 14 (**B**) days. Data were mean ± SD of 3 samples, comparing treatment to control with Kruskal-Wallis and Dunn's multiple comparison.

Summary – These data suggest that p53 was not activated as a result of PB treatment and therefore is unlikely to be controlling the expression of miR-182/96. The significant decrease in p21 expression at 3 days PB treatment may reflect PB-induced hyperplasia, due to p21's role as an inhibitor of cell cycle progression.

4.3.2.4 ROS as a regulator of miR-182/96 expression in PB treated rats

Increased expression of *hypoxia-inducible factor-* (*Hif-*)*1α* mRNA and protein have been reported as inducible by oxidative stress (Bonello et al., 2007; Pialoux et al., 2009). Hif-1α is oxygen labile, resulting in protein levels increasing during hypoxic (low oxygen) and oxidative stress conditions. Stable Hif-1α associates with Hif-1β resulting in increasing expression of target genes involved in responding to oxidative stress, such as vascular endothelium growth factor (Vegf) (Pialoux et al., 2009). Therefore, it might be expected that if PB is inducing genes implicated in increasing oxidative stress (Dail et al., 2008; Elrick et al., 2005; Klepeisz et al., 2013), then *Hif-1α* expression might also be increased as a counter measure. However, expression of *Hif-1α* at 3 and 14 days PB treatment *in vivo* showed no significant change compared to control, which was further confirmed by lack of significant change in *Hif-1α* target, Vegf (Waterman et al., 2010).

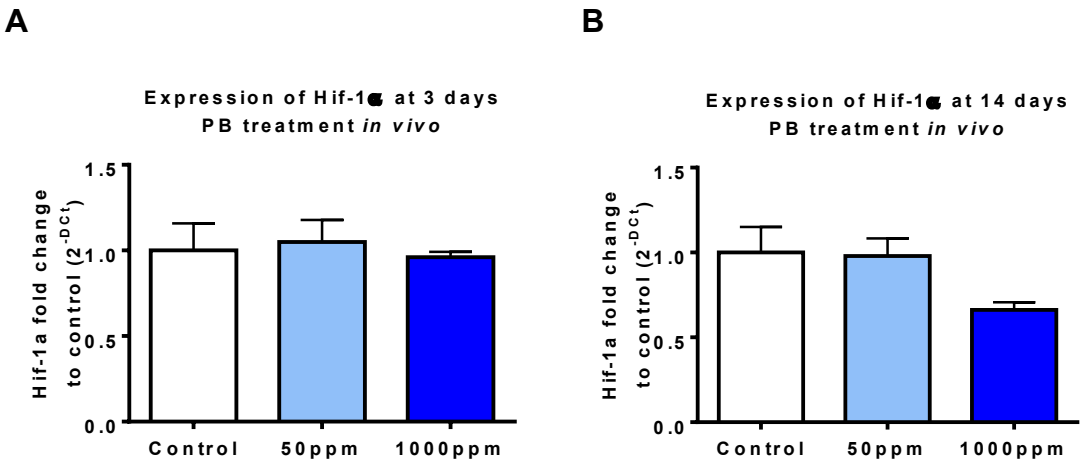


Figure 4.12: β-Gal and Hif-1α expression in PB treated rats

Figure 4.12 depitcs Hif-1α expression by qPCR after PB treatment (50ppm or 1000ppm) for 3 (**A**) or 14 (**B**) days. Data were mean ± SD of 3 samples, comparing treatment to control with Kruskal-Wallis and Dunn's multiple comparison.

Summary – These data suggest that increased ROS and subsequent oxidative stress are not likely to be involved in PB-mediated induction of miR-182/96. To confirm this, however, Hif-1α protein should also be assessed, as Hif-1α activity is determined by alteration in proteolytic degradation (Salceda & Caro, 1997).

4.3.2.5 Tgf-β as a regulator of miR-182/96 expression in PB treated rats

Expression of Tgf-β has been independently linked with PB treatment (Jirtle & Meyer, 1991) and increased miR-182 (Qiu et al., 2014). Although at 3 days, 50ppm PB appeared to induce Tgf-β1 expression, the response was not significant and demonstrated no clear dose effect (Figure 4.13 A). At 14 days PB treatment, no effect was seen (Figure 4.13 B).

A **B**

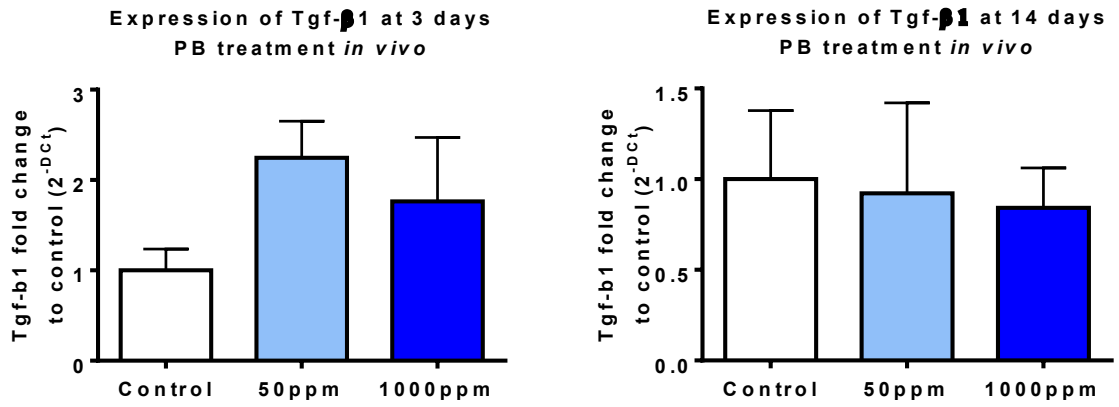


Figure 4.13: Tgf-β expression in PB treated rats

Figure 4.13 shows Tgf-β expression by qPCR after PB treatment (50ppm or 1000ppm) for 3 (**A**) or 14 (**B**) days. Data were mean ± SD of 3 samples, comparing treatment to control with Kruskal-Wallis and Dunn's multiple comparison.

Summary – These data suggest that increased Tgf-β expression is unlikely to be involved in the induction of miR-182/96 with PB treatment in the rat.

4.4 Conclusion

Through previous work we have identified miR-182/96 and miR-429/200b as PB-inducible miRNAs (Koufaris et al., 2012, 2013) (Figure 4.4). In this study we attempted to explore the expression of miR-182/96 and miR-429/200b in wild type and Car knockout rats in order to begin to interrogate the molecular changes underpinning the miRNA response.

Car as a miRNA regulator I demonstrated that there was little difference in the expression of the miRNAs between control and 500ppm PB treatment in wild type and knockout rats (Figure 4.6 and Figure 4.7). However, it was shown that miR-96 was significantly induced by PB (500ppm) compared to control in Car knockout rats (Figure 4.6 D), suggesting that this miRNA is not regulated by Car. MiR-96 and miR-182 are expressed from the same cluster from the same promoter (S. Xu, Witmer, Lumayag, Kovacs, & Valle, 2007) and exhibited significant positive correlation with PB treatment *in vivo* (Figure 4.4 B). Therefore this would suggest that the lack of significant expression of miR-182 is likely a dose-dependent issue. Furthermore, lack of increased expression of the other miRNAs examined indicates that a higher dose of PB may confirm the claim that miR-96 (and its cluster partner miR-182) are not regulated by Car.

B13/H cells Using the B13/H cells, which we have demonstrated are capable of increasing the expression of miR-182/96 in response to PB (chapter 2.3.3), I sought to confirm whether miR-182/96 were regulated by Car in the context of PB exposure *in vitro*. Unfortunately under the conditions used here to evaluate the effect of OAA, I

was unable to stimulate PB-mediated induction of *Cyp2b1/2*, in the presence of 0.1% v/v DMSO. It is unclear why, but suggests that the presence of 0.1% v/v DMSO as the vehicle may have contributed to this. Future work to repeat this experiment using ethanol to solvate OAA are indicated.

Hnf-4α as a miRNA regulator Car has been shown to exhibit an antagonistic relationship with Hnf-4α, despite Hnf-4α being sensitive to PB treatment (Bell & Michalopoulos, 2006; Miao et al., 2006). Due to the time-dependent expression of miR-182/96 and the apparent Car independent expression of miR-96 I hypothesised that the miRNA may be under the control of Hnf-4α. This was supported by the presence of Hnf-4α binding sites upstream of miR-96 (Koufaris, 2011). However, analysis of transcriptomic data from PB treated rats (Waterman et al., 2010) showed there was no change in the Hnf-4α regulated Cyp7a1 across the time when these miRNAs are induced, indicating that Hnf-4α is unlikely to control the expression of miR-182/96.

Other regulators From the literature I identified a number of PB-responsive pathways, which are also associated with increased miR-182/96 expression (Figure 4.1). However, transcriptomic or site-specific methylation analysis showed no changes to indicate regulation of miR-182/96 expression. Having only assessed one regulatory site by methylation analysis, it is possible that the key genomic regulatory region was overlooked and thus methylation could still play an important role in miRNA-mediated expression (Figure 4.14).

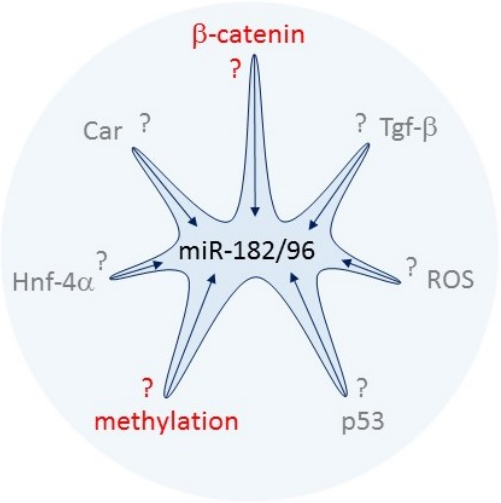


Figure 4.14: β-Catenin or methylation as miR-182/96 regulators

Figure 4.14 Potential regulators of PB-mediated miR-182/96 expression.

PB is reported as selecting for activating mutations in the *β-catenin* gene (Aydinlik et al., 2001) in mice treated with DEN (single intraperitoneal injection of 90µg/g body weight) followed by PB (on a diet of 0.05% PB) after 3 weeks rest, for 39 weeks. β-Catenin has been shown to be required for PB-mediated tumour promotion in the mouse (Rignall et al., 2011). It has been reported that β-catenin may contribute to PB-mediated carcinogenesis through altering cell adhesion, and not through a direct transcriptional response in the mouse (Aydinlik et al., 2001). As well as undergoing nuclear translocation after PB treatment, Car has also been shown to associate at the cell membrane (Koike et al., 2005). It would be interesting to see if after PB treatment Car is involved in interacting with β-catenin as a signalling complex, and if this association is conserved between the rat and the mouse.

Active β-catenin is also associated with increased expression of miR-182 in human breast cancer, although this is reported to be through a direct response (Chiang,

Hou, & Hung, 2013), suggesting that β-catenin could be involved in PB-mediated induction of miR-182/96 (Figure 4.14). Induction of miR-182/96 (and miR-200a/b/429) by PB is a rat specific event (Koufaris et al., 2012, 2013) as similar responses are not reported in the mouse (Lempiäinen et al., 2013). If β-catenin does regulate miR-182/96, then it may be that miR-182/96 are protecting the rat from PB-mediated tumour formation. This could be explored further through assessing associations of β-catenin with cell adhesion targets such as α-catenin (Aydinlik et al., 2001), or even Car, in comparison between rat and mouse models, both *in vivo* and *in vitro*. If this hypothesis is true then the function of miR-182/96 would be to maintain hepatic homeostasis, and therefore understanding miRNA function is the focus of the following chapter.

Chapter 4 Conclusions – In the rat, PB-mediated regulation of miR-182/96 could be through either epigenetic mechanisms or alteration of β-catenin activity state to maintain homeostasis. To explore if miR-182/96 are acting to preserve homeostasis, the function of these miRNAs will be interrogated next.

5. Function of phenobarbital-induced miRNAs

5.1 Introduction

In chapter 4 I explored potential regulators of the PB-inducible miR-182/96 cluster and suggest that β-catenin and methylation changes could potentially be involved. The function of these miRNAs have not been fully discussed however, and so will be the focus of this chapter.

5.1.1 PB responsive miRNAs in the mouse

One year PB treatment (0.05% w/v) of male B6C3F$_1$ mice is known to induce liver tumours (Becker, 1982). It has also been reported that the same treatment over 13 weeks induced expression of the noncoding RNA cluster, *Dlk1-Dio3*, which has been suggested as a candidate marker for hepatic tumour promotion in the mouse (Lempiäinen et al., 2013). The *Dlk1-Dio3* cluster contains 53 miRNAs (Benetatos et al., 2013; Lempiäinen et al., 2013), which are reported to be involved in cell signalling, cell morphology and a variety of cancers (Benetatos et al., 2013). Furthermore, it was demonstrated that PB-mediated expression of the *Dlk1-Dio3* cluster was dependent on both Car and β-catenin, therefore implicating this ncRNA in PB-induced tumourigenesis (Lempiäinen et al., 2013), unlike miR-96 in the rat, which appears to be regulated independently of Car (chapter 4.3.1.2). In a separate study, male C3H/HeJ mice were treated with DEN (single intraperitoneal injection of 90mg/kg body weight) for 2 weeks, followed by a diet of PB (0.05%w/w) for 39 weeks (Unterberger et al., 2014). DEN/PB tumour promotion studies are known to induce growth of β-catenin activated tumours (Aydinlik et al., 2001; Rignall et al., 2011; Unterberger et al., 2014), yet the data presented by Unterberger *et al.,*

(Unterberger et al., 2014) identified different deregulated miRNAs following DEN/PB treatment compared to PB alone (by Lempiainen *et al.,* (Lempiäinen et al., 2013)); although only three were detected as significantly changed.

These data suggest that the different treatments used to induce tumours in rodents *via* PB result in disparate effects on the miRNAome; although it must be noted that different mouse strains were used. Nonetheless, miRNA expression as a result of PB treatment in the mouse appear representative of the tumour promoting phenotype. However in the rat, as PB does not induce tumours without pre-treatment with a DNA damaging agent, it is thought that PB-mediated miRNA expression changes may be involved in maintaining homeostasis (Koufaris et al., 2012, 2013).

5.1.2 PB responsive miRNAs in the rat

PB time- and dose-dependently induces miR-200a/b/429 and miR-182/96 in the rat (Koufaris et al., 2012, 2013). The miR-200 cluster are reported to be involved in antagonising tumourigenesis through inhibiting EMT in bladder cancer cells (Adam et al., 2009), breast cancer cells (Gregory et al., 2011) and in the context of PB exposure in rats (Koufaris et al., 2013). Interestingly, miR-96 has also been shown to inhibit EMT. In HCT116 colorectal cancer cells, over expression of the EMT transcription factor Zeb1 supressed miR-96 and miR-200a/b expression, which was reversed in Zeb1 knockdown experiments (X. L. Li et al., 2013). This confirmed previous work reporting a negative feedback loop between Zeb and miR-200 expression (Bracken et al., 2008), but also demonstrated that miR-96 is sensitive to this regulation. Zeb1/2 protein expression has already been identified as down-

regulated in the livers of PB treated rats (Koufaris et al., 2013) and so will not be discussed here.

MiR-182/96 have been shown to act as oncomiRs in a number of cancers, including hepatocellular carcinoma (T.-H. Wang, Yeh, Ho, Ng, & Chen, 2015), prostate cancer (Tsuchiyama et al., 2013) breast cancer (Guttilla & White, 2009) and bladder cancer (Hirata et al., 2012). MiR-182 has also been reported as a tumour suppressor in some cancers, such as uveal melanoma (Yan et al., 2012) and renal cell carcinoma (Xin Xu et al., 2014), while miR-96 has been reported to act as a tumour suppressor in prostate cancer (Yu et al., 2010). This suggests that miRNA function is highly context dependent. In fact, miR-182/96 have been predicted to be involved in maintaining mitoinhibition in the livers of PB treated rats. This was reported due to predicted targets in pathways involved in growth factor signalling, such as MAPK/erbb, and the temporal induction of these miRNAs coinciding with the cessation of the hyperplastic response (Koufaris et al., 2013). However, no targets have been confirmed for miR-182/96 in the context of PB exposure. Here I identify a number of targets associated with miR-182/96, which are also deregulated as a result of PB treatment *in vivo*.

5.1.3 Hypothesis

MiRNA targets can be identified using *in silico* analyses of the expression of miRNAs in *in vivo* PB treated samples. Identified targets will be context-specific and indicative of the PB phenotype.

5.1.4 Aims

1. Use *in silico* analyses to identify potential targets of miR-182/96.
2. Confirm targets through selected targeted analysis.

5.2 Methods

5.2.1 Tissue samples

As described in chapter 3.2.1

5.2.2 In silico analysis

In silico analyses were performed using miRWalk (Dweep, Sticht, Pandey, & Gretz, 2011) and TargetScan (B. P. Lewis, Shih, Jones-Rhoades, Bartel, & Burge, 2003) to identify miRNA targets. TargetScan identified putative miRNA targets based on sequence matches between the miRNA seed sequence and the 3'UTR of genes, and assessed surrounding sequences for added complementarity (B. P. Lewis et al., 2003). MiRWalk identified putative targets in a similar manner but allowed comparison between other miRNA target prediction algorithms for miRNA binding to the 3'UTR of genes. MiRWalk also contained a curated database of experimentally validated targets from the literature (Dweep et al., 2011).

5.2.3 qRT-PCR

As described in chapter 2.2.6

5.3 Results and Discussion

5.3.1 Aim 1: Use *in silico* analyses to identify potential targets of miR-182/96.

5.3.1.1 miR-182/96 sequence

Despite the fact that miR-182 and miR-96 both have the same seed sequence (nucleotides 2-7) they have been shown to exhibit unique target specification due to miR-96 containing a cytidine at position 8, and miR-182 with an adenosine (Jalvy-Delvaille et al., 2012) (Figure 5.1). Others have reported that miR-182 and miR-96 have overlapping targets (Guttilla & White, 2009). The work presented here assessed both unique and common targets between these two miRNAs. As discussed in chapter 1.3.1, functional miRNAs can be generated from the cleavage of double stranded pre-miRNA hairpin structures, and either the 5p or 3p end of the pre-miRNA hairpin becomes the mature miRNA; it is the 5p end of the miRNAs (Figure 5.1) that are referred to in this work and not the miRNA-3p form. However, as the 3p form of miRNAs also exhibits functional effects (J.-S. Yang et al., 2011) it would be interesting to explore miR-182/96-3p expression and potential targets in future work.

Rno-miR-182	5’-UUUGGCAAUGGUAGAACUCACACCG-3’
Rno-miR-96-5p	5’-UUUGGCACUAGCACAUUUUUGCU-3’

Figure 5.1: MiR-182/96 sequence

Figure 5.1 shows the seed sequence, 2-7+nt8 (shown in red with sequence differences underlined), for Rno-miR-182/96-5p (obtained from www.mirbase.org (Kozomara & Griffiths-Jones, 2014)). Rno, *Rattus norvegicus*.

5.3.1.2 Validated miR-182/96 targets

Validated targets of miR-182 and/or miR-96 were identified using miRWalk (Dweep et al., 2011). This generated 30 high probability targets for rno-miR-182, and 39 for rno-miR-96. To further clarify these putative targets, they were then assessed for significant changes in expression with PB treatment *in vivo*, using published data from Waterman *et al.,* (Waterman et al., 2010), whereby $p<0.001$ by two way ANOVA with Benjamini and Hochberg false discovery rate across 14 days PB treatment (0, 50, 500, 1000ppm). This concluded in 3 targets for miR-182: *Egfr*, *Radixin* and *Slc12a2* (solute carrier family 12a2/sodium potassium chloride cotransporter (NKCC1)). In order to substantiate these targets, their expression at 3, 7 and 14 days PB treatment (0, 50, 500, 1000ppm) from Waterman *et al.,* (Waterman et al., 2010) were correlated with the expression of miR-96 using microarray data generated by Koufaris (Koufaris, 2011). MiR-182 expression could not be used in this instance as the expression level was too variable to be quantified by array (Koufaris, 2011), although both miRNAs demonstrated highly correlative expression (Figure 4.4). Furthermore, due to the data available, correlations compare average gene/miRNA expression over multiple time points and doses and therefore complicates data interpretation. Only one target passed these selection criteria: *Slc12a2*.

Slc12a2 Using Spearman correlation, Slc12a2 significantly negatively correlated with miR-96 and was therefore identified as a potential target (Figure 5.2 A and B). *Slc12a2* is a gene encoding for a cotransporter associated with increasing intracellular neuronal Cl^- levels in neonates (Dzhala et al., 2005). Therefore, miRNA-

mediated inhibition of *Slc12a2* might be to modulate the chronic effects of PB exposure and Cl^- influx.

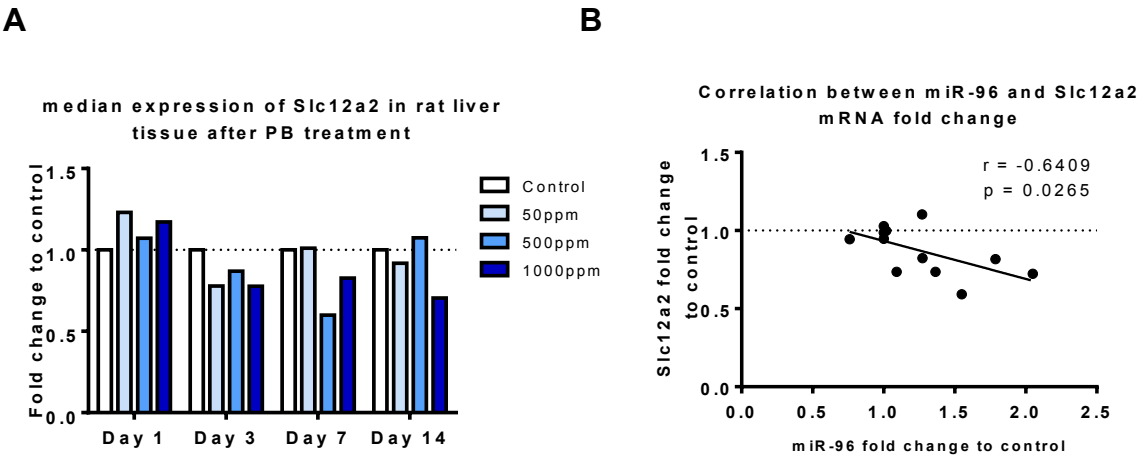


Figure 5.2: In silico analysis of validated miRNA targets (1)

Figure 5.2 shows median expression and miR-96 Spearman correlation with Slc12a2 (**A**/**B**). mRNA data were obtained from Waterman *et al.,* (Waterman et al., 2010), and miRNA expression from Koufaris (Koufaris, 2011). Data were representative of 4-5 samples.

MiR182/96 targets were also identified through literature searches in the same manner as described above. Through this method I determined a selection of miRNA targets whose expression were significantly altered by PB *in vivo*, and also significantly negatively correlate with miR-96 expression.

Smad4 Mothers against decapentaplegic homolog 4 (Smad4) was identified as a validated target for miR-182 (Hirata et al., 2012) (Figure 5.3 A and B). Smad4 is a downstream component of Tgf-β signalling that is bound by receptor activated Smads (Smad2/3), which then translocate into the nucleus to modulate gene expression (Moustakas, Souchelnytskyi, & Heldin, 2001). Smad4 is also downstream

of bone morphogenetic protein signalling (Moustakas et al., 2001). Smad4 has been reported as decreased in prostate cancer, yet appears to be important in disease progression only in the presence of other gene dysregulation (Z. Ding et al., 2011). It has also been demonstrated that Smad4 is decreased in GST-P positive foci in the livers of rats treated with DEN-PB to promote tumourigenesis (Ichimura et al., 2010). Yet, Smad4 has also been shown to be increased in patients with hepatocellular carcinomas (Hernanda et al., 2014), demonstrating that Smad4 is associated with both tumour suppression and tumour growth. Interestingly, Smad4 knockdown has been reported to abrogate up-regulation of Zeb (Gregory et al., 2011), suggesting that miR-182 might be acting in concert with the miR-200 cluster to suppress EMT.

Rb1 The retinoblastoma (Rb1) tumour-suppressor gene was also identified as a validated target for miR-182 (Krishnan, Steptoe, Martin, Wani, & Nones, 2012) (Figure 5.3 C and D). Rb1 is a regulator of cell cycle progression, cellular differentiation and survival; the loss of which is associated with myriad tissue defects and cancers (reviewed in (Goodrich, 2006)). Interestingly, loss of Rb1 function leads to the activation of multiple components of glycolysis, increasing lactate production (Clem & Chesney, 2012), which is also reported to be increased in the plasma of PB treated rats (Waterman et al., 2010).

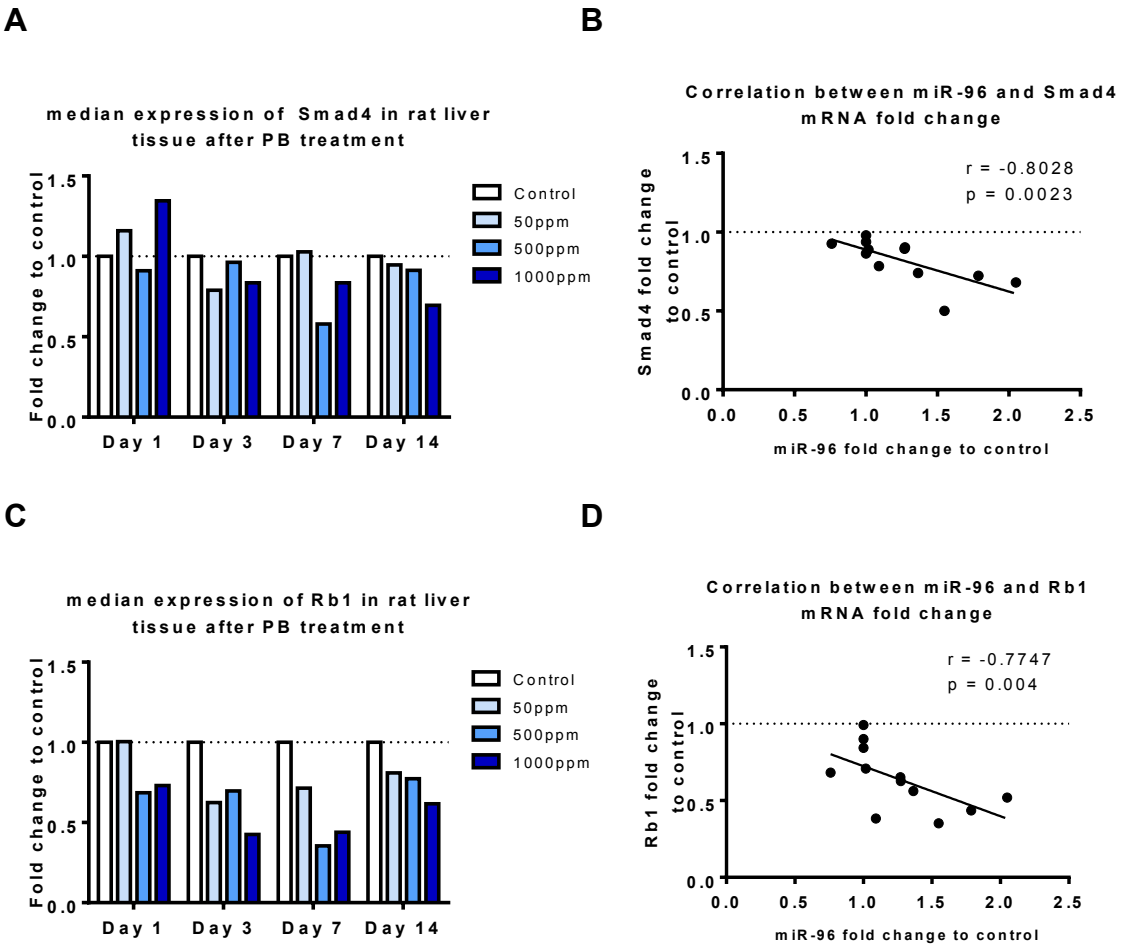


Figure 5.3: In silico analysis of validated miRNA targets (2)

Figure 5.3 shows median expression and miR-96 Spearman correlation with Smad4 (**A**/**B**) and Rb1 (**C**/**D**). mRNA data were obtained from Waterman *et al.,* (Waterman et al., 2010), and miRNA expression from Koufaris (Koufaris, 2011). Data were representative of 4-5 samples.

FoxO1 FoxO1 has been reported as a validated target for miR-96 and miR-182 (Guttilla & White, 2009), and is important in the regulation of gluconeogenic genes such as phosphoenolpyruvate carboxykinase (Pepck) and glucose-6-phosphatase (G6pase) (Puigserver et al., 2003), as well as acting as a co-activator for Car target genes (Kodama et al., 2004). Therefore FoxO1 was also interrogated as a potential miRNA target. Although FoxO1 was not reported as significantly changed by Waterman *et al.,* (Waterman et al., 2010), my preliminary data showed that FoxO1 significantly negatively correlated with miR-182 expression by qPCR (Figure 5.4),

suggesting that the above criteria used to select targets are quite stringent and are likely to be excluding other positive target matches.

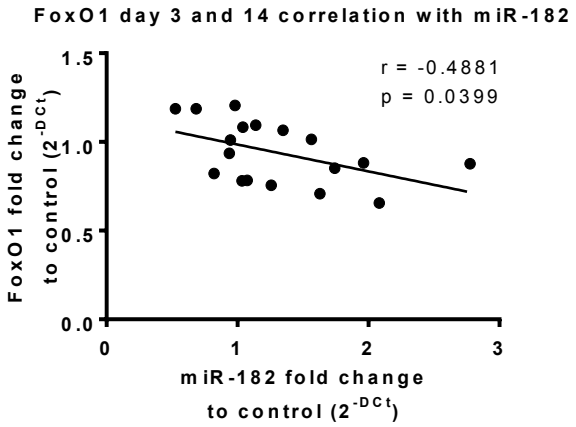


Figure 5.4: In vivo FoxO1 correlation with miR-182

Figure 5.4 shows the correlation between FoxO1 and miR-182 by qPCR at 3 and 14 days PB treatment (0, 50 and 1000ppm) using Spearman correlation.

Summary – These data demonstrate that the validated miRNA targets: Slc12a2, Smad4, Rb1 and FoxO1 exhibited expression changes and correlations indicative of miRNA regulation in the context of PB exposure *in vivo*.

5.3.1.3 Predicted miR-182/96 targets

I also explored predicted miRNA targets in the context of PB exposure. In order to limit the number of mRNA targets identified, through miRWalk, I first selected targets that were only consistently predicted (by at least 4 of the 8 programs searched by miRWalk). This generated 248 targets for rno-miR-182, and 231 targets for rno-miR-96. Using a threshold of 3 matches between search programs would have selected 629 potential targets of miR-182 and 578 for miR-96. Therefore using $\geq$4 programs concordance cut-off, produced a large, but not overwhelming number of targets.

Targets were again assessed for significant change in expression with PB treatment using data from Waterman *et al.,* (Waterman et al., 2010), and further stratified by significant negative correlation with miR-96 expression from Koufaris (Koufaris, 2011). Only those that passed both criteria were selected, and are discussed below.

Pc Pyruvate carboxylase (Pc) was identified as a putative target for both miR-182 and miR-96 (Figure 5.5 A and B). Pc catalyses the carboxylation of pyruvate to oxaloacetate in gluconeogenesis (Jitrapakdee & Wallace, 1999). Therefore, miR-182/96-mediated decrease of Pc might be predicted to decrease gluconeogenesis. Decreased hepatic glucose is a hallmark of PB treatment (Waterman et al., 2010), suggesting this may be mediated in part by miR-182/96.

Slc12a2 Slc12a2 was identified as a potential target for miR-182 and miR-96, and as a validated target for miR-182 (Figure 5.2 A and B), suggesting this gene may be a common target for both miRNAs.

Slc37a4 A second transporter was also identified as a putative target for miR-182; solute carrier family 37 (glycerol-6-phosphate transporter), member 4 (G6pt/Slc37a4) (Figure 5.5 C and D). Slc37a4 transports glucose-6-phosphate into the lumen of the endoplasmic reticulum to enable de-phosphorylation to glucose *via* glucose-6-phosphatase (Chou & Mansfield, 2014). Therefore, miR-182 mediated suppression of Slc37a4, as with FoxO1 and Pc, may contribute to PB-mediated decrease in hepatic glucose.

Map2k1 mitogen-activated protein kinase kinase 1 (Mek1/Map2k1) was identified as a putative target for miR-96 (Figure 5.5 E and F). Map2k1 is an upstream kinase for the activation of Erk. Indeed inhibition of Map2k1 has been reported to potentiate PB-mediated Cyp induction, potentially through Erk inhibition (Florence Joannard et al., 2006). This suggests that miR-96 could be involved in modulating gene induction by PB through effecting Erk activation.

Olr59 Olfactory receptor 59 (Olr59) was identified as a putative target for miR-96 (Figure 5.5 G & H). The expression of rat *Olr59* is reported to be male specific (Babelova et al., 2015), although there is very little else reported on this gene in the literature. *Olr59* was shown to be expressed in rat mesenteric arterial tissue, as was the mouse homologue, *Olfr78*, in mouse arteries. Olfr78 was reported to bind short chain fatty acids to modulate vasodilation (Reho, Shetty, Dippold, Mahurkar, & Fisher, 2015). PB has been shown to increase the uptake of fatty acids in the livers of treated rats, potentially involved in endoplasmic reticulum growth (Waterman et al., 2010). It would be interesting to determine the role of Olr59 in this context, and whether miR-96 could be reducing expression of this gene to mediate Olr59's response to the influx of fatty acids.

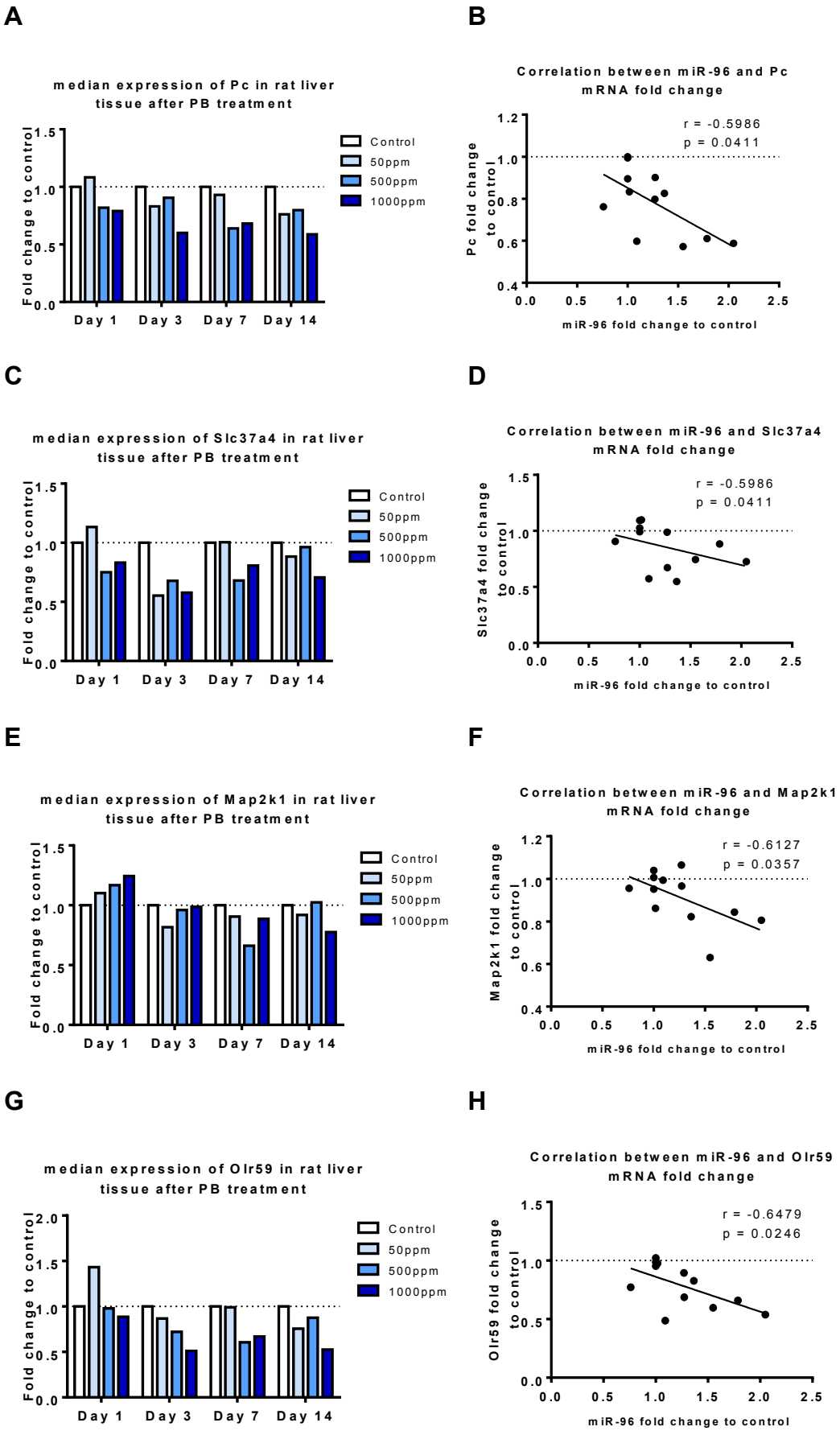


Figure 5.5: In silico analysis of predicted miRNA targets

Figure 5.5 shows median expression and miR-96 Spearman correlation with Pc (**A**/**B**), Slc37a4 (**C**/**D**), Map2k1 (**E**/**F**) and Olr59 (**G**/**H**). mRNA data were obtained from Waterman *et al.,* (Waterman et al., 2010), and miRNA expression from Koufaris (Koufaris, 2011). Data were representative of 4-5 samples.

Gnmt Glycine *N*-methyltransferase (Gnmt) was identified in preliminary work as significantly reduced by PB treatment in the rat (Figure 5.6 A). Using multiple comparisons in MiRWalk, Gnmt was not detected as a target for miR-182. Due to the stringent criteria selected for target identification, I also used TargetScan (B. P. Lewis et al., 2003) and found Gnmt was a predicted target for miR-182. Furthermore, Gnmt expression also correlated with the expression of miR-96 (Figure 5.6 B). Gnmt catalyses glycine methylation to sarcosine (and *S*-adenosylhomocysteine) using the methyl donor, *S*-adenosylmethionine. Gnmt is thought to be a major regulator of methylation of DNA/protein due to the use of *S*-adenosylmethionine in cellular methylation reactions (Luka, Mudd, & Wagner, 2009). Interestingly, Gnmt knockout mice present with hypoglycaemia due to decreased expression of fructose 1,6-bisphosphatase, phosphoenolpyruvate carboxykinase, and Slc37a4, as well as showing hepatomegaly (Liu et al., 2007), all of which are associated with the PB phenotype (Waterman et al., 2010). These suggest that PB-mediated DNA methylation changes might be influenced by miR-182 inhibition of Gnmt expression, resulting in an increase in available methyl groups for DNA methylation, as well as affecting glucose metabolism.

A **B**

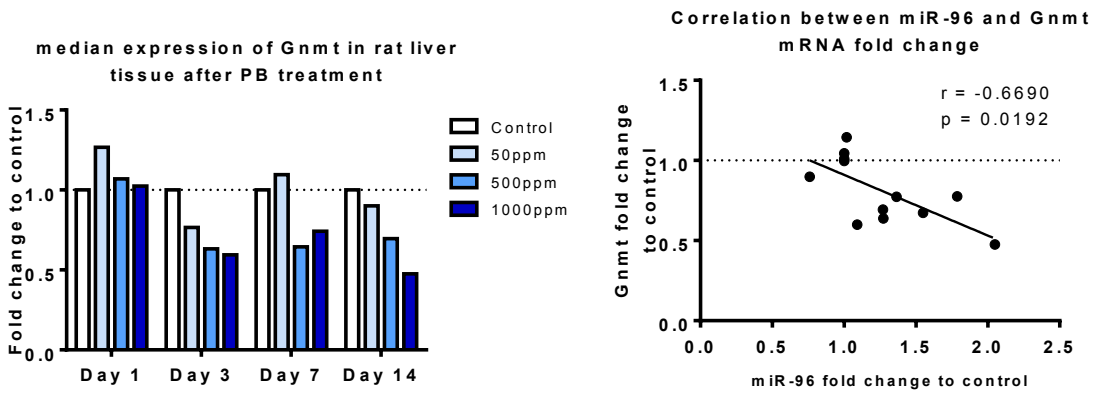


Figure 5.6: In silico Gnmt correlation with miR-96

Figure 5.6 shows the media expression of Gnmt (**A**) with PB treatment and Spearman correlation with miR-96 (**B**). mRNA data were obtained from Waterman *et al.,* (Waterman et al., 2010), and miRNA expression from Koufaris (Koufaris, 2011). Data were representative of 4-5 samples.

Summary - These data demonstrate that the predicted miRNA targets: Pc, Slc37a4, Map2k1, Olr59 and Gnmt displayed expression changes and correlations consistent with miRNA regulation in the context of PB exposure *in vivo*.

5.3.2 Aim 2: Confirm targets through selected targeted analysis.

5.3.2.1 MiR-182/96 targets chosen for validation in vivo

From the *in silico* analysis I have identified a number of validated and predicted targets for miR-182/96 (Table 5.1).

Table 5.1: MiR-182/96 targets

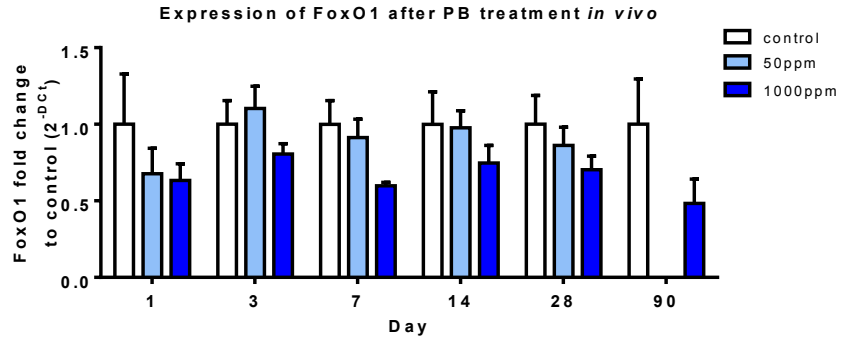
Gene	**Rno-miR-182**	**Rno-miR-96**
Slc12a2	Validated	Predicted
Smad4	Validated	-
Rb1	Validated	-
FoxO1	Validated	Validated
Pc	Predicted	Predicted
Slc37a4	Predicted	-
Map2k1	-	Predicted
Olr59	-	Predicted
Gnmt	Predicted	-

Table 5.1 shows validated (in green) and predicted (in blue) targets of miR-182 and miR-96.

In order to assess the strength of the *in silico* analysis, I chose two targets to profile using qPCR across 1-90 days PB treatment *in vivo*, and correlated their expression to miRNA expression in matched samples. As the only validated target for both miRNAs as well as due to its role in gluconeogenesis, FoxO1 was selected for validation. Gnmt was also selected as a predicted target of miR-182 and due to its role in regulating methylation and glucose metabolism both of which are affected by PB treatment (Koufaris et al., 2013; Waterman et al., 2010).

FoxO1 mRNA The validated target FoxO1, showed a trend for decreased expression at all time-points tested with PB (1000ppm) compared to control (Figure 5.7 A). Furthermore, in matched samples FoxO1 significantly negatively correlated with miR-182 (Figure 5.7 B), suggesting that FoxO1 could be a target of miR-182/96. It is interesting to note that FoxO1 expression appears decreased regardless of the time-dependent effect of PB on miR-182 (Figure 4.4). This could indicate that the miRNAs are working in concert with other factors to help maintain FoxO1 levels, or that the two may be independent. To further clarify this FoxO1 protein levels were assessed.

A



B

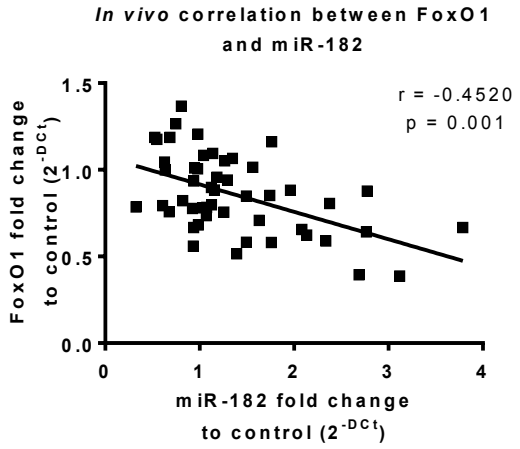
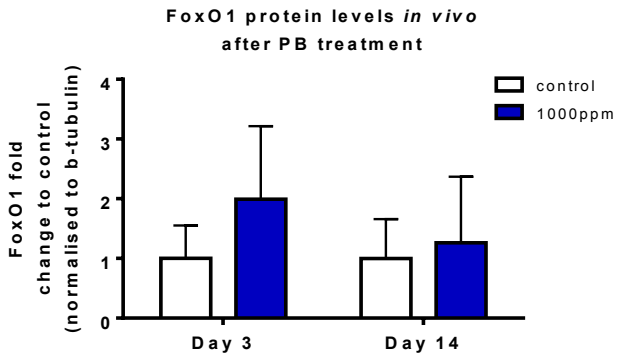


Figure 5.7: FoxO1 as a target for miR-182

Figure 5.7 shows the expression of FoxO1 mRNA in the livers of PB treated rats (**A**). Data shown were mean ± SD of 3 samples. Y-axis is fold change to control using the $2^{-\Delta Ct}$ method. Kruskal-Wallis with Dunn's multiple comparison to control was used to determine statistical significance, as well as Spearman's correlation between FoxO1 and miR-182 fold change from matched samples (**B**).

FoxO1 protein Immunoblots for FoxO1 protein were performed, which spanned the PB-mediated time-dependent change in miRNA expression. The data in Figure 5.8 shows that PB (1000ppm) did not significantly change FoxO1 expression at either time point relative to control. However there does appear to be decreased FoxO1 expression over time, which could be indicative of the miRNA expression changes.

A



B

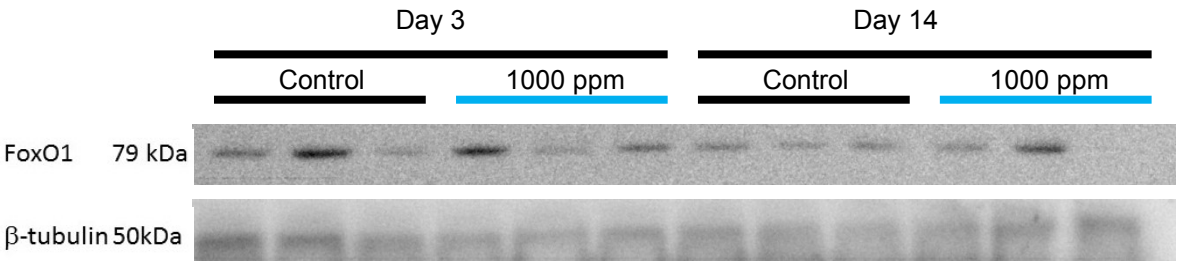


Figure 5.8: In vivo FoxO1 protein expresion

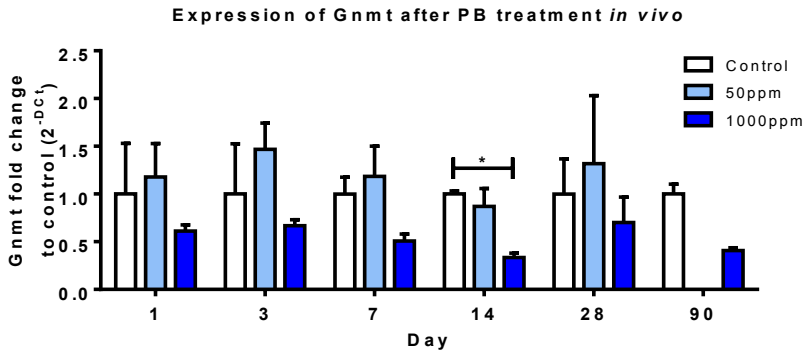
Figure 5.8 shows the expression of FoxO1 protein in the livers of PB treated rats at days 3 and 14 (**A**). Data shown were mean ± SD of 3 samples, with Y-axis as fold change to control, after normalisation to β-tubulin. Mann-Whitney tests were used to compare control with treatment. Representative blot shown (**B**).

Summary – The data presented suggests that PB does not significantly alter expression of FoxO1 mRNA or protein. However treatment with PB consistently lowers the mean FoxO1 mRNA levels and correlation analysis and change in protein

over time suggest that miR-182/96 may contribute to FoxO1 regulation in the context of PB exposure.

Gnmt mRNA The predicted miR-182 target, Gnmt, was also shown to be consistently decreased throughout high dose PB (1000ppm) treatment *in vivo* (Figure 5.9 A), with significant suppression at 14 days. Significant negative correlation with miR-182 suggests Gnmt expression may be controlled by miR-182 (Figure 5.9 B), in a similar manner to that described for FoxO1.

A



B

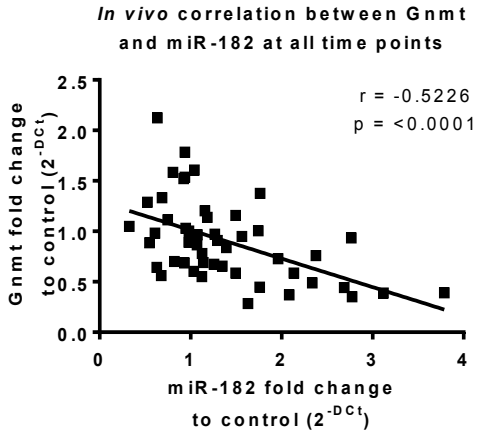
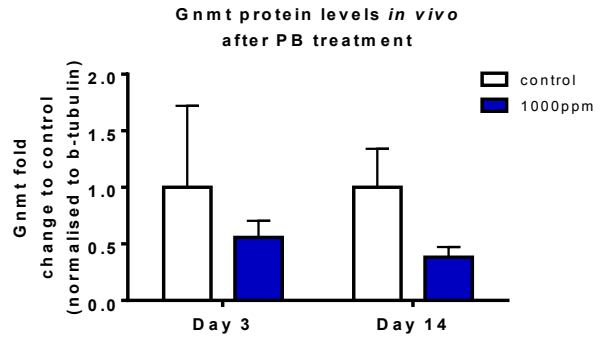


Figure 5.9: Gnmt as a target for miR-182

Figure 5.9 shows the expression of Gnmt mRNA in the livers of PB treated rats (**A**). Data shown were mean ± SD of 3 samples. Y-axis is fold change to control using the $2^{-\Delta Ct}$ method. Kruskal-Wallis with Dunn's multiple comparison to control was used to determine statistical significance, as well as Spearman's correlation between Gnmt and miR-182 fold change from matched samples (**B**). *p<0.05.

Gnmt protein Gnmt protein expression was then determined to further explore the potential effects of miR-182 on Gnmt. The data in Figure 5.10 A shows that Gnmt protein was decreased at both time points, and although not significant by Mann-Whitney, was significantly decreased by t test at day 14 (p=0.0383). This would suggest that Gnmt may be a target for miR-182 (Figure 5.10 A & B).

A



B

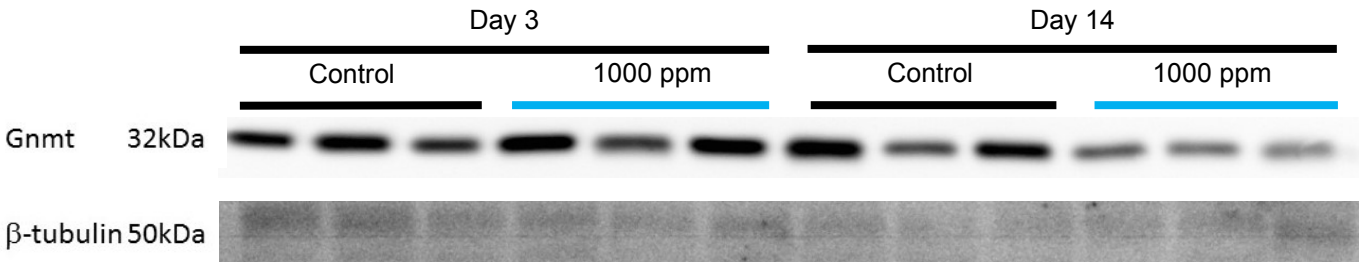


Figure 5.10: In vivo Gnmt protein expression

Figure 5.10 shows the expression of Gnmt protein in the livers of PB treated rats at days 3 and 14 (**A**). Data shown were mean ± SD of 3 samples, with Y-axis as fold change to control, after normalisation to β-tubulin. Mann-Whitney tests were used to compare control with treatment. Representative blot shown (**B**).

Summary – These data suggest that PB may influence expression of Gnmt through miR-182.

5.4 Conclusion

From the *in silico* analysis I have identified a number of validated and predicted targets of miR-182/96. The assessment of 2 targets, *FoxO1* and *Gnmt*, across a sub-chronic PB treatment plan *in vivo* suggests that these targets may be regulated by miR-182/96. It is tempting to speculate that the remaining *in silico* identified targets are also likely to be regulated by miR-182/96.

To verify the above targets I would need to perform transfection studies. Preliminary studies in B13/H (and B13 cells) demonstrated that 96 hours transfection increased both miR-182 and miR-96 expression levels but failed to affect the validated target FoxO1 (data not shown). These experiments suggested that further transfection optimisation is required. There are a number of miRNA targets that are predicted to be specific to either miR-182 or miR-96 (Table 5.1) and further transfection optimisation would enable these specific miRNA-mRNA interactions to be confirmed.

Glycolysis FoxO1 was identified as a validated target for both miR-182/96, Rb1 as a validated target for miR-182, Pc as a novel predicted target for both, while Slc37a4 and Gnmt were novel predicted targets of miR-182, and Map2k1 for miR-96. PB treatment has been shown to reduce hepatic glucose (Waterman et al., 2010), which could be due in part to miRNA-mediated glycolysis *via* suppression of Rb1, FoxO1, Pc, Slc37a4 and Gnmt (Table 5.2 and Figure 5.11). PB has been reported to increase malic enzyme activity (Waterman et al., 2010), which would result in the conversion of malate to pyruvate and the generation of NADPH (Jitrapakdee & Wallace, 1999) (Figure 5.11). Together, it might be that these miRNA targets

coupled with altered malic enzyme are involved in increasing NADPH generation for hepatic Cyp-mediated hydroxylation, which is significantly upregulated by PB treatment (Waterman et al., 2010).

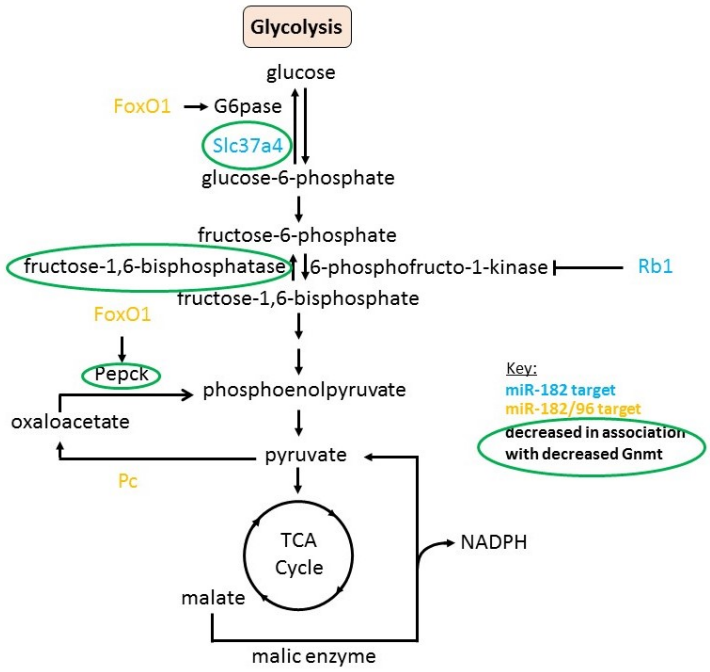


Figure 5.11: MiRNA-mediated glycolysis

Figure 5.11 demonstrates the predicted effect of miR-182/96 targets on glycolysis based on target gene function from the literature, described in text.

Table 5.2: Proposed function of miR-182/96

Gene	Rno-miR-182	Rno-miR-96	MiR function
Slc12a2	Validated	Predicted	Modulating Cl^- influx
Smad4	Validated	-	Inhibit EMT
Rb1	Validated	-	Glycolysis
FoxO1	Validated	Validated	Glycolysis
Pc	Predicted	Predicted	Glycolysis
Slc37a4	Predicted	-	Glycolysis
Map2k1	-	Predicted	Car activation
Olr59	-	Predicted	Lipid response
Gnmt	Predicted	-	Increased methylation
			Glycolysis

Table 5.2 shows proposed gene functions related to the PB-phenotype: glucose metabolism (pale red).

Furthermore, miR-96-mediated targeting of Map2k1 could control downstream Erk activation. This might be predicted to modulate PB-induction of Cyp genes over extended treatments, as Erk has been shown to inhibit PB-induced gene expression in the rat (Florence Joannard et al., 2006). Reduced expression of the above miRNA target genes are indicative of increased glycolysis, which is a hallmark of cancer development (Hanahan & Weinberg, 2011). However in the rat PB does not induce cancer without an initiating event, therefore taken together it might be that the miRNA-mediated changes discussed here are involved in controlling PB-mediated Cyp induction and controlling glycolysis activity to allow production of NADPH for biotransformation.

Methylation Gnmt was identified as a novel predicted target for miR-182. PB treatment has been shown to cause transient global hypermethylation in the rat (Koufaris et al., 2013). Interestingly, this methylation change in the rat is seen at 14 days treatment and corresponds to the decrease in Gnmt mRNA and protein expression shown here (Figure 5.9 A, and Figure 5.10 A). Decreased Gnmt levels would result in an increased availability of methyl donor groups for DNA methylation (Figure 5.12). MiR-29b has also been identified as decreased at 14 days PB treatment in the rat (Koufaris, 2011). MiR-29b directly targets DNA methyltransferase enzymes (Dnmt)3a/3b, and indirectly targets Dnmt1 (Garzon et al., 2009), which might be expected to result in increased levels of Dnmts and subsequent DNA methylation. This suggests that miR-182 and miR-29b may work in concert to induce global hypermethylation in response to PB treatment (Table 5.2 and Figure 5.12). The function of this methylation change, and its transient nature are currently unknown.

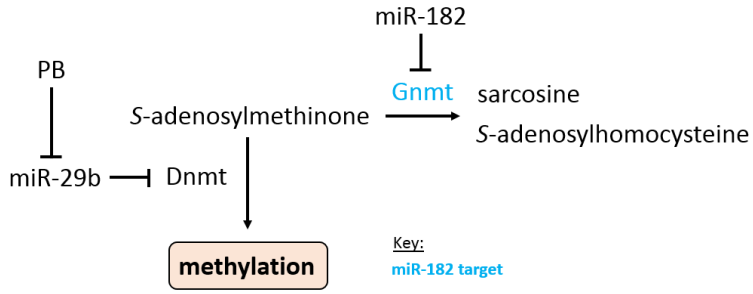


Figure 5.12: MiRNA-mediated methylation

Figure 5.12 demonstrates the predicted effect of the miR-182 target, Gnmt, in methylation patterns with another PB-sensitive miRNA, miR-29b based on target gene function from the literature, described in text.

Other – Slc12a2 inhibition by miR-182 (and miR-96) could be involved in reducing PB-potentiated neuronal Cl^- influx (Dzhala et al., 2005; Löscher & Rogawski, 2012). Smad4 suppression has been shown to inhibit increased Zeb expression (Gregory et al., 2011), therefore miR-182-mediated suppression of Smad4 may act in concert with miR-200a/b/429 and miR-96 on the suppressive effects on EMT (Figure 5.13). The role of Olr59**,** the novel putative target for miR-96, is uncertain but Olr59 inhibition by miR-96 might be to reduce the receptor's response to the influx of fatty acids as a result of PB treatment.

5. Function of phenobarbital-induced miRNAs

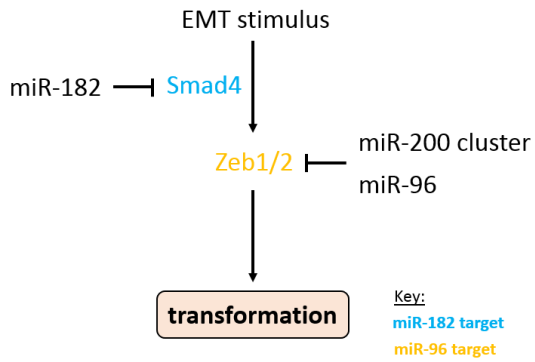


Figure 5.13: MiR-mediated effect on EMT

Figure 5.13 demonstrates the predicted effect of the miR-182 target, Smad4, on cell transformation with other PB-sensitive miRNAs based on target gene function from the literature, described in text.

Chapter 5 Conclusions – In conclusion the work presented here has identified 4 validated miR-182/96 targets, and 5 novel targets (Table 5.2). Due to the functions of these genes and the PB-phenotype I propose that miR-182/96 are induced as a result of PB treatment in the rat in order to promote glycolysis and facilitate DNA methylation changes, as well as inhibiting cell transformation, and potentially modulating Car activation, neuronal Cl^- influx, and lipid responses, and that miR-182/96 accomplish this through shared and unique targets.

Overall, I surmise that miR-182/96 work co-operatively with other miRNAs to maintain homeostasis during PB treatment in the rat.

6. Discussion

6.1 General conclusions and future work

The first 2 aims of this thesis were concerned with the use of a cell culture model of PB treatment. This was explored using the rat hepatocyte-like B13/H cell model. Aims 3 and 4 of this thesis pertained to the *in vivo* regulatory control and function of the PB inducible miR-182/96.

6.1.1 Thesis aim 1: Characterise the B13/H cell line and its response to PB and PB-like compounds.

Background MiRNAs have been reported as being regulators of homeostasis, as well as contributing to disease when dysregulated (Ebert & Sharp, 2012). PB treatment in the rat progressively induced miRNA changes across a 90 day treatment study (Koufaris et al., 2012, 2013) (Figure 4.4). In order to begin understanding this response *in vitro* requires extended chemical treatments beyond the 2-3 days typically associated with optimal primary hepatocyte treatment (Soldatow et al., 2013). To circumvent the problem inherent with primary hepatocyte cultures, the hepatocyte-like B13/H cells were used, which are reported to maintain an hepatocyte-like phenotype up to 30 days (Marek et al., 2003).

Results & Conclusion Generation of hepatocyte-like B13/H cells requires transdifferentiation from the pancreatic progenitor, B13, cell. This work confirmed that, in our hands, transdifferentiation to B13/H cells can be reliably performed through 2 weeks dexamethasone (10nM) treatment, with molecular and phenotypic

alteration towards an hepatocyte-like phenotype. Furthermore, B13/H cells responded to PB in an hepatocyte-like manner. However, the PB-responsive nuclear receptor, Car, appeared to reside in the nucleus, which is more representative of immortalised cells rather than primary hepatocytes; where Car can shuttle between the cytoplasm and the nucleus. Despite this caveat, I was able to use the transdifferentiated B13/H cells to reproduce PB-type responses. Finally, we showed that the *in vivo* PB-inducible miRNAs (miR-182/96) were also sensitive to PB treatment *in vitro* (B13/H cells) and demonstrated similar temporal expression patterns.

Therefore, the B13/H cells are a useful model for exploring PB treatment in the rat, and offer a useful *in vitro* system for mechanistic studies that appear comparable to *in vivo* data.

Future work Due to the nuclear localisation of Car in B13/H cells and the responsiveness of Car and Pxr to PB, understanding the extent of Car activation in the B13/H cells following PB treatment would be an important next step. This could be explored through the use of transient knock-down of Car in transdifferentiated B13/H cells using siRNA-mediated transfections. Additionally, I show that miR-122 was decreased with PB treatment, and this has been reported to be involved in the activation of Car. Assessing dose- and time-dependent effects of PB on miR-122 and Car-mediated gene expression would help to consolidate an interaction between miR-122 and Car. Furthermore, it would be necessary to perform a more extensive dose and time range of PB treatment to gain a better understanding of the miR-

182/96 induction profile. This sample set would also allow one to explore the mechanistic effects of these miRNAs by assessing the expression of potential targets and regulators (such as those discussed below).

6.1.2 Thesis aim 2: Explore the interaction with PB and growth factor signalling in vitro and in vivo.

Background Mutoh *et al.,* (Mutoh et al., 2013) report that PB indirectly activated Car through inhibition of the Egfr in the mouse. This is corroborated by previous work, which demonstrated that activation of the downstream Egfr signalling kinase, Erk, is inhibitory to Car activation in the mouse (Koike et al., 2007; Osabe & Negishi, 2011). Inhibition of Erk signalling has also been shown to increase expression of PB target genes in rat primary hepatocytes (F Joannard et al., 2000; Florence Joannard et al., 2006). However, PB treatment in rat primary hepatocytes has also been reported to increase Erk activation (Florence Joannard et al., 2006).

Results & Conclusion The data presented in this thesis suggests that B13/H cells respond to growth factors in a similar manner as rat primary hepatocytes, based on the literature, which is different to that of the mouse. B13/H cells respond to PB with increased Erk activation, as seen in rat primary hepatocytes (Florence Joannard et al., 2006), which is dependent on Egf. Joannard *et al.,* (F Joannard et al., 2000; Florence Joannard et al., 2006) demonstrate suppression of PB-induced genes with Erk activation suggesting that Erk may act as a negative-feedback loop to control the magnitude of Car activation during PB exposure.

Egf or Hgf in combination with PB caused an increase in Akt activity compared to growth factors alone, which might suggest that PB augments pathway activity downstream of a growth factor receptor. Furthermore, through *in vivo* analysis I showed that changes in growth factor signalling appears to be a transient early effect with the most prominent changes taking place within 24 hours treatment, as indicated with the B13/H cells. However, the data also suggests that *in vivo* Akt/FoxO1 activity may be increased after 3 days PB (1000ppm) treatment compared to control, which indicates that Akt activation may be associated with the PB-induced transient hyperplasia reported at this time (Waterman et al., 2010).

Future work In order to explore the function of Erk in PB-mediated activation of Car it would be necessary to assess expression of Car target genes following PB treatment in samples with increased or decreased Erk activation. It would be interesting to determine how PB affects Erk signalling. As Erk activation appears specific to Egf and not Hgf, it could be that this is a Egfr-mediated response. To determine the function of PB-induced Akt activation will be difficult as B13/H cells, like primary hepatocytes, are refractory to cell division (Cho, Berthiaume, Tilles, & Yarmush, 2008; Philip M E Probert et al., 2014), although analysis of downstream targets, such as FoxO1, could be used instead. Again, how PB interacts with Akt is unknown, but as this appears to be common between Egf and Hgf it suggests that PB affects the pathway downstream of the receptor. In order to begin to determine where PB interacts with both Erk and Akt signalling it would be necessary to perform a systematic study of the activation of the kinases within each pathway.

6.1.3 Thesis aim 3: Identify potential regulators of PB-induced miRNAs in vivo.

Background Treatment with PB (1000ppm) in the rat for more than 14 days significantly increases 2 families of miRNAs (miR-182/96 and miR-200a/b/429) (Koufaris et al., 2013). There are many potential regulators of these miRNAs cited in the literature, but they appear to be highly context dependent. I identified a number of potential regulators that are associated with PB exposure.

Results & Conclusion From the data presented, it is unlikely that miR-182/96 are regulated by Car, Hnf-4α, p53, ROS or Tgf-β. Changes in methylation patterns or through β-catenin-mediated alteration in cell adhesion signalling may contribute to the altered expression of miR-182/96 and miR-200a/b/429. PB is known to disrupt gap junction signalling to induce tumours in mice (Moennikes et al., 2000), and has been shown to stimulate cell membrane localisation of Car (Koike et al., 2005). Taken together it might be considered that PB induces cell membrane localisation of Car and alteration of β-catenin-mediated cell adhesion. Through altered β-catenin it might be that the PB-induced miRNAs are expressed, although the exact mechanisms behind this remain uncertain.

Could it be possible that the induction of these miRNAs are a homeostatic response to PB treatment in the rat to inhibit tumourigenesis through β-catenin? This is an intriguing possibility as the mouse is more susceptible to PB-induced tumours than the rat, and the expression of miR-182/96 and miR-200a/b/429 are only increased after PB treatment in the rat (Koufaris, 2011) and not the mouse (Lempiäinen et al., 2013). There are 3 main points to consider regarding this hypothesis:

(1) Does β-catenin only regulate the expression of miR-182/96 in the rat and not the mouse; as β-catenin is mutated in tumours from DEN/PB mouse studies (Aydinlik et al., 2001) and is in fact required for tumourigenesis in the mouse (Rignall et al., 2011)?

(2) Is β-catenin affected by PB in the rat?

(3) Are β-catenin and miRNA expression differentially regulated between tumours and healthy tissue in the livers of DEN/PB treated rats?

Future work Further methylation analysis of the upstream sequence of miR-182/96 and miR-200a/b/429 would aid in determining the extent methylation changes play in the expression of these miRNAs. Identification of common regulatory sequences within these rat miRNAs that are not present in the mouse would be interesting to explore. It would also be important to assess the localisation of Car and β-catenin over time in correlation with these miRNAs to determine if the above proposed interaction is plausible.

6.1.4 Thesis aim 4: Elucidate the potential function of PB-induced miRNAs in vivo.

Background As with the regulators of these miRNAs, their function also appears to be highly context dependent. In order to identify putative mRNA targets I used *in silico* prediction programs as well as selecting validated targets from the literature. From here I screened targets based on (1) a significant change in expression with PB treatment in the rat *in vivo*, and (2) by significant negative correlation with miR-96 over a 14 day PB treatment study in the rat.

Results & Conclusion By this approach I identified 4 validated targets for miR-182 (Slc12a2, Smad4, Rb1, FoxO1), and 1 for miR-96 (FoxO1), as well as 3 predicted targets for miR-182 (Pc, Slc37a4, Gnmt) and 4 for miR-96 (Slc12a2, Pc, Map2k1, Olr59). Two targets, Gnmt and FoxO1, were analysed over an extended sample set to include up to 90 days PB treatment, and both targets maintained significant negative correlations with miR-182. Protein levels were also assessed and were suggestive of these targets being controlled by miRNA regulation.

From the reported functions of these miRNA targets I proposed that miR-182/96 are involved in promoting glycolysis, possibly to allow production of NADPH through the *tricarboxylic acid (TCA) cycle* for Cyp450-mediated metabolism (Figure 5.11).

Additionally, through miR-96 targeting of Map2k1, an upstream kinase involved in Erk activation, I suggest that miR-96 may be acting to modulate Erk activation and hence its purported target, Car. Data in Figure 3.10 demonstrated that *in vivo* Erk activity in response to PB (1000ppm), although variable, was not significantly changed from control, indicating that either miR-96 may not influence this pathway, or that the presence of miR-96 with PB treatment may be maintaining pathway activity relative to control. This distinction would be important to determine in future work and could be assessed by suppressing miR-96 and overexpressing its target, Map2k1, to determine the effect on Erk activity and Car phosphorylation and activity.

MiR-182 is predicted to target the mRNA Gnmt, which is involved in regulating methylation, possibly by controlling availability of *S*-adenosylmethionine. As PB is

reported to alter methylation in the rat (Koufaris et al., 2013), it could be that this is in part mediated by miR-182 in concert with miR-29b, which Koufaris *et al.,* (Koufaris et al., 2013) reported as decreased by PB treatment and has been identified as a regulator of the methylation enzymes Dnmt3a/3b (Garzon et al., 2009).

PB treatment in the rat is reported to reduce expression of the EMT-associated transcription factors, Zeb1/2 (Koufaris et al., 2013). Both miR-200a/b/249 (Bracken et al., 2008; Gregory et al., 2008) and miR-96 (X. L. Li et al., 2013) have been reported to target Zeb1/2, suggesting these miRNAs may contribute to the maintenance of normal cell morphology through inhibiting EMT. This hypothesis is strengthened by the proposal that miR-182 targets Smad4. Knockdown of Smad4 has been reported to suppress induction of Zeb1/2 mRNA (Gregory et al., 2011). Therefore these miRNAs may act in concert to prevent Zeb1/2 induction and suppress residual levels.

PB potentiates Cl^- influx in response to GABA (Löscher & Rogawski, 2012). The $Na^+/K^+/2Cl^-$ cotransporter, Scl12a2, is also reported to increase neuronal Cl^- influx in neonates (Dzhala et al., 2005). Therefore, it could be that miR-182/96 targeting of Scl12a2 may act to modulate PB-induced neuronal Cl^- influx. This is interesting as it could suggest that miR-182/96 may possess extra-hepatic effects.

Finally, miR-96-mediated suppression of Olr59 could be involved in reducing the intracellular response to the influx of fatty acids associated with PB treatment, although the function of this is currently unknown.

Future work To confirm these proposed putative targets it would be necessary to perform miRNA transfection studies to experimentally manipulate the expression of the mRNAs. Furthermore, to identify the *in vivo* effects of these miRNAs, performing a miR-182/96 knockout study in the rat with PB treatment would help to determine if, for example, the miRNAs are acting to regulate Car activity or NADPH production for Cyp450 activities. Due to the proposed role in homeostasis and potential regulation by β-catenin it would be interesting to determine the expression of these miRNAs and their targets following a DEN/PB tumour initiation study in the rat.

6.2 Consolidation – the big picture

We demonstrated that the B13/H cell model appears to act in an hepatocyte-like manner and provide a model system with which we can begin to explore the molecular effects of PB in the rat and explore the roles and regulation of the PB-inducible miRNAs; miR-182/96. Furthermore, we suggest that the mechanism by which PB indirectly activates Car in the rat is different to that of the mouse. While both organisms seem to involve Erk activity, PB in the mouse inhibits Erk activation, while in the rat PB appears to increase activation.

The data presented in this thesis suggests that miR-182/96 may have a homeostatic role in the context of PB exposure in the rat, and through future work determining the effect of the loss of these miRNAs with PB treatment, I propose will identify these small ncRNAs as indicative of resistance to PB-induced tumourigenesis.

6.2.1 If not Egfr, what could be the rat PB receptor?

The data presented in chapter 3 showed that Erk activity was increased with PB treatment in combination with Egf in B13/H cells, in agreement with primary rat hepatocytes (Florence Joannard et al., 2006). This suggests that PB does not antagonise the Egfr to activate Car, as reported in the mouse. I argued in chapter 1 that Ampk activation may be involved in the full activation of nuclear Car, which is associated with decreased miR-122 expression shown in Figure 2.10, and by others (Kazantseva et al., 2015). PB-induced down regulation of miR-122 is reported to be a transient event occurring within the first 24 hours of treatment (Shizu et al., 2012). It has been suggested that PB reduces expression of miR-122 through nuclear Car-mediated inhibition of Hnf-4α target gene transcription (of which miR-122 is a target) (Kazantseva et al., 2015); although PB-induced Pxr is also reported to inhibit Hnf-4α target gene transcription (Bhalla et al., 2004). Furthermore, miR-122 is also reported to be an indirect target of glycogen synthase kinase 3β (Gsk-3β) (Zeng et al., 2010). Gsk-3β is a kinase of high basal activity, reported to be involved in glucose metabolism and Wnt signalling (Aydinlik et al., 2001; Sakamaki et al., 2012). Gsk-3β is inhibited by Erk-mediated phosphorylation (Q. Ding et al., 2005), which is activated by PB treatment (Figure 3.6). Additionally, β-catenin levels increase as a result of Gsk-3β inhibition due to decreased β-catenin phosphorylation and ubiquitin-proteaseomal degradation (Q. Ding et al., 2005). These suggest that PB may reduce miR-122 expression levels through Car/Pxr-mediated inhibition of Hnf-4α target gene transcription and/or through Erk activation and subsequent Gsk-3β inhibition, and that this process may also influence β-catenin (Figure 6.1).

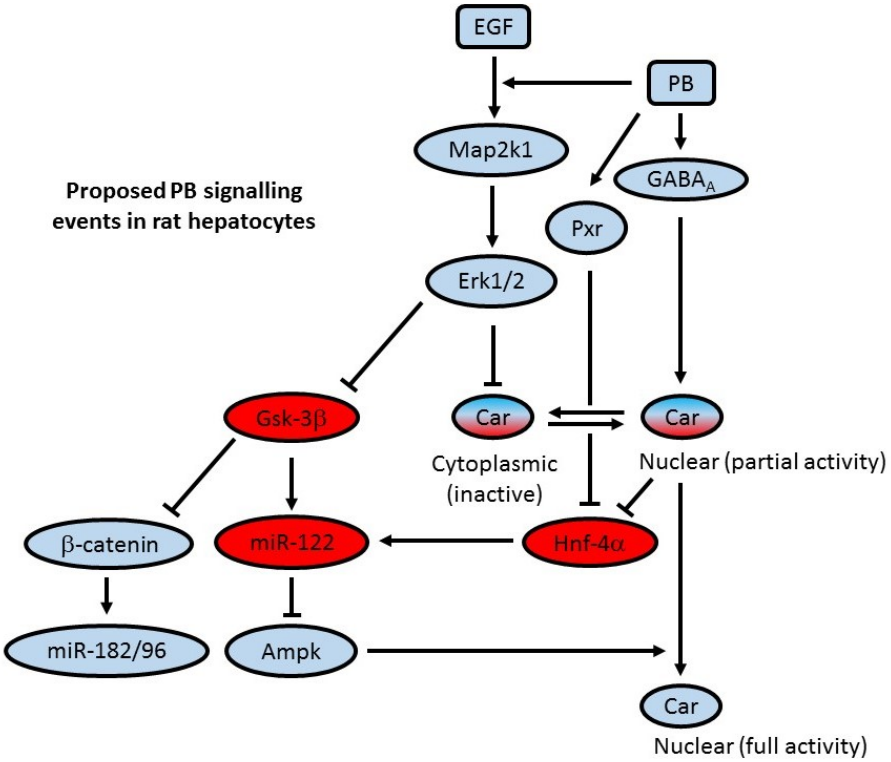


Figure 6.1: Proposed PB signalling pathway in rat hepatocytes

Figure 6.1 PB through $GABA_A$, causes the nuclear translocation of Car. Due to Car's structure it displays constitutive activity once in the nucleus, but is thought to require further molecular changes for full activation. Either inhibition of Hnf-4α, or Gsk-3β results in transiently reduced levels of miR-122 and subsequent activation of Ampk. Active Ampk provides the necessary signal for full activation of Car.

Inhibition of Gsk-3β increases the stability of β-catenin, which may induce the miR-182/96 cluster in association with cell membrane bound Car.

Induction of miR-182/96 can feedback to regulate Erk activation, and glycolysis for NADPH generation for Cyp450 genes induced by Car.

Blue colouration depicts increased activity/expression, while decreased activity/expression is shown in red. Discussed in text and adapted from: (Aydinlik et al., 2001; Kazantseva et al., 2015; Rignall et al., 2011; Shizu et al., 2012; Zeng et al., 2010).

Interestingly, increased Ampk activity is known to decrease gluconeogenesis in the liver (Lochhead, Salt, Walker, Hardie, & Sutherland, 2000), which is associated with PB exposure. This coincides with the data presented in chapter 5 suggesting that

miR-182/96 may also be involved in inhibiting gluconeogenesis, through targets such as Rb1, FoxO1, Pc, Slc37a4 and Gnmt (Figure 5.11).

However, nuclear activation of Car by Ampk still does not explain what the cell signal is that causes Car translocation into the nucleus. If not Egfr in the rat, then what? PB is known to exert its anti-epileptic effects through the $GABA_A$ receptor (Löscher & Rogawski, 2012), which has been shown to be present in the liver (Sun et al., 2003). Interestingly, $GABA_A$-β3 expression has been reported to be lost in certain human hepatocellular carcinoma cell lines (Sun et al., 2003), and the induction of Cyp2b by PB is also attenuated in preneoplastic lesions of rat livers (Numazawa et al., 2005). Taken together this implies that, in the rat, Car may be induced to translocate into the nucleus as a result of PB binding to $GABA_A$, and that complete nuclear activation is controlled by Ampk activation (Figure 6.1). If this is the case, then $GABA_A$ activation in the liver might result in an influx of Cl^- into hepatocytes following PB treatment. Therefore, miR-182/96 targeting of the $K^+/Na^+/2Cl^-$ cotransporter, Slc12a2, may be to modulate both neuronal and hepatic Cl^- influx. The role of $GABA_A$ activation in the indirect activation of Car is an intriguing possibility and could be explored using the B13/H cell model.

6.2.2 Thesis hypothesis

“I hypothesise that the rat hepatocyte-like, B13/H, cell system can provide robust mechanistic insights into the PB phenotype. Additionally, that the regulation and function of PB-induced miRNAs can be explored using *in vivo* samples, and provide context-specific relationships relevant to chronic PB exposure.”

I believe that the work presented herein confirms my hypothesis and provides the necessary background to fully explore these miRNAs as a homeostatic response to the resistance of PB-induced tumours, as well as interrogating PB-mediated activation of Car, in the rat.

References

Adam, L., Zhong, M., Choi, W., Qi, W., Nicoloso, M., Arora, A., … Dinney, C. (2009). miR-200 expression regulates epithelial-to-mesenchymal transition in bladder cancer cells and reverses resistance to epidermal growth factor receptor therapy. *Clinical Cancer Research : An Official Journal of the American Association for Cancer Research*, *15*(16), 5060–72. http://doi.org/10.1158/1078-0432.CCR-08-2245

Adams, D. R., Ron, D., & Kiely, P. a. (2011). RACK1, A multifaceted scaffolding protein: Structure and function. *Cell Communication and Signaling : CCS*, *9*(1), 22. http://doi.org/10.1186/1478-811X-9-22

Ahmed, S. a, Gogal, R. M., & Walsh, J. E. (1994). A new rapid and simple non-radioactive assay to monitor and determine the proliferation of lymphocytes: an alternative to [3H]thymidine incorporation assay. *Journal of Immunological Methods*, *170*(2), 211–224. http://doi.org/10.1016/0022-1759(94)90396-4

Aigner, K., Dampier, B., Descovich, L., Mikula, M., Sultan, A., Schreiber, M., … Schweifer, N. (2007). The transcription factor ZEB1 (δEF1) promotes tumour cell dedifferentiation by repressing master regulators of epithelial polarity. *Oncogene*, *26*(49), 6979–6988. http://doi.org/10.1038/sj.onc.1210508.The

Akinci, E., Banga, A., Greder, L. V, Dutton, J. R., & Slack, J. M. W. (2012). Reprogramming of pancreatic exocrine cells towards a beta (β) cell character using Pdx1, Ngn3 and MafA. *The Biochemical Journal*, *442*(3), 539–50. http://doi.org/10.1042/BJ20111678

Al-Adsani, A., Burke, Z. D., Eberhard, D., Lawrence, K. L., Shen, C.-N., Rustgi, A. K., … Tosh, D. (2010). Dexamethasone treatment induces the reprogramming of pancreatic acinar cells to hepatocytes and ductal cells. *PloS One*, *5*(10), e13650. http://doi.org/10.1371/journal.pone.0013650

Alessandro Chiarolini, Maria Teresa. (1997). Comparison of rat hepatocyte and differentiated hepatoma cell line cultures as bio indicators of CYP 1A1 inducers in urban air. *Biomarkers*, *2*(5), 279–285. http://doi.org/10.1080/135475097231508

Ames, B., McCann, J., & Yamasaki, E. (1975). Methods for detecting carcinogens and mutagens with the salmonella/mammalian-microsome mutagenicity test. *Mutation Research*, *31*, 347–364.

Antunović, B., Barlow, S., Chesson, A., Flynn, A., Hardy, A., Jany, K., … Vannier, P. (2011). Guidance on Default assumptions used by the EFSA Scientific Panels and Committee , and EFSA Units in the absence of actual measured data. *EFSA Public Consultation*.

Aranda, a, Aranda, a, Pascual, a, & Pascual, a. (2001). Nuclear hormone receptors and gene expression. *Physiological Reviews*, *81*(3), 1269–304. Retrieved from http://www.ncbi.nlm.nih.gov/pubmed/11427696

Aubrecht, J., Hirsch-Ernst, K. I., Becker-Rabbenstein, V., Kahl, G. F., Taniguchi, H., & Hohne, M. W. (1995). Induction of cytochrome P-4502B1-related mouse cytochrome P450 and regulation of its expression by epidermal growth factor/transforming growth factor ?? in primary hepatocyte culture. *Biochemical Pharmacology*, *50*(6), 781–785. http://doi.org/10.1016/0006-2952(95)00200-J

Audet-Walsh, É., & Anderson, A. (2009). Dexamethasone induction of murine CYP2B genes requires the glucocorticoid receptor. *Drug Metabolism and Disposition*, *37*(3), 580–588. http://doi.org/10.1124/dmd.108.022772

Aydinlik, H., Nguyen, T. D., Moennikes, O., Buchmann, a, & Schwarz, M. (2001). Selective pressure during tumor promotion by phenobarbital leads to clonal outgrowth of beta-catenin-mutated mouse liver tumors. *Oncogene*, *20*(53), 7812–7816. http://doi.org/10.1038/sj.onc.1204982

Babelova, A., Burckhardt, B. C., Salinas-Riester, G., Pommerenke, C., Burckhardt, G., & Henjakovic, M. (2015). Next generation sequencing of sex-specific genes in the livers of obese ZSF1 rats. *Genomics*. http://doi.org/10.1016/j.ygeno.2015.07.006

Beaudet, M.-J., Desrochers, M., Lachaud, A. A., & Anderson, A. (2005). The CYP2B2 phenobarbital response unit contains binding sites for hepatocyte nuclear factor 4, PBX-PREP1, the thyroid hormone receptor beta and the liver X receptor. *The Biochemical Journal*, *388*(Pt 2), 407–418. http://doi.org/10.1042/BJ20041556

Becker, F. F. (1982). Morphological classification of mouse liver tumors based on biological characteristics. *Cancer Research*, *42*(10), 3918–3923.

Behm-Ansmant, I., Rehwinkel, J., & Izaurralde, E. (2006). MicroRNAs Silence Gene Expression by Repressing Protein Expression and / or by Promoting mRNA Decay MicroRNAs Silence Gene Expression by Repressing Protein Expression and / or by Promoting mRNA Decay. *Spring*, *LXXI*, 523–530. http://doi.org/10.1101/sqb.2006.71.013

Bell, A. W., & Michalopoulos, G. K. (2006). Phenobarbital regulates nuclear expression of HNF-4alpha in mouse and rat hepatocytes independent of CAR and PXR. *Hepatology (Baltimore, Md.)*, *44*(1), 186–94.

Benetatos, L., Hatzimichael, E., Londin, E., Vartholomatos, G., Loher, P., Rigoutsos, I., & Briasoulis, E. (2013). The microRNAs within the DLK1-DIO3 genomic region: involvement in disease pathogenesis. *Cellular and Molecular Life Sciences : CMLS*, *70*(5), 795–814. http://doi.org/10.1007/s00018-012-1080-8

Berasain, C., Perugorria, M. J., Latasa, M. U., Castillo, J., Goñi, S., Santamaría, M., … Avila, M. a. (2009). The epidermal growth factor receptor: a link between inflammation and liver cancer. *Experimental Biology and Medicine (Maywood, N.J.)*, *234*(7), 713–725. http://doi.org/10.3181/0901-MR-12

Berthou, S., Aebersold, D. M., Schmidt, L. S., Stroka, D., Heigl, C., Streit, B., … Zimmer, Y. (2004). The Met kinase inhibitor SU11274 exhibits a selective inhibition pattern toward

different receptor mutated variants. *Oncogene*, *23*(31), 5387–5393. http://doi.org/10.1038/sj.onc.1207691

Bhalla, S., Ozalp, C., Fang, S., Xiang, L., & Kemper, J. K. (2004). Ligand-activated pregnane X receptor interferes with HNF-4 signaling by targeting a common coactivator PGC-1??. Functional implications in hepatic cholesterol and glucose metabolism. *Journal of Biological Chemistry*, *279*(43), 45139–45147. http://doi.org/10.1074/jbc.M405423200

Bird, A. (2007). Perceptions of epigenetics. *Nature*, *447*(7143), 396–398. http://doi.org/10.1038/nature05913

Blanco-Bose, W. E., Murphy, M. J., Ehninger, A., Offner, S., Dubey, C., Huang, W., … Trumpp, A. (2008). C-Myc and its target FoxM1 are critical downstream effectors of constitutive androstane receptor (CAR) mediated direct liver hyperplasia. *Hepatology (Baltimore, Md.)*, *48*(4), 1302–11. http://doi.org/10.1002/hep.22475

Blättler, S. M., Rencurel, F., Kaufmann, M. R., & Meyer, U. a. (2007). In the regulation of cytochrome P450 genes, phenobarbital targets LKB1 for necessary activation of AMP-activated protein kinase. *Proceedings of the National Academy of Sciences of the United States of America*, *104*(3), 1045–1050. http://doi.org/10.1073/pnas.0610216104

Bollen, M., Keppens, S., & Stalmans, W. (1998). Specific features of glycogen metabolism in the liver. *The Biochemical Journal*, *336 (Pt 1*, 19–31.

Bonello, S., Zähringer, C., BelAiba, R. S., Djordjevic, T., Hess, J., Michiels, C., … Görlach, A. (2007). Reactive oxygen species activate the HIF-1α promoter via a functional NFκB site. *Arteriosclerosis, Thrombosis, and Vascular Biology*, *27*(4), 755–761. http://doi.org/10.1161/01.ATV.0000258979.92828.bc

Boobis, A. R., Cohen, S. M., Doerrer, N. G., Galloway, S. M., Haley, P. J., Hard, G. C., … Wright, J. (2009). A data-based assessment of alternative strategies for identification of potential human cancer hazards. *Toxicologic Pathology*, *37*(6), 714–732. http://doi.org/10.1177/0192623309343779

Boon, R. a, & Vickers, K. C. (2013). Intercellular transport of microRNAs. *Arteriosclerosis, Thrombosis, and Vascular Biology*, *33*(2), 186–92. http://doi.org/10.1161/ATVBAHA.112.300139

Botts, S., Ennulat, D., Francke-Carroll, S., Graham, M., Maronpot, R. R., & Mohutsky, M. (2010). Introduction to hepatic drug metabolizing enzyme induction in drug safety evaluation studies. *Toxicologic Pathology*, *38*(5), 796–798. http://doi.org/10.1177/0192623310374330

Bracken, C. P., Gregory, P. a, Kolesnikoff, N., Bert, A. G., Wang, J., Shannon, M. F., & Goodall, G. J. (2008). A double-negative feedback loop between ZEB1-SIP1 and the microRNA-200 family regulates epithelial-mesenchymal transition. *Cancer Research*, *68*(19), 7846–54. http://doi.org/10.1158/0008-5472.CAN-08-1942

Braeuning, A. (2013). The connection of β-catenin and phenobarbital in murine hepatocarcinogenesis: a critical discussion of Awuah et al., PLoS ONE 7(6):e39771, 2012. *Archives of Toxicology*, *87*(3), 401–2. http://doi.org/10.1007/s00204-012-1002-4

Braeuning, A. (2014). Liver cell proliferation and tumor promotion by phenobarbital: relevance for humans? *Archives of Toxicology*, *88*(10), 1771–1772. http://doi.org/10.1007/s00204-014-1331-6

Braeuning, A., Gavrilov, A., Brown, S., Wolf, C. R., Henderson, C. J., & Schwarz, M. (2014). Phenobarbital-Mediated Tumor Promotion in Transgenic Mice with Humanized CAR and PXR. *Toxicological Sciences : An Official Journal of the Society of Toxicology*, *140*(2), 259–70. http://doi.org/10.1093/toxsci/kfu099

Brodie, M. J., & Kwan, P. (2012). Current position of phenobarbital in epilepsy and its future. *Epilepsia*, *53 Suppl 8*, 40–6. http://doi.org/10.1111/epi.12027

Buck, E., Eyzaguirre, A., Haley, J. D., Gibson, N. W., Cagnoni, P., & Iwata, K. K. (2006). Inactivation of Akt by the epidermal growth factor receptor inhibitor erlotinib is mediated by HER-3 in pancreatic and colorectal tumor cell lines and contributes to erlotinib sensitivity. *Molecular Cancer Therapeutics*, *5*(8), 2051–9. http://doi.org/10.1158/1535-7163.MCT-06-0007

Burke, D. M., & Mayer, R. T. (1974). Ethoxyresorufin : Microsomal Preferentially Direct Which Assay Is of O-Dealkylation By 3-Methylcholanthrene. *Drug Metabolism and Disposition*, *2*(6), 583–588.

Burke, M., Thompson, S., Weaver, R., Wolf, C., & Mayer, R. (1994). Cytochrome P450 specificities of alkoxyresorufin O-dealkylation in human and rat liver. *Biochem Pharmacol.*, *48*(5), 923–36.

Burke, Z. D., Shen, C. N., Ralphs, K. L., & Tosh, D. (2006). Characterization of liver function in transdifferentiated hepatocytes. *Journal of Cellular Physiology*, *206*(1), 147–159. http://doi.org/10.1002/jcp.20438

Butch, E. R., & Guan, K. L. (1996). Characterization of ERK1 activation site mutants and the effect on recognition by MEK1 and MEK2. *Journal of Biological Chemistry*, *271*(8), 4230–4235. http://doi.org/10.1074/jbc.271.8.4230

Butler, W. H. (1978). Long-term effects of phenobarbitone-Na on male Fischer rats. *British Journal of Cancer*, *37*, 418–423.

Carthew, P., Edwards, R. E., & Nolan, B. M. (1998). The quantitative distinction of hyperplasia from hypertrophy in hepatomegaly induced in the rat liver by phenobarbital. *Toxicological Sciences : An Official Journal of the Society of Toxicology*, *44*(1), 46–51. http://doi.org/10.1006/toxs.1998.2473

Carthew, R. W., & Sontheimer, E. J. (2009). Origins and Mechanisms of miRNAs and siRNAs. *Cell*, *136*(4), 642–55. http://doi.org/10.1016/j.cell.2009.01.035

Chamberlain, M. P., Haines, C., & Elcombe, C. R. (2014). Characterisation of the Hepatic Effects of Phenobarbital in Constitutive Androstane Receptor (CAR, NR1I3) Knockout Rats (Poster Abstract 1134). *The Toxicologist: Supplement to Toxicological Sciences*.

Chang, T. T., & Hughes-Fulford, M. (2014). Molecular mechanisms underlying the enhanced functions of three-dimensional hepatocyte aggregates. *Biomaterials*, *35*(7), 2162–71. http://doi.org/10.1016/j.biomaterials.2013.11.063

Chen, C., Ridzon, D. a., Broomer, A. J., Zhou, Z., Lee, D. H., Nguyen, J. T., … Guegler, K. J. (2005). Real-time quantification of microRNAs by stem-loop RT-PCR. *Nucleic Acids Research*, *33*(20), 1–9. http://doi.org/10.1093/nar/gni178

Chen, T., Chen, Q., Xu, Y., Zhou, Q., Zhu, J., Zhang, H., … Yu, C. (2012). SRC-3 is required for CAR-regulated hepatocyte proliferation and drug metabolism. *Journal of Hepatology*, *56*(1), 210–7. http://doi.org/10.1016/j.jhep.2011.07.015

Chen, Y., Ferguson, S. S., Negishi, M., & Goldstein, J. a. (2004). Induction of human CYP2C9 by rifampicin, hyperforin, and phenobarbital is mediated by the pregnane X receptor. *The Journal of Pharmacology and Experimental Therapeutics*, *308*(2), 495–501. http://doi.org/10.1124/jpet.103.058818.CYP2C9

Chhabra, R. (2000). NTP technical report on the toxicity studies of benzophenone (CAS No. 119-61-9). Administered in feed to F344/N rats and B6C3F mice. *Toxic Rep Ser.*, *61*, 1–53.

Chiang, C.-H., Hou, M.-F., & Hung, W.-C. (2013). Up-regulation of miR-182 by β-catenin in breast cancer increases tumorigenicity and invasiveness by targeting the matrix metalloproteinase inhibitor RECK. *Biochimica et Biophysica Acta (BBA) - General Subjects*, *1830*(4), 3067–3076. http://doi.org/10.1016/j.bbagen.2013.01.009

Cho, C. H., Berthiaume, F., Tilles, A. W., & Yarmush, M. L. (2008). A new technique for primary hepatocyte expansion in vitro. *Biotechnology and Bioengineering*, *101*(2), 345–356. http://doi.org/10.1002/bit.21911

Choi, J. M., Oh, S. J., Lee, S. Y., Im, J. H., Oh, J. M., Ryu, C. S., … Kim, S. K. (2014). HepG2 cells as an in vitro model for evaluation of cytochrome P450 induction by xenobiotics. *Archives of Pharmacal Research*. http://doi.org/10.1007/s12272-014-0502-6

Chomczynski, P., & Sacchi, N. (2006). The single-step method of RNA isolation by acid guanidinium thiocyanate–phenol–chloroform extraction: twenty-something years on. *Nature Protocols*, *1*(2), 581–595. http://doi.org/10.1038/nprot.2006.83

Chou, J. Y., & Mansfield, B. C. (2014). The SLC37 Family of Sugar-Phosphate/Phosphate Exchangers, *1*, 1–25. http://doi.org/10.1016/B978-0-12-800223-0.00010-4

Clem, B. F., & Chesney, J. (2012). Molecular pathways: regulation of metabolism by RB. *Clinical Cancer Research : An Official Journal of the American Association for Cancer Research*, *18*(22), 6096–100. http://doi.org/10.1158/1078-0432.CCR-11-3164

Czekaj, P. (2000). Phenobarbital-induced expression of cytochrome P450 genes. *Acta Biochimica Polonica*, *47*(4), 1093–1105.

Dail, M. B., Shack, L. A., Chambers, J. E., & Burgess, S. C. (2008). Global liver proteomics of rats exposed for 5 days to phenobarbital identifies changes associated with cancer and with CYP metabolism. *Toxicological Sciences : An Official Journal of the Society of Toxicology*, *106*(2), 556–69. http://doi.org/10.1093/toxsci/kfn198

Damm, G., Pfeiffer, E., Burkhardt, B., Vermehren, J., Nüssler, A. K., & Weiss, T. S. (2013). Human parenchymal and non-parenchymal liver cell isolation, culture and characterization. *Hepatology International*, *7*(4), 951–958. http://doi.org/10.1007/s12072-013-9475-7

Das, F., Ghosh-Choudhury, N., Dey, N., Bera, a., Mariappan, M. M., Kasinath, B. S., & Ghosh Choudhury, G. (2014). High Glucose Forces a Positive Feedback Loop Connecting Akt Kinase and FoxO1 Transcription Factor to Activate mTORC1 Kinase for Mesangial Cell Hypertrophy and Matrix Protein Expression. *Journal of Biological Chemistry*, *289*(47), 32703–32716. http://doi.org/10.1074/jbc.M114.605196

Dawson, M. I., & Xia, Z. (2012). The retinoid X receptors and their ligands. *Biochimica et Biophysica Acta (BBA) - Molecular and Cell Biology of Lipids*, *1821*(1), 21–56. http://doi.org/10.1016/j.bbalip.2011.09.014

De Waziers, I., Bouguet, J., Beaune, P., Gonzalez, F., Ketterer, B., & Barouki, R. (1992). Effects of ethanol, dexamethasone and RU 486 on expression of cytochromes P450 2B, 2E, 3A and glutathione transferase pi in a rat hepatoma cell line (Fao). *Pharmacogenetics*, *2*(1), 12–8.

Decaens, C., Durand, M., Grosse, B., & Cassio, D. (2008). Which in vitro models could be best used to study hepatocyte polarity? *Biology of the Cell / under the Auspices of the European Cell Biology Organization*, *100*(7), 387–398. http://doi.org/10.1042/BC20070127

Ding, Q., Xia, W., Liu, J. C., Yang, J. Y., Lee, D. F., Xia, J., … Hung, M. C. (2005). Erk associates with and primes GSK-3β for its inactivation resulting in upregulation of β-catenin. *Molecular Cell*, *19*(2), 159–170. http://doi.org/10.1016/j.molcel.2005.06.009

Ding, Z., Wu, C., Chu, G., Xiao, Y., Ho, D., Zhang, J., … DePinho, R. (2011). SMAD4–dependent barrier constrains prostate cancer growth and metastatic progression. *Nature*, *470*. http://doi.org/10.1016/j.biotechadv.2011.08.021.Secreted

Doench, J. G., & Sharp, P. a. (2004). Specificity of microRNA target selection in translational repression. *Genes & Development*, *18*(5), 504–11. http://doi.org/10.1101/gad.1184404

Doxakis, E. (2013). Principles of miRNA-Target Regulation in Metazoan Models. *International Journal of Molecular Sciences*, *14*, 16280–16302. http://doi.org/10.3390/ijms140816280

Dussault, I., Lin, M., Hollister, K., Fan, M., Termini, J., Sherman, M. A., & Forman, B. M. (2002). A Structural Model of the Constitutive Androstane Receptor Defines Novel Interactions That Mediate Ligand-Independent Activity, *22*(15), 5270–5280. http://doi.org/10.1128/MCB.22.15.5270

Dweep, H., Sticht, C., Pandey, P., & Gretz, N. (2011). MiRWalk - Database: Prediction of possible miRNA binding sites by " walking" the genes of three genomes. *Journal of Biomedical Informatics*, *44*(5), 839–847. http://doi.org/10.1016/j.jbi.2011.05.002

Dzhala, V. I., Talos, D. M., Sdrulla, D. a, Brumback, A. C., Mathews, G. C., Benke, T. a, … Staley, K. J. (2005). NKCC1 transporter facilitates seizures in the developing brain. *Nature Medicine*, *11*(11), 1205–1213. http://doi.org/10.1038/nm1301

Ebert, M. S., & Sharp, P. a. (2012). Roles for microRNAs in conferring robustness to biological processes. *Cell*, *149*(3), 515–24. http://doi.org/10.1016/j.cell.2012.04.005

Elcombe, C. R., Peffer, R. C., Wolf, D. C., Bailey, J., Bars, R., Bell, D., … Lake, B. G. (2014). Mode of action and human relevance analysis for nuclear receptor-mediated liver toxicity: A case study with phenobarbital as a model constitutive androstane receptor (CAR) activator. *Critical Reviews in Toxicology*, *44*(1), 64–82. http://doi.org/10.3109/10408444.2013.835786

Elrick, M. M., Kramer, J. a, Alden, C. L., Blomme, E. a G., Bunch, R. T., Cabonce, M. a, … Morris, D. L. (2005). Differential display in rat livers treated for 13 weeks with phenobarbital implicates a role for metabolic and oxidative stress in nongenotoxic carcinogenicity. *Toxicologic Pathology*, *33*(1), 118–126. http://doi.org/10.1080/01926230590888298

Ennulat, D., Walker, D., Clemo, F., Magid-Slav, M., Ledieu, D., Graham, M., … Boone, L. (2010). Effects of hepatic drug-metabolizing enzyme induction on clinical pathology parameters in animals and man. *Toxicologic Pathology*, *38*(5), 810–828. http://doi.org/10.1177/0192623310374332

Fabbri, M. (2012). TLRs as miRNA receptors. *Cancer Research*, *72*(24), 6333–7. http://doi.org/10.1158/0008-5472.CAN-12-3229

Finnberg, N., Stenius, U., & Högberg, J. (2000). Xenobiotics modulate the p53 response to DNA damage in preneoplastic enzyme-altered foci in rat liver; effects of diethylnitrosamine and phenobarbital. *Toxicological Sciences : An Official Journal of the Society of Toxicology*, *54*(1), 95–103. Retrieved from http://www.ncbi.nlm.nih.gov/pubmed/10746936

Fletcher, K., Orton, T. C., Chipman, J. K., & Strain, a J. (1997). The response of hepatocytes isolated from phenobarbitone treated mice to mitogenic growth factors. *Archives of Toxicology*, *71*(7), 422–8. Retrieved from http://www.ncbi.nlm.nih.gov/pubmed/9209687

Forman, B. M., Tzameli, I., Choi, H. S., Chen, J., Simha, D., Seol, W., … Moore, D. D. (1998). Androstane metabolites bind to and deactivate the nuclear receptor CAR-beta. *Nature*, *395*(6702), 612–615. http://doi.org/10.1038/26996

Fournier, T., Mejdoubi, N., Lapoumeroulie, C., Hamelin, J., Elion, J., Durand, G., & Porquet, D. (1994). Transcriptional regulation of rat alpha 1-acid glycoprotein gene by phenobarbital. *The Journal of Biological Chemistry*, *269*(44), 27175–27178.

Frommer, M., McDonald, L. E., Millar, D. S., Collis, C. M., Watt, F., Grigg, G. W., … Paul, C. L. (1992). A genomic sequencing protocol that yields a positive display of 5-methylcytosine residues in individual DNA strands. *Proceedings of the National Academy of Sciences of the United States of America*, *89*(5), 1827–1831. http://doi.org/10.1073/pnas.89.5.1827

Garzon, R., Liu, S., Fabbri, M., Liu, Z., Heaphy, C. E. a, Callegari, E., … Marcucci, G. (2009). MicroRNA-29b induces global DNA hypomethylation and tumor suppressor gene reexpression in acute myeloid leukemia by targeting directly DNMT3A and 3B and indirectly DNMT1. *Blood*, *113*(25), 6411–6418. http://doi.org/10.1182/blood-2008-07-170589

Gerets, H. H. J., Tilmant, K., Gerin, B., Chanteux, H., Depelchin, B. O., Dhalluin, S., & Atienzar, F. a. (2012). Characterization of primary human hepatocytes, HepG2 cells, and HepaRG cells at the mRNA level and CYP activity in response to inducers and their predictivity for the detection of human hepatotoxins. *Cell Biology and Toxicology*, *28*(2), 69–87. http://doi.org/10.1007/s10565-011-9208-4

Goldring, J. (2012). *Protein Electrophoresis Methods in Molecular Biology. Chapter 3*. (B. Kurien & R. Scofield, Eds.)*Springer Protocols* (Vol. 869). Humana Press. http://doi.org/10.1007/978-1-61779-821-4

Gonzales, a J., Christensen, J. G., Preston, R. J., Goldsworthy, T. L., Tlsty, T. D., & Fox, T. R. (1998). Attenuation of G1 checkpoint function by the non-genotoxic carcinogen phenobarbital. *Carcinogenesis*, *19*(7), 1173–83. Retrieved from http://www.ncbi.nlm.nih.gov/pubmed/9683175

Goodrich, D. W. (2006). The retinoblastoma tumor-suppressor gene, the exception that proves the rule. *Oncogene*, *25*(38), 5233–5243. http://doi.org/10.1038/sj.onc.1209616

Goodwin, B., Hodgson, E., D'Costa, D. J., Robertson, G. R., & Liddle, C. (2002). Transcriptional regulation of the human CYP3A4 gene by the constitutive androstane receptor. *Molecular Pharmacology*, *62*(2), 359–365. http://doi.org/10.1124/mol.62.2.359

Goodwin, B., Moore, L. B., Stoltz, C. M., McKee, D. D., & Kliewer, S. a. (2001). Regulation of the human CYP2B6 gene by the nuclear pregnane X receptor. *Molecular Pharmacology*, *60*(3), 427–431.

Gregory, P. a, Bert, A. G., Paterson, E. L., Barry, S. C., Tsykin, A., Farshid, G., … Goodall, G. J. (2008). The miR-200 family and miR-205 regulate epithelial to mesenchymal transition by targeting ZEB1 and SIP1. *Nature Cell Biology*, *10*(5), 593–601. http://doi.org/10.1038/ncb1722

Gregory, P. a, Bracken, C. P., Smith, E., Bert, A. G., Wright, J. a, Roslan, S., … Goodall, G. J. (2011). An autocrine TGF-beta/ZEB/miR-200 signaling network regulates

establishment and maintenance of epithelial-mesenchymal transition. *Molecular Biology of the Cell*, *22*(10), 1686–98. http://doi.org/10.1091/mbc.E11-02-0103

Grimson, A., Farh, K. K.-H., Johnston, W. K., Garrett-Engele, P., Lim, L. P., & Bartel, D. P. (2007). MicroRNA targeting specificity in mammals: determinants beyond seed pairing. *Molecular Cell*, *27*(1), 91–105. http://doi.org/10.1016/j.molcel.2007.06.017

Gripon, P., Rumin, S., Urban, S., Le Seyec, J., Glaise, D., Cannie, I., … Guguen-Guillouzo, C. (2002). Infection of a human hepatoma cell line by hepatitis B virus. *Proceedings of the National Academy of Sciences of the United States of America*, *99*(24), 15655–15660. http://doi.org/10.1073/pnas.232137699

Guttilla, I. K., & White, B. a. (2009). Coordinate regulation of FOXO1 by miR-27a, miR-96, and miR-182 in breast cancer cells. *The Journal of Biological Chemistry*, *284*(35), 23204–16. http://doi.org/10.1074/jbc.M109.031427

Hagiwara, a, Miyata, E., Tamano, S., Sano, M., Masuda, C., Funae, Y., … Shirai, T. (1999). Non-carcinogenicity, but dose-related increase in preneoplastic hepatocellular lesions, in a two-year feeding study of phenobarbital sodium in male F344 rats. *Food and Chemical Toxicology : An International Journal Published for the British Industrial Biological Research Association*, *37*(8), 869–79. Retrieved from http://www.ncbi.nlm.nih.gov/pubmed/10506011

Hammond, A., & Fry, J. (1992). Effect of serum-free medium on cytochrome P450-dependent metabolism and toxicity in rat cultured hepatocytes. *Biochem Pharmacol.*, *44*(7), 1461–4.

Han, J., Lee, Y., Yeom, K.-H., Kim, Y.-K., Jin, H., & Kim, V. N. (2004). The Drosha-DGCR8 complex in primary microRNA processing. *Genes & Development*, *18*(24), 3016–27. http://doi.org/10.1101/gad.1262504

Hanahan, D., & Weinberg, R. a. (2011). Hallmarks of cancer: The next generation. *Cell*, *144*(5), 646–674. http://doi.org/10.1016/j.cell.2011.02.013

Hardisty, J. F., & Brix, A. E. (2005). Comparative hepatic toxicity: prechronic/chronic liver toxicity in rodents. *Toxicologic Pathology*, *33*(1), 35–40. http://doi.org/10.1080/01926230590522077

Harper, J. W., Adami, G. R., Wei, N., Keyomarsi, K., & Elledge, S. J. (1993). The p21 Cdk-interacting protein Cip1 is a potent inhibitor of G1 cyclin-dependent kinases. *Cell*, *75*(4), 805–816. http://doi.org/10.1016/0092-8674(93)90499-G

Henderson, C. J., Cameron, A. R., Chatham, L., & Stanley, L. A. (2015). Evidence that the capacity of non-genotoxic carcinogens to induce oxidative stress is subject to marked variability.

Hernanda, P. Y., Chen, K., Das, a M., Sideras, K., Wang, W., Li, J., … Pan, Q. (2014). SMAD4 exerts a tumor-promoting role in hepatocellular carcinoma. *Oncogene*, (November), 1–14. http://doi.org/10.1038/onc.2014.425

Hernández, L. G., van Steeg, H., Luijten, M., & van Benthem, J. (2009). Mechanisms of non-genotoxic carcinogens and importance of a weight of evidence approach. *Mutation Research - Reviews in Mutation Research*, *682*(2-3), 94–109. http://doi.org/10.1016/j.mrrev.2009.07.002

Hirata, H., Ueno, K., Shahryari, V., Tanaka, Y., Tabatabai, Z. L., Hinoda, Y., & Dahiya, R. (2012). Oncogenic miRNA-182-5p targets Smad4 and RECK in human bladder cancer. *PloS One*, *7*(11), e51056. http://doi.org/10.1371/journal.pone.0051056

Honkakoski, P., Zelko, I., Sueyoshi, T., & Negishi, M. (1998). The nuclear orphan receptor CAR-retinoid X receptor heterodimer activates the phenobarbital-responsive enhancer module of the CYP2B gene. *Molecular and Cellular Biology*, *18*(10), 5652–5658.

Horie-Inoue, K., Bono, H., Okazaki, Y., & Inoue, S. (2004). Identification and functional analysis of consensus androgen response elements in human prostate cancer cells. *Biochemical and Biophysical Research Communications*, *325*(4), 1312–1317. http://doi.org/10.1016/j.bbrc.2004.10.174

Hosseinpour, F., Moore, R., Negishi, M., & Sueyoshi, T. (2006). Serine 202 Regulates the Nuclear Translocation of Constitutive Active / Androstane Receptor, *69*(4), 1095–1102. http://doi.org/10.1124/mol.105.019505.CAR

Hu, C., & Li, L. (2015). In vitro culture of isolated primary hepatocytes and stem cell-derived hepatocyte-like cells for liver regeneration. *Protein & Cell*. http://doi.org/10.1007/s13238-015-0180-2

Huang, W., Zhang, J., Chua, S. S., Qatanani, M., Han, Y., Granata, R., & Moore, D. D. (2003). Induction of bilirubin clearance by the constitutive androstane receptor (CAR). *Proceedings of the National Academy of Sciences of the United States of America*, *100*(7), 4156–4161. http://doi.org/10.1073/pnas.0630614100

Huang, W., Zhang, J., Washington, M., Liu, J., Parant, J. M., Lozano, G., & Moore, D. D. (2005). Xenobiotic stress induces hepatomegaly and liver tumors via the nuclear receptor constitutive androstane receptor. *Molecular Endocrinology (Baltimore, Md.)*, *19*(6), 1646–53. http://doi.org/10.1210/me.2004-0520

Ichimura, R., Mizukami, S., Takahashi, M., Taniai, E., Kemmochi, S., Mitsumori, K., & Shibutani, M. (2010). Disruption of Smad-dependent signaling for growth of GST-P-positive lesions from the early stage in a rat two-stage hepatocarcinogenesis model. *Toxicology and Applied Pharmacology*, *246*(3), 128–140. http://doi.org/10.1016/j.taap.2010.04.016

Ilangaratne, N. B., Mannakkara, N. N., Bell, G. S., & Sander, J. W. (2012). Phenobarbital: missing in action. *Bulletin of the World Health Organization*, *90*(12), 871–871A. http://doi.org/10.2471/BLT.12.113183

Imaoka, S., Osada, M., Minamiyama, Y., Yukimura, T., Toyokuni, S., Takemura, S., … Funae, Y. (2004). Role of phenobarbital-inducible cytochrome P450s as a source of active oxygen species in DNA-oxidation. *Cancer Letters*, *203*(2), 117–125. http://doi.org/10.1016/j.canlet.2003.09.009

Isenberg, J. S., Kamendulis, L. M., Ackley, D. C., Smith, J. H., Pugh, G., Lington, A. W., … Klaunig, J. E. (2001). Reversibility and persistence of Di-2-ethylhexyl phthalate (DEHP)- and phenobarbital-induced hepatocellular changes in rodents. *Toxicological Sciences*, *64*(2), 192–199. http://doi.org/10.1093/toxsci/64.2.192

Jalvy-Delvaille, S., Maurel, M., Majo, V., Pierre, N., Chabas, S., Combe, C., … Grosset, C. F. (2012). Molecular basis of differential target regulation by miR-96 and miR-182: the Glypican-3 as a model. *Nucleic Acids Research*, *40*(3), 1356–65. http://doi.org/10.1093/nar/gkr843

Jirtle, R. L., & Meyer, S. a. (1991). Liver tumor promotion: effect of phenobarbital on EGF and protein kinase C signal transduction and transforming growth factor-beta 1 expression. *Digestive Diseases and Sciences*, *36*(5), 659–68. Retrieved from http://www.ncbi.nlm.nih.gov/pubmed/2022168

Jitrapakdee, S., & Wallace, J. C. (1999). Structure, function and regulation of pyruvate carboxylase. *The Biochemical Journal*, *340 (Pt 1*, 1–16.

Joannard, F., Galisteo, M., Corcos, L., Guillouzo, a, & Lagadic-Gossmann, D. (2000). Regulation of phenobarbital-induction of CYP2B and CYP3A genes in rat cultured hepatocytes: involvement of several serine/threonine protein kinases and phosphatases. *Cell Biology and Toxicology*, *16*(5), 325–37. Retrieved from http://www.ncbi.nlm.nih.gov/pubmed/11201056

Joannard, F., Rissel, M., Gilot, D., Anderson, A., Orfila-Lefeuvre, L., Guillouzo, A., … Lagadic-Gossmann, D. (2006). Role for mitogen-activated protein kinases in phenobarbital-induced expression of cytochrome P450 2B in primary cultures of rat hepatocytes. *Toxicology Letters*, *161*(1), 61–72. http://doi.org/10.1016/j.toxlet.2005.08.006

Kachaylo, E. M., Pustylnyak, V. O., Lyakhovich, V. V, & Gulyaeva, L. F. (2011). Constitutive androstane receptor (CAR) is a xenosensor and target for therapy. *Biochemistry. Biokhimiia*, *76*(10), 1087–97. http://doi.org/10.1134/S0006297911100026

Kakehashi, A., Hagiwara, A., Imai, N., Nagano, K., Nishimaki, F., Banton, M., … Wanibuchi, H. (2013). Mode of action of ethyl tertiary-butyl ether hepatotumorigenicity in the rat: evidence for a role of oxidative stress via activation of CAR, PXR and PPAR signaling pathways. *Toxicology and Applied Pharmacology*, *273*(2), 390–400. http://doi.org/10.1016/j.taap.2013.09.016

Kang, L.-I., Mars, W. M., & Michalopoulos, G. K. (2012). Signals and cells involved in regulating liver regeneration. *Cells*, *1*(4), 1261–92. http://doi.org/10.3390/cells1041261

Kanno, N., LeSage, G., Glaser, S., Alvaro, D., & Alpini, G. (2000). Functional Heterogeneity of the Intrahepatic Biliary Epithelium. *Hepatology*, *31*(3), 555–561.

Kanno, Y., & Inouye, Y. (2008). Molecular Basis of the Intracellular Localization of the Constitutive Androstane Receptor (CAR). *Journal of Health Science*, *54*(3), 261–266. http://doi.org/10.1248/jhs.54.261

Kanno, Y., Miyama, Y., Ando, M., & Inouye, Y. (2009). Dependence on the Microtubule Network and 90-kDa Heat Shock Protein of Phenobarbital-Induced Nuclear Translocation of the Rat Constitutive Androstane Receptor □. http://doi.org/10.1124/mol.109.060434.

Kanno, Y., Miyazaki, Y., & Inouye, Y. (2010). The nuclear import of the constitutive androstane receptor by importin/Ran-GTP systems. *Biochimica et Biophysica Acta*, *1803*(8), 968–74. http://doi.org/10.1016/j.bbamcr.2010.05.004

Kanno, Y., Suzuki, M., Miyazaki, Y., Matsuzaki, M., Nakahama, T., Kurose, K., … Inouye, Y. (2007). Difference in nucleocytoplasmic shuttling sequences of rat and human constitutive active/androstane receptor. *Biochimica et Biophysica Acta - Molecular Cell Research*, *1773*(6), 934–944. http://doi.org/10.1016/j.bbamcr.2007.03.020

Kanno, Y., Suzuki, M., Nakahama, T., & Inouye, Y. (2005). Characterization of nuclear localization signals and cytoplasmic retention region in the nuclear receptor CAR. *Biochimica et Biophysica Acta - Molecular Cell Research*, *1745*(2), 215–222. http://doi.org/10.1016/j.bbamcr.2005.06.012

Kawai, S., & Amano, A. (2012). BRCA1 regulates microRNA biogenesis via the DROSHA microprocessor complex. *The Journal of Cell Biology*, *197*(2), 201–8. http://doi.org/10.1083/jcb.201110008

Kawamoto, T., Sueyoshi, T., Zelko, I., Moore, R., Washburn, K., & Negishi, M. (1999). Phenobarbital-responsive nuclear translocation of the receptor CAR in induction of the CYP2B gene. *Molecular and Cellular Biology*, *19*(9), 6318–6322.

Kawamura, a, Yoshida, Y., Kimura, N., Oda, H., & Kakinuma, a. (1999). Phosphorylation/Dephosphorylation steps are crucial for the induction of CYP2B1 and CYP2B2 gene expression by phenobarbital. *Biochemical and Biophysical Research Communications*, *264*(2), 530–536. http://doi.org/10.1006/bbrc.1999.1544

Kazantseva, Y. a., Yarushkin, A. a., Mostovich, L. a., Pustylnyak, Y. a., & Pustylnyak, V. O. (2015). Xenosensor CAR mediates down-regulation of miR-122 and up-regulation of miR-122 targets in the liver. *Toxicology and Applied Pharmacology*, *288*(1), 26–32. http://doi.org/10.1016/j.taap.2015.07.004

Kent, W., Sugnet, C., Furey, T., Roskin, K., Pringle, T., Zahler, A., & Haussler, D. (2002). The human genome browser at UCSC. *Genome Research*, *12*(6), 996–1006.

Khan, M. a, Qadri, S. Y., Tomar, S., Fish, D., Gururajan, L., & Poria, M. S. (1998). Induction of hepatic cytochrome P-450 by phenobarbital in semi-aquatic frog (Rana pipiens). *Biochemical and Biophysical Research Communications*, *244*(3), 737–744. http://doi.org/10.1006/bbrc.1998.8281

Khetani, S. R., Szulgit, G., Del Rio, J. a., Barlow, C., & Bhatia, S. N. (2004). Exploring interactions between rat hepatocytes and nonparenchymal cells using gene expression profiling. *Hepatology*, *40*(3), 545–554. http://doi.org/10.1002/hep.20351

Kim, J., Min, G., & Kemper, B. (2001). Chromatin Assembly Enhances Binding to the CYP2B1 Phenobarbital-responsive Unit (PBRU) of Nuclear Factor-1, which Binds Simultaneously with Constitutive Androstane Receptor (CAR)/Retinoid X Receptor (RXR) and Enhances CAR/RXR-mediated Activation of the PB. *Journal of Biological Chemistry*, *276*(10), 7559–7567. http://doi.org/10.1074/jbc.M008090200

Kim, Y.-K., & Kim, V. N. (2007). Processing of intronic microRNAs. *The EMBO Journal*, *26*(3), 775–783. http://doi.org/10.1038/sj.emboj.7601512

Kishida, T., Muto, S., Hayashi, M., Tsutsui, M., Tanaka, S., Murakami, M., & Kuroda, J. (2008). Strain differences in hepatic cytochrome P450 1A and 3A expression between Sprague-Dawley and Wistar rats. *The Journal of Toxicological Sciences*, *33*(4), 447–457. http://doi.org/10.2131/jts.33.447

Klepeisz, P., Sagmeister, S., Haudek-Prinz, V., Pichlbauer, M., Grasl-Kraupp, B., & Gerner, C. (2013). Phenobarbital induces alterations in the proteome of hepatocytes and mesenchymal cells of rat livers. *PloS One*, *8*(10), e76137. http://doi.org/10.1371/journal.pone.0076137

Kliewer, S. a, & Willson, T. M. (2002). Regulation of xenobiotic and bile acid metabolism by the nuclear pregnane X receptor. *Journal of Lipid Research*, *43*(3), 359–364.

Kliewer, S. a., Moore, J. T., Wade, L., Staudinger, J. L., Watson, M. a., Jones, S. a., … Lehmann, J. M. (1998). An orphan nuclear receptor activated by pregnanes defines a novel steroid signaling pathway. *Cell*, *92*(1), 73–82. http://doi.org/10.1016/S0092-8674(00)80900-9

Knowles, B., Howe, C., & Aden, D. (1980). Human Hepatocellular Carcinoma Cell Lines Secrete the Major Plasma Proteins and Hepatitis B Surface Antigen. *Science*, *209*, 497–499.

Kobayashi, K., Sueyoshi, T., Inoue, K., Moore, R., & Negishi, M. (2003). Cytoplasmic accumulation of the nuclear receptor CAR by a tetratricopeptide repeat protein in HepG2 cells. *Molecular Pharmacology*, *64*(5), 1069–75. http://doi.org/10.1124/mol.64.5.1069

Kodama, S., Koike, C., Negishi, M., & Yamamoto, Y. (2004). Nuclear Receptors CAR and PXR Cross Talk with FOXO1 To Regulate Genes That Encode Drug-Metabolizing and Gluconeogenic Enzymes. *Molecular and Cellular Biology*, *24*(18), 7931–7940. http://doi.org/10.1128/MCB.24.18.7931

Koike, C., Moore, R., & Negishi, M. (2005). Localization of the nuclear receptor CAR at the cell membrane of mouse liver. *FEBS Letters*, *579*(30), 6733–6736. http://doi.org/10.1016/j.febslet.2005.10.070

Koike, C., Moore, R., & Negishi, M. (2007). Extracellular signal-regulated kinase is an endogenous signal retaining the nuclear constitutive active/androstane receptor (CAR) in the cytoplasm of mouse primary hepatocytes. *Molecular Pharmacology*, *71*(5), 1217–1221. http://doi.org/10.1124/mol.107.034538

Kostka, G., Urbanek, K., & Ludwicki, J. K. (2007). The effect of phenobarbital on the methylation level of the p16 promoter region in rat liver. *Toxicology*, *239*(1-2), 127–35. http://doi.org/10.1016/j.tox.2007.07.003

Kot, M., & Daniel, W. a. (2007). Effect of cytochrome P450 (CYP) inducers on caffeine metabolism in the rat. *Pharmacological Reports*, *59*(3), 296–305.

Koufaris, C. (2011). *Using liver miRNA profiles to predict chemical carcinogenesis*. Imperial College London.

Koufaris, C., Wright, J., Currie, R. a., & Gooderham, N. J. (2012). Hepatic MicroRNA profiles offer predictive and mechanistic insights after exposure to genotoxic and epigenetic hepatocarcinogens. *Toxicological Sciences*, *128*(2), 532–543. http://doi.org/10.1093/toxsci/kfs170

Koufaris, C., Wright, J., Osborne, M., Currie, R. a, & Gooderham, N. J. (2013). Time and dose-dependent effects of phenobarbital on the rat liver miRNAome. *Toxicology*, *314*(2-3), 247–53. http://doi.org/10.1016/j.tox.2013.10.004

Kozomara, A., & Griffiths-Jones, S. (2014). MiRBase: Annotating high confidence microRNAs using deep sequencing data. *Nucleic Acids Research*, *42*(D1), 68–73. http://doi.org/10.1093/nar/gkt1181

Krishnan, K., Steptoe, A. L., Martin, H. C., Wani, S., & Nones, K. (2012). MicroRNA-182-5p targets a network of genes involved in DNA repair MicroRNA-182-5p targets a network of genes involved in DNA repair. http://doi.org/10.1261/rna.034926.112

Lambert, N. J., Gu, S. G., & Zahler, A. M. (2011). The conformation of microRNA seed regions in native microRNPs is prearranged for presentation to mRNA targets. *Nucleic Acids Research*, *39*(11), 4827–4835. http://doi.org/10.1093/nar/gkr077

Langouët, S., Mahéo, K., Berthou, F., Morel, F., Lagadic-Gossman, D., Glaise, D., … Guillouzo, A. (1997). Effects of administration of the chemoprotective agent oltipraz on CYP1A and CYP2B in rat liver and rat hepatocytes in culture. *Carcinogenesis*, *18*(7), 1343–1349. http://doi.org/10.1093/carcin/18.7.1343

Lee, I., Ajay, S. S., Yook, J. I., Kim, H. S., Hong, S. H., Kim, N. H., … Athey, B. D. (2009). New class of microRNA targets containing simultaneous 5'-UTR and 3'-UTR interaction sites. *Genome Research*, *19*(7), 1175–83. http://doi.org/10.1101/gr.089367.108

Lee, R. C., Feinbaum, R. L., & Ambros, V. (1993). The C. elegans heterochronic gene lin-4 encodes small RNAs with antisense complementarity to lin-14. *Cell*, *75*(5), 843–54. Retrieved from http://www.ncbi.nlm.nih.gov/pubmed/8252621

Lee, Y., Ahn, C., Han, J., Choi, H., Kim, J., Yim, J., … Kim, V. N. (2003). The nuclear RNase III Drosha initiates microRNA processing. *Nature*, *425*(6956), 415–9. http://doi.org/10.1038/nature01957

Lee, Y., Kim, M., Han, J., Yeom, K.-H., Lee, S., Baek, S. H., & Kim, V. N. (2004). MicroRNA genes are transcribed by RNA polymerase II. *The EMBO Journal*, *23*(20), 4051–60. http://doi.org/10.1038/sj.emboj.7600385

Lee, Y.-S., & Jeong, W.-I. (2012). Retinoic acids and hepatic stellate cells in liver disease. *Journal of Gastroenterology and Hepatology*, *27 Suppl 2*, 75–9. http://doi.org/10.1111/j.1440-1746.2011.07007.x

Legendre, A., Baudoin, R., Alberto, G., Paullier, P., Naudot, M., Bricks, T., … Leclerc, E. (2013). Metabolic Characterization of Primary Rat Hepatocytes Cultivated in Parallel Microfluidic Biochips, *102*(9), 13–15. http://doi.org/10.1002/jps

Lehmann, J. M., McKee, D. D., Watson, M. a., Willson, T. M., Moore, J. T., & Kliewer, S. a. (1998). The human orphan nuclear receptor PXR is activated by compounds that regulate CYP3A4 gene expression and cause drug interactions. *Journal of Clinical Investigation*, *102*(5), 1016–1023. http://doi.org/10.1172/JCI3703

Lempiäinen, H., Couttet, P., Bolognani, F., Müller, A., Dubost, V., Luisier, R., … Moggs, J. G. (2013). Identification of Dlk1-Dio3 imprinted gene cluster noncoding RNAs as novel candidate biomarkers for liver tumor promotion. *Toxicological Sciences*, *131*(2), 375–386. http://doi.org/10.1093/toxsci/kfs303

LePecq, J., & Paoletti, C. (1967). A fluorescent complex between ethidium bromide and nucleic acids. Physical-chemical characterization. *J Mol Biol.*, *27*(1), 87–106.

Lewis, B., Burge, C., & Bartel, D. (2005). Conserved seed pairing, often flanked by adenosines, indicates that thousands of human genes are microRNA targets. *Cell*, *120*(1), 15–20.

Lewis, B. P., Shih, I., Jones-Rhoades, M. W., Bartel, D. P., & Burge, C. B. (2003). Prediction of mammalian microRNA targets. *Cell*, *115*(7), 787–98. Retrieved from http://www.ncbi.nlm.nih.gov/pubmed/14697198

Li, T., & Chiang, J. Y. L. (2014). Bile Acid Signaling in Metabolic Disease and Drug Therapy. *Pharmacological Reviews*, *66*(4), 948–983. http://doi.org/10.1124/pr.113.008201

Li, X. L., Hara, T., Choi, Y., Subramanian, M., Francis, P., Bilke, S., … Lal, a. (2013). A p21-ZEB1 Complex Inhibits Epithelial-Mesenchymal Transition through the MicroRNA 183-96-182 Cluster. *Molecular and Cellular Biology*, *34*(3), 533–550. http://doi.org/10.1128/MCB.01043-13

Lindroos, P., Tsai, W. H., Zarnegar, R., & Michalopoulos, G. K. (1992). Plasma levels of HGF in rats treated with tumor promoters. *Carcinogenesis*, *13*(1), 139–141.

Ling, H., Sayer, J. M., Plosky, B. S., Yagi, H., Boudsocq, F., Woodgate, R., … Yang, W. (2004). Crystal structure of a benzo[a]pyrene diol epoxide adduct in a ternary complex with a DNA polymerase. *Proceedings of the National Academy of Sciences of the United States of America*, *101*(8), 2265–2269. http://doi.org/10.1073/pnas.0308332100

Liu, S.-P., Li, Y.-S., Chen, Y.-J., Chiang, E.-P., Li, A. F.-Y., Lee, Y.-H., … Chen, Y.-M. A. (2007). Glycine N-methyltransferase-/- mice develop chronic hepatitis and glycogen storage disease in the liver. *Hepatology (Baltimore, Md.)*, *46*(5), 1413–25. http://doi.org/10.1002/hep.21863

Lochhead, P. a., Salt, I. P., Walker, K. S., Hardie, D. G., & Sutherland, C. (2000). 5-Aminoimidazole-4-carboxamide riboside mimics the effects of insulin on the expression of the 2 key gluconeogenic genes PEPCK and glucose-6- phosphatase. *Diabetes*, *49*(6), 896–903. http://doi.org/10.2337/diabetes.49.6.896

Longnecker, D., Lilja, H., French, J., Kuhlmann, E., & Noll, W. (1979). Transplantation of azaserine-induced carcinomas of pancreas in rats. *Cancer Lett.*, *7*, 197–202.

Löscher, W., & Rogawski, M. a. (2012). How theories evolved concerning the mechanism of action of barbiturates. *Epilepsia*, *53 Suppl 8*, 12–25. http://doi.org/10.1111/epi.12025

Lu, J., Einhorn, S., Venkatarangan, L., Miller, M., Mann, D. A., Paul, B., & Lecluyse, E. (2015). Morphological and Functional Characterization and Assessment of iPSC-derived Hepatocytes for In Vitro Toxicity Testing.

Luisier, R., Lempiäinen, H., Scherbichler, N., Braeuning, A., Geissler, M., Dubost, V., … Moggs, J. G. (2014). Phenobarbital induces cell cycle transcriptional responses in mouse liver humanized for constitutive androstane and pregnane x receptors. *Toxicological Sciences : An Official Journal of the Society of Toxicology*, *139*(2), 501–11. http://doi.org/10.1093/toxsci/kfu038

Luka, Z., Mudd, S. H., & Wagner, C. (2009). Glycine N-methyltransferase and regulation of S-adenosylmethionine levels. *Journal of Biological Chemistry*, *284*(34), 22507–22511. http://doi.org/10.1074/jbc.R109.019273

Maglich, J. M., Parks, D. J., Moore, L. B., Collins, J. L., Goodwin, B., Billin, A. N., … Moore, J. T. (2003). Identification of a novel human constitutive androstane receptor (CAR) agonist and its use in the identification of CAR target genes. *Journal of Biological Chemistry*, *278*(19), 17277–17283. http://doi.org/10.1074/jbc.M300138200

Malarkey, D. E., Johnson, K., Ryan, L., Boorman, G., & Maronpot, R. R. (2005). New insights into functional aspects of liver morphology. *Toxicologic Pathology*, *33*(1), 27–34. http://doi.org/10.1080/01926230590881826

Malumbres, M. (2012). miRNAs and cancer: an epigenetics view. *Molecular Aspects of Medicine*, *34*(4), 863–74. http://doi.org/10.1016/j.mam.2012.06.005

Maniataki, E., & Mourelatos, Z. (2005). A human, ATP-independent, RISC assembly machine fueled by pre-miRNA. *Genes & Development*, *19*(24), 2979–90. http://doi.org/10.1101/gad.1384005

Manning, B., & Cantley, L. (2007). AKT/PKB Signalling: Navigating Downstream. *Cell*, *129*(7), 1261–1274. http://doi.org/10.1016/j.cell.2007.06.009.AKT/PKB

Mansbach, J. M., Mills, J. J., Boyer, I. J., De Souza, a T., Hankins, G. R., & Jirtle, R. L. (1996). Phenobarbital selectively promotes initiated cells with reduced TGF beta receptor levels. *Carcinogenesis*, *17*(1), 171–4. Retrieved from http://www.ncbi.nlm.nih.gov/pubmed/8565130

Marek, C. J., Cameron, G. a, Elrick, L. J., Hawksworth, G. M., & Wright, M. C. (2003). Generation of hepatocytes expressing functional cytochromes P450 from a pancreatic progenitor cell line in vitro. *The Biochemical Journal*, *370*(Pt 3), 763–9. http://doi.org/10.1042/BJ20021545

Mashima, H., Ohnishi, H., Wakabayashi, K., Mine, T., Miyagawa, J. I., Hanafusa, T., … Kojima, I. (1996). Betacellulin and activin A coordinately convert amylase-secreting pancreatic AR42J cells into insulin-secreting cells. *Journal of Clinical Investigation*, *97*(7), 1647–1654. http://doi.org/10.1172/JCI118591

Mashima, H., Shibata, H., Mine, T., & Kojima, I. (1996). Formation of insulin-producing cells from pancreatic acinar AR42J cells by hepatocyte growth factor. *Endocrinology*, *137*(9), 3969–76.

Matallanas, D., Birtwistle, M., Romano, D., Zebisch, A., Rauch, J., von Kriegsheim, A., & Kolch, W. (2011). Raf family kinases: old dogs have learned new tricks. *Genes & Cancer*, *2*(3), 232–260. http://doi.org/10.1177/1947601911407323

Matsui, T., Nagoshi, T., & Rosenzweig, A. (2003). Akt and PI 3-Kinase Signaling in Cardiomyocyte Hypertrophy nd sc ie nc e . DISEASE ot fo rib. *Cell Cycle*, (June), 220–223.

Miao, J., Fang, S., Bae, Y., & Kemper, J. K. (2006). Functional inhibitory cross-talk between constitutive androstane receptor and hepatic nuclear factor-4 in hepatic lipid/glucose metabolism is mediated by competition for binding to the DR1 motif and to the common coactivators, GRIP-1 and PGC-1alpha. *The Journal of Biological Chemistry*, *281*(21), 14537–46. http://doi.org/10.1074/jbc.M510713200

Miyazaki, M., Mars, W. M., Runge, D., Kim, T. H., Bowen, W. C., & Michalopoulos, G. K. (1998). Phenobarbital suppresses growth and accelerates restoration of differentiation markers of primary culture rat hepatocytes in the chemically defined hepatocyte growth medium containing hepatocyte growth factor and epidermal growth factor. *Experimental Cell Research*, *241*(2), 445–457. http://doi.org/10.1006/excr.1998.4085

Moennikes, O., Buchmann, a., Romualdi, a., Ott, T., Werringloer, J., Willecke, K., & Schwarz, M. (2000). Lack of phenobarbital-mediated promotion of hepatocarcinogenesis in Connexin32-null mice. *Cancer Research*, *60*(18), 5087–5091.

Moore, L. B., Parks, D. J., Jones, S. a, Bledsoe, R. K., Consler, T. G., Stimmel, J. B., … Kliewer, S. a. (2000). Orphan nuclear receptors constitutive androstane receptor and pregnane X receptor share xenobiotic and steroid ligands. *The Journal of Biological Chemistry*, *275*(20), 15122–7. http://doi.org/10.1074/jbc.M001215200

Moustakas, a, Souchelnytskyi, S., & Heldin, C. H. (2001). Smad regulation in TGF-beta signal transduction. *Journal of Cell Science*, *114*(Pt 24), 4359–4369. http://doi.org/10.1152/ajpgi.00208.2007.

Mutoh, S., Sobhany, M., Moore, R., Perera, L., Pedersen, L., Sueyoshi, T., & Negishi, M. (2013). Phenobarbital indirectly activates the constitutive active androstane receptor (CAR) by inhibition of epidermal growth factor receptor signaling. *Science Signaling*, *6*(274), ra31. http://doi.org/10.1126/scisignal.2003705

Nakabayashi, H., Taketa, K., Miyano, K., Yamane, T., & Sato, J. (1982). Growth of Human Hepatoma Cell Lines with Differentiated Functions in Chemically Defined Medium Growth of Human Hepatoma Cell Lines with Differentiated Chemically Defined Medium, *42*(September), 3858–3863.

Nugraha, B., Hong, X., Mo, X., Tan, L., Zhang, W., Chan, P. M., … Yu, H. (2011). Galactosylated cellulosic sponge for multi-well drug safety testing. *Biomaterials*, *32*(29), 6982–6994. http://doi.org/10.1016/j.biomaterials.2011.05.087

Numazawa, S., Shindo, S., Maruyama, K., Chibana, F., Kawahara, Y., Ashino, T., … Yoshida, T. (2005). Impaired nuclear translocation of CAR in hepatic preneoplastic lesions: Association with an attenuated CYP2B induction by phenobarbital. *FEBS Letters*, *579*(17), 3560–3564. http://doi.org/10.1016/j.febslet.2005.05.028

Ogihara, T., Fujitani, Y., Uchida, T., Kanno, R., Choi, J. B., Hirose, T., … Watada, H. (2008). Combined expression of transcription factors induces AR42J-B13 cells to differentiate into insulin-producing cells. *Endocrine Journal*, *55*(4), 691–698. http://doi.org/10.1507/endocrj.K07E-169

Omiecinski, C. J., Coslo, D. M., Chen, T., Laurenzana, E. M., & Peffer, R. C. (2011). Multi-species analyses of direct activators of the constitutive androstane receptor. *Toxicological Sciences : An Official Journal of the Society of Toxicology*, *123*(2), 550–62. http://doi.org/10.1093/toxsci/kfr191

Orton, T. C., Doughty, S. E., Kalinowski, a E., Lord, P. G., & Wadsworth, P. F. (1996). Expression of growth factors and growth factor receptors in the liver of C57BL/10J mice following administration of phenobarbitone. *Carcinogenesis*, *17*(5), 973–81. Retrieved from http://www.ncbi.nlm.nih.gov/pubmed/8640946

Osabe, M., & Negishi, M. (2011). Active ERK1/2 protein interacts with the phosphorylated nuclear constitutive active/androstane receptor (CAR; NR1I3), repressing dephosphorylation and sequestering car in the cytoplasm. *Journal of Biological Chemistry*, *286*(41), 35763–35769. http://doi.org/10.1074/jbc.M111.284596

Osabe, M., Sugatani, J., Takemura, A., Yamazaki, Y., Ikari, A., Kitamura, N., … Miwa, M. (2008). Expression of CAR in SW480 and HepG2 cells during G1 is associated with cell proliferation. *Biochemical and Biophysical Research Communications*, *369*(4), 1027–33. http://doi.org/10.1016/j.bbrc.2008.02.140

Park, Y., Li, H., & Kemper, B. (1996). Phenobarbital induction mediated by a distal CYP2B2 sequence in rat liver transiently transfected in situ. *Journal of Biological Chemistry*, *271*(39), 23725–23728. http://doi.org/10.1074/jbc.271.39.23725

Pascussi, J. M., Drocourt, L., Fabre, J. M., Maurel, P., & Vilarem, M. J. (2000). Dexamethasone induces pregnane X receptor and retinoid X receptor-alpha expression in human hepatocytes: synergistic increase of CYP3A4 induction by pregnane X receptor activators. *Molecular Pharmacology*, *58*(2), 361–372.

Pascussi, J. M., Drocourt, L., Gerbal-Chaloin, S., Fabre, J. M., Maurel, P., & Vilarem, M. J. (2001). Dual effect of dexamethasone on CYP3A4 gene expression in human hepatocytes. Sequential role of glucocorticoid receptor and pregnane X receptor. *European Journal of Biochemistry / FEBS*, *268*(24), 6346–6358.

Pascussi, J. M., Gerbal-Chaloin, S., Fabre, J. M., Maurel, P., & Vilarem, M. J. (2000). Dexamethasone enhances constitutive androstane receptor expression in human hepatocytes: consequences on cytochrome P450 gene regulation. *Molecular Pharmacology*, *58*(6), 1441–50. Retrieved from http://www.ncbi.nlm.nih.gov/pubmed/11093784

Phillips, J. M., Burgoon, L. D., & Goodman, J. I. (2009). The constitutive active/androstane receptor facilitates unique phenobarbital-induced expression changes of genes involved in key pathways in precancerous liver and liver tumors. *Toxicological Sciences : An Official Journal of the Society of Toxicology*, *110*(2), 319–33. http://doi.org/10.1093/toxsci/kfp108

Phillips, J. M., Yamamoto, Y., Negishi, M., Maronpot, R. R., & Goodman, J. I. (2007). Orphan nuclear receptor constitutive active/androstane receptor-mediated alterations in DNA methylation during phenobarbital promotion of liver tumorigenesis. *Toxicological Sciences : An Official Journal of the Society of Toxicology*, *96*(1), 72–82. http://doi.org/10.1093/toxsci/kfl188

Pialoux, V., Mounier, R., Brown, A. D., Steinback, C. D., Rawling, J. M., & Poulin, M. J. (2009). Relationship between oxidative stress and HIF-1α mRNA during sustained hypoxia in humans. *Free Radical Biology and Medicine*, *46*(2), 321–326. http://doi.org/10.1016/j.freeradbiomed.2008.10.047

Pitot, H., Peraino, C., Morse, P., & Potter, V. (1964). Hepatomas in tissue culture compared with adapting liver in vivo. *Natl Cancer Inst Monogr*, *13*, 229–45.

Probert, P. M. E., Chung, G. W., Cockell, S. J., Agius, L., Mosesso, P., White, S. a, … Wright, M. C. (2014). Utility of B-13 progenitor-derived hepatocytes in hepatotoxicity and genotoxicity studies. *Toxicological Sciences : An Official Journal of the Society of Toxicology*, *137*(2), 350–70. http://doi.org/10.1093/toxsci/kft258

Probert, P. M. E., Meyer, S. K., Alsaeedi, F., Axon, A. a., Fairhall, E. a., Wallace, K., … Wright, M. C. (2015). An expandable donor-free supply of functional hepatocytes for toxicology. *Toxicol. Res.*, *4*(2), 203–222. http://doi.org/10.1039/C4TX00214H

Puigserver, P., Rhee, J., Donovan, J., Kitamura, Y., Altomonte, J., & Dong, H. (2003). Insulin-regulated hepatic gluconeogenesis through FOXO1 – PGC-1 a interaction. *Nature*, *423*(May), 550–555. http://doi.org/10.1038/nature01606.1.

Pustylnyak, V. O., Zakharova, L. Y., Mikhailova, O. N., Rice, R. H., Gulyaeva, L. F., & Lyakhovich, V. V. (2005). In vivo effects of protein kinase and phosphatase inhibitors on CYP2B induction in rat liver. *Toxicology*, *207*(2), 315–22. http://doi.org/10.1016/j.tox.2004.10.003

Qiu, Y., Luo, X., Kan, T., Zhang, Y., Yu, W., Wei, Y., … Jiang, X. (2014). TGF-β upregulates miR-182 expression to promote gallbladder cancer metastasis by targeting CADM1. *Molecular bioSystems*, *10*(3), 679–85. http://doi.org/10.1039/c3mb70479c

Ravichandran, K. S. (2001). Signaling via Shc family adapter proteins. *Oncogene*, *20*(44), 6322–6330. http://doi.org/10.1038/sj.onc.1204776

Reddy, J. K., Rao, M. S., Qureshi, S. a., Reddy, M. K., Scarpelli, D. G., & Lalwani, N. D. (1984). Induction and origin of hepatocytes in rat pancreas. *Journal of Cell Biology*, *98*(6), 2082–2090. http://doi.org/10.1083/jcb.98.6.2082

Reho, J. J., Shetty, A., Dippold, R. P., Mahurkar, A., & Fisher, S. a. (2015). Unique gene program of rat small resistance mesenteric arteries as revealed by deep RNA sequencing. *Physiological Reports*, *3*(7), n/a–n/a. http://doi.org/10.14814/phy2.12450

Rencurel, F., Stenhouse, A., Hawley, S. a, Friedberg, T., Hardie, D. G., Sutherland, C., & Wolf, C. R. (2005). AMP-activated protein kinase mediates phenobarbital induction of CYP2B gene expression in hepatocytes and a newly derived human hepatoma cell line. *The Journal of Biological Chemistry*, *280*(6), 4367–73. http://doi.org/10.1074/jbc.M412711200

Rendic, S. (2015). Summary of information on human CYP enzymes: human P450 metabolism data. *Drug Metabolism Reviews*, *34*(1-2), 83–448. http://doi.org/10.1081/DMR-120001392

Reschly, E. J., & Krasowski, M. D. (2006). Evolution and function of the NR1I nuclear hormone receptor subfamily (VDR, PXR, and CAR) with respect to metabolism of xenobiotics and endogenous compounds. *Current Drug Metabolism*, *7*(4), 349–365. http://doi.org/10.2174/138920006776873526

Reuber, M. D. (1961). A transplantable bile-secreting hepatocellular carcinoma in the rat. *Journal of the National Cancer Institute*, *26*, 891–899.

Rignall, B., Braeuning, A., Buchmann, A., & Schwarz, M. (2011). Tumor formation in liver of conditional β-catenin-deficient mice exposed to a diethylnitrosamine/phenobarbital tumor promotion regimen. *Carcinogenesis*, *32*(1), 52–57. http://doi.org/10.1093/carcin/bgq226

Rodriguez, A., Griffiths-Jones, S., Ashurst, J. L., & Bradley, A. (2004). Identification of mammalian microRNA host genes and transcription units. *Genome Research*, *14*(10 A), 1902–1910. http://doi.org/10.1101/gr.2722704

Ross, J., Plummer, S. M., Rode, A., Scheer, N., Bower, C. C., Vogel, O., … Elcombe, C. R. (2010). Human constitutive androstane receptor (CAR) and pregnane X receptor (PXR) support the hypertrophic but not the hyperplastic response to the murine nongenotoxic hepatocarcinogens phenobarbital and chlordane in vivo. *Toxicological Sciences : An Official Journal of the Society of Toxicology*, *116*(2), 452–66. http://doi.org/10.1093/toxsci/kfq118

Roth, A., Looser, R., Kaufmann, M., Blättler, S. M., Rencurel, F., Huang, W., … Meyer, U. a. (2008). Regulatory cross-talk between drug metabolism and lipid homeostasis: constitutive androstane receptor and pregnane X receptor increase Insig-1 expression. *Molecular Pharmacology*, *73*(4), 1282–1289. http://doi.org/10.1124/mol.107.041012

Royo, J. L., Hidalgo, M., & Ruiz, A. (2007). Pyrosequencing protocol using a universal biotinylated primer for mutation detection and SNP genotyping. *Nature Protocols*, *2*(7), 1734–1739. http://doi.org/10.1038/nprot.2007.244

Saini, H. K., Griffiths-Jones, S., & Enright, A. J. (2007). Genomic analysis of human microRNA transcripts. *Proceedings of the National Academy of Sciences of the United States of America*, *104*(45), 17719–17724. http://doi.org/10.1073/pnas.0703890104

Sakamaki, J., Daitoku, H., Kaneko, Y., Hagiwara, A., Ueno, K., & Fukamizu, A. (2012). GSK3β regulates gluconeogenic gene expression through HNF4α and FOXO1. *Journal of Receptor and Signal Transduction Research*, *32*(2), 96–101. http://doi.org/10.3109/10799893.2012.660531

Salceda, S., & Caro, J. (1997). Hypoxia-inducible Factor 1a (HIF-1a) Protein Is Rapidly Degraded by the Ubiquitin-Proteasome System under Normoxic Conditions. *J . Biol. Chem.*, *272*(36), 22642–22647. http://doi.org/10.1091/mbc.E02

Salmena, L., Poliseno, L., Tay, Y., Kats, L., & Pandolfi, P. P. (2011). A ceRNA hypothesis: the Rosetta Stone of a hidden RNA language? *Cell*, *146*(3), 353–8. http://doi.org/10.1016/j.cell.2011.07.014

Schettino, C., Bareschino, M. A., Ricci, V., & Ciardiello, F. (2008). Erlotinib: an EGF receptor tyrosine kinase inhibitor in non-small-cell lung cancer treatment. *Expert Review of Respiratory Medicine*, *2*(2), 167–178. http://doi.org/10.1586/17476348.2.2.167

Schmittgen, T. D., & Livak, K. J. (2008). Analyzing real-time PCR data by the comparative C(T) method. *Nature Protocols*, *3*(6), 1101–1108. http://doi.org/10.1038/nprot.2008.73

Schwarz, D. S., Hutvágner, G., Du, T., Xu, Z., Aronin, N., & Zamore, P. D. (2003). Asymmetry in the assembly of the RNAi enzyme complex. *Cell*, *115*(2), 199–208. Retrieved from http://www.ncbi.nlm.nih.gov/pubmed/14567917

Shaw, P. M., Adesnik, M., Weiss, M. C., & Corcos, L. (1993). The phenobarbital-induced transcriptional activation of cytochrome P-450 genes is blocked by the glucocorticoid-progesterone antagonist RU486. *Molecular Pharmacology*, *44*(4), 775–83. Retrieved from http://www.ncbi.nlm.nih.gov/pubmed/8232228

Shen, C. N., Slack, J. M., & Tosh, D. (2000). Molecular basis of transdifferentiation of pancreas to liver. *Nature Cell Biology*, *2*(12), 879–87. http://doi.org/10.1038/35046522

Shindo, S., Numazawa, S., & Yoshida, T. (2007). A physiological role of AMP-activated protein kinase in phenobarbital-mediated constitutive androstane receptor activation and CYP2B induction. *The Biochemical Journal*, *401*(3), 735–41. http://doi.org/10.1042/BJ20061238

Shizu, R., Benoki, S., Numakura, Y., Kodama, S., Miyata, M., Yamazoe, Y., & Yoshinari, K. (2013). Xenobiotic-induced hepatocyte proliferation associated with constitutive active/androstane receptor (CAR) or peroxisome proliferator-activated receptor α (PPARα) is enhanced by pregnane X receptor (PXR) activation in mice. *PloS One*, *8*(4), e61802. http://doi.org/10.1371/journal.pone.0061802

Shizu, R., Shindo, S., Yoshida, T., & Numazawa, S. (2012). MicroRNA-122 down-regulation is involved in phenobarbital-mediated activation of the constitutive androstane receptor. *PLoS ONE*, *7*(7), 1–10. http://doi.org/10.1371/journal.pone.0041291

Sidhu, J. S., & Omiecinski, C. J. (1997). An okadaic acid-sensitive pathway involved in the phenobarbital-mediated induction of CYP2B gene expression in primary rat hepatocyte cultures. *The Journal of Pharmacology and Experimental Therapeutics*, *282*(2), 1122–1129.

Soldatow, V., LeCluyse, E., Griffith, L., & Rusyn, I. (2013). In vitro models for liver toxicity testing. *Toxicology Research*, *2*(1), 23–39. http://doi.org/10.1039/C2TX20051A.In

Staudinger, J. L., Goodwin, B., Jones, S. a, Hawkins-Brown, D., MacKenzie, K. I., LaTour, a, … Kliewer, S. a. (2001). The nuclear receptor PXR is a lithocholic acid sensor that protects against liver toxicity. *Proceedings of the National Academy of Sciences of the United States of America*, *98*(6), 3369–3374. http://doi.org/10.1073/pnas.051551698

Sturgill, M. G., & Lambert, G. H. (1997). Xenobiotic-induced hepatotoxicity: Mechanisms of liver injury and methods of monitoring hepatic function. *Clinical Chemistry*, *43*(8 SUPPL.), 1512–1526.

Sueyoshi, T., Kawamoto, T., Zelko, I., Honkakoski, P., & Negishi, M. (1999). The repressed nuclear receptor CAR responds to phenobarbital in activating the human CYP2B6 gene. *Journal of Biological Chemistry*, *274*(10), 6043–6046. http://doi.org/10.1074/jbc.274.10.6043

Sueyoshi, T., Moore, R., Sugatani, J., & Matsumura, Y. (2008). PPP1R16A , The Membrane Subunit of Protein Phosphatase 1 ␣ , Signals Nuclear Translocation of the Nuclear Receptor Constitutive Active / Androstane Receptor, *73*(4), 1113–1121. http://doi.org/10.1124/mol.107.042960.al.

Suino, K., Peng, L., Reynolds, R., Li, Y., Cha, J.-Y., Repa, J. J., … Xu, H. E. (2004). The nuclear xenobiotic receptor CAR: structural determinants of constitutive activation and heterodimerization. *Molecular Cell*, *16*(6), 893–905. http://doi.org/10.1016/j.molcel.2004.11.036

Sun, D., Gong, Y., Kojima, H., Wang, G., Ravinsky, E., Zhang, M., & Minuk, G. Y. (2003). Increasing cell membrane potential and GABAergic activity inhibits malignant hepatocyte growth. *American Journal of Physiology. Gastrointestinal and Liver Physiology*, *285*(1), G12–G19. http://doi.org/10.1152/ajpgi.00513.2002

Takai, D., & Jones, P. a. (2002). Comprehensive analysis of CpG islands in human chromosomes 21 and 22. *Proceedings of the National Academy of Sciences of the United States of America*, *99*(6), 3740–3745. http://doi.org/10.1073/pnas.052410099

Tamasi, V., Juvan, P., Beer, M., Rozman, D., & Meyer, U. A. (2009). Transcriptional Activation of PPARr by Phenobarbital in the Absence of CAR and PXR Viola. *Molecular Pharmaceutics*, *6*(5), 1573–1581.

Tan, S., Guo, J., Huang, Q., Chen, X., Li-Ling, J., Li, Q., & Ma, F. (2007). Retained introns increase putative microRNA targets within 3??? UTRs of human mRNA. *FEBS Letters*, *581*(6), 1081–1086. http://doi.org/10.1016/j.febslet.2007.02.009

Thomson, J. P., Hunter, J. M., Lempiäinen, H., Müller, A., Terranova, R., Moggs, J. G., & Meehan, R. R. (2013). Dynamic changes in 5-hydroxymethylation signatures underpin early and late events in drug exposed liver. *Nucleic Acids Research*, 1–16. http://doi.org/10.1093/nar/gkt232

Thomson, J. P., Lempiäinen, H., Hackett, J. A., Nestor, C. E., Müller, A., Bolognani, F., … Meehan, R. R. (2012). Non-genotoxic carcinogen exposure induces defined changes in the 5-hydroxymethylome. *Genome Biology*, *13*(10), R93. http://doi.org/10.1186/gb-2012-13-10-R93

Thomson, J. P., Moggs, J. G., Wolf, C. R., & Meehan, R. R. (2013). Epigenetic profiles as defined signatures of xenobiotic exposure. *Mutation Research - Genetic Toxicology and Environmental Mutagenesis*, *764-765*, 3–9. http://doi.org/10.1016/j.mrgentox.2013.08.007

Tojima, H., Kakizaki, S., Yamazaki, Y., Takizawa, D., Horiguchi, N., Sato, K., & Mori, M. (2012). Ligand dependent hepatic gene expression profiles of nuclear receptors CAR and PXR. *Toxicology Letters*, *212*(3), 288–97. http://doi.org/10.1016/j.toxlet.2012.06.001

Tomson, T., Battino, D., Bonizzoni, E., Craig, J., Lindhout, D., Sabers, A., … Vajda, F. (2011). Dose-dependent risk of malformations with antiepileptic drugs: An analysis of data from the EURAP epilepsy and pregnancy registry. *The Lancet Neurology*, *10*(7), 609–617. http://doi.org/10.1016/S1474-4422(11)70107-7

Treyer, A., & Musch, A. (2013). Hepatocyte Polarity. *Compr Physiol*, *3*, 243–287. http://doi.org/10.1002/cphy.c120009.Hepatocyte

Tsai, W., & Michalopoulos, G. (1991). Responsiveness of hepatocytes to epidermal growth factor, transforming growth factor-beta and norepinephrine during treatment with xenobiotic hepatic tumor promoters. *Cancer Letters*, *57*(1), 83–90.

Tsai, W., Zarnegar, R., & Michalopoulos, G. (1991). Long-term treatment with hepatic tumor promoters inhibits mitogenic responses of hepatocytes to acidic fibroblast growth factor and hepatocyte growth factor. *Cancer Letters*, *59*(2), 103–8.

Tsuchiyama, K., Ito, H., Taga, M., Naganuma, S., Oshinoya, Y., Nagano, K.-I., … Itoh, H. (2013). Expression of microRNAs associated with Gleason grading system in prostate cancer: miR-182-5p is a useful marker for high grade prostate cancer. *The Prostate*, *73*(8), 827–34. http://doi.org/10.1002/pros.22626

Tzameli, I., Pissios, P., Schuetz, E. G., & Moore, D. D. (2000). The xenobiotic compound 1,4-bis[2-(3,5-dichloropyridyloxy)]benzene is an agonist ligand for the nuclear receptor CAR. *Molecular and Cellular Biology*, *20*(9), 2951–2958. http://doi.org/10.1128/MCB.20.9.2951-2958.2000

Ueda, A., Hamadeh, H. K., Webb, H. K., Yamamoto, Y., Sueyoshi, T., Afshari, C. a, … Negishi, M. (2002). Diverse roles of the nuclear orphan receptor CAR in regulating hepatic genes in response to phenobarbital. *Molecular Pharmacology*, *61*(1), 1–6. Retrieved from http://www.ncbi.nlm.nih.gov/pubmed/11752199

Unterberger, E. B., Eichner, J., Wrzodek, C., Lempiäinen, H., Luisier, R., Terranova, R., … Schwarz, M. (2014). Ha-ras and β-catenin oncoproteins orchestrate metabolic programs in mouse liver tumors. *International Journal of Cancer*, *135*(7), 1574–1585. http://doi.org/10.1002/ijc.28798

Vermeulen, A., Behlen, L., Reynolds, A., Wolfson, A., Marshall, W. S., Karpilow, J., & Khvorova, A. (2005). The contributions of dsRNA structure to Dicer specificity and efficiency. *RNA (New York, N.Y.)*, *11*(5), 674–682. http://doi.org/10.1261/rna.7272305

Wagner, E. F., & Nebreda, A. R. (2009). Signal integration by JNK and p38 MAPK pathways in cancer development. *Nature Reviews. Cancer*, *9*(8), 537–549. http://doi.org/10.1038/nrc2694

Wallace, B. D., & Redinbo, M. R. (2013). Xenobiotic-sensing nuclear receptors involved in drug metabolism: a structural perspective. *Drug Metabolism Reviews*, *45*(1), 79–100. http://doi.org/10.3109/03602532.2012.740049

Wallace, K., Fairhall, E. a, Charlton, K. a, & Wright, M. C. (2010). AR42J-B-13 cell: an expandable progenitor to generate an unlimited supply of functional hepatocytes. *Toxicology*, *278*(3), 277–87. http://doi.org/10.1016/j.tox.2010.05.008

Wallace, K., Long, Q., Fairhall, E. a, Charlton, K. a, & Wright, M. C. (2011). Serine/threonine protein kinase SGK1 in glucocorticoid-dependent transdifferentiation of pancreatic acinar cells to hepatocytes. *Journal of Cell Science*, *124*(Pt 3), 405–413. http://doi.org/10.1242/jcs.077503

Wallace, K., Marek, C. J., Currie, R. a., & Wright, M. C. (2009). Exocrine pancreas trans-differentiation to hepatocytes-A physiological response to elevated glucocorticoid in vivo. *Journal of Steroid Biochemistry and Molecular Biology*, *116*(1-2), 76–85. http://doi.org/10.1016/j.jsbmb.2009.05.002

Wallace, K., Marek, C. J., Hoppler, S., & Wright, M. C. (2010). Glucocorticoid-dependent transdifferentiation of pancreatic progenitor cells into hepatocytes is dependent on transient suppression of WNT signalling. *Journal of Cell Science*, *123*(Pt 12), 2103–2110. http://doi.org/10.1242/jcs.070722

Wang, H., & Negishi, M. (2003). Transcriptional regulation of cytochrome p450 2B genes by nuclear receptors. *Current Drug Metabolism*, *4*(6), 515–25. Retrieved from http://www.ncbi.nlm.nih.gov/pubmed/14683479

Wang, T.-H., Yeh, C.-T., Ho, J.-Y., Ng, K.-F., & Chen, T.-C. (2015). OncomiR miR-96 and miR-182 promote cell proliferation and invasion through targeting ephrinA5 in hepatocellular carcinoma. *Molecular Carcinogenesis*, (June), n/a–n/a. http://doi.org/10.1002/mc.22286

Wang, Y.-M., Ong, S. S., Chai, S. C., & Chen, T. (2012). Role of CAR and PXR in xenobiotic sensing and metabolism. *Expert Opinion on Drug Metabolism & Toxicology*, *8*(7), 803–17. http://doi.org/10.1517/17425255.2012.685237

Waterman, C. L., Currie, R. a, Cottrell, L. a, Dow, J., Wright, J., Waterfield, C. J., & Griffin, J. L. (2010). An integrated functional genomic study of acute phenobarbital exposure in the rat. *BMC Genomics*, *11*, 9. http://doi.org/10.1186/1471-2164-11-9

Waxman, D. J. (1999). P450 Gene Induction by Structurally Diverse Xenochemicals : Central Role of Nuclear. *Archives of Biochemistry and Biophysics*, *369*(1), 11–23.

Wei, P., Zhang, J., Egan-Hafley, M., Liang, S., & Moore, D. D. (2000). The nuclear receptor CAR mediates specific xenobiotic induction of drug metabolism. *Nature*, *407*(6806), 920–923. http://doi.org/10.1038/35038112

Wiebel, F., Kiefer, F., & Murdia, U. (1984). Phenobarbital induces cytochrome P-450- and cytochrome P-448-dependent monooxygenases in rat hepatoma cells. *Chem Biol Interact*, *52*(2), 151–62.

Williams, G. M., & Whysner, J. (1996). Epigenetic carcinogens: evaluation and risk assessment. *Experimental and Toxicologic Pathology : Official Journal of the Gesellschaft Fur Toxikologische Pathologie*, *48*(2-3), 189–195. http://doi.org/10.1016/S0940-2993(96)80041-8

Wu, S.-Y., Hsieh, C.-C., Wu, R.-R., Susanto, J., Liu, T.-T., Shen, C.-R., … Shen, C.-N. (2010). Differentiation of pancreatic acinar cells to hepatocytes requires an intermediate cell type. *Gastroenterology*, *138*(7), 2519–30. http://doi.org/10.1053/j.gastro.2010.02.011

Xu, S., Witmer, P. D., Lumayag, S., Kovacs, B., & Valle, D. (2007). MicroRNA (miRNA) transcriptome of mouse retina and identification of a sensory organ-specific miRNA cluster. *Journal of Biological Chemistry*, *282*(34), 25053–25066. http://doi.org/10.1074/jbc.M700501200

Xu, X., Lu, Z., Qiang, W., Vidimar, V., Kong, B., Kim, J. J., & Wei, J. J. (2014). Inactivation of AKT induces cellular senescence in uterine leiomyoma. *Endocrinology*, *155*(4), 1510–1519. http://doi.org/10.1210/en.2013-1929

Xu, X., Wu, J., Li, S., Hu, Z., Xu, X., Zhu, Y., … Xie, L. (2014). Downregulation of microRNA-182-5p contributes to renal cell carcinoma proliferation via activating the AKT/FOXO3a signaling pathway. *Molecular Cancer*, *13*(1), 109. http://doi.org/10.1186/1476-4598-13-109

Yamada, T., Okuda, Y., Kushida, M., Sumida, K., Takeuchi, H., Nagahori, H., … Kawamura, S. (2014). Human Hepatocytes Support the Hypertrophic but not the Hyperplastic Response to the Murine Nongenotoxic Hepatocarcinogen Sodium Phenobarbital in an In Vivo Study Using a Chimeric Mouse with Humanized Liver. *Toxicological Sciences*, *142*(1), 137–157. http://doi.org/10.1093/toxsci/kfu173

Yamamoto, Y., Moore, R., Goldsworthy, T. L., Negishi, M., & Maronpot, R. R. (2004). The orphan nuclear receptor constitutive active/androstane receptor is essential for liver tumor promotion by phenobarbital in mice. *Cancer Research*, *64*(20), 7197–7200. http://doi.org/10.1158/0008-5472.CAN-04-1459

Yamamoto, Y., & Negishi, M. (2008). The Antiapoptotic Factor Growth Arrest and DNA-Damage- Inducible 45 beta Regulates the Nuclear Receptor Constitutive Active/Androstane Receptor-Mediated Transcription. *Drug Metabolism and Disposition*, *36*(7), 1189–1193. http://doi.org/10.1124/dmd.108.020628.to

Yan, D., Dong, X. Da, Chen, X., Yao, S., Wang, L., Wang, J., … Tu, L. (2012). Role of microRNA-182 in posterior uveal melanoma: regulation of tumor development through MITF, BCL2 and cyclin D2. *PloS One*, *7*(7), e40967. http://doi.org/10.1371/journal.pone.0040967

Yang, H., Garzel, B., Heyward, S., Moeller, T., Shapiro, P., & Wang, H. (2014). Metformin represses drug-induced expression of CYP2B6 by modulating the constitutive androstane receptor signaling. *Molecular Pharmacology*, *85*(2), 249–60. http://doi.org/10.1124/mol.113.089763

Yang, J.-S., Phillips, M. D., Betel, D., Mu, P., Ventura, A., Siepel, A. C., … Lai, E. C. (2011). Widespread regulatory activity of vertebrate microRNA* species. *RNA (New York, N.Y.)*, *17*(2), 312–326. http://doi.org/10.1261/rna.2537911

Yarushkin, a a, Kachaylo, E. M., & Pustylnyak, V. O. (2013). The constitutive androstane receptor activator 4-[(4R,6R)-4,6-diphenyl-1,3-dioxan-2-yl]-N,N-dimethylaniline inhibits the gluconeogenic genes PEPCK and G6Pase through the suppression of HNF4α and FOXO1 transcriptional activity. *British Journal of Pharmacology*, *168*(8), 1923–32. http://doi.org/10.1111/bph.12090

Ye, J., Coulouris, G., Zaretskaya, I., Cutcutache, I., Rozen, S., & Madden, T. (2012). Primer-BLAST: a tool to design target-specific primers for polymerase chain reaction. *BMC Bioinformatics*, *13*.

Yi, R., Qin, Y., Macara, I. G., & Cullen, B. R. (2003). Exportin-5 mediates the nuclear export of pre-microRNAs and short hairpin RNAs. *Genes & Development*, *17*(24), 3011–6. http://doi.org/10.1101/gad.1158803

Yoshinari, K., Kobayashi, K., Moore, R., Kawamoto, T., & Negishi, M. (2003). Identification of the nuclear receptor CAR:HSP90 complex in mouse liver and recruitment of protein phosphatase 2A in response to phenobarbital. *FEBS Letters*, *548*(1-3), 17–20. http://doi.org/10.1016/S0014-5793(03)00720-8

Yu, S., Lu, Z., Liu, C., Meng, Y., Ma, Y., Zhao, W., … Chen, J. (2010). miRNA-96 suppresses KRAS and functions as a tumor suppressor gene in pancreatic cancer. *Cancer Research*, *70*(14), 6015–6025. http://doi.org/10.1158/0008-5472.CAN-09-4531

Yusof, Y. a, & Edwards, a M. (1990). Stimulation of DNA synthesis in primary rat hepatocyte cultures by liver tumor promoters: interactions with other growth factors. *Carcinogenesis*, *11*(5), 761–70. Retrieved from http://www.ncbi.nlm.nih.gov/pubmed/1692266

Zelko, I., Sueyoshi, T., Kawamoto, T., Moore, R., & Negishi, M. (2001). The Peptide Near the C Terminus Regulates Receptor CAR Nuclear Translocation Induced by Xenochemicals in Mouse Liver, *21*(8), 2838–2846. http://doi.org/10.1128/MCB.21.8.2838

Zeng, C., Wang, R., Li, D., Lin, X. J., Wei, Q. K., Yuan, Y., … Zhuang, S. M. (2010). A novel GSK-3 beta-C/EBP alpha-miR-122-insulin-like growth factor 1 receptor regulatory circuitry in human hepatocellular carcinoma. *Hepatology*, *52*(5), 1702–1712. http://doi.org/10.1002/hep.23875

Zhang, B., Pan, X., Cobb, G. P., & Anderson, T. a. (2007). microRNAs as oncogenes and tumor suppressors. *Developmental Biology*, *302*(1), 1–12. http://doi.org/10.1016/j.ydbio.2006.08.028

Zhang, L., Hou, D., Chen, X., Li, D., Zhu, L., Zhang, Y., … Zhang, C.-Y. (2012). Exogenous plant MIR168a specifically targets mammalian LDLRAP1: evidence of cross-kingdom regulation by microRNA. *Cell Research*, *22*(1), 107–26. http://doi.org/10.1038/cr.2011.158

Zhang, Q., Bae, Y., Kemper, J. K., & Kemper, B. (2006). Analysis of multiple nuclear receptor binding sites for CAR/RXR in the phenobarbital responsive unit of CYP2B2. *Archives of Biochemistry and Biophysics*, *451*(2), 119–127. http://doi.org/10.1016/j.abb.2006.04.016

Zhang, X., Tang, N., Hadden, T. J., & Rishi, A. K. (2011). Akt, FoxO and regulation of apoptosis. *Biochimica et Biophysica Acta - Molecular Cell Research*, *1813*(11), 1978–1986. http://doi.org/10.1016/j.bbamcr.2011.03.010

Zhou, C., Tabb, M. M., Nelson, E. L., Grün, F., Verma, S., Sadatrafiei, A., … Blumberg, B. (2006). Mutual repression between steroid and xenobiotic receptor and NF-κB signaling pathways links xenobiotic metabolism and inflammation. *Journal of Clinical Investigation*, *116*(8), 2280–2289. http://doi.org/10.1172/JCI26283